Universität Konstanz

Chemical and behavioral aspects of insect-microbe interactions

Dissertation zur Erlangung des akademischen Grades eines Doktors der Naturwissenschaften (Dr. *rer. nat.*)

an der Universität Konstanz

Mathematisch-Naturwissenschaftliche Sektion
Fachbereich Biologie

vorgelegt von

Schlesiger, Ralf

Tag der mündlichen Prüfung: 17.Oktober 2017

1. Referent: PD. Dr. Christoph Kleineidam

2. Referent: Prof. Dr. Bernhard Schink

For my

family

friends

and colleagues at

University of Würzburg

University of Konstanz

Steigenberger Inselhotel Konstanz

Landesamt für Verbraucherschutz und Lebensmittelsicherheit Niedersachsen

Acknowledgments

Scientific contributions of academics, co-workers and students are acknowledged in front of or in every chapter. They have been miscellaneous and could therefore not be generalized.

I thank the Konstanz Research School Chemical Biology (KoRS-CB) and their team for the numerous training and education opportunities, as well as financial and administrative support. The scientific course program and the events helped me to increase my knowledge not only in areas of special interest, but also in career development and as a professional.

Moreover I thank all my colleagues at the KoRS-CB for their trust in me as elected student representative and their generous support while organizing events.

I want to thank my thesis committee for guidance during my four years in Konstanz, namely Prof. Dr. D. Spiteller, Prof. Dr. B. Schink and Prof. Dr. V. Wittmann.

Furthermore, I want to thank both technicians in our lab, Daniela Starke and Karin Denger.

I thank PD Dr. D. Schleheck for his support and trust during my lectures in his seminar “Methods in Biology”.

Moreover, I am grateful for the guidance and advices of PD Dr. C. Kleineidam, Prof. Dr. F. Roces (University of Würzburg) and Prof. Dr. H. Gross (University of Tübingen).

Special thanks go to Ann-Katrin Matt and Michael Weiß for being my floor mates.

In addition, I acknowledge the advices from Grzegorz Kubik and Sarah Wallrodt (both chemistry experts) as well as Manuel Nagel and Stefanie Neupert (both ant experts) for allowing fruitful conversations.

Overview of Contributions

Students were supported with specifications for experimental design, data collection, data analysis and writing of draft. Some of my figures were shared with them.

Supervision of bachelor theses

Denis Maier wrote his bachelor thesis “Untersuchungen zur Attraktivität von *Pseudomonas* sp. D2p auf *Drosophila hydei*” (submitted in July 2015) under my supervision.

Xenia Schilke wrote her bachelor thesis “Metabolitenprofile ausgewählter Blattschneiderameisen im Vergleich” (submitted in September 2015) under my supervision.

Luca Dietrich wrote his bachelor thesis “Charakterisierung von Oktalaktonen und kutikulären Verbindungen ausgewählter Blattschneiderameisen mittels GC-MS” (submitted in August 2016) under my supervision.

Supervision of students

My DAAD RISE student Karolina Subko contributed to several projects under my supervision (Juni-August 2015).

Names of students, which worked during intense practicals in chemical ecology under my supervision, are given in front of each chapter.

1 Table of contents

2 List of abbreviations

**g*	relative centrifugal force (multiples of gravity)
16*S* rDNA	16*S* ribosomal deoxyribonucleic acid
2D	two dimensional
2TY	cultivation medium (see methods)
3-C_4PDDR	desulfonated product of 3-C_4SPC; 3-(4'-(5''-Deoxy-D-ribofuranos-5''-yl)phenyl)butanoic acid
3-C_4SPC	3-(4'-Sulfophenyl) butanoic acid
3D	three dimensional
3-PB	3-Phenyl butyrate
adH_2O	autoclaved double distilled water
APE	A plasmid Editor (software)
bp	base pairs (DNA)
CC0	licensed after Creative Commons
CFP	fluorescent protein (cyan)
Ch.	chapter
COSY	correlation spectroscopy (NMR)
ctrl	control (solvent)
DAAD RISE	Deutscher akademischer Auslandsdienst – Research Internships in Science and Engineering
DAD	diode array detector
DAS	4,4′-Diamino-stilbene-2,2′-disulfonic acid
ddH_2O	double distilled water
Dendra2	fluorescent protein (red)
DFG	Deutsche Forschungsgemeinschaft (German Research Foundation)
DMSO	Dimethyl sulfoxide
DNS	4,4'-Dinitrostilbene-2,2'-disulfonic acid
dNTP	Deoxynucleotide triphosphate
e.g.	*exempli gratia* (lat.; for example)
EDTA	Ethylenediaminetetraacetic acid
eGFP	fluorescent protein (green, enhanced)
ESI-MS	electrospray ionization - mass spectrometry
et al.	*et alteri* (lat.; further authors)
ff	following
Fig.	Figure
GC-MS	gas chromatography - mass spectrometry
GFP	fluorescent protein (green)

GSP	good scientific practice
h	hour (time, 60 min)
HDD	hard disk drive
His	histidine (amino acid)
HMBC	heteronuclear multiple bond correlation (NMR)
HPC	high performance computing
HPLC	high performance liquid chromatography
HR-MS	high resolution - mass spectrometry
$HSQC_{ed}$	heteronuclear single quantum coherence edited (NMR)
IR	infrared (spectroscopy)
IT	information technology
KoRS-CB	Konstanz Research School Chemical Biology
l	liter (volume)
LAS	linear alkylbenzene sulfonates
LC-DAD-MS	liquid chromatography - diode array detector - mass spectrometry
m	meter (distance)
m4/m5/m6/m7	cultivation media (see methods)
m/z	mass to charge ratio
MALDI	matrix-assisted laser desorption ionization
MEGA	Molecular Evolutionary Genetics Analysis (software)
MeOH	methanol
mEos2	fluorescent protein (red)
min	minute (time, 60 seconds)
MPI CE	Max Planck Institute for Chemical Ecology
MSTFA	*N*-Methyl-*N*-(trimethylsilyl) trifluoroacetamide
N3, N4, N6, N46	cultivation medium (see methods of specific chapter)
NaHMDS	Sodium bis(trimethylsilyl)amide
NCBI	National Center for Biotechnology Information, USA
NMR	nuclear magnetic resonance (spectroscopy)
NO2	cultivation medium (see methods)
NOESY	Nuclear Overhauser Enhancement spectroscopy (NMR)
p.	page
p.a.	*pro analysi* (lat.; analytical grade purity)
PCR	polymerase chain reaction
ppm	part per million
RFP	fluorescent protein (red)
RP-C_{18}	reverse phase with C_{18} modification

rpm	revolutions per min
R_t	retention time
SCC	scientific compute cluster
SDS-PAGE	Sodium dodecyl sulfate-polyacrylamide gel electrophoresis
sec	second (time)
SFG	cultivation medium (see methods)
SPC	sulfophenyl carboxylic acids
SPE	solid phase extraction
SPEt	1-(4'-Sulfophenyl) ethanol
SPME	solid phase micro extraction
STE	common buffer (see methods)
Tab.	Table
TAE	common buffer (see methods)
TB	cultivation medium (see methods)
TDDR	desulfonated product of TS; 5-Deoxy-5-tol-4'-yl-D-ribofuranose
TIC	total ion count
TL	transmitted light (microscopy)
TMSH	Trimethylsulfonium hydroxide
Tris	2-Amino-2-(hydroxymethyl)-1,3-propanediol
TS	Toluene sulfonate
U/µl	Units per µl (enzyme concentration)
USB	universal serial bus
Vertiefungskurs Chemische Ökologie	Intense practical in chemical ecology
VNC	virtual network connection
VOC	Volatile organic compound
vol	volume
VPN	virtual private network

3 Summary

Insect microbe interactions were studied with leaf-cutting ants (*Atta* and *Acromyrmex*) and *Drosophila* fruit flies. Not only chemical, but also behavioral parameters were investigated to assist in describing relationships and dependencies of interactions.

Rearrangement inside waste chambers and antimicrobial composition of waste particles from leaf-cutting ants and bramble plants as leaf source were studied.

All waste heaps had a certain slope, no matter if there was an U-shaped, a donut-like or a nugget-like heap. Fresh waste particles were observed to be released onto the heap, thereafter a passive rolling-down of particles was observed and particles from the lower part of the waste heaps were transported into holes/tunnels by ants. In areas containing fresh waste particles, temporary turnover activities with moving tunnels or surface recirculation were observed. First experiments indicated, that there might be non-mutualistic fungi, whose growth was at least tolerated by leaf-cutting ants. Waste particles and bodies of dead ants showed microbial growth, especially greenish and whitish fungal hyphae.

To compare the antimicrobial composition of leaf-cutting ants' waste from different origins, bioassay-guided fractionation was used. Several differences and similarities were spotted for tested species.

To the best of our knowledge, for the first time, bramble leaves and stems were described to contain both, antifungal and antibacterial compounds. The bioactive compounds were extracted using acidified methanol (only antibacterial) or diethyl ether-acetone mixtures (antibacterial and antifungal).

Besides investigations in leaf-cutting ants' waste, also *R*- and *S*-γ-octalactone from metapleural glands of *Acromyrmex* and *Atta* leaf-cutting ants were analyzed. They were shown to differ in dominance, enantiomer ratio and overall amount. Further experiments are necessary to prove possible influencing parameters, like communication or disinfection issues.

For flightless *Drosophila hydei*, a novel behavioral assay was developed. Bacterial cells of *Pseudomonas* sp. D2p, isolated from *Drosophila* fruit flies, were shown to attract them. Cultivation conditions for D2p were studied, to enhance production of attractive volatile compounds. Several compounds like methylated pyrazines were present in GC-MS spectra and therefore tested for their attractiveness. Real-time tracking of fruit fly distribution was achieved by analyzing recorded movies with Matlab scripts.

Further projects with different topics, like method development for chemical analysis of secondary metabolites or structure elucidation of degradation products after anaerobic desulfonation of 3-C_4-SPC, were followed as well.

4 Zusammenfassung

Interaktionen zwischen Insekten und Mikroben wurden mit Blattschneiderameisen (*Acromyrmex* und *Atta*) sowie mit Fruchtfliegen (*Drosophila*) untersucht. Nicht nur chemische, sondern auch verhaltensabhängige Parameter wurden untersucht, um die Beschreibung der Beziehungen und Abhängigkeiten von Interaktionen zu unterstützen.

Verlagerungen in Müllkammern sowie die antimikrobielle Zusammensetzung von Müllpartikeln der Blattschneiderameisen und Brombeerpflanzen als Blattquelle wurden untersucht.

Alle Müllhaufen hatten eine Steigung, unabhängig davon, ob der Müllhaufen U-förmig war oder eine donut- oder nuggetartige Form hatte. Frische Müllpartikel wurden oben auf dem Müllhaufen abgelegt, danach wurde ein passives herunterrollen beobachtet und Müllpartikel vom unteren Teil des Müllhaufens wurden von Ameisen in Löcher/Tunnel eingetragen. In Bereichen, die frische Müllpartikel enthielten, wurden kurzzeitige Effekte wie sich bewegende Tunnel und Oberflächenumwälzung beobachtet. Erste Experimente zeigten nicht-mutualistische Pilze, deren Wachstum von Blattschneiderameisen zumindest geduldet wurde. Müllpartikel und Körper toter Ameisen wiesen optisch sichtbares Mikroben-wachstum auf, vor allem grüne und weiße Pilzhyphen wurden beobachtet.

Um die antimikrobielle Zusammensetzung von Müllpartikeln verschiedenen Ursprungs zu vergleichen, wurden Fraktionen in Agardiffusionsassays getestet. Mehrere Unterschiede und Gemeinsamkeiten wurden für die untersuchten Ameisenarten identifiziert.

Soweit wir wissen, beschreiben wir zum ersten Mal das Vorhandensein von antifungalen und antibakteriellen Substanzen in Brombeerblättern und –stämmen. Die bioaktiven Substanzen wurden mittels angesäuertem Methanol (antibakteriell) oder angesäuertem Diethylether-Aceton-Gemisch (antifungal und antibakteriell) extrahiert.

Neben Untersuchungen im Müll der Blattschneiderameisen wurden auch γ-Oktalaktone aus Metapleuraldrüsen von Blattschneiderameisen (*Acromyrmex* und *Atta*) untersucht. Es wurde gezeigt, dass sich das relative Vorhandensein, das Enantiomerenverhältnis sowie der Gehalt unterscheiden. Weitere Experimente sind notwendig, um mögliche Einflussfaktoren, wie Kommunikations- oder Desinfektionszwecke, zu identifizieren.

Für flugunfähige *Drosophila hydei* wurde ein neuartiger Verhaltensassay entwickelt. Bakterienzellen von *Pseudomonas* sp. D2p, das von *Drosophila hydei* isoliert wurde, wirkten anziehend auf diese Fruchtfliegen. Um die Produktion der anziehenden flüchtigen Verbindungen zu erhöhen, wurden Kultivierungsversuche durchgeführt. Mehrere Verbindungen, wie zum Beispiel methylierte Pyrazine, waren in GC-MS-Spektren sichtbar

und wurden daher auf ihre anziehende Wirkung untersucht. Echtzeit-Verfolgung der Fruchtfliegenverteilung wurde mit der Auswertung von Videos mittels Matlab durchgeführt. Weitere Projekte mit unterschiedlichen Themen wurden ebenfalls verfolgt, wie Methodenentwicklung für die chemische Analyse von Sekundärmetaboliten oder Strukturaufklärung der Abbauprodukte von anaerober Desulfonierung von 3-C_4-SPC.

5 Ecosystem of leaf-cutting ants

5.1 Introduction

5.1.1 Overview of leaf-cutting ants

There are few examples for fungus-growing insects in nature.[1] They all share the dependency on their cultivated fungus, because they must feed on it. Thus, it is very important for fungus-growing insects to protect their fungal cultivar against pathogens.

Among fungus-growing insects, leaf-cutting ants (genera *Atta* and *Acromyrmex*) are unique because they support their fungal cultivar with fresh leaf material.[2] Their presumed evolutionary origin is the wet forest of equatorial South America, while they nowadays occur from Argentina to the southern United States. Leaf-cutting ants cultivate fungal symbionts (*Leucoagaricus*) that serve as primary food source for the larvae and as an important food source for adult ants. Leaf-cutting ants use fresh plant material to cultivate their fungal mutualist, which provides food for ants in the form of lipid and carbohydrate rich inflated hyphal tips (gongylidia).

To protect their fungal cultivar from pathogens and parasites, leaf-cutting ants provide a clean environment in underground nest chambers. Exhausted or contaminated fungus garden material is continuously deposited in waste chambers by ant workers.[3] Additionally, leaf-cutting ants show multiple hygienic behaviors: a combination of aseptic glandular secretions and symbiotic bacteria producing antibiotics.

5.1.2 Symbiotic bacteria of leaf-cutting ants

Antibiotic-producing bacterial symbionts (mainly *Pseudonocardia* and *Streptomyces*) are described to be vertically transmitted from parent to offspring nests by young queens, which furthermore take little pieces of fungal cultivar before they leave for the mating flight and foundation of a new nest.[2]

Isolation of the symbiotic bacteria is different between *Atta* and *Acromyrmex.* While their fungal cultivar and their inwards contain symbiotic bacteria, only ants of the genus *Acromyrmex* have whitish biofilms on parts of their bodies. These biofilms consist of spores from Actinobacteria, which can be scraped off and cultivated on agar plates.[4]

The origin of the symbiotic bacteria in general remains unclear. While a co-evolutionary background is discussed, it is also conceivable that the established symbiotic strains could be replaced.[5-6] While there is only a small variety of bacterial strains (mainly *Pseudonocardia* and *Streptomyces*), all ants in one nest have at least similar bacterial species.[7] This might take place by chance due to high availability of these strains.

Alternatively, ants might actively select for a favored strain because of bacterial features that would enhance ants' fitness.

Passing on of symbiotic bacteria from old leaf-cutting ants to young ants (genus *Acromyrmex*) is not completely understood. The accumulation of symbiotic bacteria, visible as whitish biofilm, is different between worker castes and status of contamination with pathogens in the nest.[8] Ants (genus *Acromyrmex*) have no bacterial biofilm when they hatch, but they somehow begin to accumulate bacteria by interaction with nest mates in their first days.

5.1.3 Threat of ants' nest by pathogens

Encroaching contamination with fungal pathogens can destroy a fungal garden completely. The filamentous fungus *Escovopsis weberi* is known as hyphal parasite of the fungus-cultivar and can be found as spores or actively growing in ants' nests.[9]

To repress fungal contamination, leaf-cutting ants show multiple hygienic behaviors combining the use of aseptic glandular secretions and symbiotic bacteria producing antibiotics.[10]

Some bacterial symbionts produce secondary metabolites under laboratory conditions which show activity against fungal pathogens in bioassays.[11] The significance of these secondary metabolites for the survival of ant colonies remains unclear. These secondary metabolites could play a role in repressing fungal pathogens, because artificially increased contamination led to increased bacterial distribution in ants' nests or on their bodies (genus *Acromyrmex*).[8] Therefore, a modulating communication between ants and bacterial symbionts is suggested. Indeed, this can even happen passive due to increased glandular secretions, which may enhance bacterial growth.

The presence of an antibiotic compound (Valinomycin) on ants' bodies was shown by MALDI-MS-Imaging.[12] Therefore, the bacterial symbionts produce antibiotics and may support ants with their metabolites.

5.2 Waste management of leaf-cutting ants

5.2.1 Ant behavior assists complete decomposition in waste chambers of *Atta vollenweideri*, *Atta laevigata* and *Acromyrmex lundii*

Contributions

Observations were made with lab colonies in Konstanz and Würzburg. I would like to thank Dr. Kleineidam, Stefanie Neupert (University of Konstanz), Prof. Dr. Flavio Roces, Dr. Daniela Roemer, Adrienne Gerber-Kurz (University of Würzburg) because of fruitful discussions and making everything possible.

Antonin Sulc (Department for Computer and Information Science) prepared MATLAB scripts, which we applied on my videos. With thank to Dr. Stefan Gerlach, the scripts could be processed on servers of the Scientific Compute Cluster (SCC), a platform for high performance computing (HPC) at the University Konstanz.

Furthermore, Xenia Schilke wrote her bachelor thesis "Metabolitenprofile ausgewählter Blattschneiderameisen im Vergleich" (submitted in September 2015) regarding mainly chemical composition but also first observations of leaf-cutting ants' waste. She was assisted by my DAAD RISE student Karolina Subko. Exemplarily shown microbes were isolated by Laura Heinzelmann, Hendrick Rusche and Nils Glücklich during "Vertiefungskurs Chemische Ökologie 2016".

Technical equipment and travel expenses were mainly private financed by myself.

5.2.1.1 Abstract

Waste management of leaf-cutting ants is most often associated with pathogen repression, either by hygienic behavior, spreading of antimicrobial compounds or strict task partitioning. Nevertheless, there must be beneficial influences of waste piles, because ants do not only throw away their wastes but take care of them.

For this project, waste chambers of *Atta vollenweideri*, *Atta laevigata* and *Acromyrmex lundii* were observed by cameras for a long time. The content of waste chambers was collected and visible and physical properties were described.

One main aim of this project was to describe building activities within waste chambers. Several behavioral motifs were identified for different time points. The start of waste deposit and turnover activities followed repeating rules, moreover the formation of tunnel systems was monitored and analyzed using MATLAB scripts. Isolation of microbes revealed not only pathogenic microbes but also possible non-mutualistic fungi with beneficial properties such as decomposition of waste particles.

5.2.1.2 Introduction

Leaf-cutting ant cultivate fungal symbionts (*Leucoagaricus*) that serve as important food source. Exhausted or contaminated fungus garden material and bodies of dead ants are continuously deposited in waste chambers by ant workers.[3] These waste chambers are often reported as highly pathogenic areas, where task partitioning and strict isolation of waste workers was observed.[13-14]

There are some differences in waste management of Attini, as external or internal waste chambers can be used.[3] Recently, Farji-Brener, et al. [15] reported that, from 20 *Acromyrmex* and 12 *Atta* species, 80% of the *Acromyrmex* species but only 17% of the *Atta* species had external refuse dumps.

Nevertheless, ants did not only throw away waste particles but took care of waste piles. Underground waste piles were speculated to assist in regulation of climatic parameters, such as air humidity, with importance for the whole nest.[16-17]

The purpose of ant behavior for waste management was assumed to be mainly removal of contaminations and to promote the decomposition rate of waste particles.

During my work with leaf-cutting ants, I observed fascinating turnover activities within their nests, especially in waste chambers (*Atta vollenweideri*). While behavior and circumstances regarding foraging activities, nestmate recognition, childhood care and effects nearby the fungal symbiont were extensively studied (Hölldobler and Wilson [16] and references therein), less is known about waste chambers. Most studies focused on pathogens, task partitioning and ant fitness.[3, 14-15, 18-21] For a nice overview, I recommend the PhD thesis of Dr. Daniela Römer (published 2014; p. 103ff).[22] She investigated the influence of temperature, humidity and carbon dioxide on waste deposition and the impact of volatile cues on waste management.

In addition, I observed a certain building sequence, following several distinct rules. Further investigations showed, that these effects were reported only as side notes before.

For example, that fresh waste is loaded onto the waste pile and that there are tunnels inside the waste pile.[3] Furthermore, not only the presence of tunnel holes was observed for both, *Atta* and *Acromyrmex*, but ants were reported to enter holes with waste particles.[14]

With this project, we describe how leaf-cutting ants start to deposit in empty waste chambers. Furthermore, there are several behavioral motifs for turnover of waste, separated in temporary and long-term effects. In the end, there will be only a black humus-like material left.

5.2.1.3 Methods

5.2.1.3.1 Origin of leaf-cutting ants and waste chambers

Waste chambers from several leaf-cutting ant colonies were monitored with cameras.

The major observations were made with *Atta vollenweideri* colonies from the group of Dr. Kleineidam (University of Konstanz). Method development such as application of camera and Raspberry Pi systems were developed in Konstanz and applied thereafter in Würzburg.

Waste chambers of *Atta laevigata* and *Acromyrmex lundii* were monitored at the University of Würzburg in the lab of Prof. Dr. Roces.

Among Dr. Kleineidam and Prof. Dr. Roces, the generous support of Stefanie Neupert, Dr. Daniela Römer and Adrienne Gerber-Kurz has to be mentioned because this work depended completely on their expertise in leaf-cutting ant cultivation.

The monitored waste chambers consisted of transparent acrylic glass or glass panes. Shapes like cylindrical, rectangular and globular boxes with one entry were provided to prevent shape specific behavioral changes.

To observe internal rearrangements of waste particles, a narrow rectangular box was manufactured. This box had holes which allowed to take out waste particles from regions of interest.

5.2.1.3.2 Recording humidity and temperature in waste chambers with cameras

Several action cams were placed around the waste chambers together with permanent illumination (Osram, Philips).

Several cameras like Xiaomi Yi (16 Megapixel), Raspberry Pi 2 cameras (5 Megapixel) and one SJcam SJ5000 (14 Megapixel), were used equipped with 32/64/128 gigabyte microSD cards from Qumox, Transcend or SanDisk. The action cams were used continuously with power supply and took pictures in time lapse mode every min (Xiaomi Yi) or every 20 seconds (SJcam SJ5000). The setup and parameters of the Raspberry Pi 2 cameras are described elsewhere (Ch. 5.2.1.3.4, p. 11ff)

The pictures were processed using XNconvert or IrfanView. The pictures were rotated, downsized and/or cropped in batches. Thereafter, the pictures were converted to video (.*avi) with 25 frames per second using Images-to-video (Version 4.0, www.cze.cz). The avi files were compressed with Freemake Video Converter (*.mp4 files; H.264/MPEG-4 AVC), with full resolution and 480p. The videos were watched with videolan player (www.videolan.org) and processed as described elsewhere either by hand (Ch. 5.2.1.3.7, p. 19) directly or after processing with MATLAB scripts (Ch. 5.2.1.3.6, p. 17).

5.2.1.3.3 Equipment to record changes in waste chambers with sensors

To control the combined temperature and humidity sensors DHT11 and DHT22, several Raspberry Pi 2 were set up with Raspbian Jessie (Build February 2016) as operating system on microSD cards. The systems were updated (Code 1; lines 1-4), thereafter cameras were enabled (Raspberry Pi configuration) and software for network control (TightVNC; Code 1; lines 6-53) was installed with the help of the terminal.

Code 1: Setup of Raspberry Pi and VNC

```
1 % update distribution
2 sudo apt-get update
3 sudo apt-get dist-upgrade
4 sudo rpi-update
5
6 % install TightVNC server
7 sudo apt-get install tightvncserver
8 tightvncserver
9 % set password
10
11 % run TightVNC at boot
12 sudo su
13 cd /etc/init.d/
14 sudo nano vncboot
15
16 %paste this code into the file
17   #! /bin/sh
18   # /etc/init.d/vncboot
19   ### BEGIN INIT INFO
20   # Provides: vncboot
21   # Required-Start: $remote_fs $syslog
22   # Required-Stop: $remote_fs $syslog
23   # Default-Start: 2 3 4 5
24   # Default-Stop: 0 1 6
25   # Short-Description: Start VNC Server at boot time
26   # Description: Start VNC Server at boot time.
27   ### END INIT INFO
28   USER=pi
29   HOME=/home/pi
30   export USER HOME
31   case "$1" in
32       start)
33   echo "Starting VNC Server"
34   #Insert your favoured settings for a VNC session
35   su - $USER -c "/usr/bin/vncserver :1 -geometry 1280x800 -depth 16 -
36   pixelformat rgb565"
37   ;;
38   stop)
39   echo "Stopping VNC Server"
40   /usr/bin/vncserver -kill :1
41   ;;
42   *)
43   echo "Usage: /etc/init.d/vncboot {start|stop}"
44   exit 1
45   ;;
46   esac
47   exit 0
48
49 % make file executable
50 chmod 755 vncboot
```

```
51
52 % update boot table
53 update-rc.d vncboot defaults
```

5.2.1.3.4 Setup of the "RPi cam control" software

After installation of the RPi cam control software (Code 2; lines 2-5), the software was configured (Code 2; lines 7-8) with apache web server for remote access of the web frontend.

Code 2: Setup of RPi cam control software

```
1 % install RPi Cam software
2 git clone https://github.com/silvanmelchior/RPi_Cam_Web_Interface.git
3 cd RPi_Cam_Web_Interface
4 chmod u+x RPi_Cam_Web_Interface_Installer.sh
5 ./RPi_Cam_Web_Interface_Installer.sh install
6
7 % configure RPi Cam software with web server, port and autostart
8 ./RPi_Cam_Web_Interface_Installer.sh autostart_yes
```

The frontend of RPi cam control software was accessed with the browser, using the IP address and the selected port (Fig. 1). The software showed an image preview directly, this function was used to arrange the camera. In the configuration panel, the camera and motion detection settings were defined.

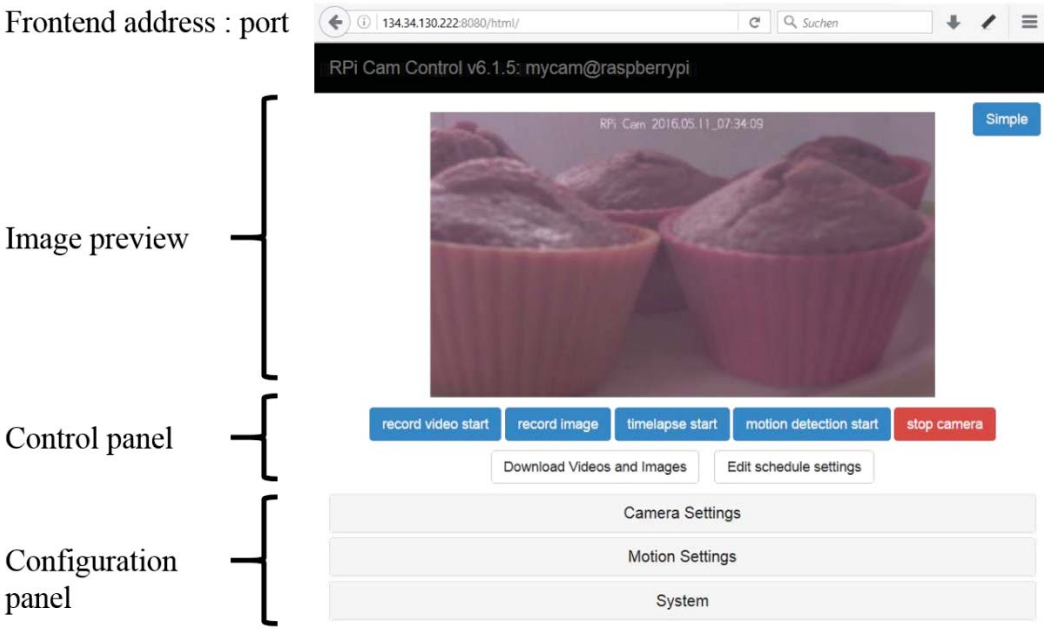

Fig. 1: Frontend of the software "RPi cam control".

After configuration of basic camera parameters (contrast, brightness, ISO - fixed or automatic adjustment), the capture parameters were set (Fig. 2). For annotation of the image and video files, the capturing date and time was embedded into the filename. In general, time lapse intervals of 60 seconds with the full resolution of 2592x1944 pixels were used.

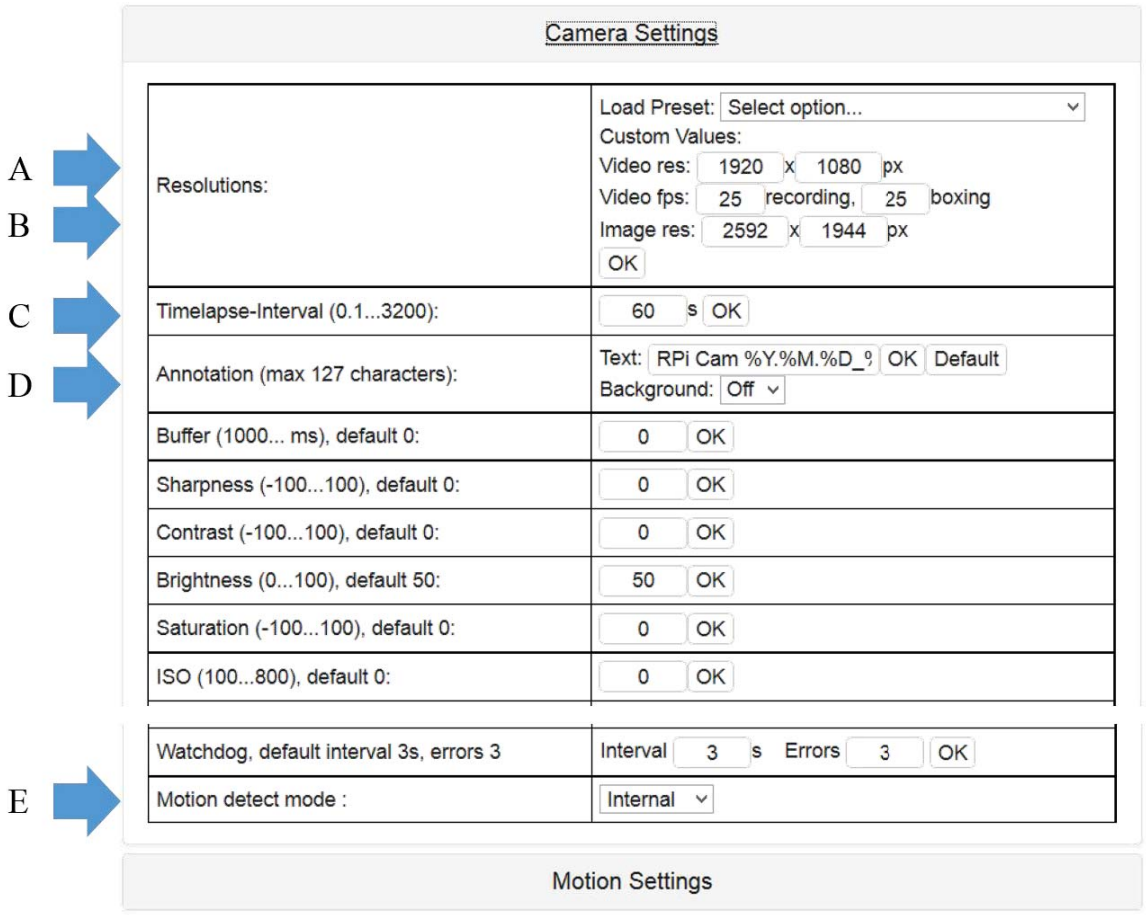

Fig. 2: Camera setting parameters. A: Resolution and frames per second of video files. B: Resolution of image files. C: Time lapse interval. D: Naming of files including time and date. E: Motion detection mode (internal or external).

For advanced approaches, time lapse was combined with internal motion detection (Fig. 2 E). The internal motion detection was easy to handle, whereas for the external motion detection the motion module needs to be installed and configured in another frontend and a configuration script.

The motion detection algorithm needed to be optimized for every setup because of contrast and light differences. The internal motion detection was set up, in order to define suitable noise level, thresholds and video duration (frames) for each experiment. In general, a video for 3 min (180 seconds) with 1 frame per second and 1920x1080 pixels was produced (Fig. 3) after detected movements.

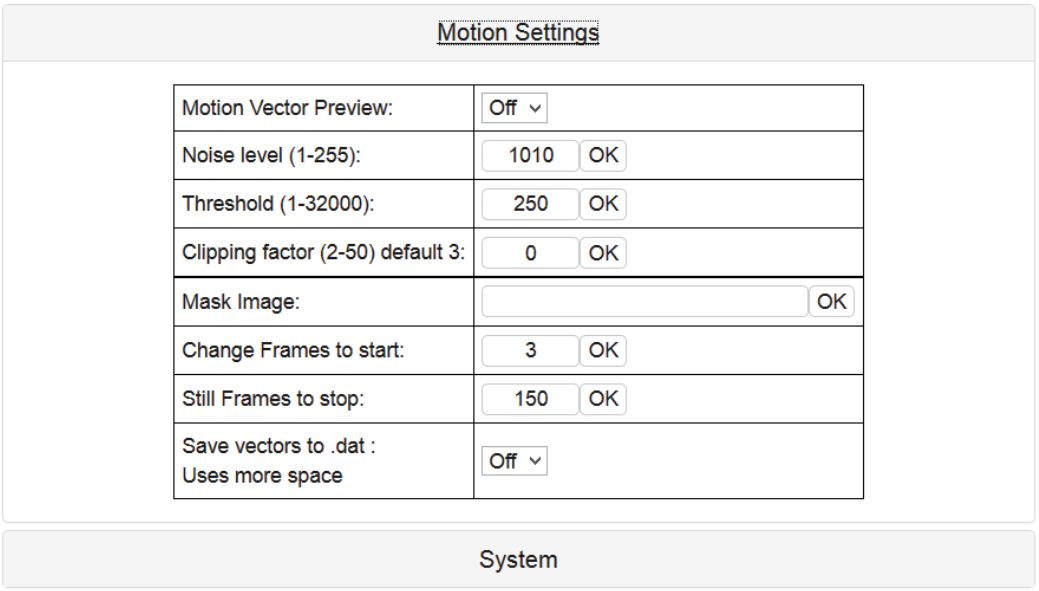

Fig. 3: Motion settings parameters to change noise level, threshold and number of frames.

The jobs with the adjusted parameters were schedules in order to start them automatically. Therefore, the schedule was set up with the "Edit schedule settings" button in the control panel.

The videos and pictures were stored in the destination folder, but could be remotely accessed with the "Download videos and images" button in the control panel (Fig. 4). The files were stored either alone (images, videos) or in batches (time lapse).

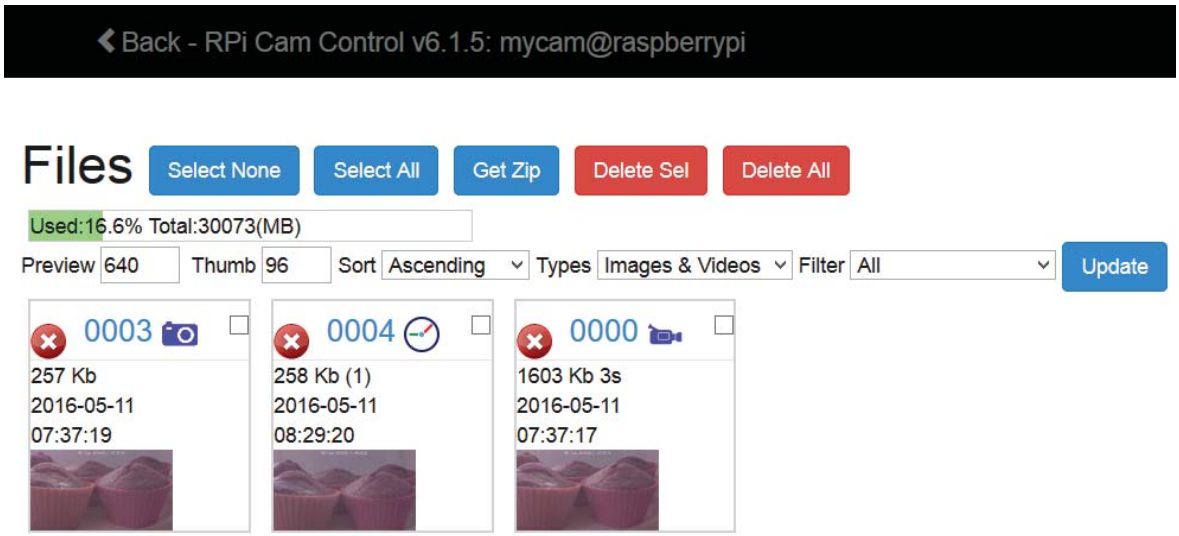

Fig. 4: File storage in the frontend to check data storage.

The image files were processed as described previously to generate *.mp4 video files (Ch. 5.2.1.3.2, p. 9).

5.2.1.3.5 Setup of combined humidity and temperature sensors

To measure the influence of humidity in several waste layers, combined humidity and temperature sensors were connected to data pins of the GPIO panel of the Raspberry Pi 2.

Therefore, DHT11 and DHT22 sensors were connected to wires of a breadboard and the GPIO. DHT11 sensors are smaller and cheaper than DHT22 sensors (Fig. 5 A; 1 € compared to 7 € each), but measurements are less precise (Tab. 1). Both sensor types were tested and results were compared to evaluate the data.

Tab. 1: Comparison of parameters from DHT11 and DHT22 sensors.

	Temperature (°C)	**Accuracy**	**Humidity (%)**	**Accuracy**
DHT11	0-50	±2,0°C	20-95,0	±5%
DHT22	-40-80	±0,5°C	0-99,9	±2%

Both sensors had the same arrangement, with a four PIN arrangement from whose three PINs needed to be connected. The first PIN is the power connector, which needs 3 Volts power supply (Fig. 5 B red). The second PIN was for data transfer (Fig. 5 B blue), furthermore it needed power supply through a resistor (4-10 kΩ; Fig. 5 B red through resistor). The third PIN was empty and not connected, but the fourth PIN was the zero conductor and was connected to the ground (Fig. 5 B green and black). The sensors were fixed in waste chambers with the solid site upwards and the open site downwards (Fig. 5 C)

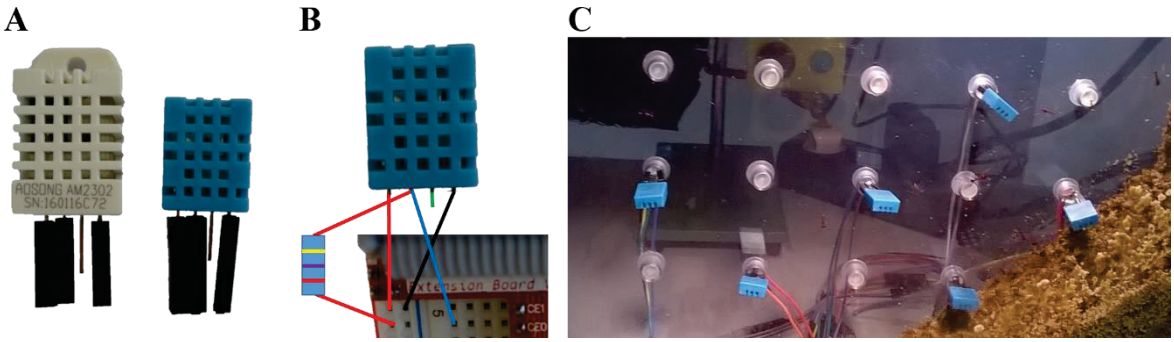

Fig. 5: Overview of the DHT sensors. A: DHT22 (left) and DHT11 (right). B: Wiring of the DHT sensors (red: 3 Volts, blue: data connection, green: not connected, black: ground). C: Example of DHT11 sensors in a waste chamber.

The sensors were programmed with the help of Python scripts. Therefore, the adafruit drivers (adafruit factory, NY, USA) and the required python packages were loaded (Code 3; lines 1-8). To communicate with the sensors, the python script (AdafruitDHT.py) as well as the sensor type (11 or 22) and the data PIN needed to be executed in the terminal (Code 3; lines 12).

Code 3: Installation and start adafruit drivers and their python scripts.

```
1 % install python packages
2 sudo apt-get update
3 sudo apt-get install build-essential python-dev python-openssl
4
```

```
% install adafruit DHT drivers
git clone https://github.com/adafruit/Adafruit_Python_DHT.git
cd Adafruit_Python_DHT
sudo python setup.py install

% start python script for communication with sensors
cd adafruit-driver-folder
sudo ./AdafruitDHT.py 11 27
sudo ./AdafruitDHT.py 22 26
```

The sensor readout data was only displayed in the terminal directly, but not written to a file (Fig. 6 A). In order to generate a tabulator with the sensor readouts, the code needed to be executed in a bash script. The values of several sensors together with the date and time were then stored in a *.csv file (Fig. 6 B).

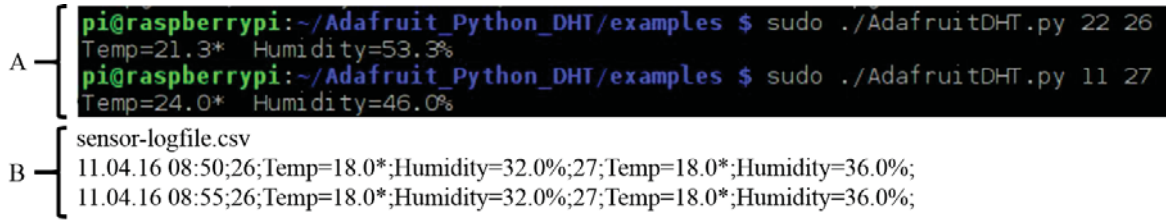

Fig. 6: Readout from sensor data. A: Readout of single sensors in the terminal. B: Example of a readout written to a *.csv file without modification.

The bash script was generated using the terminal. At first, a variable for the date and time was defined (Code 4; lines 7-8; VDATE). After that, the *.py script was executed for every sensor (Code 4; lines 14-20; for sensor 27 as DHT11 and sensor 26 as DHT22) and the readout data was stored as variables (e.g. TEMP26 and HUMI26). After collection of all sensor data, the values were written to the specified *.csv file (Code 4; lines 22-24). The values for temperature and humidity were separated with semicolons and the corresponding sensor number was stored in front (date; sensor number; sensor temperature; sensor humidity; -next sensor).

*Code 4: Generate a *.csv file from sensor readout data and execute script every 5 min.*

```
% generate script in terminal
sudo nano sensor-readout.sh

% paste this code into the *.sh file and modify parameters
      #!/bin/bash

      # create a variable for date and time
      VDATE=$(date +"%d.%m.%y %H:%M")

      # change to directory with *.py script
      cd /home/pi/adafruit-driver-folder/

      # execute the *.py script for every sensor
      VALUE27=$(sudo ./AdafruitDHT.py 11 27)
      TEMP27=$(echo $VALUE27 | awk '{print $1}')
      HUMI27=$(echo $ VALUE27 | awk '{print $2}')

```

```
18        VALUE26=$(sudo ./AdafruitDHT.py 22 26)
19        TEMP26=$(echo $VALUE26 | awk '{print $1}')
20        HUMI26=$(echo $ VALUE26 | awk '{print $2}')
21
22        # print results to *.csv file, separation of parameters with “;”
23        echo "$VDATE;27;$TEMP27;$HUMI27;26;$TEMP26;$HUMI26;" >> sensor-
24        logfile.csv
25
26 % make *.sh file executable
27 chmod u+x sensor-readout.sh
28
29 % start *.sh file manually
30 sudo ./sensor-readout.sh
31
32 % execute *.sh file automatically
33 crontab -e
34
35 % add the following line to the crontab file to execute the *.sh file
36    every 5 min “/5”
37 */5 * * * * /home/pi/adafruit-driver-folder/sensor-readout.sh
```

To plot the resulting data, only the numerary is needed without units and descriptions (Fig. 6 B). Therefore, several search and

replace operations with the software Notepad++ (https://notepad-plus-plus.org/; Version 6.9) were necessary. Microsoft EXCEL was not used, because the case sensitive replacement of "*" is not possible as it meant "all". The parameters "Temp=", "Humidity=", ".0*" and ".0%" were removed. Thereafter, the *.csv file was imported with EXCEL, defining semicolons as separators. The date was changed to numbers to plot the time points easily (Tab. 2).

Tab. 2: Example for a data set of sensor number 23 in EXCEL.

Date and time	Date as number	Sensor number	Temperature of sensor 23 (°C)	Humidity of sensor 23 (%)
11.04.2016 07:05	42471,295	23	18	35
11.04.2016 07:10	42471,298	23	18	36
11.04.2016 07:15	42471,302	23	18	31

The data sets were used to plot changes of temperature and humidity over time, which was then correlated to changes observed by camera systems.

5.2.1.3.6 Processing of videos using MATLAB scripts

To process the time-lapse videos, the software MATLAB 2015b was used with a script generated in co-operation with Antonin Sulc (Department for Computer and Information Science). With this script, the movements of individual ants were removed. Furthermore, the changes in the waste piles were visible clearly.

Downsampling (called subsampling in the code) of the videos was necessary because of the consumption of random access memory, which limited the calculations (Code 5; line 6). Parameters like WS and lambda needed to be adjusted for every video file (Code 5; line 4-5). The WS parameter influences the number of frames, which were taken for picture differentiation. If the WS parameter is too low, ant movement is visible, if the parameter is too high, the pile movement is fragmented.

The lambda parameter influences the granularity of changed areas. If the parameter is too low, some pixels of ant bodies are not recognized. If the parameter is too high, the pile movement might be not visible.

The video file is loaded by the command in line 9 (Code 5). The video output is split in three parts, with the input video on the left, the processed video in the middle and a calculated differentiation pattern on the right side. The calculated differentiation pattern was not as useful as expected, the main reason for that were the illumination and the camera systems, which led to flickering and therefore disturbed the calculations.

Code 5: MATLAB script for noise and movement reduction by calculation of difference images.

```
addpath('./animal_behavior/code/libs/SVD/')
addpath('./animal_behavior/code/libs/FPCP/')

ws = 10;
lambda = 0.001; % 2/sqrt(max(size(M))); % default lambda
subsample = 2; % divide picture size by this factor

%% reading input video
filename = './videofolder/videoname.mp4'
video = VideoReader(filename);

% for debugging: change number of frames “nf”, if limited by memory
h = uint32(video.Height/subsample);
w = uint32(video.Width/subsample);
nf = uint32(video.FrameRate * video.Duration);

%% processing of input video
I = zeros(h,w,3,nf,'uint8');
for i = 1:nf
    I(:,:,:,i) = im2uint8(imresize(readFrame(video),[h,w]));
    fprintf('reading %i-th frame of %i\n', i,nf)
end
If = (fft(I,[],4));
If = fftshift(If);
filter = zeros(size(If));
filter(:,:,:,end/2 - ws : end/2 + ws) = 1;
Ilow = abs(ifft(ifftshift(If .* filter),[],4)) / 255;
lear If filter;
Ilow = uint8(Ilow * 255);
Ilowbw = squeeze(0.2989 * Ilow(:,:,1,:) + 0.5870 * Ilow(:,:,2,:) + 0.1140
* Ilow(:,:,3,:) );
M = reshape(double(Ilowbw)/255,h*w,nf);
[L,S] = fastpcp(M,lambda);
S = reshape(S,h,w,nf);
S(S(:) == 0) = NaN;

%% produce output video
vout = VideoWriter('./videofolder/videoname-processed.avi');
open (vout);
for i=1:nf
    i1 = double(rgb2gray(I(:,:,:,i)))/255;
    i2 = double(rgb2gray(Ilow(:,:,:,i)))/255;
    i3 = mat2gray(abs(S(:,:,i)));
    Im = cat(2,i1,cat(2,i2,i3));
    writeVideo(vout,Im);
end
close(vout)
```

To overcome difficulties with limited random access memory, the calculations were processed on servers of the Scientific Compute Cluster (SCC), a platform for high performance computing (HPC) at the University Konstanz. With thank to Dr. Stefan Gerlach, the scripts were applied to HPC clusters. The video and data files were transferred using winSCP (https://winscp.net/eng/docs; Version 5.9.1). To run the MATLAB scripts, a job file and a terminal command was necessary. The job file contained commands to load the MATLAB module and run the script without graphical user interface (Code 6).

Code 6: Content of the job file job.sh to run a MATLAB script on HPC cluster.

```
1 #!/bin/bash
2 module load matlab
3 matlab -nodisplay -nodesktop -nosplash < matlabfile.m
```

The commands were transferred using Putty (http://www.putty.org/; Version 0.67), a free terminal software. After login and change of directory, the generated job file was started. The random access memory was allocated with the command h_vmem, in order to use more than the default memory (Code 7; in this case 256 Gigabyte).

Code 7: Terminal command to start job file to run MATLAB scripts.

```
1 qsub -l h_vmem=256G job.sh
```

The output video files were transferred to a local computer and further analyzed.

5.2.1.3.7 Evaluation of pictures, videos and processed videos

To visualize tunnel and surface changes, images were imported into Microsoft PowerPoint. The contour of the box as well as surface and tunnels were marked with the pencil tool. The graphs were exported as *.png with transparent background. These files could be overlaid to show changes over time. For presentations, these *.png files could be combined to a movie or animated as *.gif.

5.2.1.4 Results and Discussion

5.2.1.4.1 Process flow sequence in leaf cutting ants' waste disposal

The observations in leaf-cutting ants' waste were categorized in three main groups (Fig. 7). At first, a waste chamber is acquired and in some areas, the deposit of waste particles starts. Thereafter, the waste chamber is filled with more and more waste particles, which show a certain arrangement and turnover including tunnel systems. Even when the ants stop disposal of additional waste particles, the content of a waste chamber is not a static but a dynamic system.

The observations were assisted by camera systems, which allowed to generate time lapse videos for weeks and months. Main parts of the experiments were conducted with *Atta vollenweideri* in Konstanz, additional experiments with *Atta laevigata* and *Acromyrmex lundii* in Würzburg allowed to classify observations to be single, general or species-specific events.

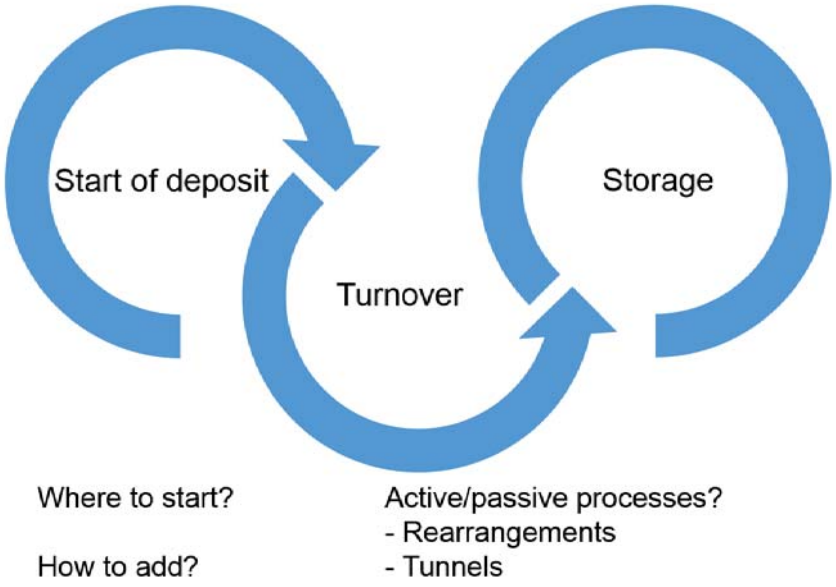

Fig. 7: General classification of observations in leaf-cutting ants' waste chambers.

At first, cylindrical waste chambers were used. The waste chambers had one connection pipe to the nest. To describe several events in the box, cameras were placed on the upside, side or backside of the cylinder (Fig. 8). For some experiments, colorful paper was cut into pieces and soaked with bramble leaf extract to generate trackable waste-like particles. The paper pieces were offered in the leaf chamber and mainly processed like leaf material by the ants.

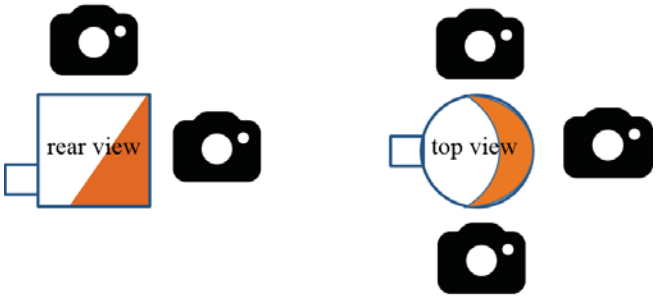

Fig. 8: Camera positions at waste chambers.

To answer specific questions about tunnel building activities, an additional waste chamber arrangement was developed. This additional waste chamber was a long, but tight box with one glass surface, to track rearrangements and tunnel building directly (Fig. 9 A). To classify those observations, additional measurements such as temperature and humidity were conducted using a Raspberry Pi system with sensors on the other side, where holes were plugged and usable for modifications (Fig. 9 B).

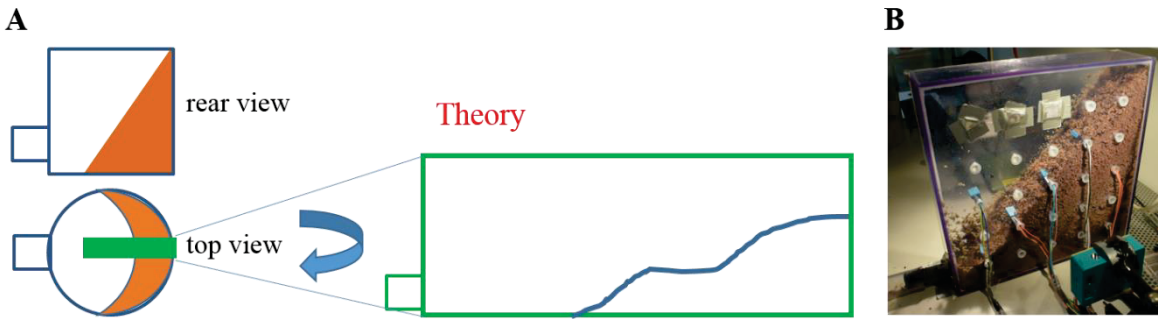

Fig. 9: Arrangement of long waste chamber. A: Theoretical approach of the long tight chamber. B: Practical usage of the long waste chamber equipped with sensors.

The chemical and physical composition of waste particles will be discussed in another chapter (Ch. 5.2.2; p. 62).

5.2.1.4.2 Start of waste deposit in waste chambers

In lab colonies, leaf-cutting ants' nests depend directly on available boxes. These waste chambers are emptied periodically. In nature, nest building behavior and climatic influences play an important role for the acquisition of waste chambers.[23]

In our experiment, an empty box was applied on a pipe, where another waste chamber was connected previously. Therefore, the trail was not altered.

Leaf-cutting ants did not start waste chambers randomly, but in the edges between the ground and wall in a certain distance to the connection pipe. In cylindrical boxes, the disposal started in a distance of one quarter from the entrance (Fig. 10 B; red arrow). Interestingly, a second waste pile started in the same distance on the other side (Fig. 10 C; red arrow).

The filling speed is related to colony size and age; therefore, no representative kinetic experiments were conducted.

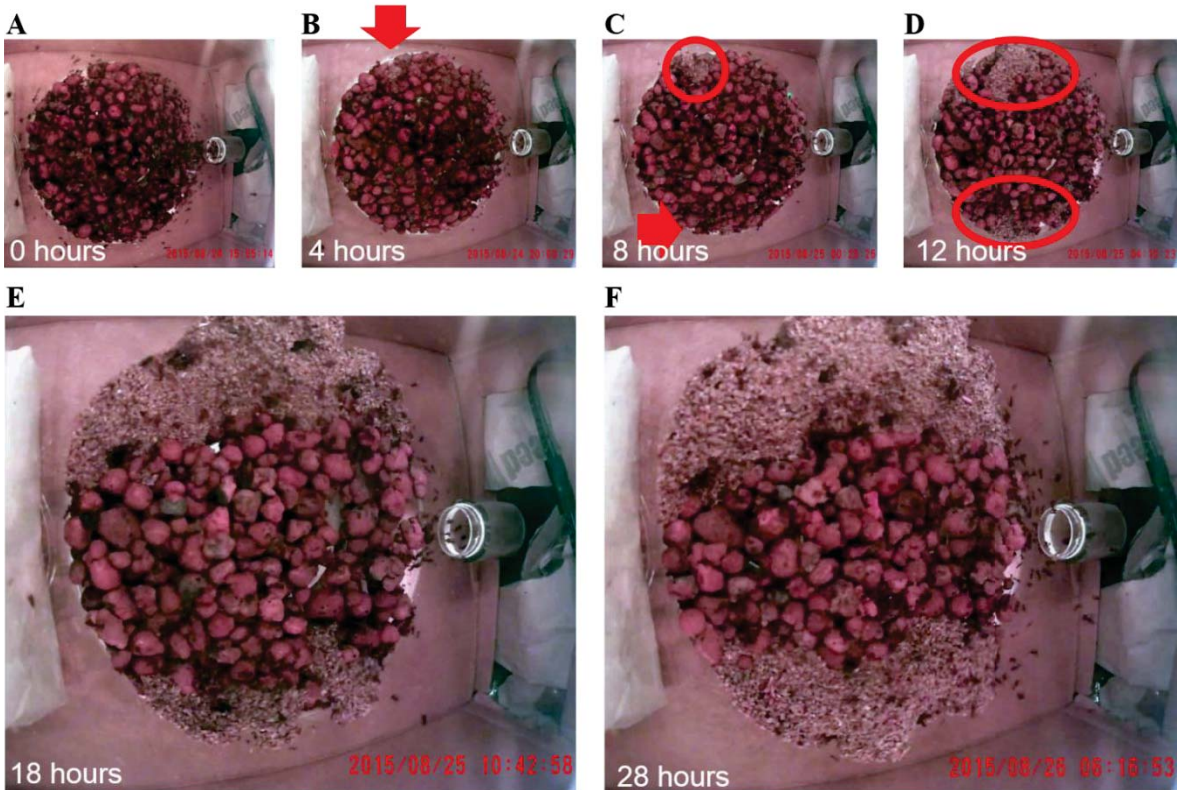

Fig. 10: Initial deposit of waste particles in cylindrical boxes (top view). First piles indicated with red arrows in B and C. Growth of waste piles in C and D indicated by red circles.

The pile is created on the opposite side of the entrance (Fig. 11). At the entrance area, a lot of ant movement was visible, but no waste particles were deposited. At the entrance area, the clay particles were visible. The waste particle transporting ants seemed to carry the particles not only until the entrance area of the waste chamber, but up to the peak of the pile.

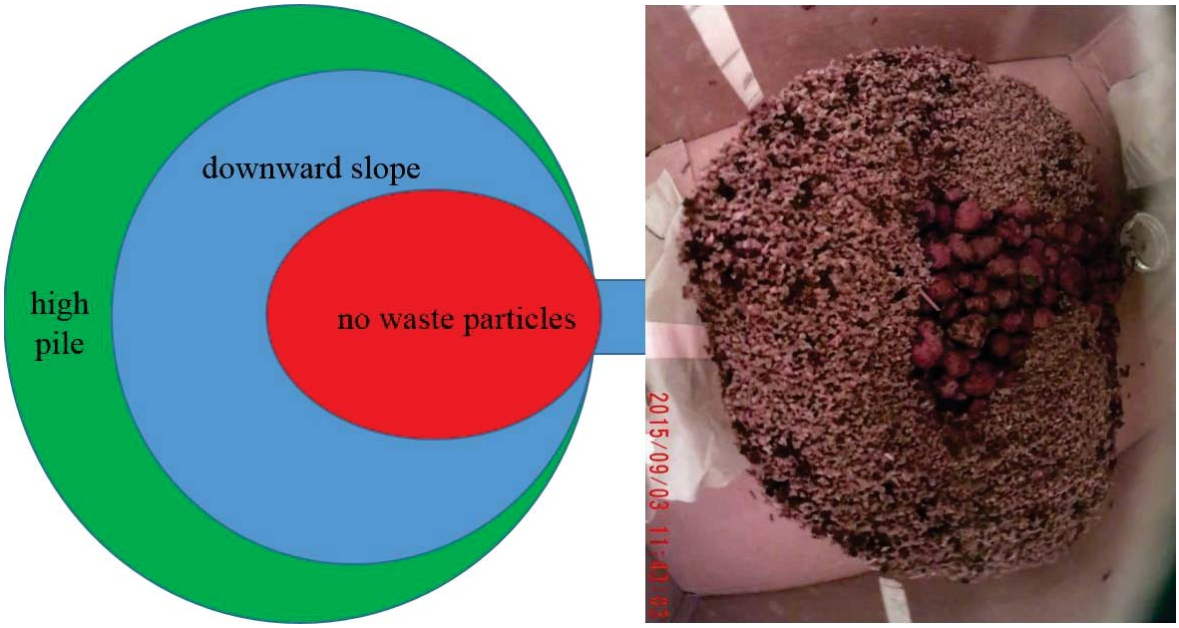

Fig. 11: Distribution of waste piles in cylindrical boxes (top view). Orientation of pile slope and peak.

In the long flat chamber, the waste disposal started in a distance of 10-15 cm from the entrance (Fig. 12 B). After a certain time, a second waste disposal area was started another 10-15 cm in distance to the first waste pile (Fig. 12 C). The second waste pile was moved another 10 cm in the direction away from the entrance and built a third pile (Fig. 12 D). Thereafter another pile in the location of the second pile was created (Fig. 12 E). Over time, the most distantly waste pile grew in height and the waste piles got connected (Fig. 12 F). Already in that state, temporary turnover indentations were visible (Fig. 12 G-H). While the initial turnover based on translocation from pile to pile, the later turnover based on translocation within one pile. This effect will be further discussed in another chapter (Ch. 5.2.1.4.8; p. 42).

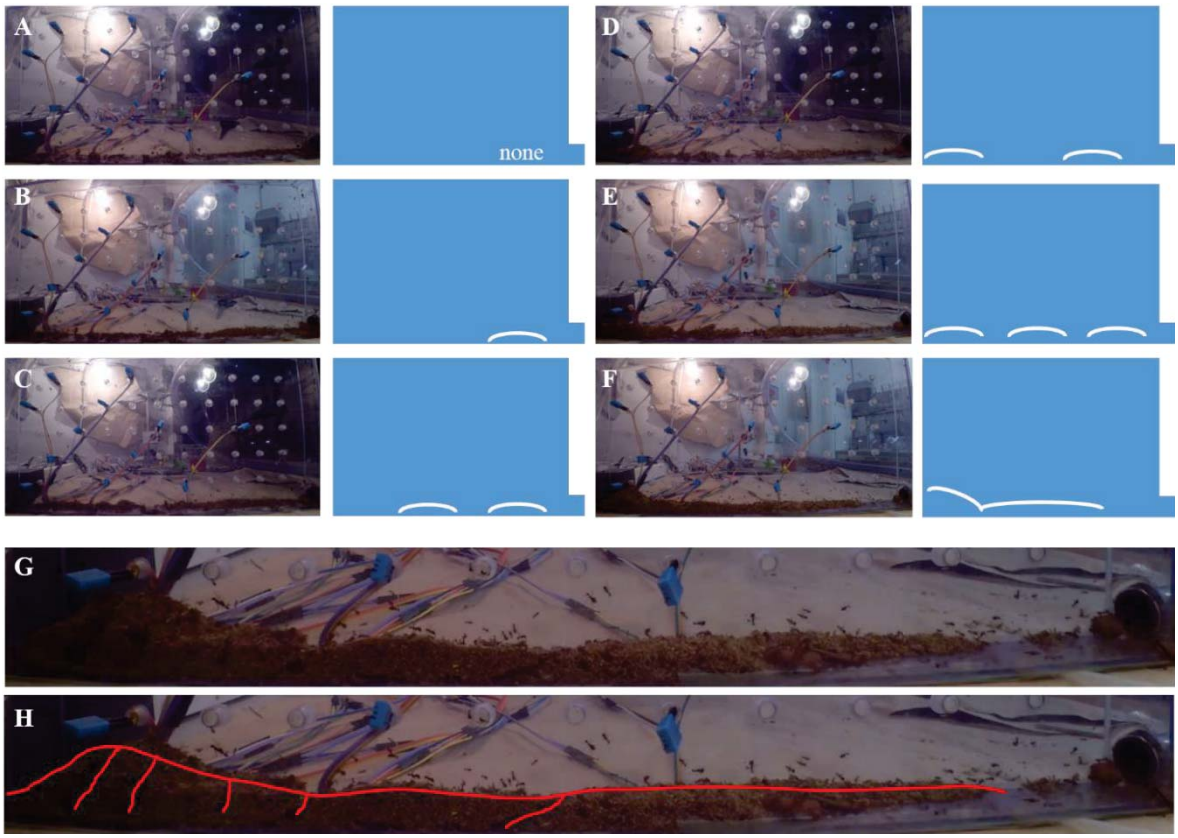

Fig. 12: Indication of beginning waste deposit in a long chamber. Several time points for a total time of 10 days. A-F: Indication of waste piles as white lines. G-H: First indication for active turnover of waste particles on waste piles. Red line in H shows surface and indentations of G.

Whether the ants start depositing waste particles after a certain distance or after a clue on the travel path is not known. The simplest possibility would be a distance related choice (Fig. 13; A1 and B1). In that scenario, an ant would go a certain distance from the entrance and deposit waste particles.

In a second scenario, the ant would move a certain distance and if there is no disturbance, move back and deposit waste particles (Fig. 13; A2 and B2). In a third scenario, the ant would move until a disturbance appears and then move back a certain distance (Fig. 13; A3 and B3).

With the available data sets, the mode of action could not be resolved. Indeed, in nature there are no cylindrical boxes but more spherical holes, where the deposit would start in the natural cavity.

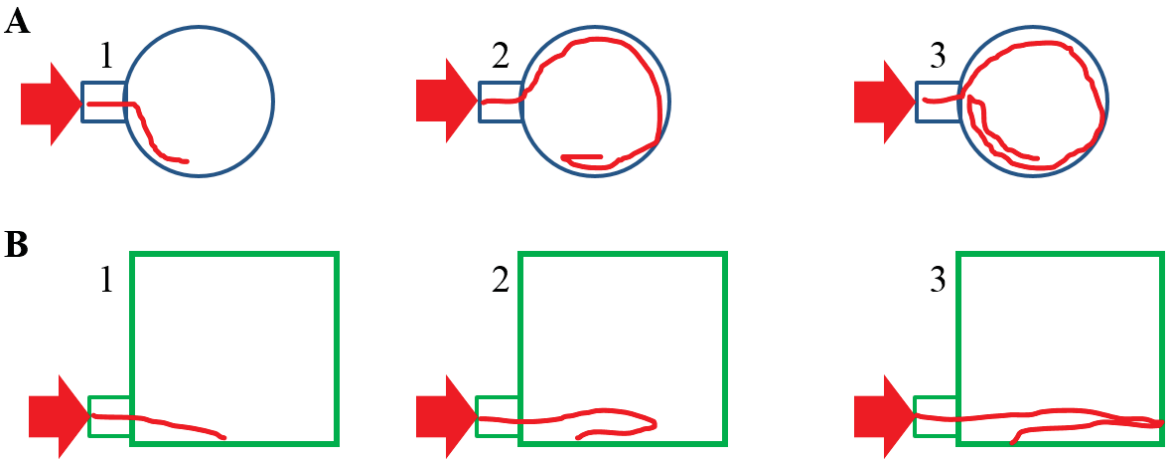

Fig. 13: Comparison of possible travel routes for initial waste deposit of leaf-cutting ants.

5.2.1.4.3 Deposit of waste particles in differently shaped waste chambers

The deposit of waste particles was tested in cylindrical boxes with entrances on the bottom, side and top. Moreover, a spherical arrangement was investigated.

For the cylindrical boxes, the waste deposit for an entrance at down sideways was already shown in the previous chapter (Fig. 14 A). The main parts of the piles started on the opposite side of the entrance, while the entrance area remains free of waste particles.

When the entrance was at the upside sideways, there was no defined pile but a donut-like structure formed (Fig. 14 B). There was no free entrance area, moreover the donut-like structure showed gradients in all directions.

A direct entrance at the downside of the box was not possible, therefore the opening pipe was extended into the box (Fig. 14 C). The pile looked similar to the down sideways arrangement without the forecourt at the entrance area. Whether an arrangement with an externally connected entrance would be different or not is not known.

When the entrance was on top of the box, the ants did not deposit waste particles (Fig. 14 D). It seemed like the ants were not able to enter the box without losing waste particles. The box was only entered by ants without waste particles. Waste particles were only transported until the end of the pipe, but were then moved into another chamber.

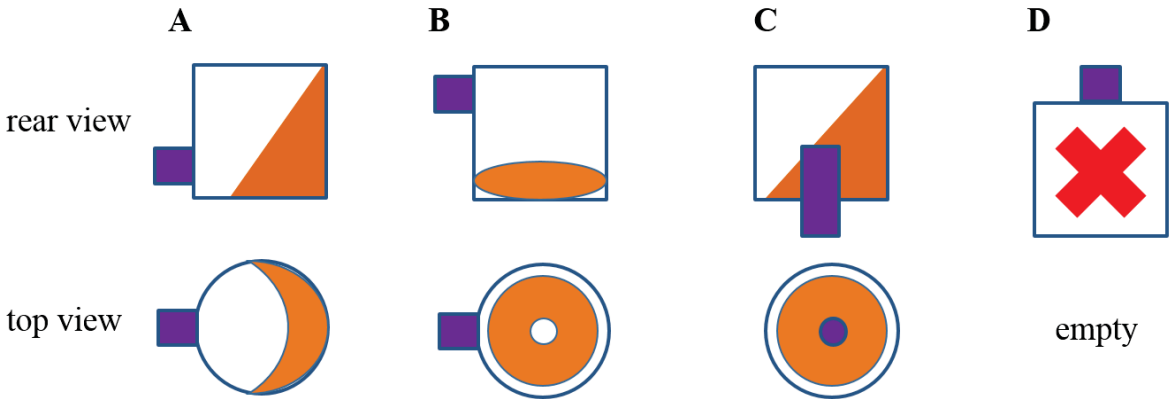

Fig. 14: Arrangement of waste piles in cylindrical boxes with different entrance orientation. A: Down sideways. B: Up sideways. C: Down downside. D: Up upside.

In a spherical chamber with sideways entrance, the waste deposit started at the lowest point. Again, waste particles were arranged in piles with certain gradients (Fig. 15). There was no forecourt at the entrance area, the waste pile was more or less central inside of the chamber and started directly at the entrance pipe.

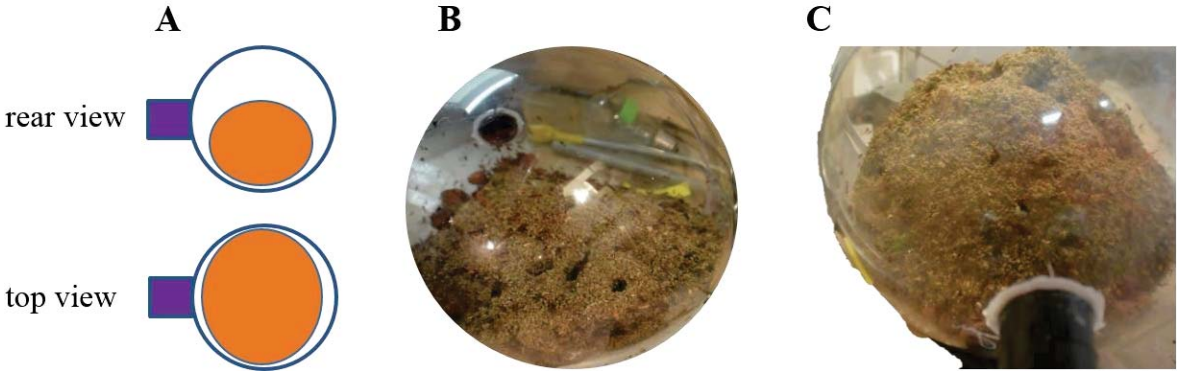

Fig. 15: Spherical waste chamber. A: Schematic drawing of waste arrangement. B: Picture of waste pile from the backside towards the entrance. C: Picture of waste pile from the entrance side.

5.2.1.4.4 Turnover of waste particles in waste chambers

While the overall deposit in waste chambers could be assumed as a static system, where new waste particles are deposit on top of older waste particles,[3] a closer look revealed a more complex process. After starting the deposit of waste particles, immediately a turnover by rearrangements began. Indeed, there are active and passive processes involved.

Using colorful pieces of paper, particles rolling down the piles were followed. Tracking one particle over time, the particle moved down the pile without long-term contact with ants (Fig. 16 A-E). Moreover, particles were not observed to move up the pile again. Like that, the pile would be flattened over time, but no flattening was observed. Therefore, another mechanism needs to be involved.

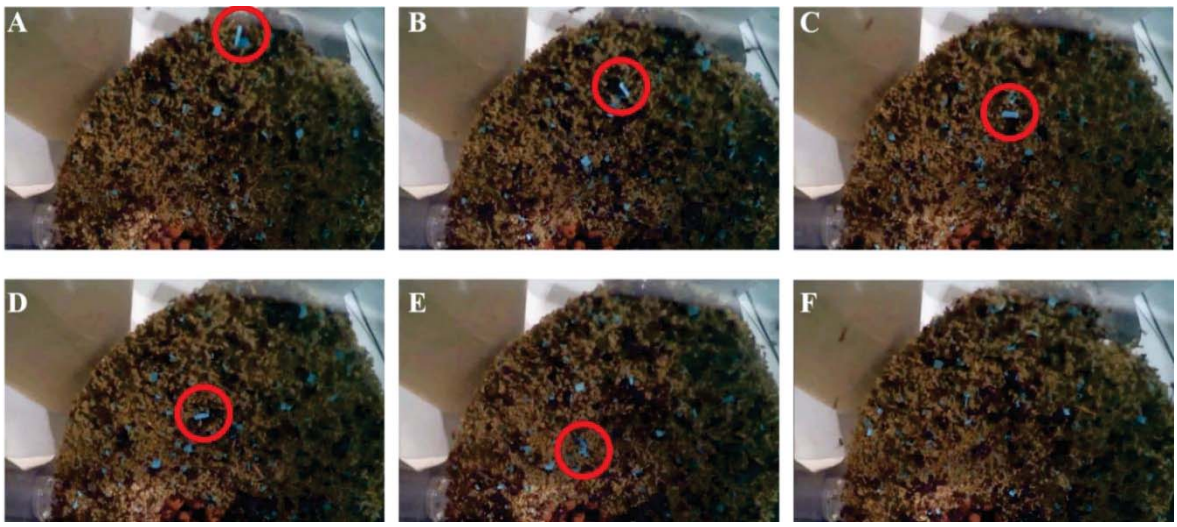

Fig. 16: Cylindrical waste chamber with top view. Tracking of a blue paper which is rolling down the pile. A-E: Tracking of a single blue piece in red circle. F: Blue piece not visible any more.

The movement of particles was monitored for a long time (weeks). Over time, the color of paper pieces was changed. Thereby, blue and orange particles could be monitored and tracked (Fig. 17 A-C). If leaf-cutting ants deposit waste particles randomly on top of the pile, distinct layers of one color should be formed (Fig. 17 E1). Because of the rolling down of particles, these layers could also be broadened (Fig. 17 E2).

However, the observed effect showed a complex mixture of colorful particles. These colorful particles were also found in deeper layers, which were already covered with older particles (Fig. 17 E3). This points towards stirring of discarded particles by ants even after weeks.

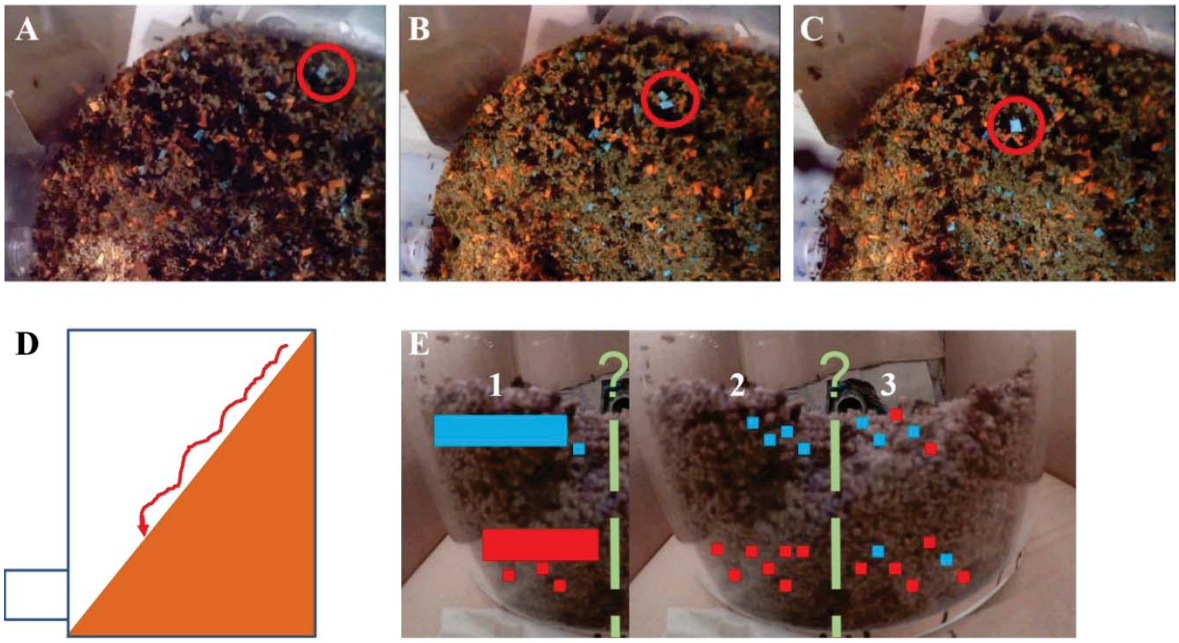

Fig. 17: Principle of passive rolling down. A-C: Tracking of another blue particle. D: Schematic drawing. E: Estimated layers of colorful paper pieces in waste piles. 1: Distinct sharp layers. 2: Distinct, but broadly mixed layers. 3: Completely mixed layers.

Further investigations showed, that in the middle or at the bottom of waste piles, there were holes visible. In time lapse videos, particles seemed to be “soaked” by these holes (Fig. 18 B, red arrow). The appearance of holes and disappearance of waste particles in the underground point towards tunnel systems in waste piles (Fig. 18 F). Presence of tunnels was mentioned before, but not investigated in more detail.[3, 14] Leaf-cutting ants were reported to translocate waste particles inside of holes in waste piles.

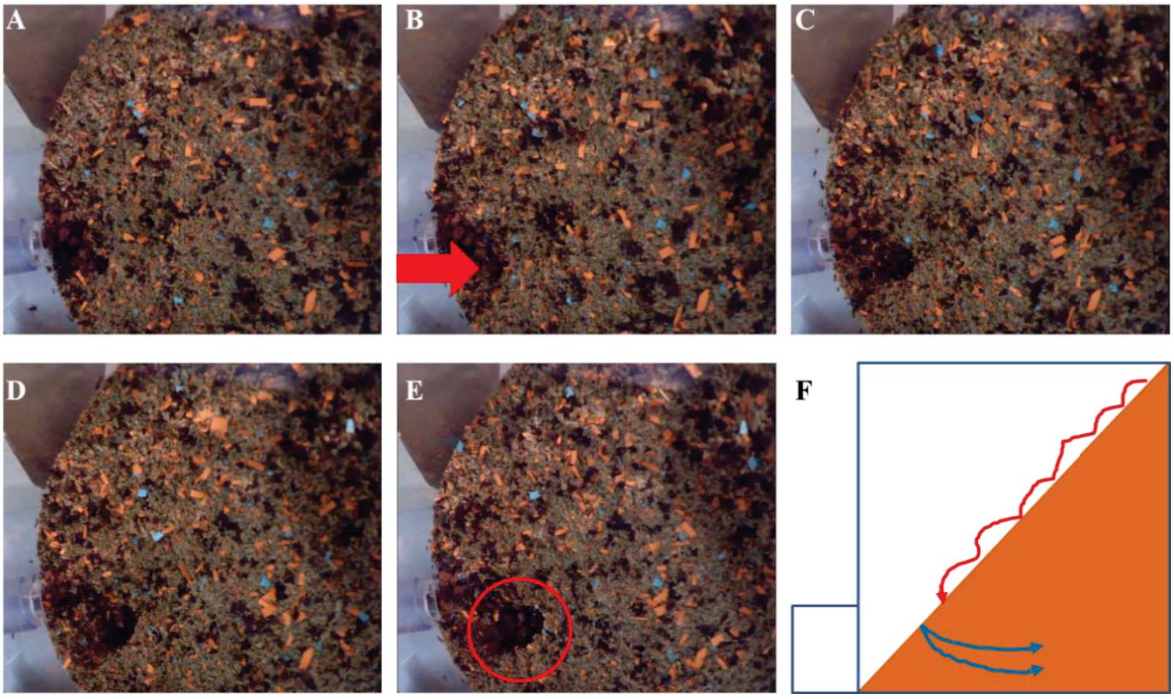

Fig. 18: Active deposition of waste particles in underground tunnels after passive roll down. A-E: Formation of a tunnel hole. F: Schematic overview with passive rolling down (red) and active transport into tunnel systems (blue).

Holes were not only observed in cylindrical waste boxes (Fig. 19 A), but also in the spherical waste box (Fig. 19 B). Looking sideways at cylindrical boxes, sometimes tunnel formation was visible. Because of the curved design, the observation of tunnel building was ineffective. Development of tunnels will be investigated in more detail with the long cross section box.

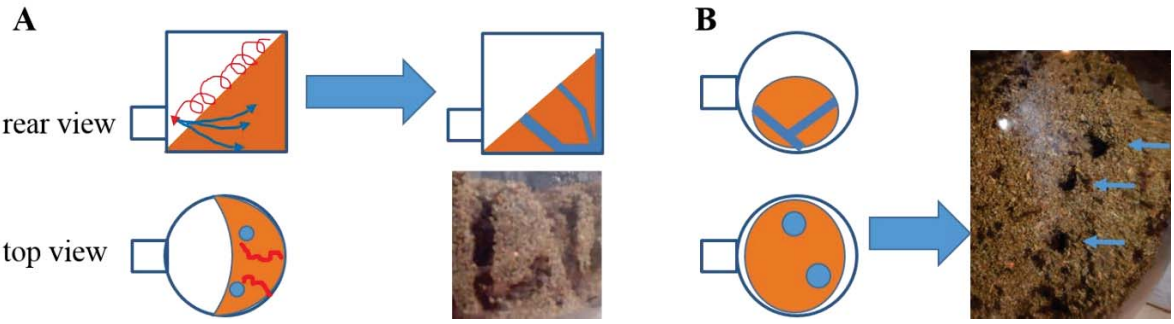

Fig. 19: Conclusion of hole formation in cylindrical (A) and spherical (B) waste boxes. Examples for tunnels (A) and holes (B, three blue arrows) indicated in pictures.

5.2.1.4.5 Development of tunnels in cylindrical waste chambers

Tunnel formation in cylindrical waste chambers was only visible at the outside. It was previously shown, that main amounts of waste particles rolled down the pile and were transported into holes at the lower part of the piles. Therefore, cylindrical boxes limited our possibilities to monitor effects below the surface.

Sometimes, tunnel formation took place at the outside (Fig. 20) and could therefore be monitored over time. From a closed surface, ants started digging directly into the waste pile

(Fig. 20 A-B). This tunnel was increased over time (Fig. 20 C-D), but was thereafter filled with waste particles again (Fig. 20 E-F) until the surface was covered with waste particles again (Fig. 20 G).

Besides this observation of temporary tunnel formation, there were permanent tunnels visible (compare Fig. 20 A and G). We were speculating about task oriented tunnel formation, using permanent tunnels for transportation and digging temporary tunnels for agitation, crushing of waste particles or removal of unwanted pathogens.

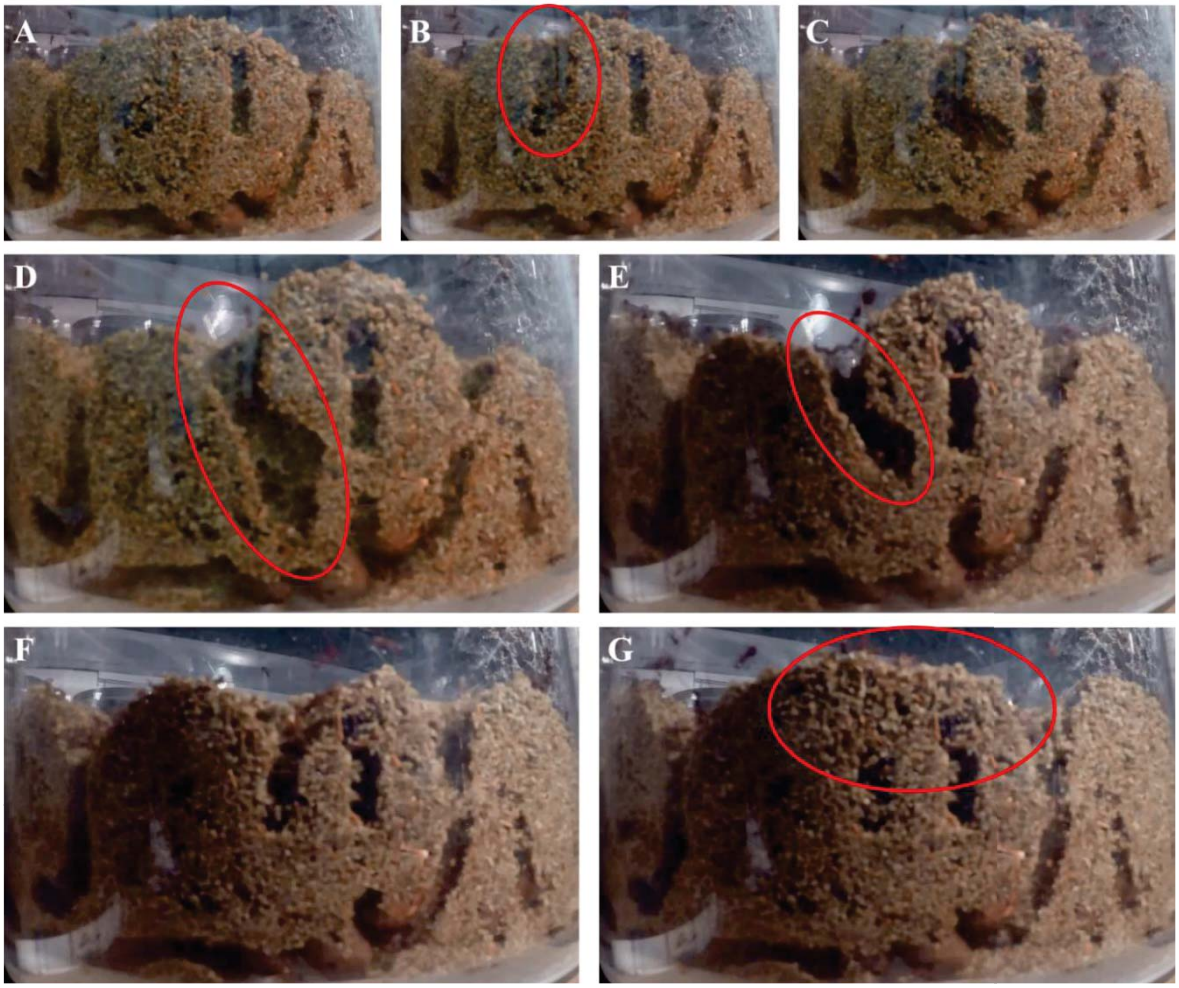

Fig. 20: Tunnel formation and turnover in a cylindrical waste chamber. A-G: Time lapse of the same waste chamber. A: Initial state. B: Formation of a new tunnel (indicated in red ellipse). D: Tunnel indicated at its maximum size. E: Tunnel is partially filled with waste particles. G: Former location of tunnel is covered with waste particles on top.

To describe the turnover of waste particles within waste chambers, the area was monitored with cameras. The cameras took time-lapse pictures, basically one picture every min. With a resolution of 16 megapixels, the cameras could take pictures for more than 20 days (microSD cards with 128 gigabytes storage) without being moved. Therefore, short term as well as long term effects could be observed.

Time-lapse pictures were converted to videos with 24 frames per second. This allowed to comfortably interpret data and saved storage, because conversion from *.jpg to *.mp4 reduced storage more than 99% without reduction of resolution. Rendering of 16 megapixel videos (4608*3456 pixels) down to 720p (1280*720 pixels; progressive) allowed to store data of two weeks only with around 80 megabytes instead of 64.000 megabytes.

To visualize changes over time, the surface and visible tunnels in waste chambers were marked with a digital pen. In order to differentiate between time points, colors were changed. The advantage of this differentiation will be obvious later.

As an example, the idea is shown in more details (Fig. 21). For the initial state, a green color was chosen (Fig. 21 A). Already after 4 hours (Fig. 21 B), a broad indention was visible while the tunnel at the right side was covered. 19 hours later, the upper layer consisted of many blue paper pieces (Fig. 21 C). After 6 hours, the waste chamber was even more filled (Fig. 21 D). Forwarding another 104 hours, the blue paper layer is obviously gone (Fig. 21 E). Furthermore, the waste chamber is even more filled but not as much as previously observed for a time frame of only 6 hours (Fig. 21 C to D; 6 hours; compared with Fig. 21 D to E; 104 hours).

This might indicate another effect, having not only a turnover of waste particles, but also compression over time to use the available space efficiently. This will be investigated in more detail.

Comparison of changes between Fig. 21 E and Fig. 21 F, which have only 40 min difference, showed major changes at the tunnel system at the upper parts close to the surface.

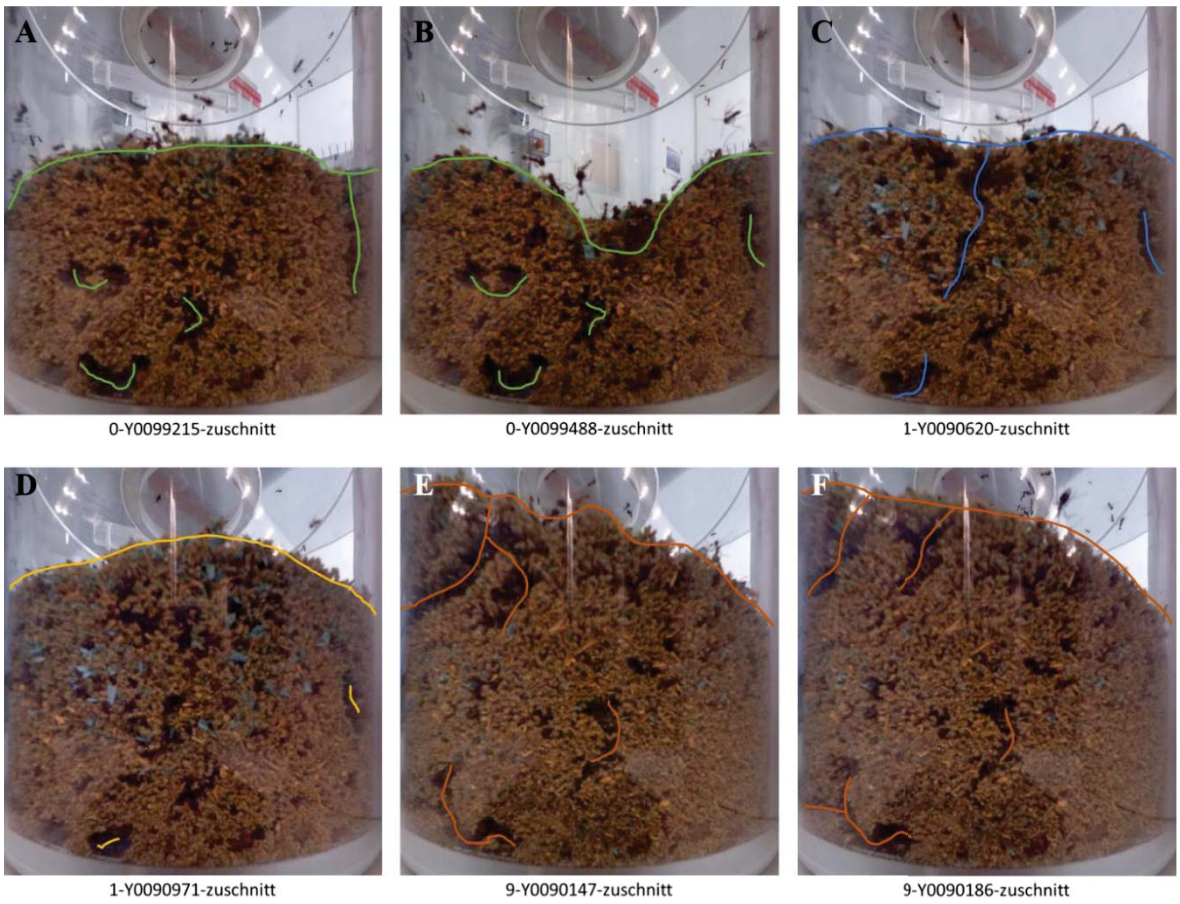

Fig. 21: Example of time resolved turnover of waste in a cylindrical box. Surface and tunnels indicated with colored lines. A: Start. B: 4 hours later. C: After 23 hours, fresh blue paper layer visible. D: After 29 hours. E: After 133 hours. F: After 133,6 hours; 40 min later than E.

To visualize changes within waste chambers over time, the drawings were uncoupled from the pictures. Background color was removed, therefore the *.png files could be overlaid and changes were visible (Fig. 22 A).

Because all lines had the same intensity, there was no differentiation between short and long term situations. To overcome that, transparency of every line was set to 5%. Now, every line had a lower intensity and when they overlapped, they aggregated their intensities and increased the overall contrast. This allowed to distinguish between short term (light color) and long term (intensive color) effects. This approach was used to visualize changes in waste chambers, because short time changes like temporary tunnel formation and permanent tunnels could be distinguished (Fig. 22 B). Effects on the surface of the waste piles were visible, too (Fig. 22 C).

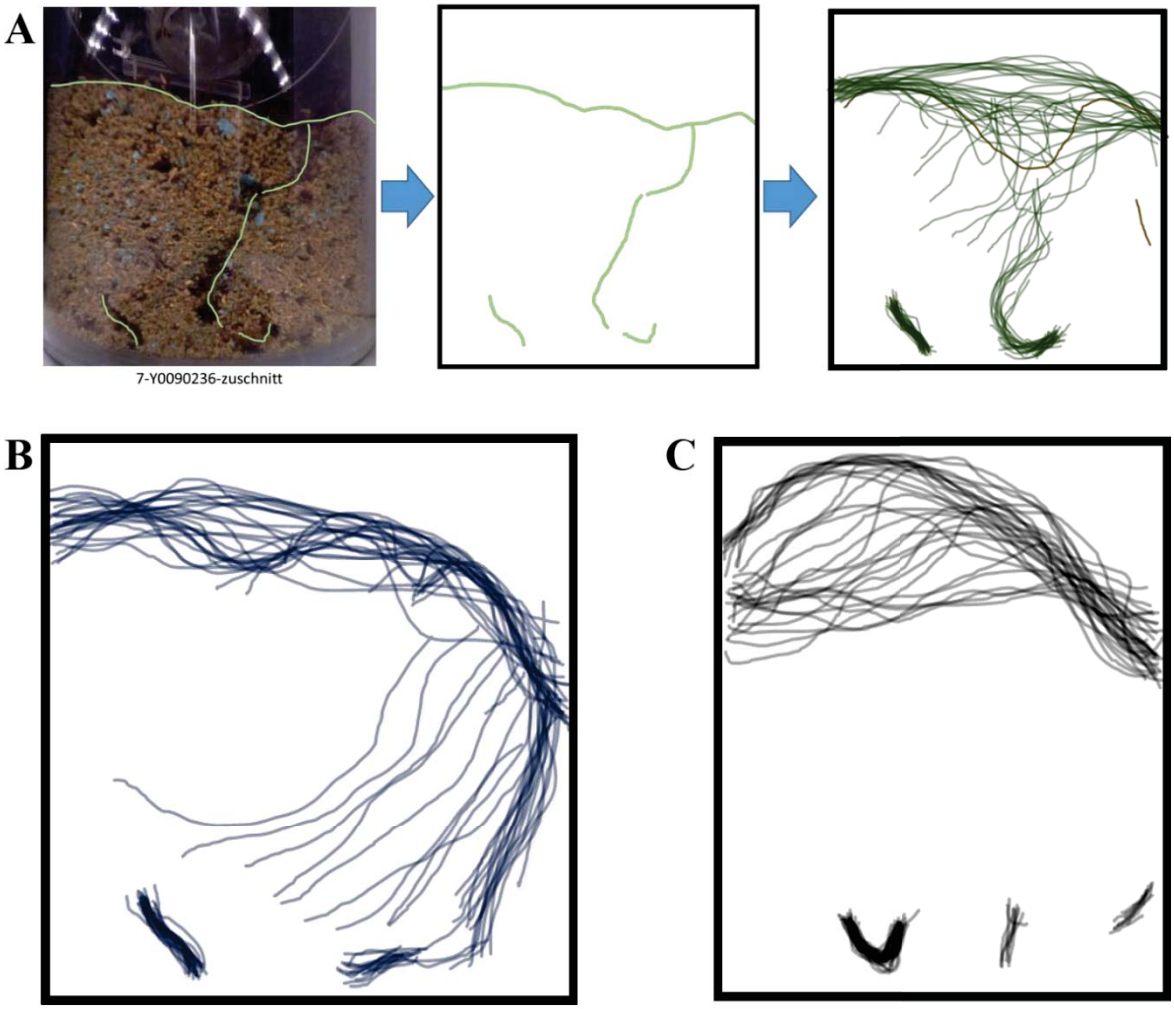

Fig. 22: Principle of data visualization for time resolved changes in waste chambers. A: Generation of drawings from pictures and overlay. B: Example for moving tunnels. C: Example for changes on the surface.

Following this visualization approach, several time-lapse observations were analyzed. Looking sideways at a waste chamber might explain why turnover effects were not studied in detail yet. In most cases, there were no noteworthy events (Fig. 23). In general, the deposit of waste particles led to a slightly fluctuating filling level.

For another dataset, there were digging activities visible between 9,5 and 27 hours (Fig. 24 B and C). Before and thereafter, again only fluctuating filling levels were visible (Fig. 24 A for before and D, E after the event). Unfortunately, this effect can only be observed by chance in cylindrical waste chambers.

It was shown before, that leaf-cutting ants deposited waste particles, which rolled down the pile, continuously inside of holes located at the lower part of the pile. Therefore, with some improvements, these effects will be investigated in more detail.

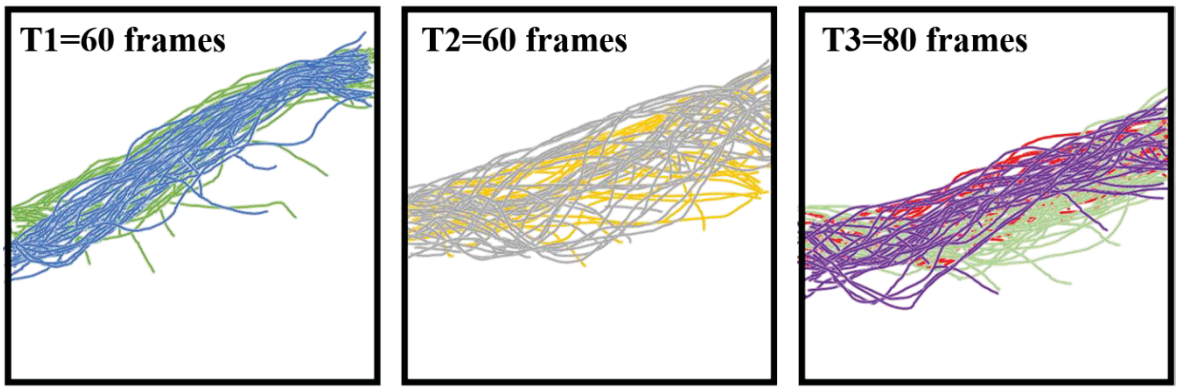

Fig. 23: Changes over time of a waste chamber monitored sideways for 100 hours in total (30 min per frame; dataset 151130-yi1-seitl).

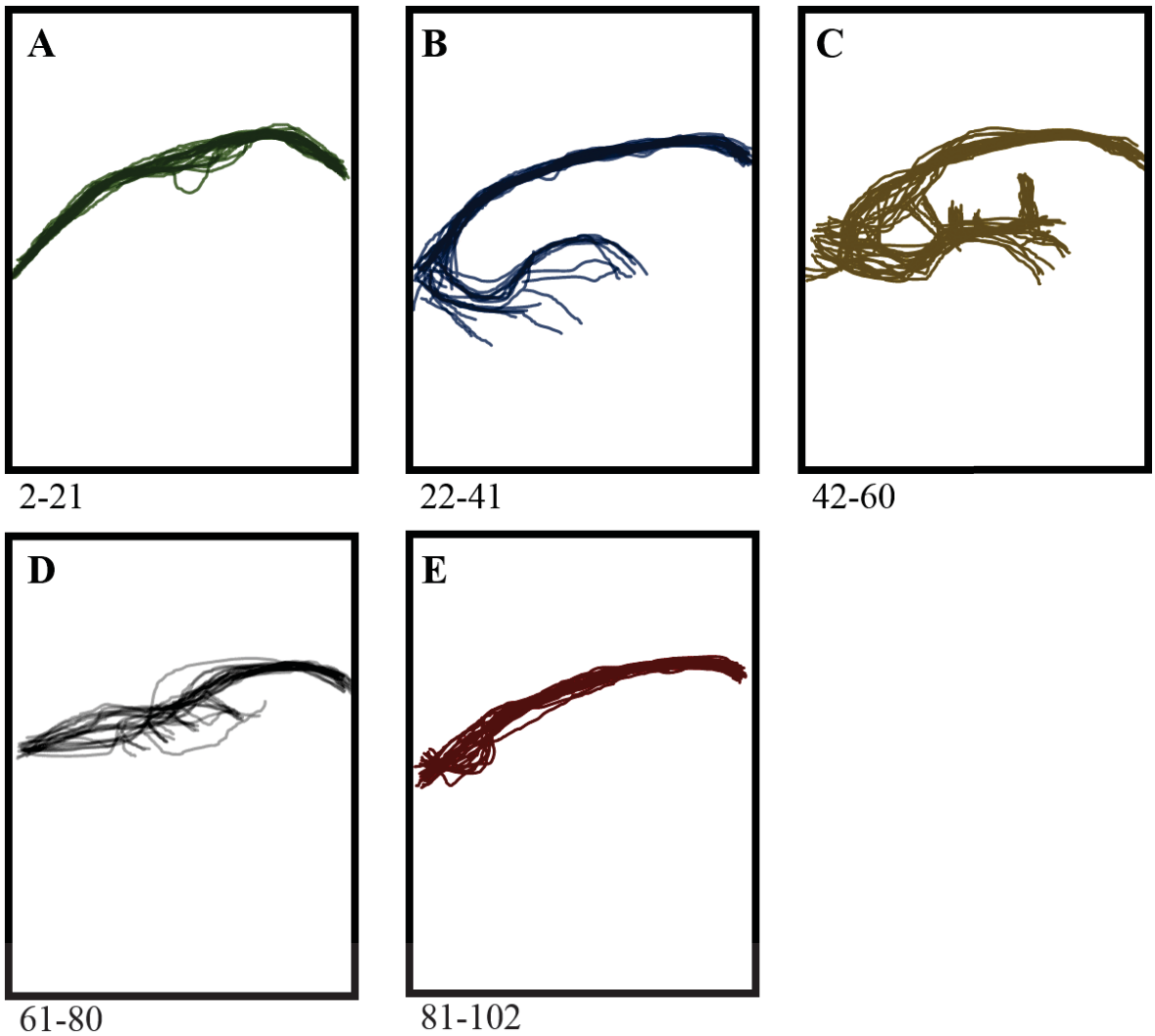

Fig. 24: Changes over time of a waste chamber monitored sideways for 52 hours in total (30 min per frame; dataset 151102-müllk-seitl-sj). A: 9,5hours. B: 9,5 hours. C: 9 hours. D: 9,5 hours. E: 10,5 hours.

Looking from the backside at a waste chamber, especially fluctuating filling levels were determined at the upper part nearby the surface (Fig. 25). Tunnel formation was observed only for short time ranges (Fig. 25 B), but permanent tunnel systems were visible in the lower part of the waste pile (Fig. 25 C-G).

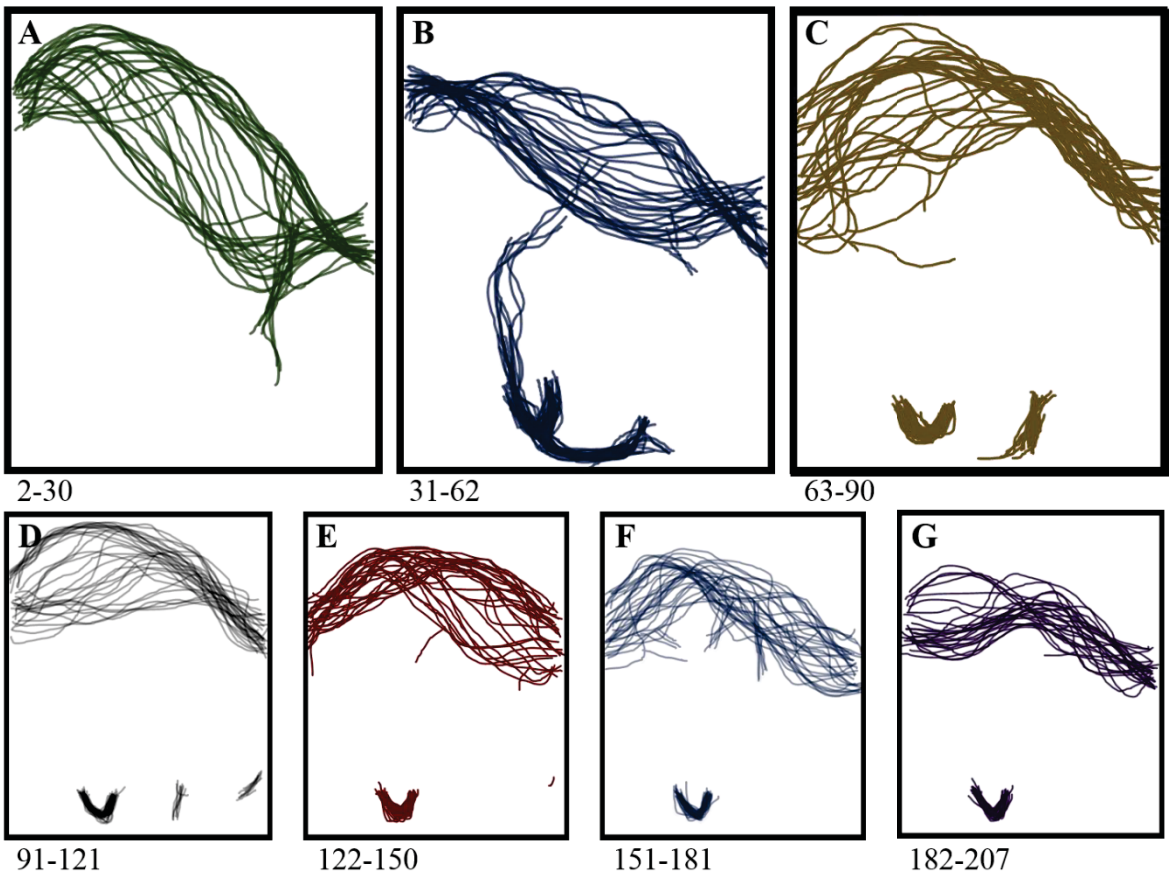

Fig. 25: Changes over time from the backside of a waste chamber monitored for 104 hours in total (30 min per frame; dataset 151130-yi0-hinten). A: 14 hours. B: 15,5 hours. C: 13,5 hours. D: 15 hours. E: 14 hours. F: 15 hours. G: 12,5 hours.

Again, there were not only steady examples, but also waste chambers with very intense turnover. High fluctuation rates at the upper surface were visible by formation of indentations/cavities (Fig. 26, especially visible in A, B, D). These depressions were thereafter refilled, as showed before with fresh waste particles (Fig. 21 C compared to B). Parts of permanent tunnels were visible again nearby the lower left corner. The formation of tunnels was visible starting mainly from the surface (Fig. 26, especially visible in F-H). Movements of tunnels themselves was observed between frame 191 and 215 (Fig. 26 H). Depending on colony size and connection time of waste chambers, there was a saturation of waste intake into chambers observed. Leaf-cutting ants did not leave full waste chambers, but there were less ants visible and they reduced their digging and turnover activities. Furthermore, translocation of waste material from old to new waste chambers was observed, but not further investigated.

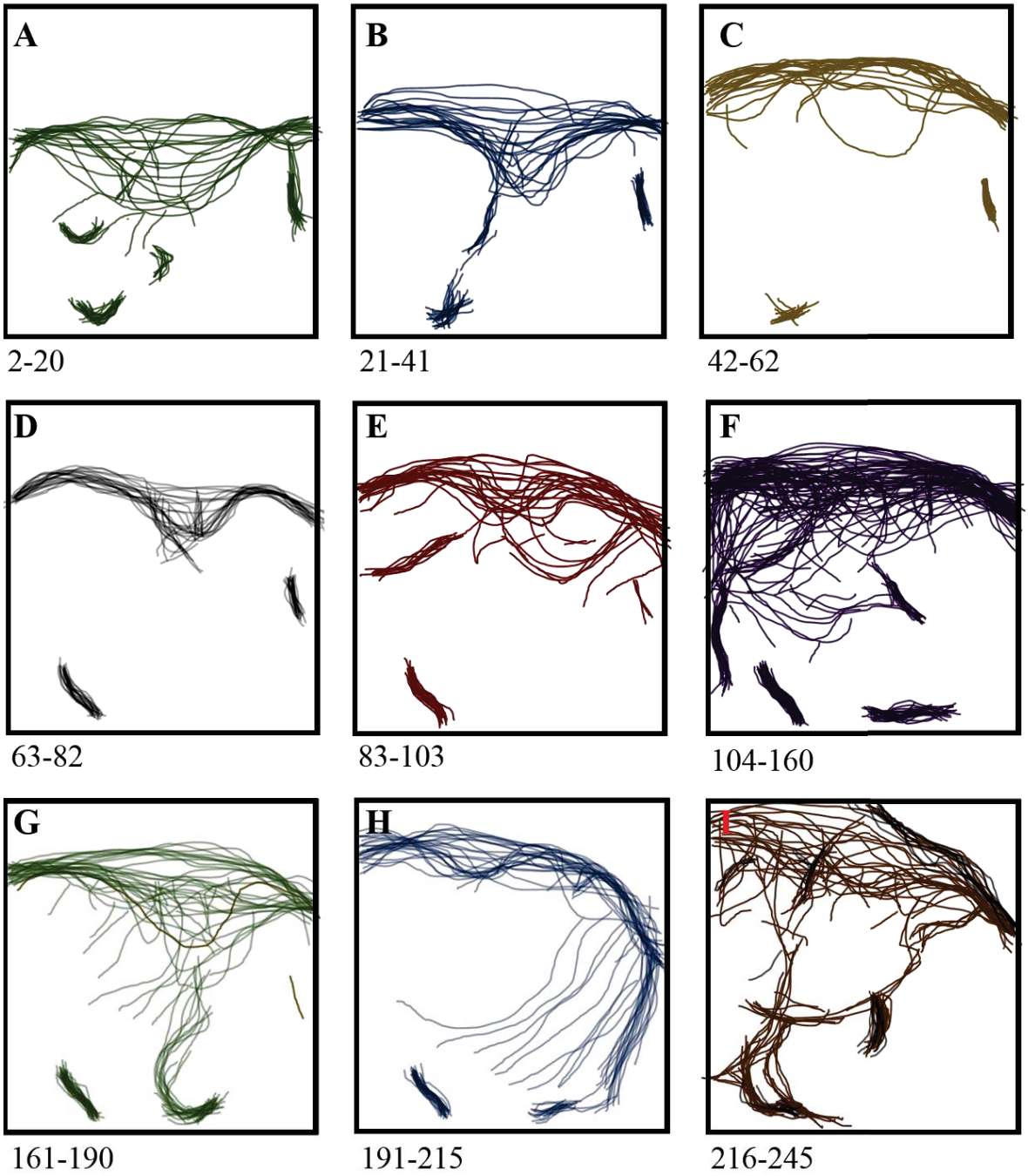

Fig. 26: Changes over time from the backside of a waste chamber monitored for 122 hours in total (30 min per frame; dataset 151030-müllk-seitl). A: 9 hours. B: 10 hours. C: 10 hours. D: 9,5 hours. E: 10 hours. F: 27 hours. G: 14,5 hours. H: 12 hours. I: 14,5 hours.

5.2.1.4.6 Improvements for monitoring target oriented rearrangement of waste management behaviour

To be able to generate data to investigate the already described effects, we developed a long, but tight rectangular box. In theory, this box would mimic a cut-out as indicated within the pile of a cylindrical box (Fig. 27 A). Indeed, we observed the formation of a pile as predicted and could monitor tunnel formation on the complete side of the box (Fig. 27 B).

On the one side, the long chamber consisted of a clear glass surface, which allowed a clear view. On the other side, there were holes applied which were covered by plastic caps. Through these plastic caps, modifications could be applied. For example, combined temperature-humidity sensors were applied and connected to a Raspberry Pi system (Fig. 27 C). With this system, every sensor was read-out in 5 min intervals.

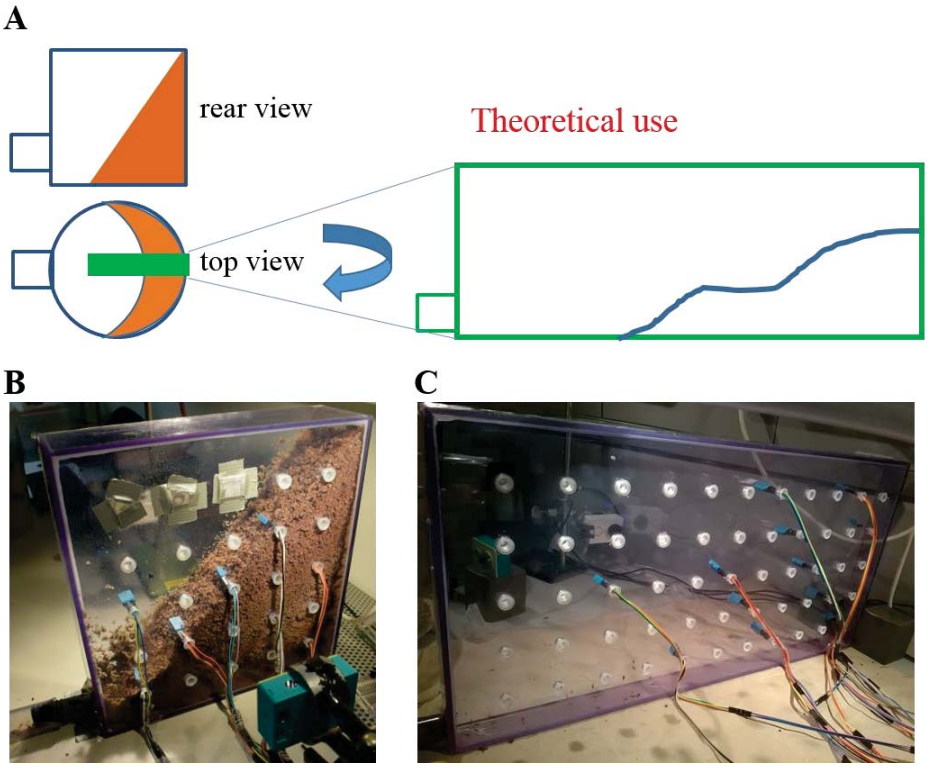

Fig. 27: Improved waste chamber with long and tight rectangular shape. A: Desired cut out indicated as green box, with the theoretical filling of waste in the novel box. B: Picture of already filled long box with camera and sensors. C: Empty long waste chamber with applied sensors.

The start of waste deposit in the long chamber was already shown (Fig. 12; p. 24).

Both sides of the long tight chamber were observed permanently. Waste piles were clearly visible at the glass surface (Fig. 28 A). Again, the surface of waste piles and tunnels were drawn by hand. Overlays of these images resulted in schemes indicating changes inside the chamber (Fig. 28 B, C).

To differentiate between short term and long term events, transparency of frames was increased. Therefore, short term events resulted in light color and long term events in lines with higher contrast (Fig. 29).

Tunnels were most often started on the flat top or at the bottom of pile slopes. In the following chapters, MATLAB scripts together with manual drawings will be used to describe effects inside of long tight waste chambers.

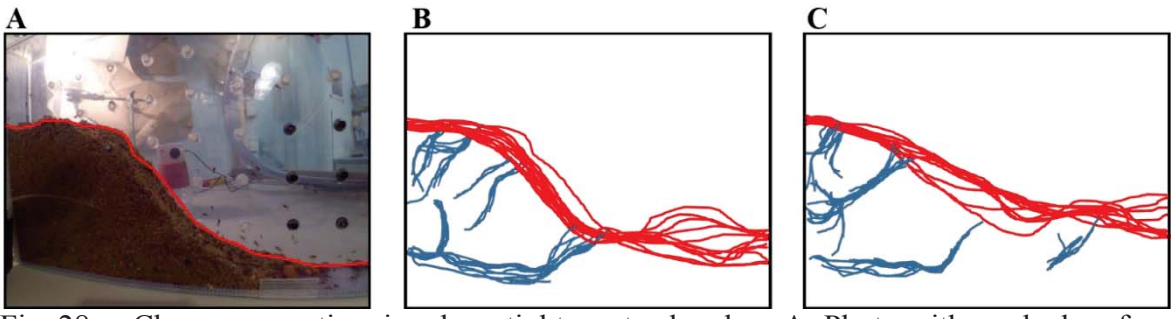

Fig. 28: Changes over time in a long tight waste chamber. A: Photo with marked surface (red. B, C: Frames with indication of tunnels (blue) and surface (red). Frames in C are follow ups of B. (dataset: 160211-langek-klar)

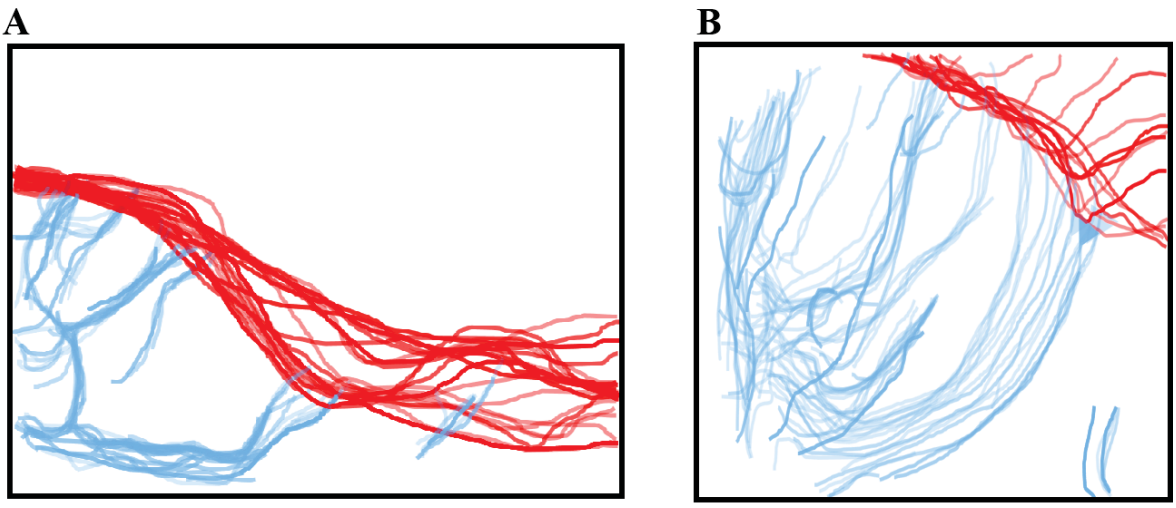

Fig. 29: Changes over time with contrast indication inside of a long tight waste chamber. A: Formation of tunnels (blue) and changes of surface (red) in a several days old chamber. Combining the dataset of Fig. 28 B, C. (dataset 160211-langek-klar). B: Formation of tunnels (blue) and changes of surface (red) in the left side of a longer connected waste chamber (magnified interesting area; dataset: 160129-langek-klar).

5.2.1.4.7 Introduction of MATLAB scripts for video processing

To generate drawings of tunnel formation and turnover automatically, a MATLAB script was adapted by Antonin Sulc with the aim to produce such graphs.

The output of the script consisted of three areas (Fig. 30 A). The initial video was shown in window 1, while window 2 showed a processed overlay of the defined number of pictures (parameter ws). In window 3, the differentiation pattern should show a contour graph to determine location and size of tunnels and to estimate the overall turnover activity. As an example, the corresponding manual drawing has at least a certain similarity, but the MATLAB pattern showed dominant background noise (Fig. 30 A3 and B3).

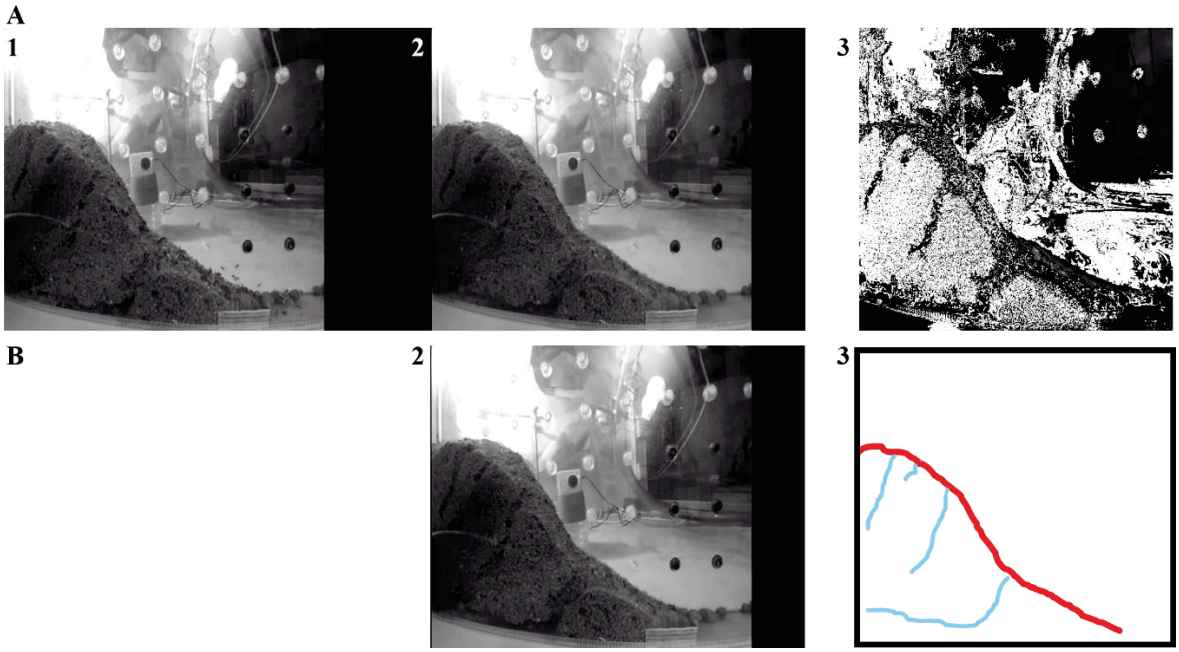

Fig. 30: Comparison of MATLAB processed data (A) and manual drawing (B). 1: Original video frame. 2: Processed overlay frame. 3: Calculated (A) or drawn (B) differentiation pattern.

As mentioned before, processing of available videos with MATLAB requires powerful computer systems (Ch. 5.2.1.3.6; p. 17). Furthermore, videos were only processed in greyscale instead of colored, because otherwise every pixel would contain more information (RGB) and increase processing time exponentially.

Downsampling of the videos was necessary because of the consumption of random access memory, which limited the calculations (Code 5; line 6). The reduction of pixels led to a loss of information and imprecise views (Fig. 31), I therefore only used high numbers (up to 16) for fast screenings and factor 1 (no downsampling) or 2 for result videos.

Parameters like WS and lambda needed to be adjusted for every video file (Code 5; line 4-5). The lambda parameter influences the granularity of changed areas (Fig. 32). If the parameter is too low, some pixels of ant bodies are not recognized. If the parameter is too high, the pile movement might be not visible (Fig. 32 B).

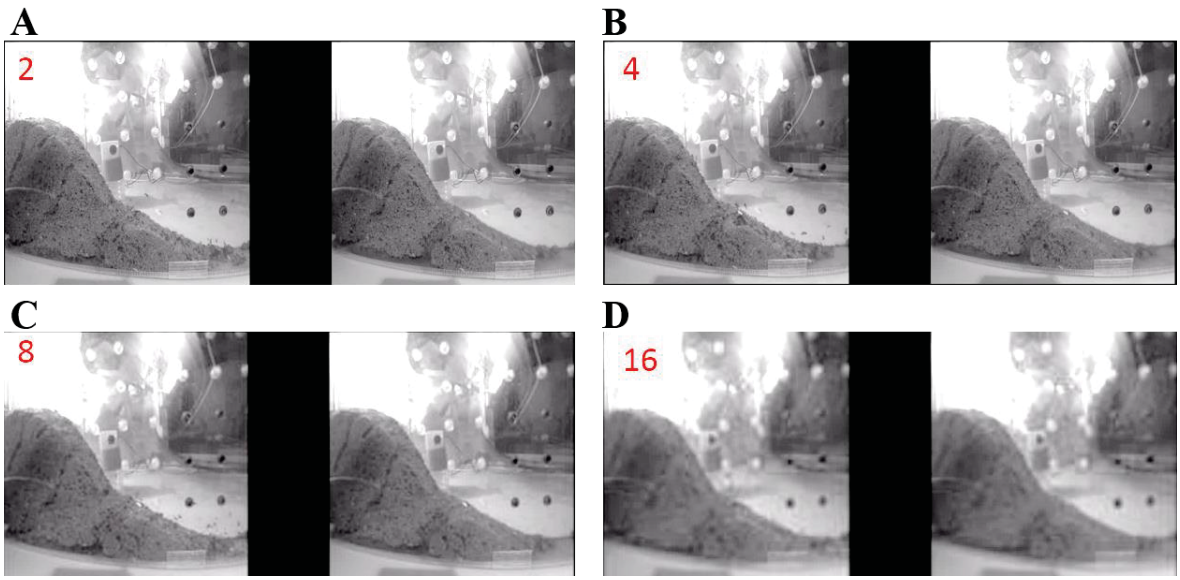

Fig. 31: Reduction of video/image resolution by downsampling with the factor 2 (A), 4 (B), 8 (C) and 16 (D).

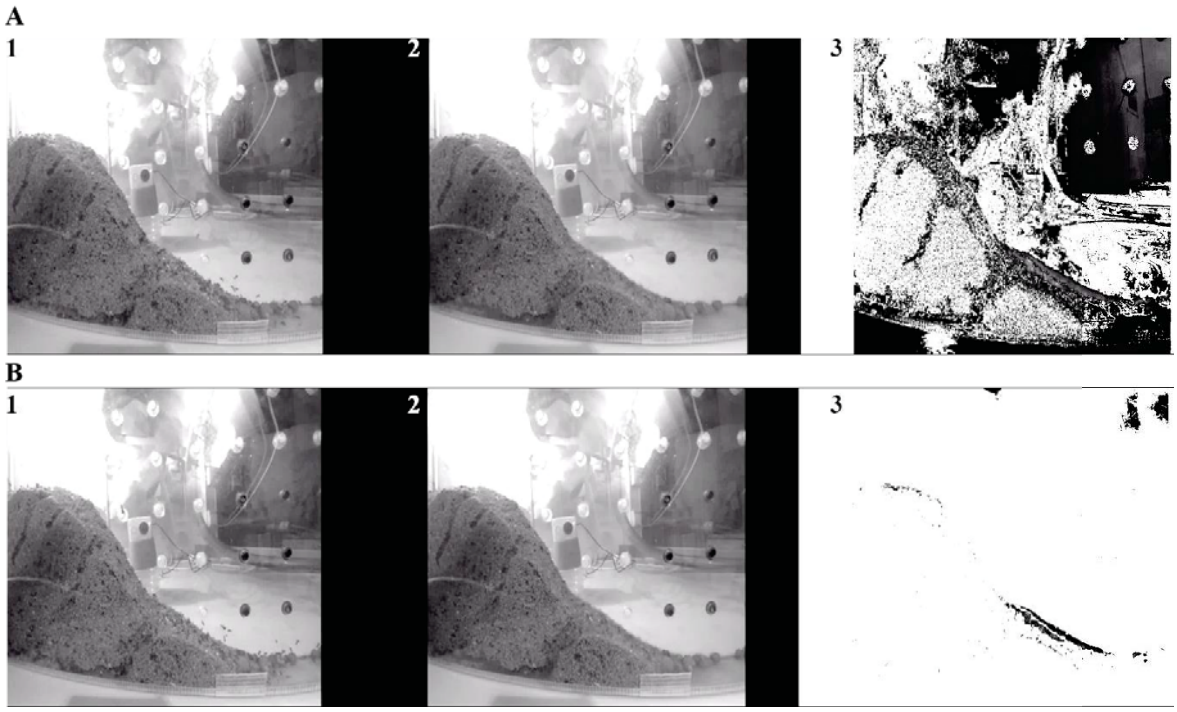

Fig. 32: Comparison of two lambda settings. The resulting differentiation patterns (3) differed in their granularity. A: WS10; lambda0,005; downsample2. B: WS10; lambda0,05; downsample2. (Dataset 160209-langk-1000f; position 15 seconds).

The WS parameter influences the number of frames, which were taken for picture differentiation. If the WS parameter is too low, ant movement is visible, if the parameter is too high, the pile movement is fragmented. The WS parameter was adjusted for every movie by try and error, best results were obtained with parameters between 5 and 10 (Fig. 33).

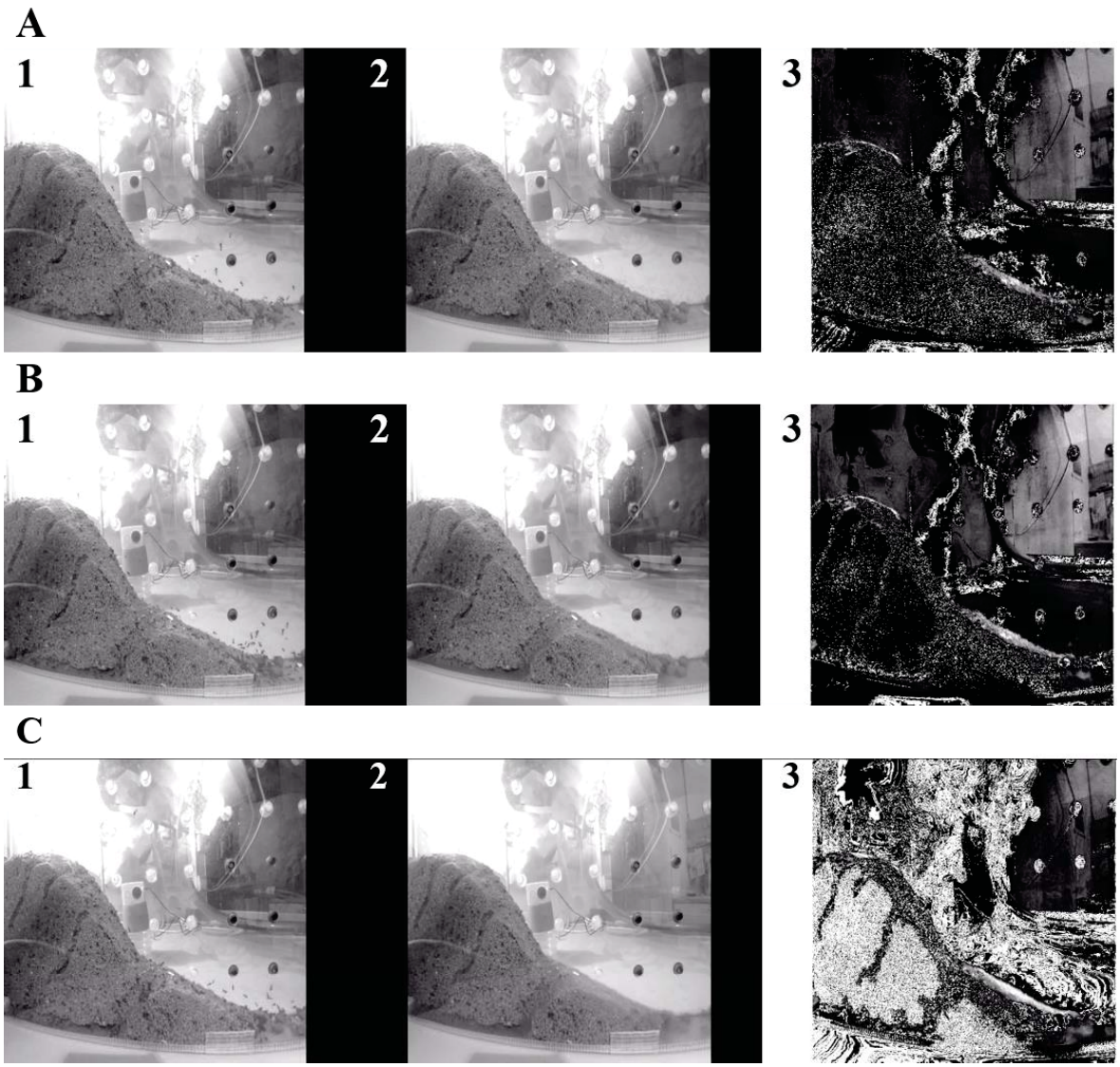

Fig. 33: Altered frequency led to either loss of information by generation of random noise (A3) or generation of heavy background artefacts (C3). A: WS50; lambda0,002; downsample2. B: WS10; lambda0,002; downsample2. C: WS1; lambda0,002; downsample2. (Dataset 160209-langk-1000f; position 26 seconds).

After determination of suitable settings for the variable parameters, I compared the resulting patterns with manual drawings or optical impressions. While there was a flickering visible, mainly caused by frequencies of light sources, the algorithm itself seemed to generate artefacts.

To show one distinct example, there was a differentiation pattern visible after about 75 frames (Fig. 34 A3) which did not fit to the waste pile because there were no tunnels at all visible (Fig. 34 A2). The unique pattern fitted to the tunnel systems of the waste pile after about 550 frames (Fig. 34 B2; indicated by arrow). It remains unknown, which circumstances led to the creation of artefacts.

Because of high background noise levels and creation of artefacts, the differentiation patterns were not used for further analysis. The idea behind and possibilities of valid graphs will be

discussed. Whether the flickering could be reduced by better light sources and camera sensors, was not tested. All tested light sources, such as light bulbs, halogen spots, neon tubes and LED products had their advantages and disadvantages. Besides flickering, there were production of heat (halogen spot), reduced contrast and falsified colors (neon tubes and LED). A high quality light support together with a backplane shield might result at least less random noise.

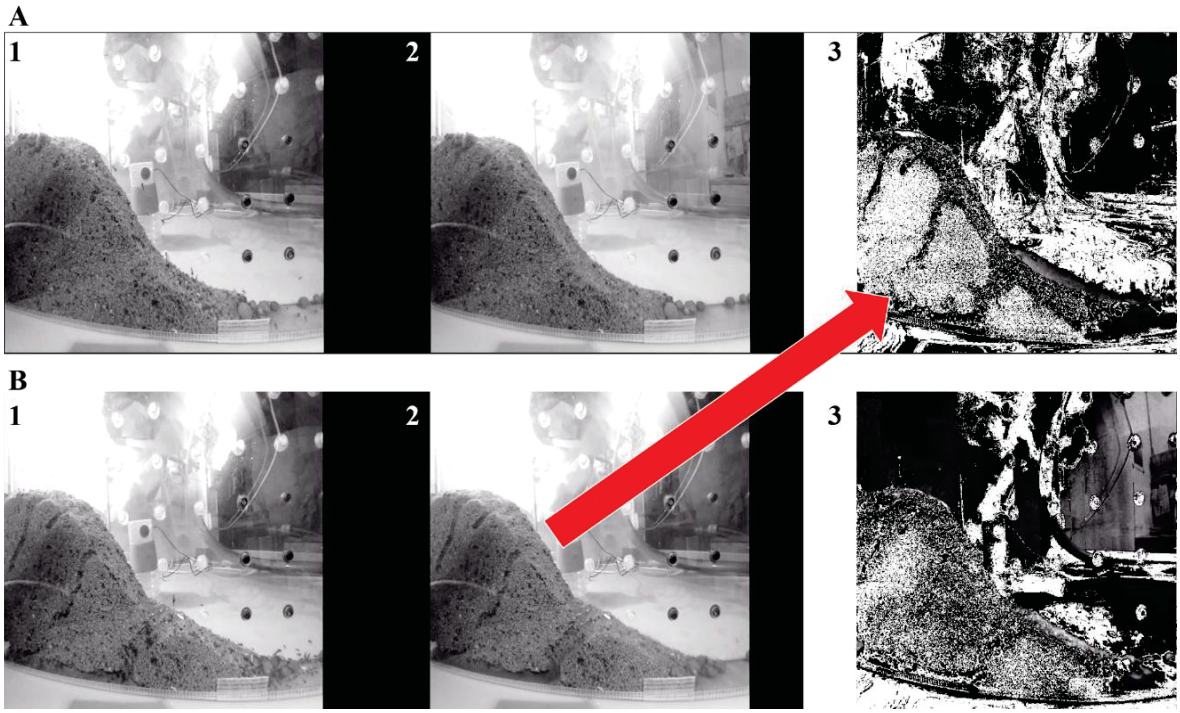

Fig. 34: Artefact generation by the algorithm. Differentiation patterns A3, taken after 3 seconds, matched to the tunnel pattern after 23 seconds (Dataset 160209-langk-1000f-ws10.005-2).

5.2.1.4.8 Description of influencing parameters for tunnel formation and elongation

As mentioned before, there were time ranges with less activity and time ranges with higher activity inside of waste chambers. Therefore, there are several types of videos and only partially interesting moments therein.

On the following pages, I will focus on only some few processed videos to present evidence pictures for observed effects. A compilation of all effects will be given as a conclusion later, because the complex chronology of effects request a differentiated scheme.

As shown for cylindrical waste chambers, waste particles roll down the pile and are translocated in tunnels at the lower part of the waste pile. Starting with a closed surface of waste particles (Fig. 35 A), the ants dug a tunnel with an angle of about 45° (Fig. 35 B). The front of this initial tunnel seemed to stay untouched for 10 hours, but indeed the opening moved from left of the black plug 3 cm to the right (Fig. 35 B-E) and ant movements at least

indicated some underground activity. For some reason, prolongation of the tunnel happened in the following 10 hours (Fig. 35 F-H).

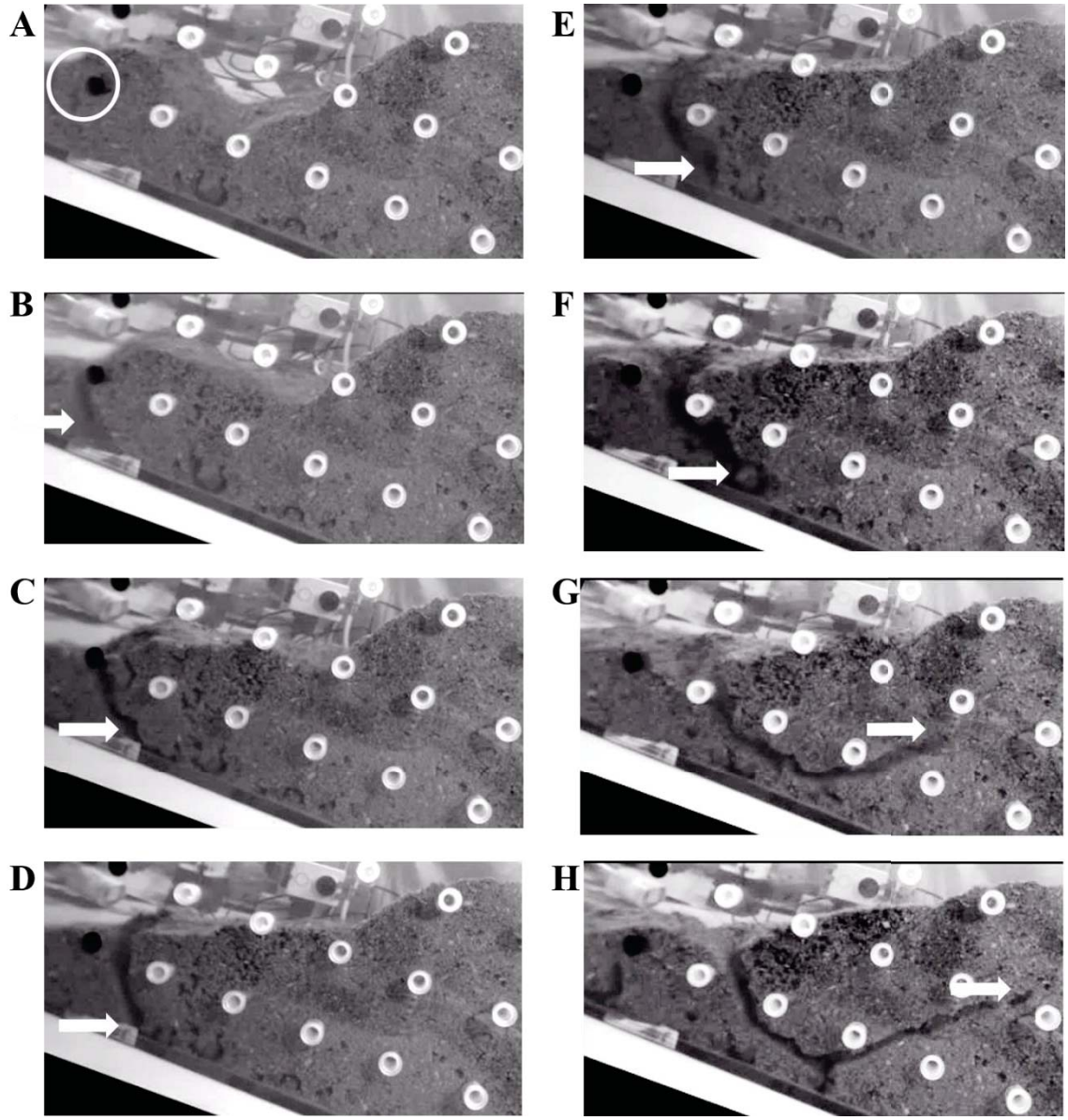

Fig. 35: Generation of a permanent transportation tunnel, monitored for 24 hours. Circle: Complete covered with waste particles. Arrows: Front of tunnel formation activities. A: Start. B: 4 hours. C: 8 hours. D: 12 hours. E: 14 hours. F: 16 hours. G: 20 hours. H: 24 hours. (Dataset 160209-langek-zuro2-ws10.002-3-pr).

The overall process of tunnel formation from starting to its first end took about 8 hours for a distance of 17,5 cm (Fig. 36 A). The same tunnel was prolonged some hours later to reach the top of the waste pile (Fig. 36 B). Digging the distance of 10,5 cm took them again about 8 hours.

Calculation of digging speeds yield 2,2 cm/hour (Fig. 36 A) and 1,3 cm/hour (Fig. 36 B).

In comparison to another digging activity from inside of the waste pile, the digging speed was determined with 5,4 cm/hour (Fig. 37 A). The starting point is marked with a dot and

the tunnel route indicated with a line (Fig. 37 A4), the tunnel started on the other side of the waste chamber and was connected to another, already existing, tunnel.

As a combination of both, tunnel formation from the surface and underground prolongation, another video was analyzed. In this case, there was a temporary digging activity (Fig. 37 B1) which moved to the left side and was used as a starting point for tunnel formation (Fig. 37 B2).

At first, the tunnel was prolonged with a speed of 4 cm/hour (Fig. 37 B3). But thereafter, tunnel prolongation took place with a speed of 9,8 cm/hour (Fig. 37 B4).

In summary, observed prolongation speeds for permanent tunnels ranged between roughly 1 and 10 cm/hour. The importance of influencing factors, such as ant activity, diameter of tunnels, particle size and digging purpose, can only be estimated.

With changes in the differentiation patterns of MATLAB processed video, one could estimate the overall activity and the activity within one tunnel. In theory, there must be a difference between one ant digging slowly, an optimal number of ants digging most effective and too many ants digging, which disturb each other. With such a parameter, one could maybe calculate an average or normalized speed.

The diameter of tunnels is important, because this limits the number of ants therein. Furthermore, it is still unknown whether every tunnel prolongation required removal of waste particles or if waste particles were only broken down and released with less space required. Indeed, for some tunnels ants were observed to transport particles out of the tunnel, but most of the time there was tunnel formation and influx of ants with waste particles (personal detail observations). The change of waste particle size will be discussed later (Ch. 5.2.1.4.9).

One digging purpose is of course the turnover of fresh waste particles. Another purpose is the observed permanent transportation of waste particles into the waste pile. As a third factor, the defense against pathogens will be discussed later (Ch. 5.2.1.4.10).

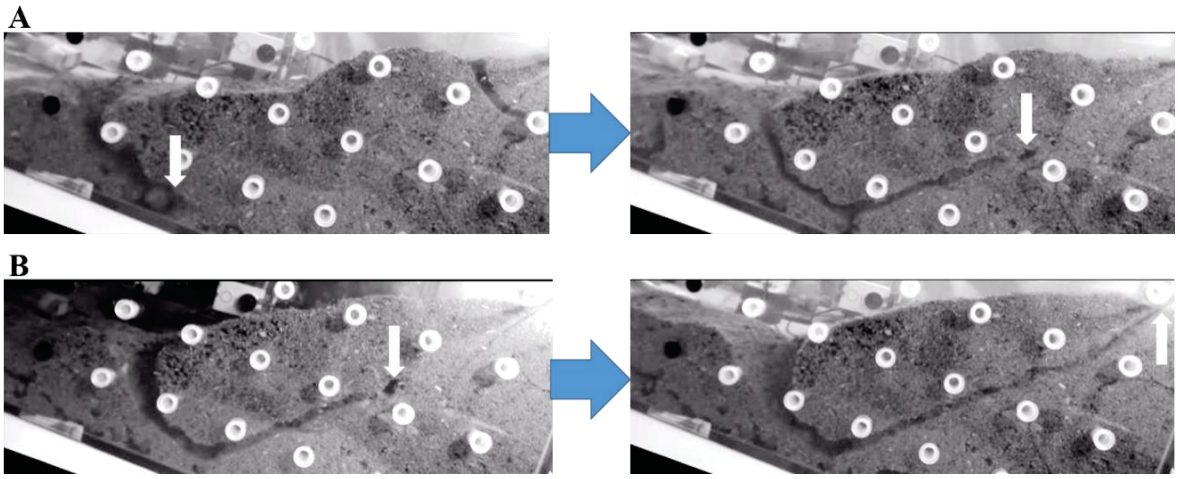

Fig. 36: Determination of tunnel building kinetics. Arrows: Front of tunnel formation activities. A: Formation of a tunnel with a length of 17 cm in 8 hours. B: Elongation of the tunnel after several hours with a distance of 10,8 cm in 8 hours. (Datasets 160209-langek-zuro2-ws10.002-3-pr and 160209-langek-zuro3-ws10.002-3-pr).

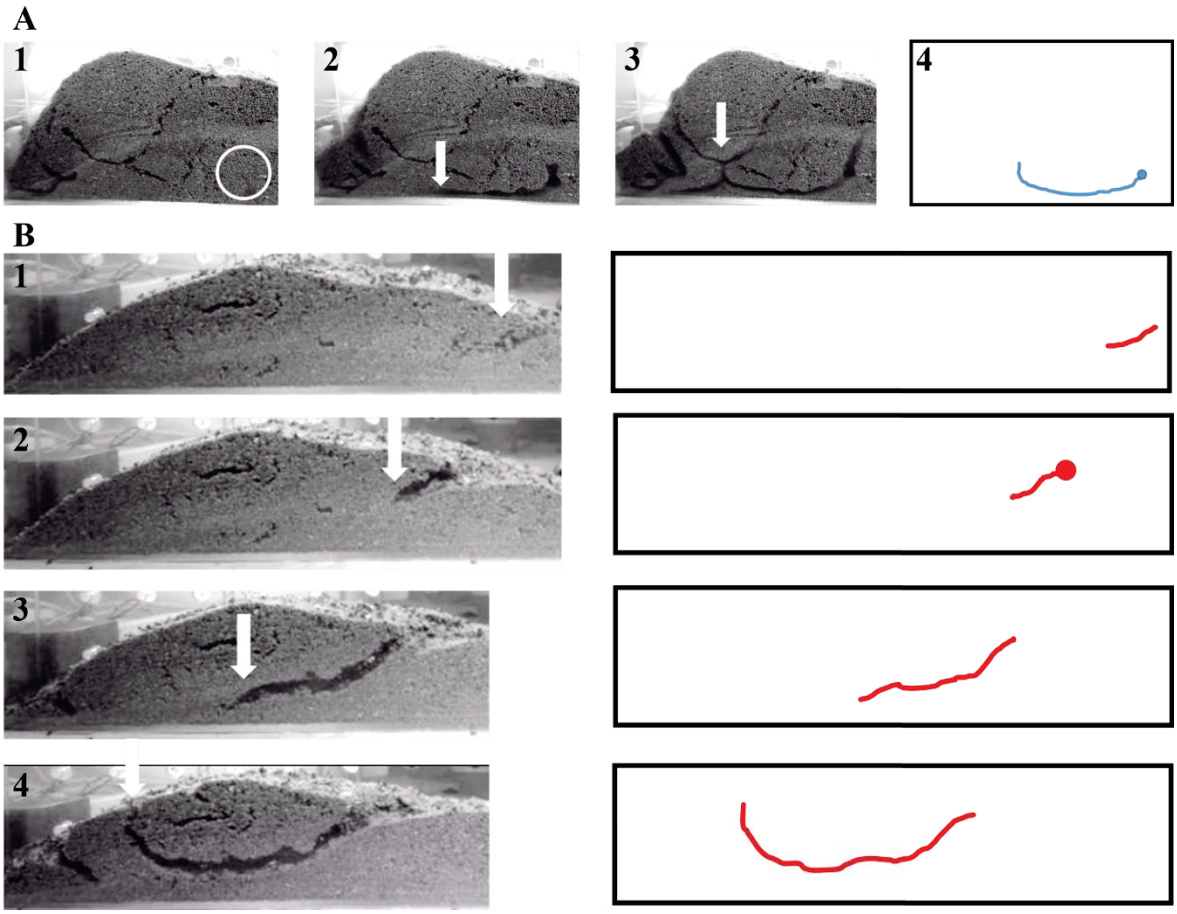

Fig. 37: Determination of starting points for the observation of tunnel development. A: Tunnel formation starting in the waste pile. B: Tunnel formation starting on top of the pile. A1: Start. A2: 2,4 hours. A3: 1,6 hours. B1: Start. B2: 1,6 hours. B3: 3,2 hours. B4: 1,2 hours. (Datasets A: 160223-langk-kl-links-4-5-ws10.002-2 B: 160331-langek-klar-zuschnittrot0-ws10.002-3.)

Temporary short tunnels at the surface were already described before, they were especially observed for areas containing fresh waste material. In this case, the complete tunnel was

moved with a speed of about 5 cm/hour (Fig. 38). Temporary tunnels were generally not visible in the MATLAB processed videos, when they were operated with a WS>10. The tunnels move too fast and are therefore removed, similarly to the intended removal of ant movement.

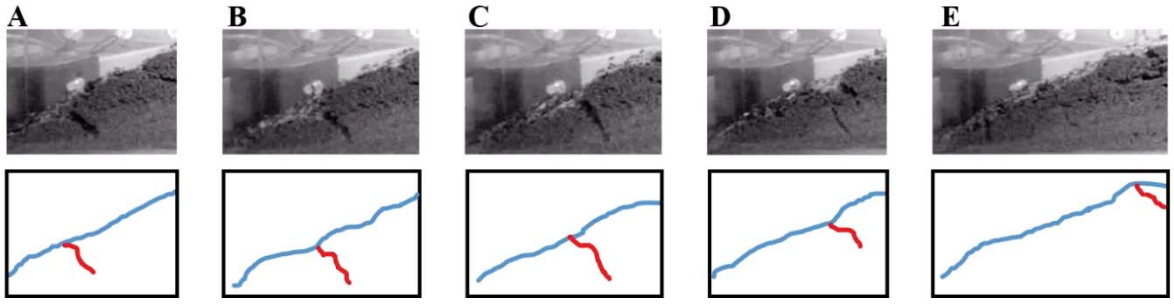

Fig. 38: Temporary tunnel formation as part of a surface turnover. A-E: Each taken after 20 frames (frame distance: 1 min; dataset 160331-langek-klar-zuschnittrot0-ws10.002-3; 0-5 sec).

Besides permanent tunnels, which are used for several days, there are also short term transportation tunnels, which were dug and used but filled up again within one day. Starting with a closed surface of waste particles (Fig. 39 A), ants started digging a tunnel with the length of about 10 cm in 8 hours (Fig. 39 B-E). The shape of this tunnel did not change for 24 hours (Fig. 39 E to F), but thereafter it was prolonged to the surface (Fig. 39 G, H). The new part of the tunnel was filled with waste particles again (Fig. 39 I), 6 hours later the complete tunnel was gone (Fig. 39 J).

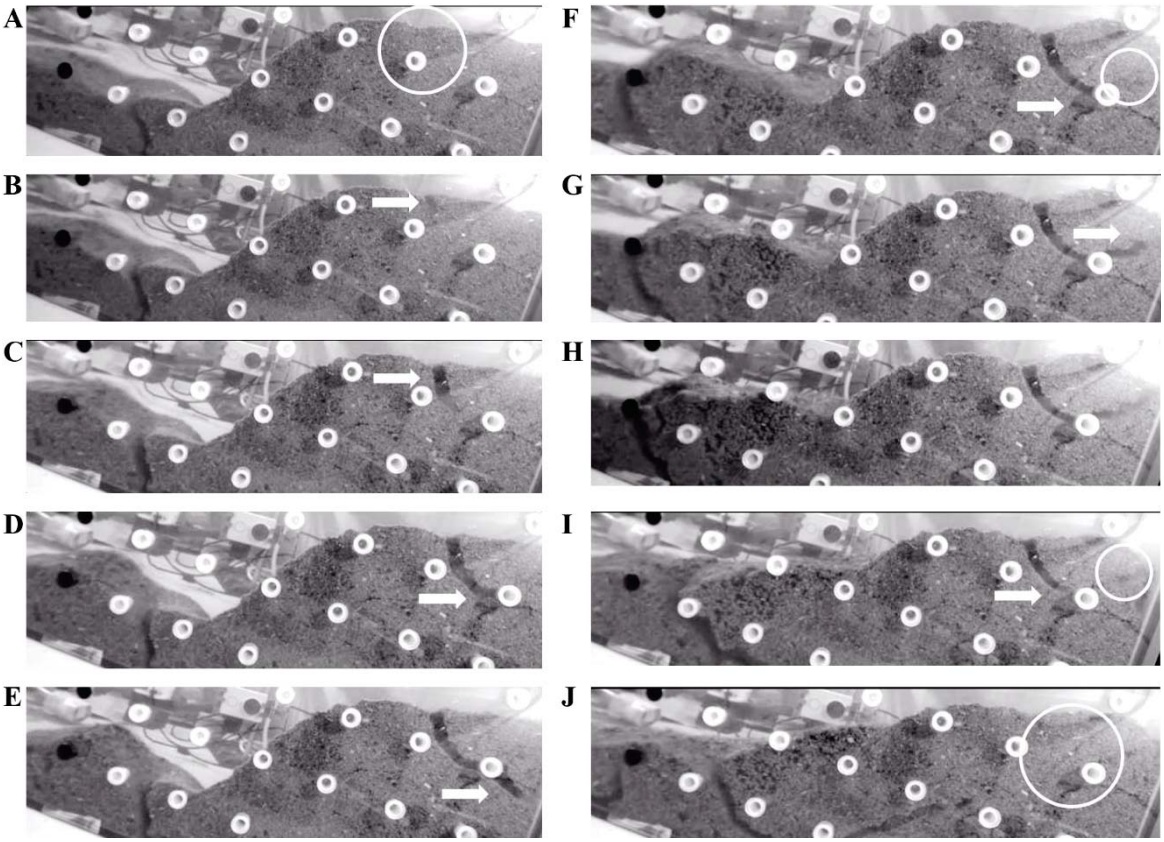

Fig. 39: Tunnel formation followed by a fill up, monitored for 48 hours. Circles: Complete covered with waste particles. Arrows: Front of tunnel formation activities. A: Start. B: 2 hours. C: 4 hours. D: 6 hours. E: 8 hours. F: 32 hours. G: 34 hours. H: 36 hours. I: 42 hours. J: 48 hours. (Datasets 160209-langek-zuro2-ws10.002-3 and 160209-langek-zuro3-ws10.002-3).

Observations over a long period (several weeks) yielded different results. Fresh waste chambers reached a certain filling level within two days, thereafter the filling level seemed to be nearly constant and the rise of the waste pile was slower. Of course there were sometimes effects, like an increased intake after change of the waste chamber, but in average I did not observe a systematic change.

What I observed was, that turnover and relocation of waste particles together with size reduction led to less required space and therefore the possibility to store more waste within the same volume.

As an example, I monitored a half filled, established waste chamber for one week. Every color represent data from another day (Fig. 40). In the beginning, particles were relatively big and ants dug everywhere (Fig. 40 A). Later, digging activity was visible especially in the fresh waste pile nearby the entrance of the chamber (Fig. 40 B). The next days, digging activities stopped under the surface in the front parts of the waste chamber, instead deposit and turnover of fresh waste material was observed (Fig. 40 C).

The layers inside of a waste chamber will be investigated in more detail.

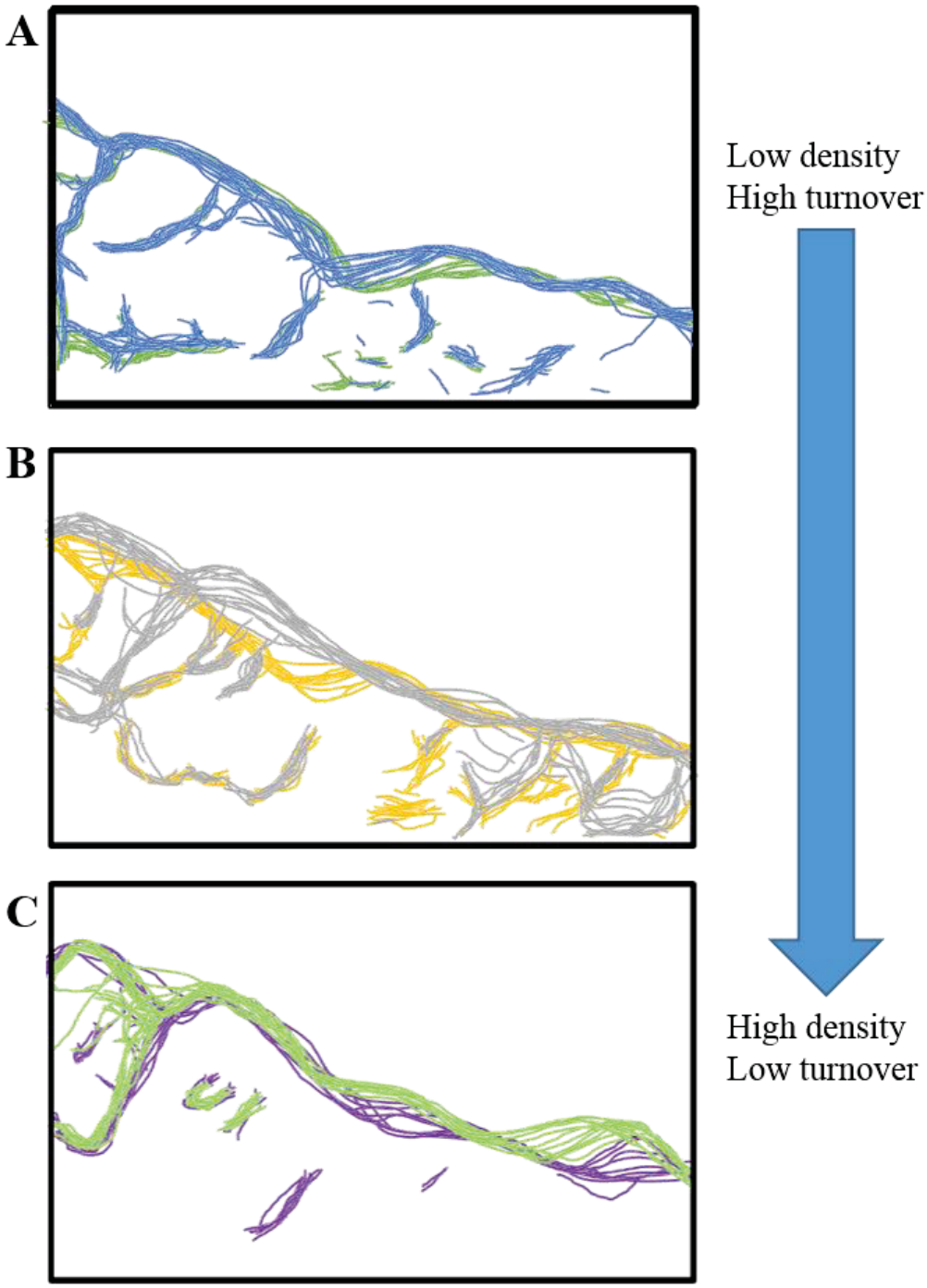

Fig. 40: Digging activity and tunnel rearrangement as an example. Overlay of frames, each color represents one day. A: Day 1 green and Day 2 blue. B: Day 3 yellow and Day 4 grey. C: Day 5 purple and Day 6 green (Dataset 160215-langk-klar).

All examples in this chamber were prepared with material from *Atta vollenweideri* (Konstanz). For *Atta laevigata* and *Acromyrmex lundii* (both Würzburg), the observations were the same. The only difference was, that *Acromyrmex lundii* started small waste piles on the DHT sensors and took care of them in small groups. Nevertheless, they operated a big waste pile with the same shape as both *Atta*.

5.2.1.4.9 Water content and appearance of waste particles in different layers of waste chambers

To understand processes inside of the waste pile, waste particles were analyzed. Parameters such as water content, granularity and color were determined from every layer.

Data from the applied DHT sensors were recorded permanently. While temperature data was not of interest in a climate chamber, the relative humidity showed some effects. After an initial starting phase, until leaf-cutting ants started to deposit waste particles, the overall humidity in the waste chamber was lower. When the ants started to deposit, the humidity increased. When a sensor was covered with waste material, the relative humidity increased again up to 96-100% (Fig. 41 Aa1). This event was filmed by a camera and the time point could be linked to the event. Another sensor was covered by waste material for a short time, but cleared again (Fig. 41 Ab2). The increase of relative humidity decreased again. After some hours, this sensor was permanently covered with waste material (Fig. 41 Ab3).

These effects were observed several times, where sensors nearby the ground were covered very fast (Fig. 42 A) while other sensors were temporarily (Fig. 42 B 1,3,4) covered and thereafter permanently (Fig. 42 B 2,5).

Some of the sensors broke down due to corrosion after a certain time. Nevertheless, with some measurements, the formation of tunnels was shown by temporary decrease of relative humidity of about 5-10%. As the sensors were prepared with the grid to the downside and the solid side to the upside, it remains unknown if these measurements are reliable. If the grid was still covered, the measurement could indicate a closed layer of waste instead of a tunnel.

The measurement showed, that the relative humidity inside of the waste pile was close to 100% and therefore saturated in gas phase.

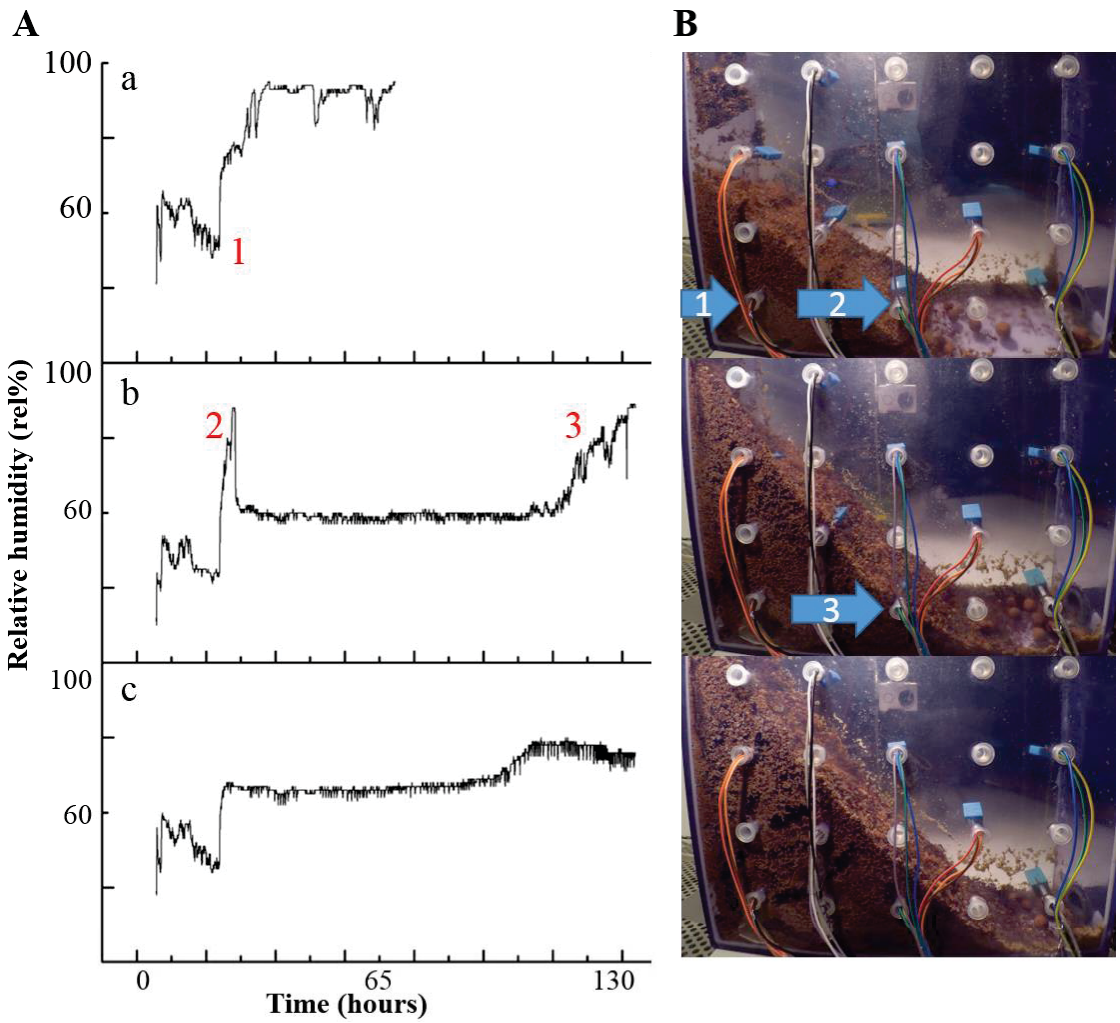

Fig. 41: Comparison of relative humidity from DHT-sensors connected to Raspberry Pi systems. Every graph represents data from one sensor. A: Sensor data. B: Waste chambers after several time points. Location of sensors and events indicated by arrows and numbers. Event 1: Sensor covered with waste material. Event 2: Sensor covered with waste material which was removed thereafter. Event 3: Sensor got covered again with waste particles.

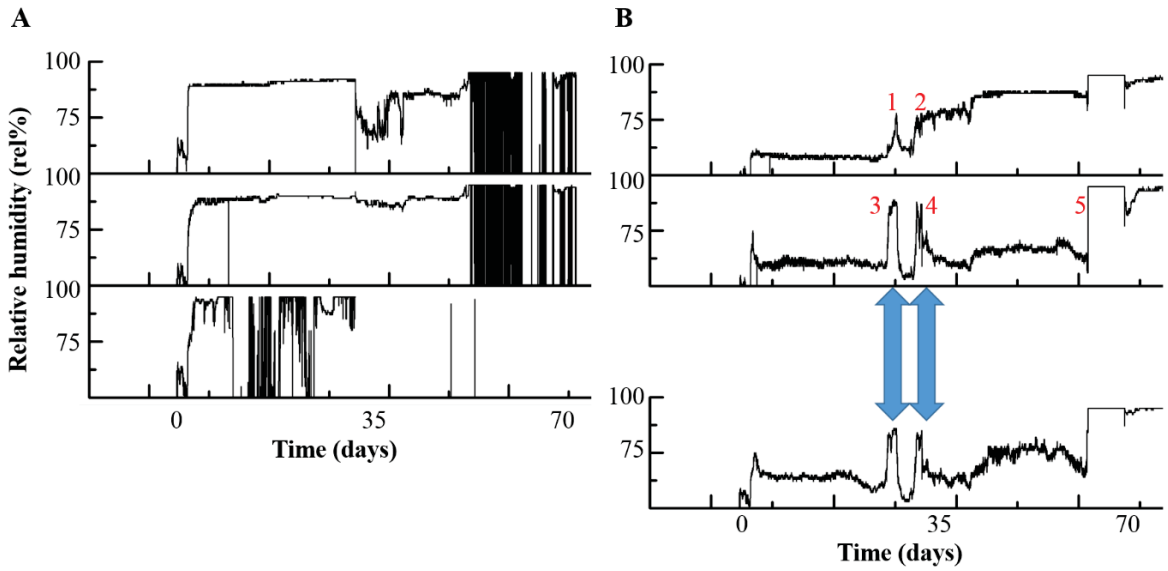

Fig. 42: Graphs of relative humidity of DHT sensors. Every graph represents data of one sensor. A: Sensors which were covered with waste particles very fast. B: Sensors which were covered with waste particles over time. Event 1, 3, 4: Sensor got covered and cleared after a certain time. Event 2, 5: Sensor got covered permanently.

Gravimetric determination of water content from waste particles originated in several layers of the waste chamber showed, that the absolute water content ranged from 50% on the upper surface to 40% in lower layers and up to 70% at the bottom of the box (Fig. 43).

Due to the preparation procedure, not only water but at least all chemicals with a boiling point less than 100°C would have been evaporated and were therefore removed. Degradation of waste particles was not observed.

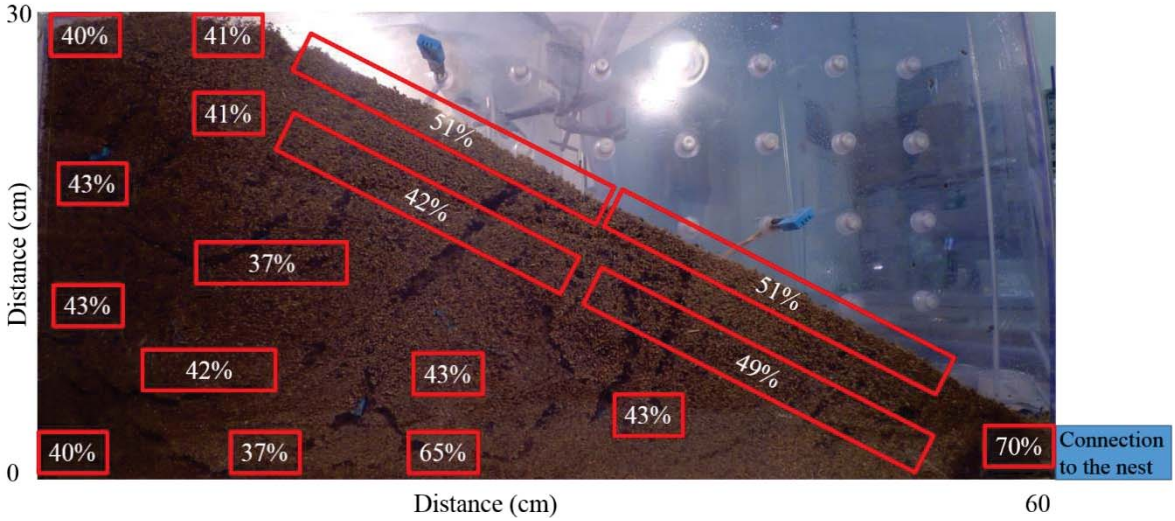

Fig. 43: Water content (weight %) of waste particles collected from indicated areas.

Waste particles of defined areas in the waste chamber of *Atta vollenweideri* were collected (Fig. 44). In the upper layer, the typical brownish particles were found (Fig. 44 Aa and BCa). In a lower layer (Fig. 44 Ac and BCc) the waste particles had a whitish cover. Moreover, the

particle size was reduced compared to particles from the upper layer. Waste particles from the bottom (Fig. 44 Ad and BCd) were smaller and had a darker color.

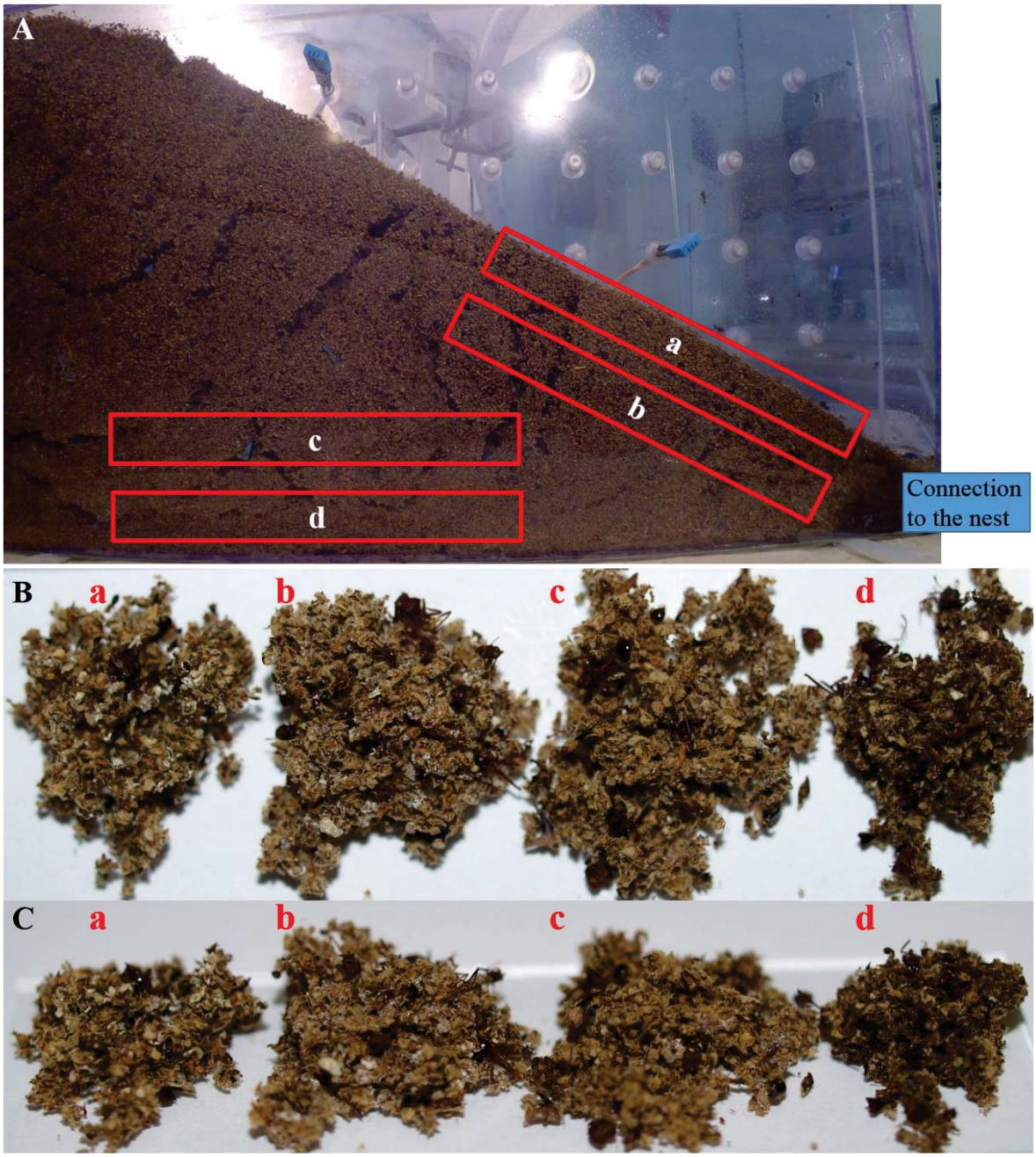

Fig. 44: Collection areas of waste particles from a leaf-cutting ant waste chamber. A: Indication of collection area. B: Waste particles from the areas in detail. *Atta vollenweideri*, Konstanz.

These effects were studied in more detail with waste particles of *Atta laevigata* from Würzburg, where three distinct layers were identified by eye (Fig. 45 A-C). There was a brownish crumbly layer on top. Inside of the waste pile, there was a whitish layer which was more compressed than the top layer. The third layer was black and had a consistence like humus (Fig. 45 D).

The water content was determined to be 18% for the brownish top layer, 40% for the intermediate whitish layer and 75% for the black layer.

Interestingly, the brownish waste particles seemed to be metabolized and degraded to a black humus like layer. Therefore, microbes were isolated from the layers.

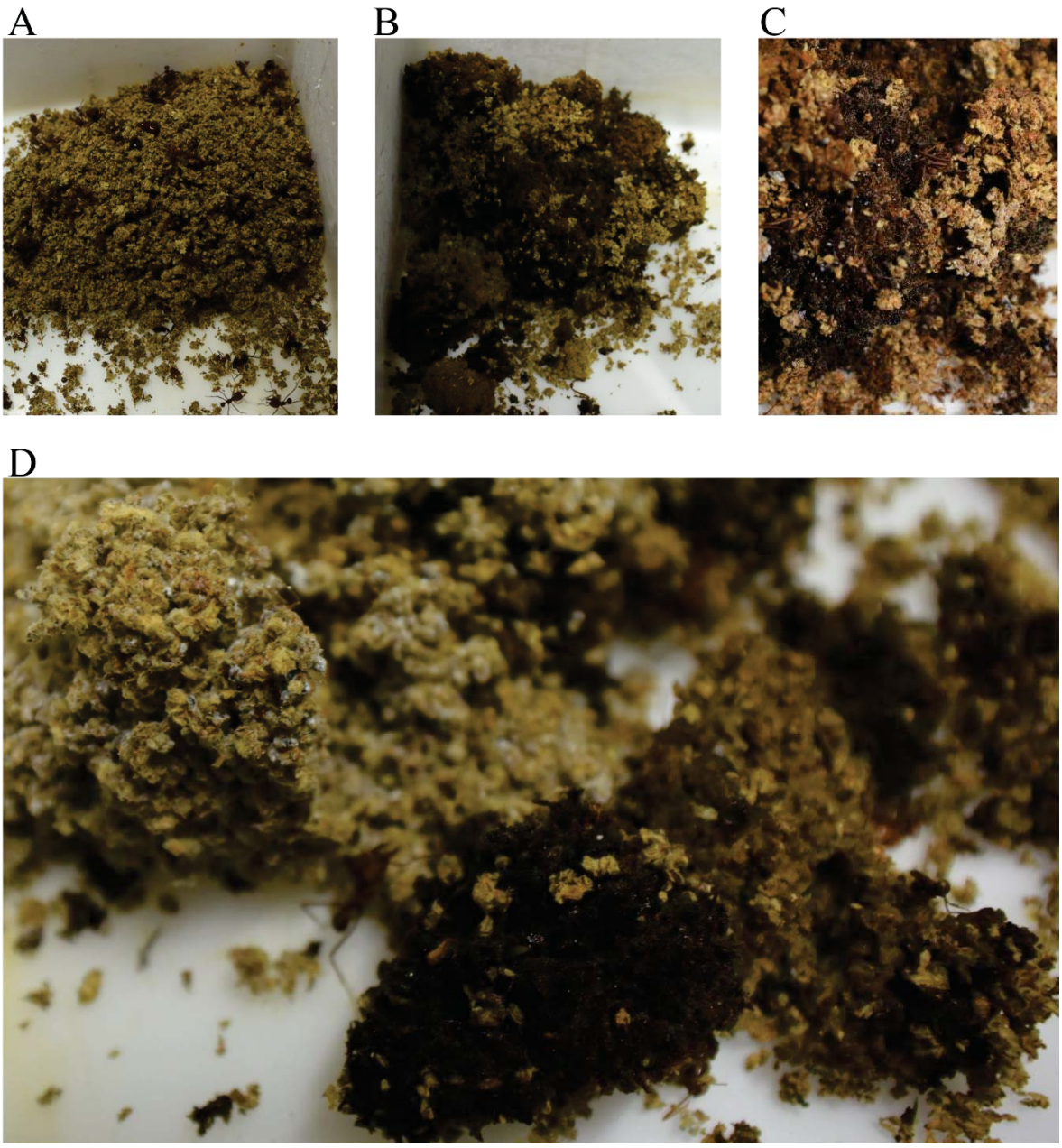

Fig. 45: Photographs of waste particles from several layers. A: Top layer, brownish crumbly particles. B: Layers from inside the waste pile. C: Bottom layer, consisted mainly black humus like material. D: Comparison of particles from all layers. Left whitish, front black and right brownish waste material. *Atta laevigata* (Würzburg).

5.2.1.4.10 Growth of microorganisms in different layers of waste chambers

The previously described waste particles from the three layers were collected and photographed using a binocular (Fig. 46 A). The particles differed in color and granularity. Especially particles of the black layer stacked together. The brownish particles had a hard and even surface. In contrast, the surface of the whitish particles was smoother and small

hair-like structures were visible (Fig. 46 B). Looking closer at the hairs, fungal hyphae were visible with higher magnification (Fig. 46 D). The main fungus had a greenish color, while there were whitish aggregates.

Particles of the black layer consisted of fungal hyphae, which were also visible on body parts of dead leaf-cutting ants (Fig. 46 C).

This observation led to the hypothesis, that already inside of laboratory waste chambers, there was degradation of waste particles resulting in humus-like material. The circumstances and steps of waste particle degradation were not investigated so far.

Besides reports of increased waste worker mortality investigated after infectious events and stringent task partitioning,[3, 13-14] my observations showed accepted or at least tolerated visible fungal growth in waste chambers. Previous studies on non-mutualistic fungal cultures revealed many species, which were believed to be "alien" or pathogens without benefits. [19, 24-25]

Among them, Rodrigues, et al. [26] identified several fungal species, such as *Syncephalastrum racemosum* (54%), *Trichoderma harzianum* (38%), *Fusarium oxysporum* (23%) and *Escovopsis weberi* (21%) in leaf-cutting ants' gardens and wastes. Three years later, Rodrigues, et al. [18] reported 33 fungal species found in leaf-cutting ants' nests. *Escovopsis weberi* is well known as hyphal parasite of the fungal cultivar and can be found as spores or actively growing in nests of leaf-cutting ants.[9]

There are for sure some pathogens present, but maybe there are some underestimated beneficial microbes in the ecosystem of leaf-cutting ants? As an example, nitrogen fixating bacteria were described in 2009.[27]

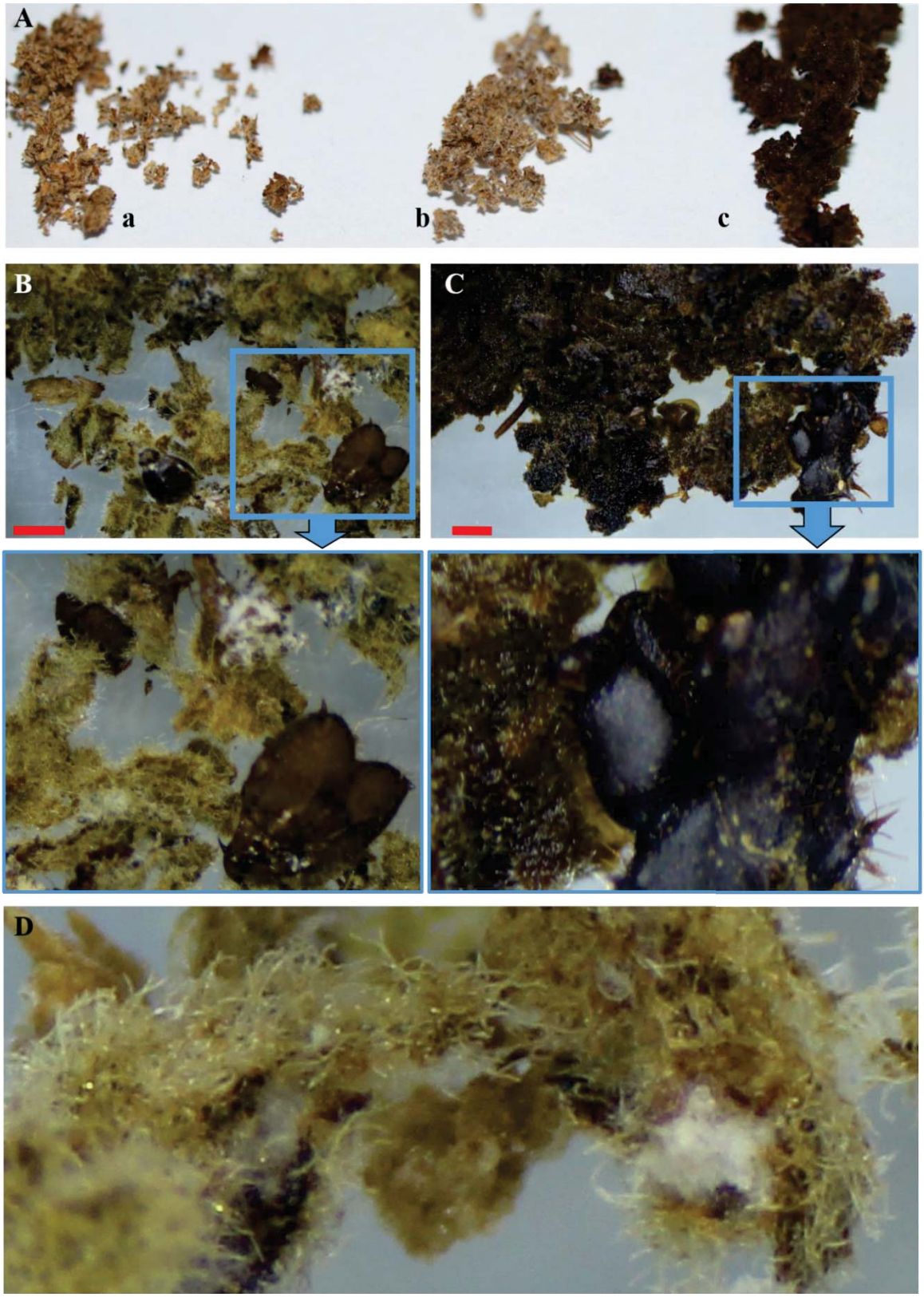

Fig. 46: Waste particles from leaf-cutting ants and microbes therein. A: Waste particles from three distinct layers. B: Detail picture of whitish waste material and zoom (blue box). C: Detail picture of black waste material and zoom (blue box). D: Visible fungal hyphae on whitish waste material with higher magnification. Red bars: 1 cm.

5.2.1.4.11 Preliminary results for prospective experiments

To investigate the reaction of leaf-cutting ants when confronted with waste material, a behavioral assay was developed.

In this assay, ants could dig tunnels to reach a prepared sample. Samples were fresh waste, incubated waste or waste inoculated with isolated microbes. Waste was autoclaved to make sure, that only the inoculated strain grew. Waste particles were inoculated with microbes and incubated for several days (28°C).

The experiment was documented with time-lapse pictures taken by action cams.

First results of this experiment with isolated microbes (Fig. 47 A; for protocols see Ch. 7.2; p. 177) were conducted with *Atta vollenweideri* and *Atta laevigata*. Both ant species showed, that when there were "interesting" microbes growing, they started digging within the first three hours. Tunnels were clearly visible (Fig. 47 C), sometimes ants were observed to process treated waste particles with their mandibles.

Another setup, where samples could be applied in syringes and connected to waste piles with cannulas through plastic caps, ants dug to the front of cannulas with "interesting" samples and tried to get closer than the thorn (Fig. 48 A). Both experiments were conducted with variation of samples and controls. Wetting of waste showed comparable effects after incubation, therefore the growth of microbes was assumed to be responsible for some effects.

For another screening experiment, where the natural surroundings of waste heaps should be mimicked, an artificial waste heap was prepared on top of clay granulate (Fig. 48 B). Ants mixed waste particles and clay granulate. There were holes of tunnels visible, moreover waste particles were visible in underground layers at the glass surface (Fig. 48 C). In contrast to laboratory colonies, which were limited by glass surfaces, such experiments might help to understand what happens in underground waste chambers. This screening experiment was not connected to an ant colony and only conducted for several days.

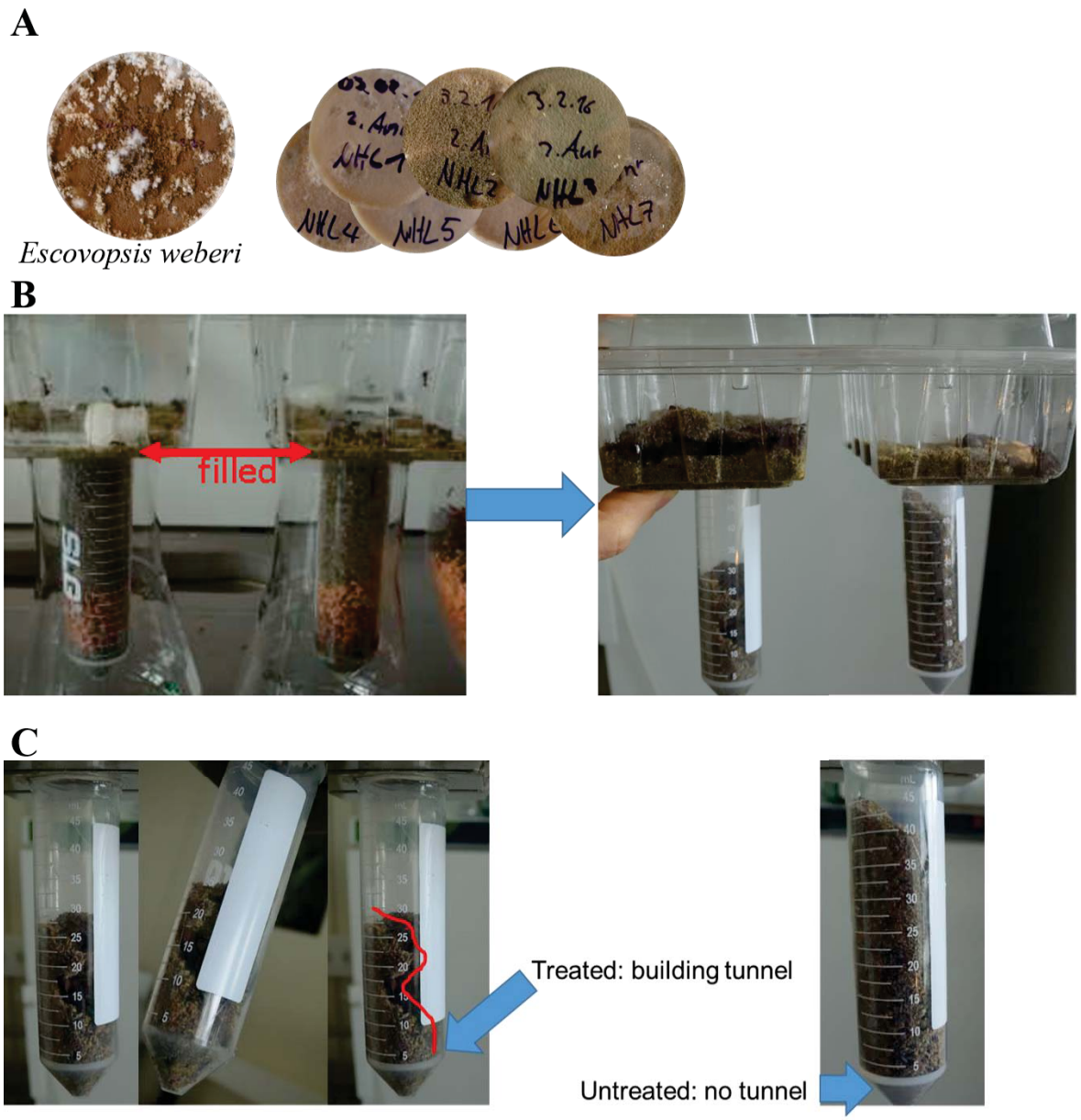

Fig. 47: Behavioral assay to determine impact of isolated microbes. A: Available microbes. B: Binary choice experiment before and after ants were added. C: Detailed view on tubes with treated (left) and untreated (right) waste.

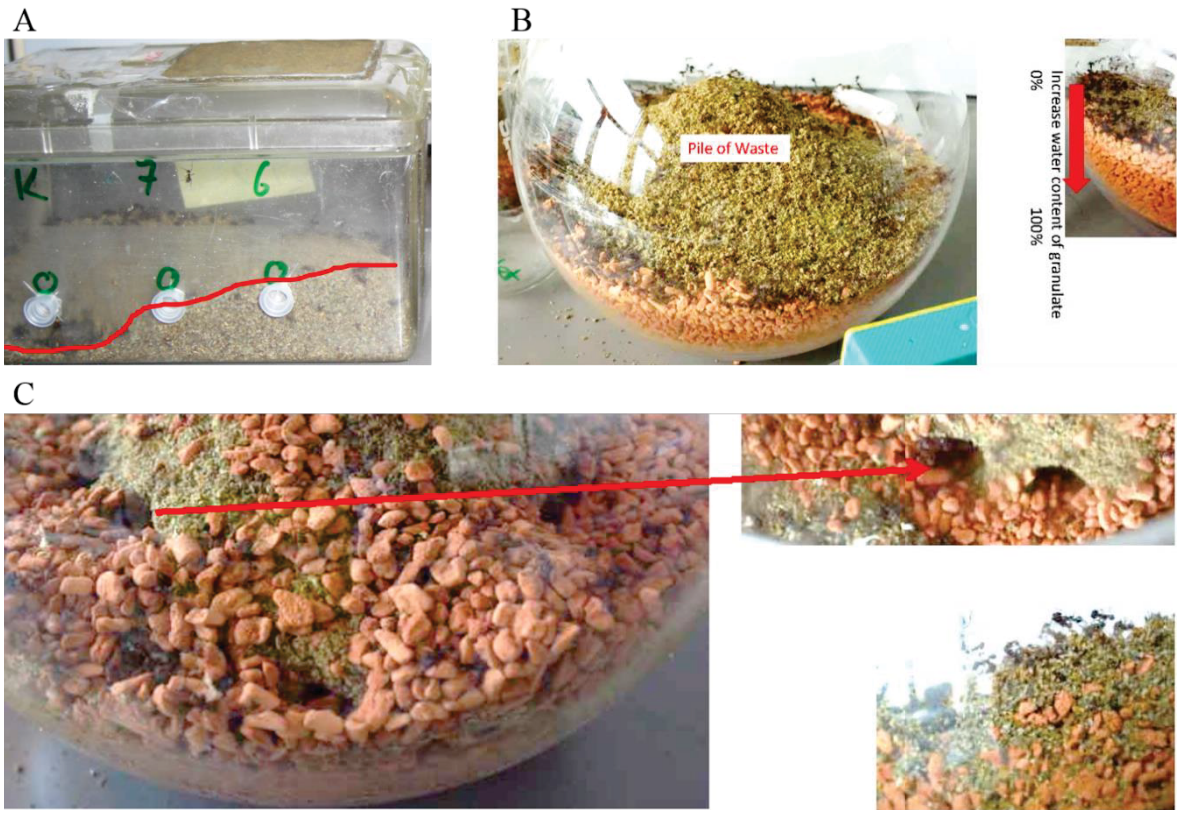

Fig. 48: Screenings for ant behavior. A: Artificial waste piles, where syringes with cannulas were applied through plastic caps and ants dug to samples. B: Artificial waste pile on top of clay granulate with different water content before ants were added. C: Artificial waste pile after ants were added. Ants mixed waste particles with granulate, intake in tunnels.

Nevertheless, the first observations were not reproduced yet. There is an enormous amount of control experiments necessary to produce meaningful results.

To-do list (incomplete)

- Phylogeny of isolated microbes with 18*S* rDNA primers, PCR, sequencing and database comparison
- Difference between wet and dry waste; before and after incubation
- Difference between autoclaved and non-autoclaved waste
    - Microbial
    - Chemical
    - Recognition (waste flavoring with cryo trap distillation, see Ch. 6.1.3.6, p. 148)
- Difference between time points after inoculation with microbes
    - Time series
- Difference of microbial growth with supplements
    - Application of carbon/nitrogen sources to allow/speed up growth
- Difference between waste workers and other castes

- Experiments with “real” waste chamber - connected to a colony
    - transfer inoculated waste particles inside a plastic syringe and connect this using a cannula with the waste chamber (penetrate trough plastic plugs)

5.2.1.5 Conclusion

Several repetitive effects were observed during the connection time of a waste chamber to laboratory colonies.

Start of waste deposit was observed in a certain distance to the entrance for cylindrical and long boxes (Fig. 49 A, B). It remains unclear, whether the ants choose a certain distance by chance (Fig. 49 A, B; both 1) or if there is a trigger like space limitations (Fig. 49 A, B; both 2 and 3). For a differentiation, very close observations with macro objectives might help to identify travel paths of waste particle transporting ants.

All waste heaps had a certain slope, no matter if it was an U-shaped, a donut-like or a nugget-like heap. Comparisons of slopes showed a high diversity. For obviously wet waste, the slope was higher than for "normal" waste. I would predict, that the slope was influenced by passive physical effects. Indeed, fresh waste particles were observed to be released onto the heap, thereafter a passive rolling-down of particles was observed and particles from the lower part of the waste heaps were transported inside of holes/tunnels by ants (Fig. 49 D). In areas containing fresh waste particles, temporary turnover activities with moving tunnels (Fig. 49 E1-5) or surface recirculation were observed (Fig. 49 E6).

Permanent transportation tunnels were most often present at the crossover area of the main slope and a flatter area in front (Fig. 49 F1). Movement of tunnels was sometimes observed passively due to collapse of upstream layers or actively by ants digging into heaps and refilling tunnels with waste particles (Fig. 49 F1-2).

Exhausted or contaminated fungus garden material appeared as fresh brownish waste particles especially in the upper layers of the waste heap. Translocation inside the heap led to a mixture of already decomposed and fresh waste particles. Three layers were identified by eye, a brownish, whitish and black layer (Fig. 49 G1-2). Particles and bodies of dead ants showed microbial growth, especially greenish and whitish fungal hyphae (Fig. 49 G3).

First experiments indicated, that there might be non-mutualistic fungi, which are tolerated and must no longer be considered as pathogens but as helpful.

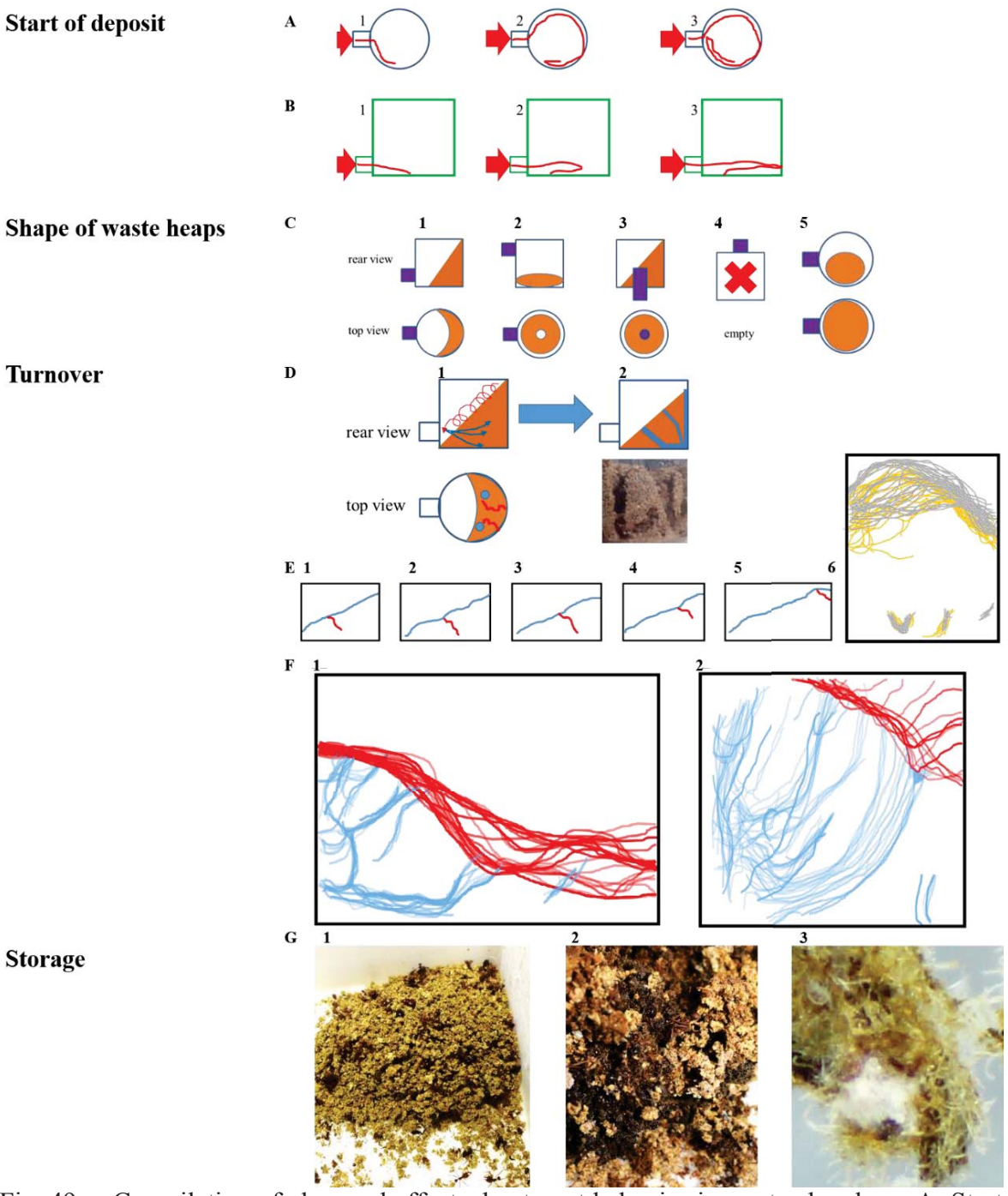

Fig. 49: Compilation of observed effects due to ant behavior in waste chambers. A: Start in cylindrical boxes, three possible mechanisms. B: Start in long waste chamber, three possible mechanisms. C: Shape of waste heaps 1: Cylindrical box with entrance downside. 2: Cylindrical box with entrance upside. 3: Cylindrical box with entrance at the bottom. 4: Cylindrical box with entrance on top. 5: Spherical box with entrance sideways. D: Active and passive turnover processes. 1: Rolling down of particles intake into waste heap. 2: Formation of tunnels. E: Turnover of fresh waste particles at the surface 1-5: Moving temporary tunnel. 6: Surface turnover. F: Drawing of tunnel formation. 1: Permanent tunnel systems. 2: Temporary moving tunnels. G: Decomposition of waste particles over time. 1: Fresh brownish particles. 2: Decomposed whitish and black particles. 3: Microbial growth on waste particles.

5.2.2 Chemical defense against pathogens in leaf-cutting ants' ecosystem (several *Atta*/*Acromyrmex*) in particular in their waste

Contributions

This project was initially started in the Emmy Noether junior group of Prof. Dr. D. Spiteller at the Max Planck Institute for Chemical Ecology (MPI CE, Jena, Germany) associated with the group of Prof. Dr. Boland. Dr. Ilka Schoenian described initial parts in her PhD thesis (available online http://d-nb.info/1017079013; urn:nbn:de:gbv:27-20111109-142430-0), my findings are independent from her methods and results. I will only summarize some of her suggested methods and results shortly.

Furthermore, Xenia Schilke wrote her bachelor thesis "Metabolitenprofile ausgewählter Blattschneiderameisen im Vergleich" (submitted in September 2015) regarding leaf-cutting ants' waste.

Additional purification efforts of waste samples were topic of "Vertiefungskurs Chemische Ökologie" in 2016, prepared by Hendrik Rusche and Laura Heinzelmann.

5.2.2.1 Abstract

Leaf-cutting ants evolved several mechanisms to protect their fungal cultivar, *Leucoagaricus gongylophyrus*. During the processes along the food chain from bramble leaves to waste substrate, there are many intermediate steps which are susceptible to contaminations. In particular, attacks by the specialized parasite *Escovopsis weberi* were described to weaken ant colonies.

The combination of leaf-cutting ants' behavior, together with glandular secretions and antibiotics from microorganisms were described on the basis of model systems which considered only parts of the performed defense mechanisms. Nevertheless, descriptions of chemical compounds involved in these processes were not determined on colony level. Synergistic effects of inter-coordinated pieces of this puzzle are therefore still hidden.

One main aim of this project was to identify and describe antibiotic compounds found in the ecosystem of leaf-cutting ants, in particular in the place where they accumulate: in leaf-cutting ants' waste.

Several variables in the ecosystem of leaf-cutting ants were identified to be relevant investigation targets. Bramble leaves were found to contain antibacterial and antifungal compounds. Separation of waste particles and contained bodies of dead ants both showed bioactivity. The bioactivity of dead bodies is surprising and was not reported before.

Nevertheless, the described methods with the novel findings contribute to the understanding of yet unstudied influence factors. Due to lacking material from the ecosystem of leaf-cutting ants and sensitive instruments, chemical structures could not be elucidated.

5.2.2.2 Introduction

Among social insects, especially fungus growing ants live in complex ecosystems. Leaf-cutting ants (*Atta* and *Acromyrmex*) provide their fungal cultivar with fresh leaf material. This task is performed by mayor workers with huge heads. The leaf material is cleaned from contaminations, cut down to pieces and interlaced between fungal hyphae by small workers in the fungal chamber. Besides childcare, they also maintain their fungal cultivar. Old fungal material is removed and transported to the waste chamber. Contaminated fungal material is stored in these chambers as well. While leaf-cutting ants take care about waste particles, there is no expansion of contamination. After leaf-cutting ants left their nests, the waste material could be completely overgrown with pathogenous fungi.[14]

Leaf-cutting ants execute a combination of behavioral and chemical defense to keep their nest under suitable conditions. While they spare no effort to keep their fungal cultivar healthy, they also maintain their individual fitness and welfare.[21]

In literature, the chemical defense mechanisms are usually only considered in isolated model systems. On the one hand, these limited conditions help to understand the fundamental interactions between various effects.[28-30] On the other hand, there is no overview to interconnect fundamental relations. Therefore, the investigated parts can not be linked and ranked.

Indeed, in leaf-cutting ants' ecosystem, there are numerous possibilities to respond to infection related happenings. Furthermore, there might not only be one answer, but again huge differences between species. Waste management of leaf-cutting ants was discussed very controversial, as some specific findings were suggested to be true for all *Attini* ants, while they were only specific for some species.[3, 13, 31]

With this project, we aimed to identify antibiotic compounds which are present in leaf-cutting ants' waste. Leaf-cutting ants' waste was found to contain bioactive compounds.[32] The waste chambers (or heaps) are the ultimate destination for exhausted or contaminated particles from the nest. Moreover, the waste of leaf-cutting ants contains dead ants' bodies and for example infrabuccal pellets. These pellets are produced by the mouthparts of ants and were described to be directly related to contaminations.[33] They were produced in higher numbers when pathogens are present in leaf-cutting ants' nests.

Furthermore, the origin of the bioactive compounds should be estimated and related according to their relative bioactivity. The visible parts of the ecosystem (leaves, ants, fungal symbiont and waste particles) can be divided in more complex pieces (Fig. 50 A, B). For example, leaf-cutting ants were shown to use their glandular secretions[34-36] as well as antibiotics from bacterial symbionts[5, 37] to defend against pathogens (Fig. 50 C). The symbiont of the fungus-growing ant *Cyphomyrmex minutus*, *Tyridiomyces formicarum*, was found to produce several antifungal diketopiperazines which were suspected to protect the fungal cultivar or its host.[38]

By comparison of waste particles from several leaf-cutting ant species, I aimed to differentiate between general and unique defending mechanisms and antibiotics. After isolation of bacterial symbionts, their bioactivity can be estimated in bioassays against pathogens. By cultivation of these bacterial strains, the chemical structures of produced antibiotics can be elucidated after extraction of culture media and bioassay-guided fractionation.

To compare bioactivity profiles of waste samples, they were separated with identical chromatographic conditions. Bioactivity was estimated against the specialized parasite *Escovopsis weberi* and the ubiquitous bacterium *Bacillus subtilis*. Chemical structures of pure bioactive compounds should have been elucidated with the help of NMR, IR and MS, but the available sample amount was too small for analysis.

Therefore, I present my novel findings to contribute to prospective efforts in this direction.

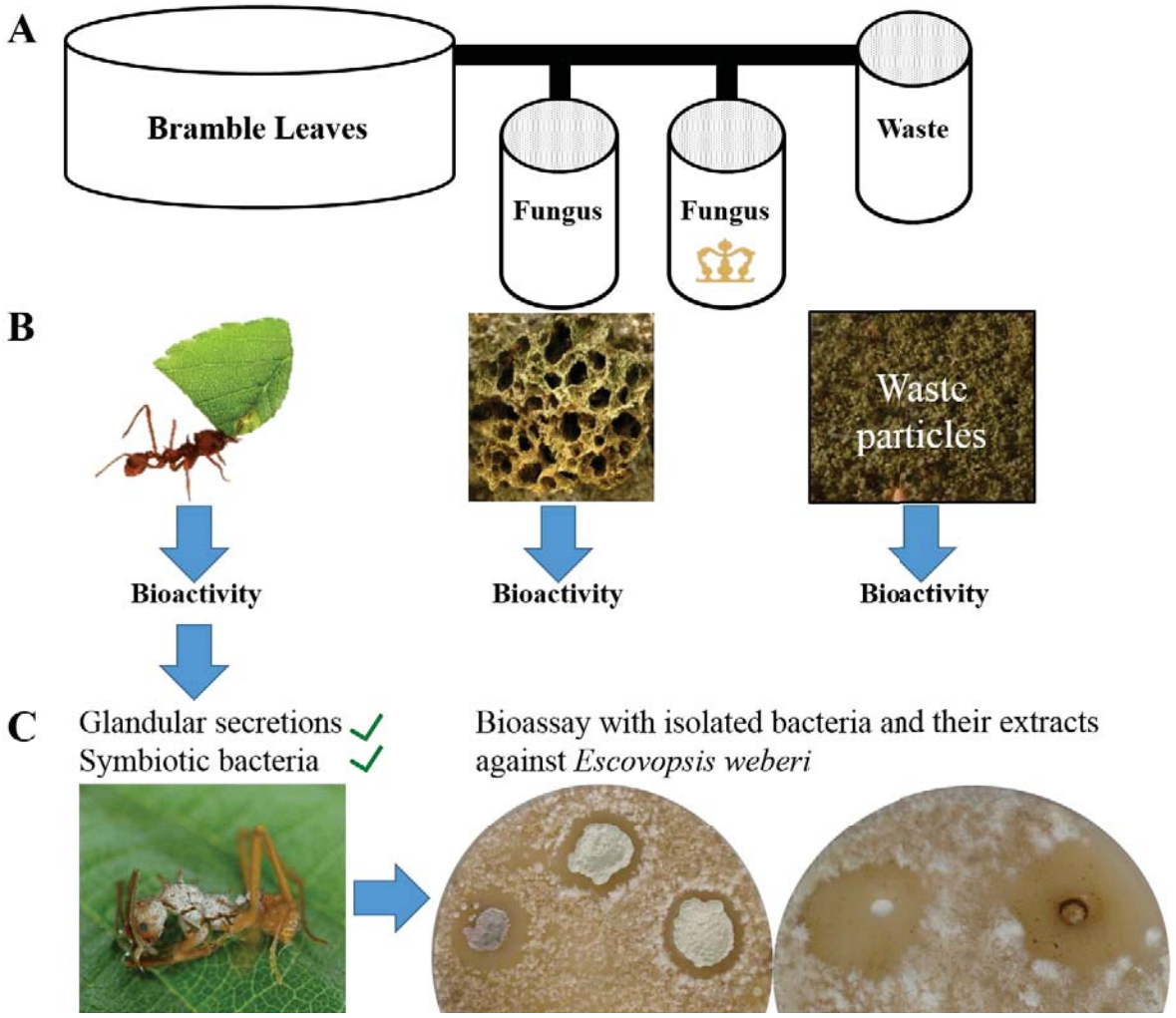

Fig. 50: Overview of leaf-cutting ants ecosystem with focus on origin of bioactive substances. A: Minimum chamber system for cultivation of leaf-cutting ants. B: Bioactive parts in the production and spreading of bioactive substances. C: Origin of bioactive substances from the bodies of leaf-cutting ants. Isolated bacteria from leaf-cutting ants' bodies and their extracts after cultivation in bioassays against *Escovopsis weberi*.

5.2.2.3 Methods

5.2.2.3.1 Origin of leaf-cutting ants' waste and storage

Waste samples from several leaf-cutting ant families were collected. The major amount was provided by the group of Dr. Kleineidam (University of Konstanz), cultivating two *Atta vollenweideri* colonies. The waste material was used directly or stored at 4°C or -20°C. Samples of *Acromyrmex echinatior* were provided by Dr. Wirth (University of Kaiserslautern), transported at room temperature and stored for years in a freezer (-20°C). Samples of *Atta colombica* were received from Prof. Dr. Roces (University of Würzburg), transported at room temperature and stored in a cold-room at 4°C. Small amounts of waste samples from *Acromyrmex lundii*, *Acromyrmex ambiguous* and *Acromyrmex heyeri* were

collected directly in Würzburg and frozen using liquid nitrogen. They were stored in a freezer at -20°C.

5.2.2.3.2 Separation of particles from leaf-cutting ants' waste

The samples of leaf-cutting ants' waste contained clay granules, which were removed by hand on a clean surface such as clingfilm.

If separation of waste substrate and leaf-cutting ant bodies was necessary, they were separated using hexane. The bodies swam on the surface and were removed using a metal sieve. The used hexane was evaporated and the residue was applied in bioassays (Ch. 7.3.2; p. 181). There was no bioactivity visible against *Escovopsis weberi*, *Fusarium* spp. or *Bacillus subtilis*.

5.2.2.3.3 Dry weight and density of leaf-cutting ants' waste

Waste material was transferred to a 2 l beaker and weighted on a balance. The waste material was not compressed, but pushed with the bottom of a conical flask (100 g; 1 Newton) into the beaker.

The wet weight was measured, then the beakers were freeze-dried (0,1 mbar; -80°C) until there was no measurable weight change any more (minimum 15 hours).

5.2.2.3.4 Agar diffusion assays and antagonistic organisms

SFG-Agar dishes were used for agar diffusion assays (composition in Ch. 7.3.2; p. 181). Liquid extracts or fractions were dissolved in a defined volume of pure methanol, water-methanol mixtures or acetone-water mixtures dependent on solubility of the residues.

Up to 7 holes were cut out of the agar plates with the backside of a Pasteur pipette, 90 µl of the test fractions were pipetted inside, allowed to diffuse inside the agar for at least 30 min. Thereafter, the test organism was spread all over the agar dish.

Bacillus subtilis, Escovopsis weberi or *Fusarium* spp. were used to observe growth inhibition. The petri dishes were incubated at 28°C and checked daily.

5.2.2.3.5 Extraction of bioactive substances

For a first screening, several solvents (hexane, petrol ether, ethyl acetate, dichloromethane, diethyl ether or methanol) were used at native or acidified pH (around pH=2) in order to evaluate their abilities to extract bioactive compounds. 20 g of waste material were used for each screening. The complete extract was applied in the agar diffusion assays.

There was no bioactivity in the extracts at native pH, therefore these conditions were used for a pre-extraction of inactive substances. Beneficial extraction abilities were obtained with a mixture of diethyl ether-acetone (9:1), acidified with hydrochloric acid (5 ml concentrated

hydrochloric acid per 2 l extraction). Afterwards, some bioactive substances were extracted using acidified methanol in a second pass.

Extraction of waste material was conducted in 2 l beakers using the principle of counter-current extraction in order to increase efficiency. The solvent was dried with sodium sulfate before evaporation using a rotavap (Büchi, Switzerland).

The extraction conditions for waste samples described by Dr. Schoenian were repeated, but the conditions revealed hydrolysis of ethyl acetate. Bottles with balanced sample material were placed on a rotary shaker and shaken overnight. They contained either waste material or water, which were acidified using hydrochloric acid (around pH=2). The organic phase was transferred and dried over sodium sulfate. In the flask attached to the rotavap, not only ethyl acetate (40°C; about 120 mbar) but also ethanol (40°C; about 70 mbar) and acetic acid (40°C; about 20 mbar) were present. The problematic circumstances of producing artefacts with acetic acid will be discussed later. Acetic acid was observed to produce bioactive artefacts and hindered the evaporation. Its boiling point of 118°C is higher than the boiling point of water (100°C). Therefore, ethyl acetate was not used for long term extractions any more, which eliminated the formation of bioactive artefacts.

5.2.2.3.6 Pre-purification of crude extracts

The viscous, tarlike crude extract was pre-purified using silica filtration through a silica plug. Sand and silica powder (60 mesh) were added to the crude extract, diethyl ether was evaporated and the sand mixture was homogenated. A silica plug with a minimum of ten times the sand mixture volume was prepared with diethyl ether. The material was filtered into two fractions, first diethyl ether and afterwards methanol. Both fractions were evaporated and analyzed in bioassays.

The diethyl ether fraction was bioactive, and used for a methanol-hexane-separation in a 100 ml bottle. The hexane layer (upper) was changed until it remained clear. Both phases were evaporated and tested in bioassays.

This procedure reduced the volume of the crude extract by around 95%, the bioactive part remained in only 5% of the initial volume.

5.2.2.3.7 Bioassay-guided fractionation of extracts and fractions

Several chromatography workflows were tested in order to identify suitable solvent mixtures.

The methanol phase (bioactive, Ch. 5.2.2.3.6) was further purified by flash chromatography using a silica gel column (20x2,5 cm), eluted with petrol ether/diethyl ether (4:1; 2:1; 1:1; 1:2) and finally methanol in 5 fractions (120 ml each). The bioactive fraction was transferred

to a RP-C_{18}-column (15x2,5 cm; Polygoprep C_{18} 60-50; Macherey-Nagel, Düren) eluted with methanol in ddH_2O (30%; 50%; 70%; 90%; 100%) in 5 fractions (120 ml each) followed by RP-HPLC fractionation.

For HPLC fractionation, an Agilent 1100 HPLC system was used. The bioactive residue was dissolved in ddH_2O/methanol (4:1) and several times (up to 30 µl each) injected into an Agilent ZORBAX Eclipse XDB C_8 column (150x4,6 mm; particle size: 5 µm). A program with ddH_2O and methanol (each 0,1% acetic acid) was used at a flow rate of 0,6 ml/min (Tab. 3). The automatic fraction collector collected 27 fractions (1 tube/min) between 1 and 28 min of the runtime.

Tab. 3: HPLC gradient program used for fractionation

Time (min)	%MeOH (in ddH_2O)
0	20
12	70
18	70
20	100
23	100
23,1	20
28	20

The collected fractions were lyophilized, residues were dissolved in methanol and tested for bioactivity in agar diffusion assays (Ch. 5.2.2.3.4).

5.2.2.4 Results and Discussion

5.2.2.4.1 Composition of waste particles and their origin in leaf-cutting ants' waste

Leaf-cutting ants' waste contained not only exhausted fungus material (brownish), but also dead ants' bodies and bramble stems. Bramble leaves were cut in small pieces by leaf-cutting ants and provided to their fungal cultivar. The fungal cultivar grows in layers, from greyish on top to brownish at the bottom. The bottom parts are removed by leaf-cutting ants and deposited into waste chambers. In addition, also bramble stems were transported into fungal and waste chambers (own observation). Whether their function is related to provide nutrients, antibiotics or stability is not known.

Dead ants' bodies were also found in waste chambers, whether the waste workers are old ants directly dying there or not is not known. They were translocated inside of the waste chamber. In deeper layers, only parts of ants' bodies were found (own observation). Most probably, they fell into pieces or were cut into pieces.

5.2.2.4.2 Water content and density of leaf-cutting ants' waste

The water content of waste material from *Atta vollenweideri*, *Atta colombica* and *Acromyrmex echinatior* was determined. According to their origin, they showed huge variation. Some waste material was very dry, while other waste material contained a lot of water. As the same colonies were not monitored over time, the results are not as comparable as they could be with repetitions. The water content of the bramble leaves alternates with the season, with dry leaves in wintertime and very wet leaves when they start growing in spring. Nevertheless, the conducted measurements resulted in an average water content of 47±5% with values between 10% (*Atta colombica*) and 60% (*Atta vollenveideri*).

The water content depends on location, surrounding area and connection time of the waste chambers to the colony. The same is true regarding density of waste inside of waste chambers. Leaf-cutting ants start filling their waste chambers with very coarse grained particles and after several time they reduce the particle size (Ch. 5.2.1.4.9; p. 49).

Waste material of *Acromyrmex echinatior* had the highest density (0,16±0,05 g/ml) while the density of *Atta* waste particles ranged around 0,08 g/ml. Because the connection time of the waste chambers from laboratory colonies is not known, these values can not be compared (waste chambers have to be emptied by staff).

5.2.2.4.3 Extraction of leaf-cutting ants' waste

The waste of leaf-cutting ants was previously described to be bioactive.[32] The origin of the bioactive compounds remained unclear.

Repetition of previous extraction protocols indicated, that the described effects might be caused by self-made artefacts rather than contained bioactive compounds. Extracts of waste particles, shaken overnight in acidic conditions with ethyl acetate, produced appreciable amounts of ethanol and acetic acid. The origin of those compounds was proven by controls: Acidified water (waste particles contain water; pH=2) was shaken overnight with ethyl acetate, which generated the same "bioactive" compounds (ethanol, acetic acid).

Acetic acid was shown to confuse some students, as they mistook acidity for microbial bioactivity. Indeed, some microorganisms produce small acidic compounds, but they should not be present in control experiments. Especially pronounced amphiphilic compounds, which got lost during separation, were shown to be very often related to small acidic compounds (data not shown, tested with formic and acetic acid).

In screenings with cooled diethyl ether and dichloromethane, the availability of volatile compounds in waste material was tested. The waste material was extracted from ice-cold waste particles, evaporation of solvents was performed using mild conditions (10°C, >500 mbar). Thereafter, fractionation with silica flash chromatography was performed (data

not shown, separation with petrol ether (boiling point 20-40°C), pentane, dichloromethane and diethyl ether). There were no indications of different compositions compared to standard conditions (extraction at room temperature; evaporation at 40°C and pressure down to 20 mbar). Possible volatile bioactive compounds could have been lost during transportation or storage of waste samples. This experiment should be repeated with fresh waste material to identify possible bioactive volatiles with bioassays and GC-MS.

In order to avoid artefacts, several chemically inert organic solvents were tested for their abilities to extract bioactive compounds. While methanol extracted not only bioactive compounds but also a lot of ions and particles, because methanol is miscible with water, unpolar solvents for liquid/liquid extractions were preferred. Several solvents with different polarities were tested, for example hexane, diethyl ether, dichloromethane, and compared to short term extractions with ethyl acetate.

Finally, a mixture of diethyl ether and acetone (9:1) was chosen to extract waste samples, hydrochloric acid was added for acidic conditions. The ultrasonic finger was used in order to support intermixture of particles in an aqueous environment and organic solvents. Artefacts were no longer observed. Unfortunately, the previously described bioactivity[32] was lower as estimated even when using ethyl acetate (without formation of acetic acid). The extraction efficacy did not differ when shaken overnight or ultrasonic assisted with chemically inert solvents.

5.2.2.4.4 Origin of bioactive compounds in leaf-cutting ants' waste

The waste consists of brownish waste particles and bodies of dead ants. In order to distinguish their contribution to the overall bioactivity, dead ants and particles were separated. Because separation by hand was very time consuming, a protocol with solvents was established. Some organic solvents were shown not to extract bioactive compounds and were therefore tested for their ability to separate bodies and particles. Hexane did not extract bioactive substances but particles stayed on the ground while ant bodies swam on the surface (Fig. 51 A). Compared to methanol (Fig. 51 B) and water (Fig. 51 C), the separation with hexane was most efficient. The bodies were removed with a kitchen strainer and extracted separately.

Fig. 51: Comparison of solvents to separate bodies of dead ants and waste particles. A: Hexane; B: Methanol; C: Water.

The waste particles come from the exhausted fungus material which arises from bramble leaves. The waste as well as the fungal cultivar and the bramble leaves contain a huge set of microorganisms, which are able to produce or degrade antibiotic compounds. Leaf-cutting ants produce antibiotic compounds in their glands and symbiotic bacteria were shown to produce further compounds. Leaf-cutting ants are able to spread those compounds on their bodies and in their nest.[21, 39-40] In order to relate antibiotic compounds with their origins, several intermediate samples were taken (Fig. 52).

At first, bramble leaves were tested for their bioactivity (Fig. 52 A). Indeed, extracts of bramble leaves showed bioactivity against bacteria as well as against fungi. This will be discussed in another chapter of this work (Ch. 5.2.3; Antifungal and antibacterial bioactivity of bramble leaves).

Unfortunately, no fungal cultivar samples or a sufficient number of living leaf-cutting ants were extracted due to a lack of material (Fig. 52 B). This would be interesting, because in the fungal chamber of leaf-cutting ants, at least one *Burkholderia* sp. bacterium was isolated and described to produce antibiotic substances.[30] The chemical defense of leaf-cutting ants working in the fungal chamber was separated in two parts. On the upside, only small workers without bacterial biofilm and on the downside merely mayor workers with bacterial biofilm were reported.[39, 41-42] This would make the process even more complex, as the fungal chamber needs to be divided in at least two areas. The symbiont of the fungus-growing ant *Cyphomyrmex minutus*, *Tyridiomyces formicarum*, was found to produce several antifungal diketopiperazines which were suspected to protect the fungal cultivar or its host.[38]

Bioactivity against *Bacillus subtilis, Escovopsis weberi* or *Fusarium* spp. was not only shown for extracts of waste particles, but also for extracts of bodies from dead ants (Fig. 52 C). Whether the bioactivity differs in several layers of leaf-cutting ants' waste is not known. I showed that there are active transportation mechanisms in leaf-cutting ants' waste (Ch. 5.2.1.4.4; p. 26). It would be nice compare the presence of bioactive compounds in the different layers of leaf-cutting ants' waste after their structures were elucidated.

A) Bramble leaves	proven
B) Fungal symbiont	
- itself?	unknown (Agar extracts)
- bacteria on fungus?	unknown (Fungus extracts)
- spreaded by ants? (glands, gut and/or bacteria?)	unknown (living ant extracts)
C) Waste chamber	proven
- remaining activity from fungal chamber?	separated
- spreaded by ants? (glands and/or bacteria?)	✓ Substrate
- bodies of ants? (as growth medium for bacteria?)	✓ Ants

Fig. 52: Possible sources of bioactive substances and sources which were proven in this study for leaf-cutting ants' waste and bramble leaves.

5.2.2.4.5 Comparison of bioactivity in leaf-cutting ants' waste

Waste samples from different collection time points of *Atta vollenweideri*, *Atta colombica* and *Acromyrmex echinatior* were separately mixed in order to homogenate the samples of each colony. The waste was weighed and the dry weight was estimated with a portion after lyophilisation. The amounts of the wet weights ranged between 440 and 520 g. The dry weights ranged between 240 and 360 g.

To the best of my knowledge, there are no examples in literature, where somebody tried to compare profiles of bioactive compounds from several leaf-cutting ant samples.

The bioactive extracts were separated using silica flash chromatography with similar protocols in order to compare bioactivities of fractions. The extracts were separated in less than 10 fractions in order to not split the bioactive compounds into too many fractions. Separation with RP-C_8 and RP-C_{18} HPLC in 28 fractions with the used columns showed no bioactivity anymore which might be due to distribution of antibiotics in many fractions and/or removal of synergistic effects. Mixtures of fractions regained their bioactivity, therefore bioactivity was not lost during these procedures.

Unfortunately, the amount of the collected waste material did not suffice for all planed experiments. The bioactivity was lower as expected, especially without the self-made activity which was described previously (Ch. 5.2.2.3.5; p. 66). Therefore, only silica flash chromatography generated reliable results. The results were already compared by Xenia Schilke in her bachelor thesis. She was supported with all initial extracts and available waste material, furthermore she compared the bioactive profile of previously prepared bramble leaf extracts (see Ch. 5.2.3; Antifungal and antibacterial bioactivity of bramble leaves).

There was antibacterial activity against *Bacillus subtilis* in fraction 5 of all waste extracts except for extracts from *Acromyrmex echinatior* (Tab. 4). All extracts showed antifungal activity against *Escovopsis weberi*. Extracts of *Acromyrmex echinatior* showed the broadest

range with antifungal compounds in fractions 1, 3 and 5. Waste particles of *Atta vollenweideri* showed the weakest antifungal activity.

Tab. 4: Profiles of bioactive fractions described by Xenia Schilke (2015). Indication of relative inhibition zone diameters (- no inhibition zone; +++ high diameter).

Bioassay organisms	*Bacillus subtilis* / *Escovopsis weberi*			
Fraction number	***Atta vollenweideri***	***Atta colombica***	***Acromyrmex echinatior***	***Bramble leaves*** *(Rubus fructicosus)*
F1	- / -	- / -	- / +++	- / -
F2	- / -	- / -	- / -	- / -
F3	- / -	- / -	- / +++	- / +++
F4	- / -	- / ++	- / -	+ / +++
F5	+++ / +	+++ / +++	- / +++	+++ / +

5.2.2.5 Outlook

The previously described extraction and purification protocol[32] was shown to be ineffective. For identification of possible volatile bioactive compounds, fresh waste material could be extracted with low boiling solvents or methods described elsewhere (Ch. 6.1.3.6; p. 148) and analyzed by GC-MS.

The newly developed extraction protocol using a diethyl ether-acetone mixture (9:1) under acidic conditions (hydrochloric acid) generated bioactive extracts reproducibly. There were no indications for a loss of bioactivity after fractionation by silica flash chromatography followed by RP-C18-HPLC. Only splitting in fractions and/or dilution effects prevented further bioassay-guided fractionation.

Therefore, this approach has to be repeated with more waste material. For screenings, around 2 to 4 liters of waste material were used. For the separation, around 10 to 15 liters of each waste sample was used (approximately 500 g). Indeed, several kilograms of waste have to be collected in order to generate reasonable results. Waste samples were shown to contain a variety of bioactive compounds, which splits bioactivity during fractionation processes (Fig. 53 A, B).

The identification of the bioactive compounds could either be started with waste material, which might be the most complex sample, or parts involved in the process of waste

generation like bramble leaves or living ants (Fig. 53 C). In Germany, bramble leaves are available all year round at waysides or edges of forests.

Bioactive compounds from bacterial isolates, which were grown under lab conditions, might also contribute to the understanding of waste compositions, but sensitive detection methods are necessary to identify the presence of these antibiotics in waste material.

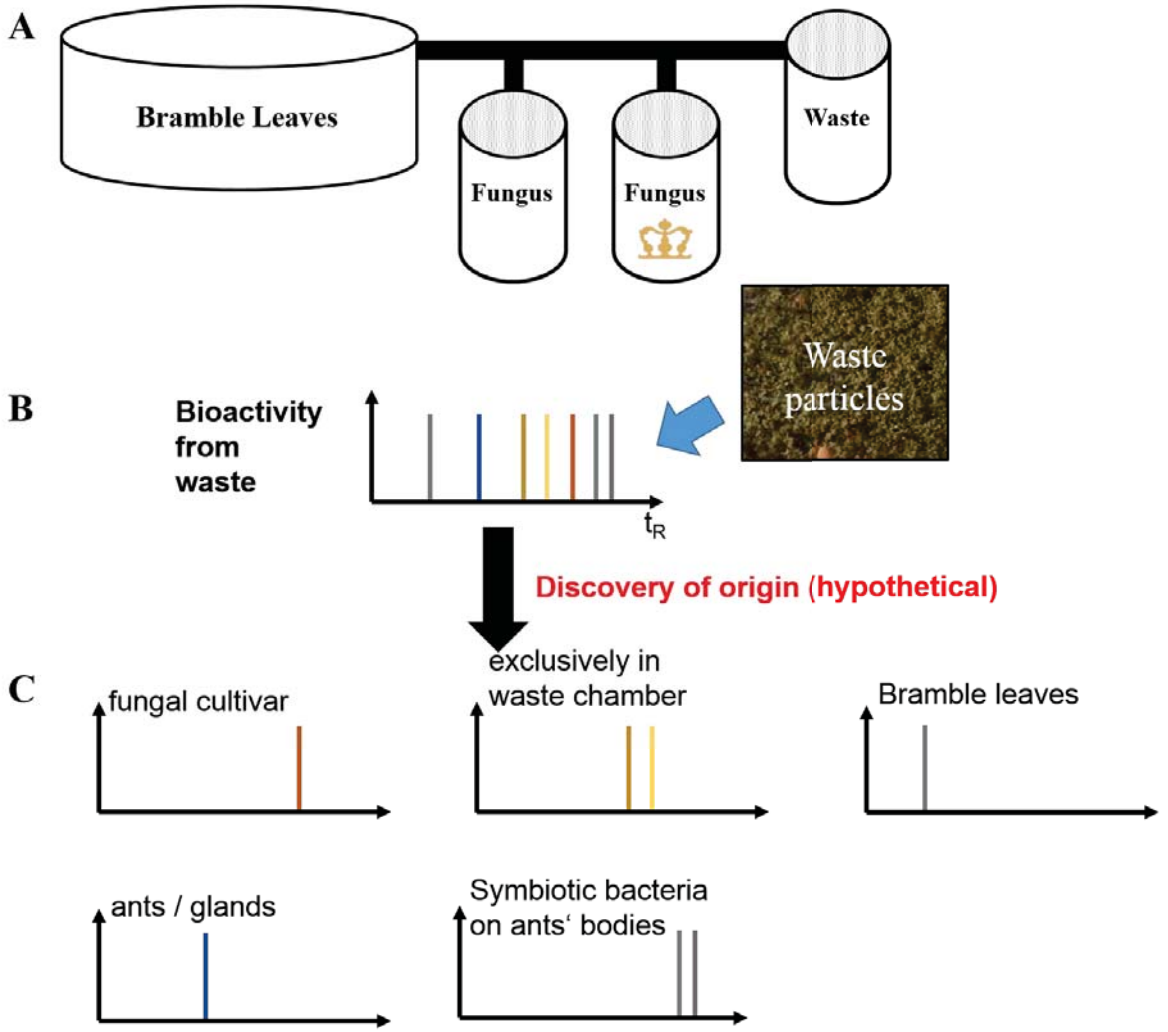

Fig. 53: Schematic overview of sources for bioactive compounds of leaf-cutting ants' waste. A: Minimum chamber system of leaf-cutting ants. B: Hypothetical composition of extracts from waste particles. C: Hypothetical origin of extracted bioactive compounds.

5.2.2.6 Conclusion

In this project, the composition of leaf-cutting ants' waste was described. Additionally, water contents of different leaf-cutting ant species and colonies were determined.

Moreover, previously described extraction and purification procedures could not be reproduced; estimated bioactivity was much higher than observed bioactivity. Verification experiments showed generation of artefacts, therefore new extraction and purification workflows were developed. Volatile bioactive compounds could have been lost during

transportation or storage of waste samples. This experiment should be repeated with fresh waste material to identify possible bioactive volatiles with bioassays and GC-MS.

Waste samples were separated in particles and dead ants' bodies, which both showed bioactivity. Bramble leaves, as initial substrate for cultivation of the fungal symbiont, were shown to be bioactive against *Escovopsis weberi* and *Bacillus subtilis*. Living ants and the fungal symbiont were not tested for bioactivity due to a lack of samples.

Waste samples of all leaf-cutting ants showed antifungal activity against *Escovopsis weberi*. Antibacterial activity was shown for *Atta vollenweideri* and *colombica*. Bioactive fractions after silica flash chromatography were separated using HPLC, where no single fractions were found to be bioactive, while a combination of all fractions remained bioactive.

This project needs to be continued with much more leaf-cutting ant waste material.

5.2.3 Antifungal and antibacterial bioactivity of bramble leaves and stem

Contributions

Extraction and purification started in 2014 with Luca Dietrich as helping scientist (HIWI; 40 hours in total), further efforts were topic of "Vertiefungskurs Chemische Ökologie" in 2015 with Jan Henkel and Franziska Kopietz.

5.2.3.1 Abstract

Blackberry fruits are known for their nutritional, cosmetic or medical use. In fact, not only fruits of *Rubus fructicosus* (family *Rosaceae*) are in focus of research, but also plant material such as leaves, stem and roots. It was shown, that methanol extracts of blackberry plant matter yielded antibacterial compounds. Their structures have not been elucidated so far.

In order to compare bioactivity found in blackberry plant material with our findings in leaf-cutting ants' waste, plant matter was extracted and tested in bioassays. To the best of our knowledge, this is the first time that the presence of antifungal compounds in leaves and stem of blackberry is described. Furthermore, the presence of at least three different bioactive compounds was shown, one antibacterial and two antifungal.

5.2.3.2 Introduction

Fruits of *Rubus fructicosus* (family *Rosaceae*) are generally known as blackberries. Besides their nutritional and flavoring characteristics, other plant parts like leaves and stem were already used in traditional medicine. Fruits and plant material were shown to function as anti-inflammatory and anti-diarrheic agents for human disease treatment.[43-44]

The antibacterial activity of fruit and plant extracts was shown, but responsible bioactive compounds were not identified yet.[45-46]

Bramble plants attracted my interest, because they are used as food supply for leaf-cutting ants in German laboratories among other *Rosaceae* plants. In order to identify bioactive substances which contribute to the repression of fungal contamination in waste chambers of leaf-cutting ants, bramble leaf extracts were analyzed. The current knowledge in conjunction with *Rubus* spp. was reviewed in 2014.[47] In addition, I found out that extracts of bramble plants contain not only antibacterial but also antifungal compounds. While screenings for antibacterial and antifungal compounds in literature was only conducted with methanol,[46] I furthermore used ethyl acetate and diethyl ether-acetone mixtures for extraction. Indeed, the acidic methanol fraction exhibited only antibacterial and no antifungal bioactivity. Whereas acidified ethyl acetate and diethyl ether extracts of bramble leaves and stems contained both, antibacterial and antifungal compounds.

The antibacterial and antifungal compounds were extracted and fractionated using bioassay assay guided isolation. The main aim was again, to identify chemical structures of bioactive compounds. Unfortunately, there was no sufficient financial and material support to overcome spotted difficulties.
Therefore, I want to support prospective efforts by description of my findings.

5.2.3.3 Methods

5.2.3.3.1 Origin of bramble plant material

Bramble leaves and stems were collected in Konstanz, Germany, with the help of garden shears. Main parts were collected in September 2014 and January 2015 between the train stations Fürstenberg and Petershausen (longitude 47.675640684288176; latitude 9.167168140411377; WGS 84).
The fresh material was transported to the University by car and processed immediately.

5.2.3.3.2 Crushing of plant material

Bramble stem were cut into small pellets of around 2-5 cm using garden shears or a garden shredder (Bosch, Germany).
Bramble leaves were frozen using liquid nitrogen and fragmented using a metal bucket as a hammer.
Weight and water content analysis was performed as described before (Ch. 5.2.2.3.3; p. 66)

5.2.3.3.3 Extraction and purification procedure

Screenings showed antifungal and antibacterial compounds in acidified ethyl acetate or diethyl ether extracts. Antibacterial compounds were extracted in screenings using acidified methanol (around pH=2; hydrochloric acid).
Extraction was performed using ethyl acetate or a diethyl ether-acetone mixture (9:1) at native pH first. This treatment removed inactive substances beforehand (very viscous crude extract with many colorful compounds). Afterwards the extraction was performed in 2 l beakers using the principle of counter-current extraction in order to increase efficiency with acidified solvents as described before (Ch. 5.2.2.3.5; p. 66).
Leaf fragments or stems were then placed in acidified water (around pH=2; hydrochloric acid) and treated with an ultrasonic finger (15 min; 70% amplitude; 4/1 sec on/off pulse). This material was extracted in 2 l beakers using the principle of counter-current extraction in order to increase efficiency of extraction. The solvent was dried over sodium sulfate before evaporation using a rotavap (Büchi, Switzerland).

The purification process of the crude extracts was performed as described before (Ch. 5.2.2.3.6, p. 67 and Ch. 5.2.2.3.7, p. 67).

5.2.3.4 Results and Discussion

Bramble plant material (*Rubus fructicosus*) was collected several times in Konstanz, Germany. The extraction procedure was simplified as condition and solvents from preliminary tests were found to be effective.

5.2.3.4.1 Water content of bramble leaves and stems

The water content of bramble leaves and stems depends on the season of collection and was estimated in February 2015. Bramble leaves contained 56±2% water (N=5), bramble stems contained 26±7% water (N=2). Drying of stems was more difficult than leaves, as the leaves were softer and could be cut in smaller pieces which resulted in bigger surfaces.

5.2.3.4.2 Bioactivity of bramble material

Comparison of ethyl acetate and methanol extractions of bramble leaves with either native or acidified conditions showed, that acidified extracts with ethyl acetate caused noteworthy inhibition zones against *Escovopsis weberi*, *Beauveria bassiana* and *Fusarium* spp. (Fig. 54 A). The antifungal and antibacterial activities of extracts obtained by different extraction conditions were compared. Both, extracts from bramble stems and leaves exhibited antibacterial and antifungal activity (Fig. 54 B, C; 1: stem 2: leaves). In contrast, extracts with acidified methanol only showed antibacterial, but no antifungal activity (Fig. 54 B, C; 3: methanol). A comparison of suitable solvents showed, that previously established protocols with diethyl ether-acetone mixtures extracted antibacterial and antifungal compounds with a similar efficiency as ethyl acetate or methanol (Fig. 54 B, C; 2: ethyl acetate; 3: methanol; 4: diethyl ether-acetone mixture).

Bramble leaves and stems extracted with acidified methanol released mainly antibacterial compounds, while acidified diethyl ether-acetone mixtures extracted both, antifungal and antibacterial compounds. Diethyl ether is an inert, volatile solvent and was shown to have advantages regarding extractions compared to ethyl acetate (Ch. 5.2.2.4.3; p. 69).

This is the first time, that antifungal compounds in *Rubus fructicosus* are described. Whether those bioactive compounds were bound in the plant material and released by acidic hydrolysis or their functional groups required acidified conditions in order to be extracted is not known yet.

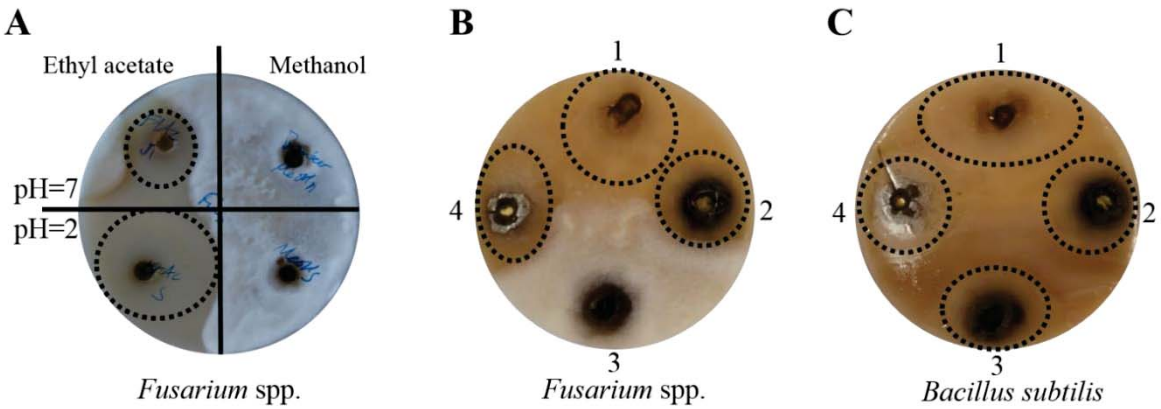

Fig. 54: Comparison of conditions for extraction of bioactive molecules from bramble leaves and stem. Circles with dashed lines indicate inhibition zones. A: Bioassay against *Fusarium* spp.. Comparison of ethyl acetate and methanol at native and acidified conditions. B: Bioassay against *Fusarium* spp. C: Bioassay against *Bacillus subtilis*. Extracts prepared with 1: Bramble stems; acidified ethyl acetate. 2: Bramble leaves; acidified ethyl acetate. 3: Bramble leaves; acidified methanol. 4: Bramble leaves; acidified diethyl ether-acetone mixture (9:1).

The crude extracts of not acidified extracts contained huge amounts of colorful plant material without bioactivity. This extraction step was used in order to already eliminate unwanted compounds. Several kilograms of bramble leaves and stem were extracted using acidified methanol or acidified diethyl ether-acetone mixtures. The extracts were treated separately and further purified using the described protocols (Ch. 5.2.2.3.6, p. 67 and Ch. 5.2.2.3.7, p. 67).

Separation of the extracts prepared with acidified diethyl ether-acetone showed at least three compounds with different lipophilic properties after separation by HPLC. Two separate fractions exhibited antifungal and one more polar fraction showed antibacterial activity. Separation of the acidified methanol extract showed at least one compound with antibacterial properties after separation by HPLC, which was more polar than the antifungal compounds. This result was also confirmed by the previously described experiment of Xenia Schilke (Ch. 5.2.2.4.5; p. 72). She was supported with extracts from bramble leaves in order to classify the bioactive compounds in her metabolic profiles of leaf-cutting ants' waste. The antibacterial fractions were more polar than the antifungal fractions (Tab. 4; p. 73).

The chemical structures of the compounds could not be elucidated due to the lack of material. For elucidation with NMR, more material needs to be extracted and purified. No additional information could be gained with application to mass spectrometry (LCQ; positive and negative tunes; see Ch. 7.5; p. 189 for approaches).

The isolation of bioactive substances has to be repeated with more plant material. Appropriate equipment for collection of bramble plant samples, as well as for the fragmentation procedure has to be purchased. Every week of handcrafted collection and

break-down of plant material only took less than one hour for extraction. As I only brought my private gardening equipment for the described experiments, suitable gardening tools will help to improve this process.

5.2.3.5 Outlook and Conclusion

To the best of our knowledge, for the first time bramble leaves and stems were described to contain both, antifungal and antibacterial compounds. The bioactive compounds were extracted using acidified methanol (only antibacterial) or diethyl ether-acetone mixtures (antibacterial and antifungal). Separation of the extracts led to a total of at least three bioactive compounds.

The structures could not be elucidated because of a lack of material caused by a lack of support. Proper equipment for cutting, transporting and breaking down of plant material is necessary before the project can be continued.

As we extracted more than five kilograms of leaves and stems (wet weight) for the screenings and the presented workflow, and we did not end up with a sufficient amount of bioactive compounds, this has to be repeated with more material.

Extracts of stems contained a smaller variety of inactive compounds. Bramble stems are on the other hand very hard, thus breaking down and extraction are very exhausting without sufficient equipment.

According to the efforts for identification of bioactive compounds in leaf-cutting ants' waste, the bioactive compounds derived from bramble leaves could be easier accessed by extraction of bramble plant material directly. After the bioactive compounds from bramble leaves are known and detectable by LC-MS, their presence could be directly estimated in extracts from leaf-cutting ants' waste.

5.3 Ratio of *R*/*S*-γ-Octalactones in glandular secretions of leaf-cutting ants

Contributions

This project was initially started in the Emmy Noether junior group of Prof. Dr. D. Spiteller at the Max Planck Institute for Chemical Ecology (MPI CE, Jena, Germany) associated with the group of Prof. Dr. Boland.

As part of her diploma thesis, Susanne Haeder analased some metapleural glands from leaf-cutting ants by SPME-GC-MS. Furthermore, she performed stereo selective synthesis of γ-octalactones as a side project.

Leaf-cutting ants were received from Dr. Wirth (University of Kaiserslautern) or were collected by myself at the University of Würzburg. I thank Prof. Dr. Flavio Roces, Dr. Daniela Roemer and Adrienne Gerber-Kurz for their support.

Furthermore, Luca Dietrich wrote his bachelor thesis "Charakterisierung von Oktalaktonen und kutikulären Verbindungen ausgewählter Blattschneiderameisen mittels GC-MS" (submitted in August 2016) regarding γ-octalactones from metapleural glands and volatile cuticular compounds of leaf-cutting ants.

Control experiments for instrumental analysis of γ-octalactones from metapleural glands were topic of "Vertiefungskurs Chemische Ökologie" in 2015, prepared by Rafael Fahrner.

Some equipment and all travel expenses were private financed by myself.

5.3.1 Abstract

The evolutionary arms race between farming insects and pathogenic microbes resulted in several defense strategies on both sides during the last 50 million years.

Leaf-cutting ants are unique among farming insects as they support their fungal cultivar with fresh leaf material. The ants provide not only beneficial growth conditions, but also perform behavioral and chemical care. While leaf-cutting ants could use antimicrobial compounds from external sources, such as *Actinomycetes*, one of their key sources for protective antibiotics are chemicals from their metapleural glands. Especially when challenged with pathogens, leaf-cutting ants start hygienic behavior like grooming and spreading of metapleural gland secretions to disinfect their bodies and nest components. The composition of metapleural gland secretions has been intensively studied and several antimicrobial compounds have been identified.

Among them, γ-octalactones attracted our interest because they possess a chiral center and are only dominantly present in the metapleural gland secretions of some leaf-cutting ant species. In order to study their occurrence, individual ants were dissected, volatiles were

collected using SPME and analyzed with the help of chiral GC-MS. Interestingly, the enantiomeric ratio of *R*- and *S*-γ-octalactone varied among individual ants.

5.3.2 Introduction

Metapleural glands are a pair of exocrine glands at the posterolateral end of the mesosoma which is unique for almost all ants (Formicidae).[48] The secretions of these glands were described to produce chemical cocktails with antibacterial as well as antifungal properties.[49-50] Especially fungus growing ants developed a variable composition of metapleural gland secretions in order to keep their nest and fungal cultivar free from encroaching pathogen contaminations.[51-52] The combination of ant behavior, together with chemical defense mechanisms from glands and symbiotic bacteria ensured the survival of fungus growing ants for several million years.[24, 53] Among fungus growing ants, especially the metapleural glands of leaf-cutting ants were intensively studied.[51] Besides the chemical composition, also morphological differences were investigated.[54-56] The chemical composition of chemical cocktails from metapleural glands were not only described, but also their antimicrobial abilities were compared against relevant pathogens and symbionts.[21, 34-35]

The antifungal abilities of γ-lactones were described against *Escovopsis weberi*, a specialized mycoparasite of the fungal cultivar.[35] Besides the antifungal abilities, γ-octalactones (Fig. 55 A) were found to be dominant only in some *Acromyrmex* species, while they were not observed for *Atta*.[57] γ-Octalactones possess a chiral center in position C_4, their presence in leaf-cutting ants was shown for extracts from *Acromyrmex crassispinus* in 1993 with one picture in a book chapter as an example for enantiomer separation with cyclodextrin columns.[58]

Investigations of several leaf-cutting ant species supported the finding, that enantiomer ratios varied not only between species, but also between individual ants (Fig. 55 B). Usage of solid phase micro extraction (SPME) together with chiral columns and gas chromatography mass spectrometry (GC-MS) measurements allowed a fast and effective measurement of single glands within 20 min.

For this project, six *Acromyrmex* and three *Atta* species were compared concerning their γ-octalactone production in metapleural glands. Individual ants of *Acromyrmex echinatior* and *octospinosus* were further investigated and compared in consideration of their chamber of origin and head sizes.

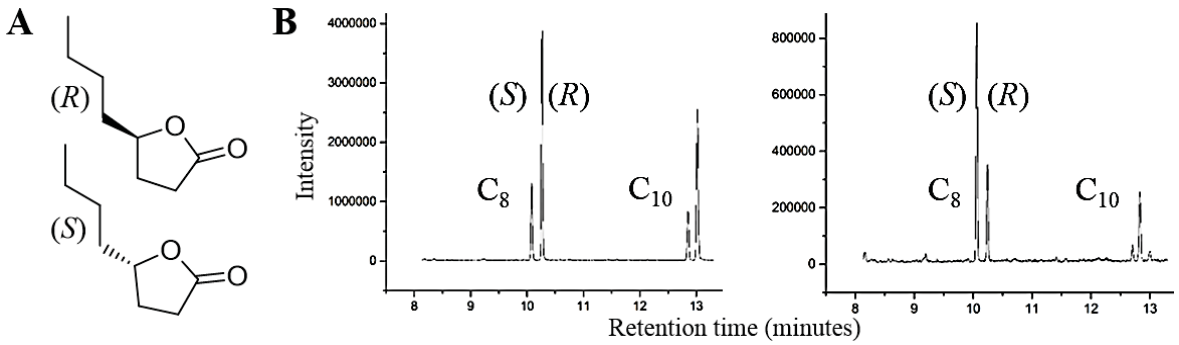

Fig. 55: A: Structures of γ-octalactone enantiomers. B: Separation of γ-octa- (C8) and γ-decalactone (C10) from metapleural glands of two individual ants (*Acromyrmex echinatior*) by chiral GC-MS (ion trace m/z=85).

5.3.3 Material and methods

5.3.3.1 Origin of leaf cutting ants

Most samples were collected by me at the University of Würzburg in the lab of Prof. Dr. Roces. I collected ants from several chambers with tweezers and transferred them directly into a pre-cooled centrifugation tube (15 or 50 ml). After collection of up to 20 ants, the tube was frozen at -20°C. Tubes were transported frozen surrounded by thermal packs in a car (travelling time around 4 hours). I collected *Acromyrmex ambiguus*, *octospinosus*, *lobicornis*, *lundii*, *heyeri*, furthermore *Atta sexdens* and *colombica* in Würzburg.

Samples of *Atta vollenweideri* and *Camponotus blandus* were collected in the lab of Dr. Kleineidam (University of Konstanz). Only ants from the leaf and waste chamber (*Atta*) or from the open arena (*Camponotus*) were collected and frozen directly (-20°C).

Samples of *Acromyrmex echinatior* and *octospinosus* were received from Dr. Wirth (University of Kaiserslautern). They were sent within a postal package equipped with thermal packs. Transportation time was around three days. They were stored frozen at -20°C after arrival.

5.3.3.2 Dissection of leaf-cutting ants

All samples were processed and stored frozen (-20°C or colder).

Leaf cutting ants were dissected using a common scalpel on dry ice (-81°C). Body parts were stored variably, depending on which measurements were planned.

For single gland analysis with SPME-GC-MS of *Acromyrmex*, the thorax part with gland was stored in a glass vial (2 ml) with insert (9 mm; 200 µl). The head was stored in a reaction tube for size measurements. Both tubes were marked with the same name.

For pooled measurements, body parts were combined in collections of 10 or 20 ants and mainly stored in a glass vial (2 ml) with insert (9 mm; 200 µl or a big insert with 500 µl).

5.3.3.3 Measurement of the head width of leaf-cutting ants

The heads were placed under a binocular and photographed with 1,6x magnification (Canon Eos D 600, 18 Megapixel, ISO 100). To determine the dimensions of the heads, a micrometer ruler was used (Bresser; Article number 5916700; Scale 0-20 mm; Increment 0,1 mm).

The software image J (Version: 1.50i; March 2016; https://imagej.nih.gov/ij/) was used for size measurements. After loading the picture, the function "Process/Find edges" was applied to increase the contrast (Fig. 56 B). The scale of the ruler was measured for a minimum of 3 mm with the measure function (CTRL+m). Shorter distances increased the measurement error.

Thereafter, the eye distance was determined with the same function (Fig. 56 C). The distance of the eyes in mm was calculated from the number of pixels in the result tabulator.

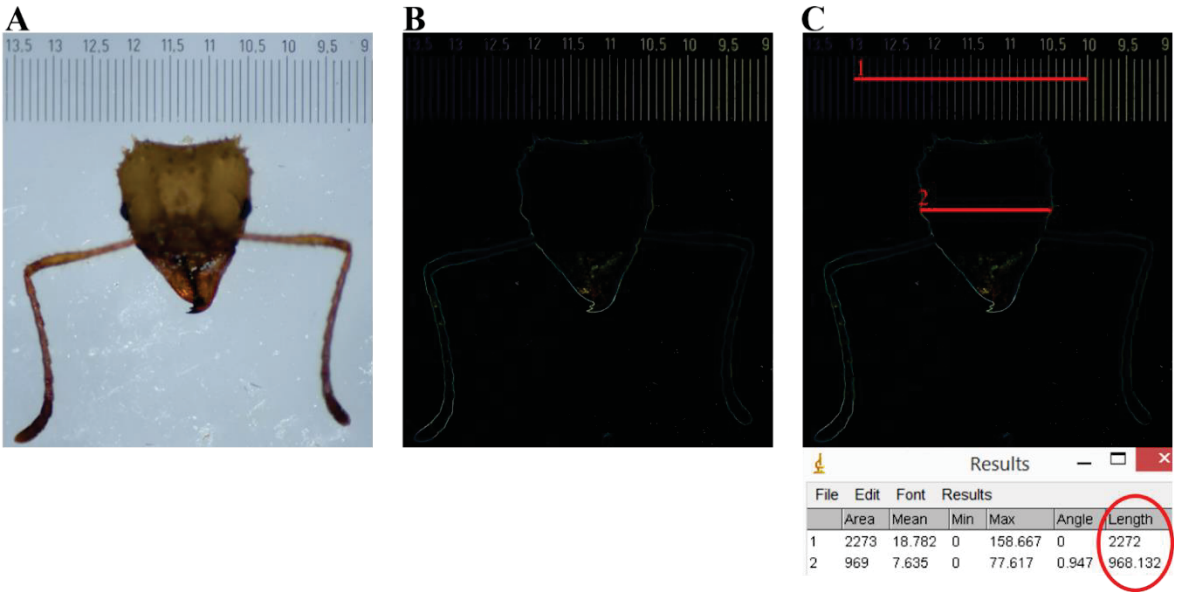

Fig. 56: Example for head size estimations of leaf-cutting ants. A: Picture of a head on the micrometer ruler. B: Transformation with the "find edges" function. C: Measurement points for head size estimation (1, 2), with the length on the ruler compared to head width in the results table (circle).

5.3.3.4 SPME-GC-MS analysis of volatile compounds

The SPME fiber was cleaned by heating in the injector of the GC oven. The cleanness of the column and the measurement instrument was ensured daily.

A SPME fiber (Supelco; red; polydimethylsiloxane) together with a ISQ Single Quadrupole GC-MS Systems (Thermo Scientific) equipped with a Hydrodex β-6TBDM (25 m x 0,25 mm, 0,25 µm, Macherey Nagel, Düren) GC-column was used for analysis.

Collection temperatures were compared from -25 to 100°C using standard mixtures, which showed reproducible results for 30, 40 and 50°C (Ch. 5.3.4.3.3, p. 90). For SPME-GC-MS

measurements, an incubation temperature of 45°C and time of 13-17 min were chosen. The SPME fiber was applied for 1 min to the injector of the GC instrument.

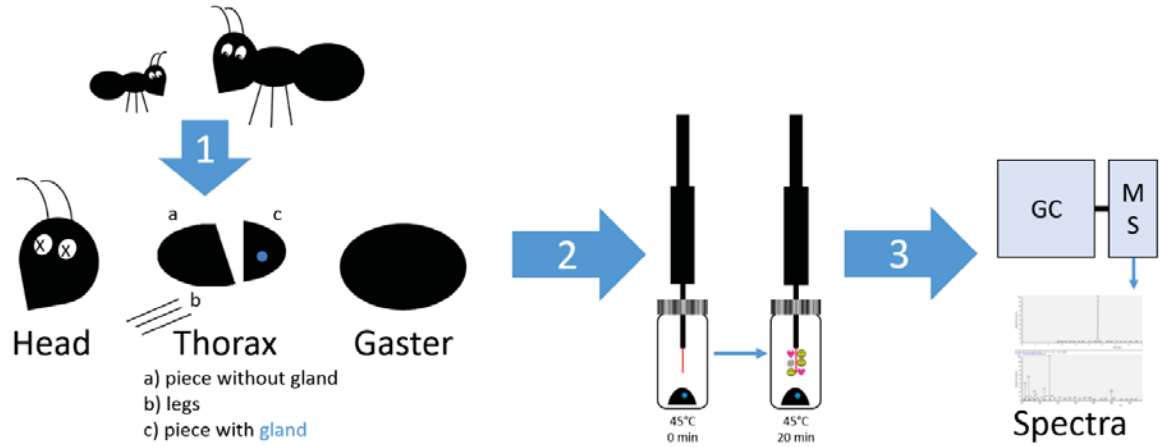

Fig. 57: Workflow of sample preparation with ant dissection, volatile collection with SPME and analysis with chiral GC-MS.

The following GC temperature program was developed to separate *R*- and *S*-γ-octalactone in a short time for single gland measurements. For pooled samples, a longer temperature gradient was used.

Tab. 5: Conditions and temperature gradients of GC-MS measurements.

Mode of injection	Splitless, constant septum purge	1,7 ml/sec Helium
Injector temperature	180°C	
	short	**long**
Initial temperature	70°C	70°C
Ramp	15°C/min until 130°C	4°C/min until 180°C
	6°C/min until 180°C → hold for 1 min	→hold for 1 min
Runtime	13,3 min	28,5 min

MS	
Ionization mode	EI (70 eV)
Runtime	5,5 min until end
Mass range	45-300/550
Scan time	0,2 s
Detector gain	$3 \cdot 10^5$

R- and *S*-isomers of γ-octalactone were synthesised previously by Susanne Haeder using the protocol of Habel and Boland [59]. Racemates of γ-octa- and γ-decalactone were purchased from Sigma Aldrich.

Retention times of identified compounds were for short and long GC method:

S-γ-octalactone (R_t = 10,0 min; 21,8 min)
R-γ-octalactone (R_t = 10,2 min; 22,3 min)
S-γ-decalactone (R_t = 12,8 min; 26,0 min)
R-γ-decalactone (R_t = 13,0 min; 26,2 min)
Heptadecane (R_t = not observed; 22,4 min)

5.3.3.5 GC-MS data analysis and processing

The software Thermo Excalibur (Version: 2.2 SP 1.48, Thermo Scientific) was used to open raw-files from the GC-MS instrument.

Peak areas in the TIC and mass selection (ion trace m/z=85) were integrated with the Genesis algorithm and exported to Microsoft EXCEL. With the peak areas, the enantiomeric ratio (*S*/*R*) was calculated.[60]

OriginLab Origin (Version 2015G (Teaching license; University of Konstanz); 64 bit; March 2016) was used for data processing and plotting.

5.3.3.6 Activity of *R*-/*S*-γ-octalactone against pathogenic fungi

The bioactivity of γ-octalactone was tested against *Escovopsis weberi* and *Beauveria bassiana*.

The bioassays were prepared on gSFG-Medium (Glucose 10 g, soy flour 10 g, Agar-Agar KobeI 15 g and Glycerol 4 g per liter ddH_2O) and incubated at 28°C. For spore preparations, the fungi were harvested after 21 days. Agar plates were flooded with adH_2O, mixed on the surface of the agar plate with fungal hyphae and transferred into a reaction tube. The liquid was filtered through cotton wool (compressed to a length of 0,5 cm in a tube) at 800 rpm. Thereafter, the liquid was transferred into another tube and centrifuged for 10 min at 3000 rpm. The supernatant was filtered again through compressed cotton wool at 800 rpm. To harvest vital hyphae, the agar plate was flooded with adH_2O after 4 (*Escovopsis weberi*) or 8 days (*Beauveria bassiana*) of growth. The suspension was vortexed and used directly. For storage, a 60% glycerol solution was used and stored at -20 or -80°C.

For bioassays, several holes with equal distances were punched in agar using the backside of a Pasteur pipette. Dilutions of octalactone with methanol were prepared, and 90 µl of the

dilution were pipetted in the hole (Tab. 6). After diffusion and evaporation of the dilution, the organism was distributed all over the plate.

The γ-octalactone racemate was tested at first from undiluted to 10^{-8}. γ-Octalactone is described with a molecular mass of 142,2 g/mol and a density of 0,97 g/l (CemicalLand21.com and TheGoodScentsCompany.com; June 2016). The racemate showed bioactivity up to a dilution of 10^{-2}, therefore *R*- and *S*-γ-octalactone were tested separately in 1:50 and 1:100 dilutions for spore suspensions of *Escovopsis weberi*.

Tab. 6: Calculation of γ-octalactone amount in dilutions.

Dilution	pure	1:50	1:100
Amount per hole	87,3 mg (600 µmol)	1,75 mg (12 µmol)	0,87 mg (6 µmol)

After inoculation, the plates were incubated at 28°C and monitored daily after 3-7 days (*Escovopsis weberi*) or 6-12 days (*Beauveria bassiana*).

5.3.4 Results

5.3.4.1 Preliminary work

The presence of γ-octalactone and its dominance in some leaf-cutting ant species was already reported in the PhD thesis of Jochen Borchert in 1987, prepared in the lab of Prof. Francke (University of Hamburg).[57] GC measurements of liquid extracts from leaf-cutting ants' thorax were shown to contain γ-octa- and γ-decalactone dominantly for *Acromyrmex crassispinus, disciger* and *niger* but not for *Acromyrmex subterraneus* or *Atta sexdens*. The first stereochemical separation was shown for extracts from *Acromyrmex crassispinus* in 1993 with one picture in a book chapter to illustrate enantiomer separation with cyclodextrin columns.[58]

In the Emmy Noether junior group of Prof. Dr. D. Spiteller at the MPI Jena, some individuals of *Acromyrmex echinatior*, *Acromyrmex niger, Acromyrmex octospinosus*, *Acromyrmex octospinosus subsp. volcanus*, *Atta colombica* and *Atta sexdens* (N=5-14 each) were analyzed using SPME-GC-MS with a chiral column. It was assumed, that γ-octalactone is present in all *Acromyrmex* but not in *Atta*.

5.3.4.2 Antifungal activity of γ-octalactone enantiomers

γ-Lactones were shown to be present in metapleural gland secretions in 2000, when secretions were collected from *Acromyrmex octospinosus* with capillaries and measured with GC-MS.[34] The bioactivity of γ-octa- and γ-decalactone was investigated by Bot, et al. [35] and

tested against relevant organisms of leaf-cutting ants like *Escovopsis weberi*, *Leucoagaricus gongylophorus* and *Beauveria bassiana*.[35]

In my bioassays, racemic mixtures of γ-octalactone showed bioactivity up to 1:100 dilution, but not for 1:300 dilution. Investigations with pure *R*- and *S*-isomers showed that the *S*-isomer is only active until 1:50 dilution (Fig. 58 C; 12 µmol per hole) but not in 1:100 dilution (Fig. 58 D; 6 µmol per hole), while the *R*-isomer is still active in 1:100 dilution (Fig. 58 B; 6 µmol per hole).

The dilutions are not comparable with the dilutions used by Bot, et al. [35] because they used a disk not a hole based assay. Furthermore, γ-octalactone is not miscible with water, therefore the diffusion into aqueous agar media might be negatively influenced. The evaporation of γ-octalactone into the airspace below the agar medium might also play a role. On the one hand, the equilibrium between gas and liquid phase could lead towards lower concentrations of γ-octalactone in the holes. I used four holes on one agar plate, because the equilibrium should be reached faster and with less loss of γ-octalactone for each hole. On the other hand, volatiles in the airspace were shown to influence fungal growth (Liu, et al. [61] and references therein). As I did not observe growth influences around the solvent control, this influence was insignificant.

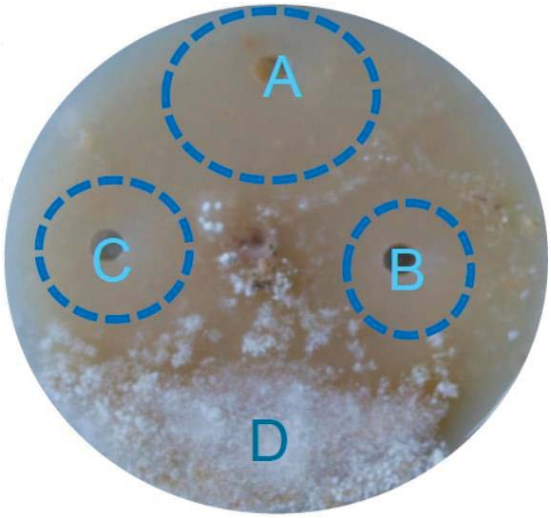

Fig. 58: Bioassay of *R*/*S*-γ-octalactone enantiomers against spores of *Escovopsis weberi*. A: *R*-γ-octalactone (1:50); B: *R*-γ-octalactone (1:100); C: *S*-γ-octalactone (1:50); D: *S*-γ-octalactone (1:100). Middle: Solvent control (methanol, not indicated).

R-γ-octalactone was more bioactive against spores of *Escovopsis weberi* than *S*-γ-octalactone. Previous investigations observed different bioactivity between *R*- and *S*-γ-lactones in bioassays against some organisms.[62] While *Candida albicans* did not discriminate between *R*- and *S*-γ-undecalactone (minimum inhibitory concentration of 102 µg/ml for both), *Aspergillus niger* was more sensitive against *R*-γ-undecalactone than *S*-γ-undecalactone (minimum inhibitory concentration of 51,2 compared to 102 µg/ml).

Our findings confirmed previous investigations which showed a comparatively poor bioactivity of γ-lactones against *Escovopsis weberi* and a discrimination between *R*- and *S*-γ-lactones with the *R*-enantiomer being more bioactive.

5.3.4.3 Evaluation of instrument parameters for SPME-GC-MS measurements

5.3.4.3.1 Determination of proportions for *R*- and *S*-γ-lactones

The usage of the terms enantiomeric excess, diastereomeric excess and enantiomer ratio in order to comparatively describe enantiomer proportions was discussed by Gawley [60] in 2008. Initially, the peak area ratio (*S*/*R*) was used to describe enantiomer proportions, but this expression was found to be not linear and therefore underestimated differences below a ratio of 1 compared to a ratio above 1 (Fig. 59; y axis; linearity as green bar on the right side). In contrast, the enantiomer ratio (*S*/*R*) showed linear distances. Mixtures of 1:4 and 4:1 have the same distance to the racemic mixture (1:1). Therefore, the enantiomer ratio will be used for the following descriptions of enantiomer proportions.

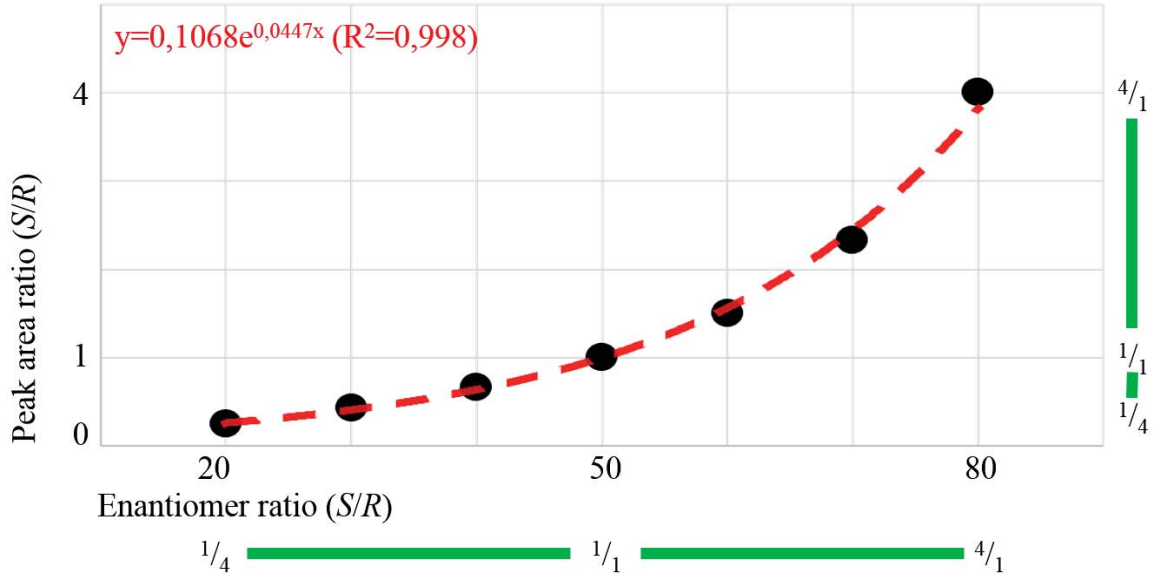

Fig. 59: Comparison of enantiomer ratio in correlation to peak area ratio. Indication of exponential fit (red line) and linearity of ratios (green lines).

5.3.4.3.2 Temperature gradient for GC separation

The previously used temperature gradient for GC separation of enantiomers was changed by comparison of several temperature programs to baseline separate *R*- and *S*-γ-octalactones. The retention times of *R*- and *S*-γ-octalactones were determined using the synthesized enantiopure compounds. Heptadecane was identified and confirmed using a reference sample with the pure compound (to be sure, multi-dimensional GC-MS has to be applied).

A long and a short method were developed. The short method (13,3 min) was used for ant species with dominant γ-octalactone and measurement of individuals or their body parts. The long method (28,5 min) was used for pooled samples with 10 or 20 ants or their body parts. Retention times were as follows for the short and the long method:

S-γ-octalactone (R_t = 10,0 min; 21,8 min)

R-γ-octalactone (R_t = 10,2 min; 22,3 min)

S-γ-decalactone (R_t = 12,8 min; 26,0 min)

R-γ-decalactone (R_t = 13,0 min; 26,2 min)

Heptadecane (R_t = not observed; 22,4 min)

5.3.4.3.3 Temperature for SPME collection of γ-octalactone

For the determination of collection time and temperature of γ-octalactone, a 1:1 mixture of the *R*- and *S*-enantiomers was prepared. The concentration of γ-octalactone was comparative to an average concentration of a single metapleural gland of *Acromyrmex echinatior*.

Collection temperatures below 0°C were hard to determine, as the signal intensities in MS spectra were very poor. This observation is positive because ant samples were stored at -20°C. The metapleural glands of the stored ants should not lose too much of the contained γ-lactone.

It was not possible to determine γ-octalactone in the total ion count for temperatures below -10°C (Fig. 60 A). Selection for the mass range (m/z=85) allowed integration of peak areas (algorithm: Genesis). Furthermore, the variation in observed peak areas and ratio were smaller for the mass range (Fig. 60 B) compared to total ion count (Fig. 60 A).

For temperatures of 30, 40 and 50°C, the calculated enantiomer ratio and the standard deviation were best compared to the prepared sample. Below 30°C, the relative standard deviation was more than 3,6%. Between 30 and 50°C, the relative standard deviation was smaller than 1,9%. Above 60°C, the relative standard deviation grew again and the calculated enantiomer ratios became incorrect.

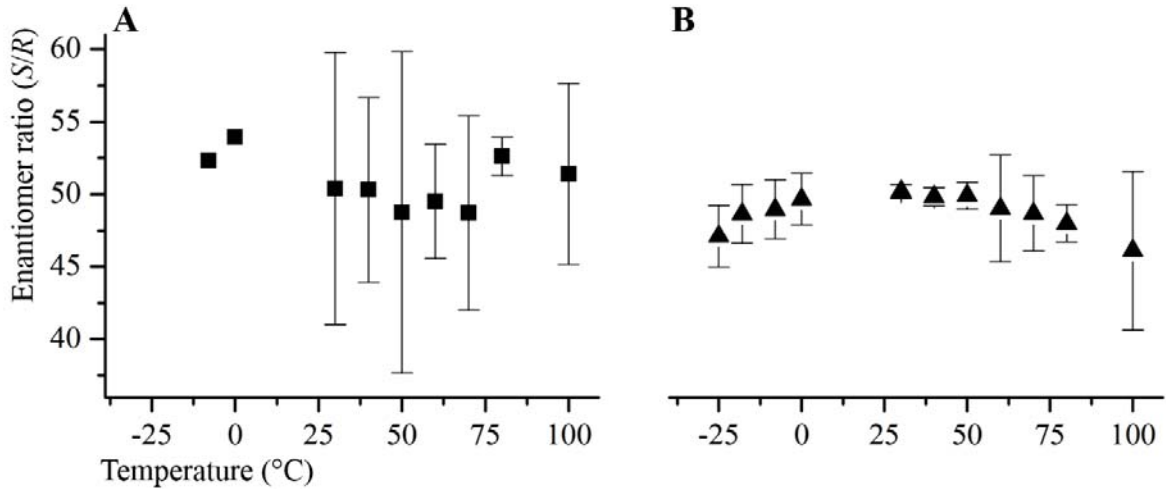

Fig. 60: Comparison of collection temperature with SPME in correlation to observed enantiomer ratio. A: Total ion count. B: Mass range (m/z=85). No signal for -24 and -18°C of A. N=1 for -10 and 0°C of A. Other signals N=2-4.

While these findings are true for prepared liquid samples, the enantiomer ratio of metapleural glands can not be measured comparatively.

The measurement time can not be estimated by comparative measurements, too. Therefore, several time points with metapleural glands were tested. Signal intensities grew up to 10 min collection time with SPME. Between 10 and 20 min, there was no difference visible. Above 20 min, the content of heavier compounds (γ-decalactones) increased compared to γ-octalactone.

With respect to surrounding tissue at the prepared thorax pieces, the temperature was set to 45°C with a collection time of 13-17 min.

5.3.4.3.4 Evaluation of enantiomer ratio for comparative γ-octalactone measurements

In order to make sure, that the chosen measurement protocol is able to determine enantiomer ratios in the estimated range, several mixtures of the *R*- and *S*-enantiomers were prepared. Unfortunately, the mixtures were prepared for the initially used peak area ratio and not for the calculated enantiomer ratio. Therefore, the measurement points are not equidistantly distributed.

The measurement was repeated two times independently with a SPME collection temperature of 45°C and a collection time of 13-17 min. The mixtures showed nice linear correlations between calculated and prepared enantiomer ratios (Fig. 61) while the estimated ratios differed from the measured ratios. This might be due to pipetting errors. The relative error for the lowest point was 33%, while the relative errors of the two high points were only 4 and 5%.

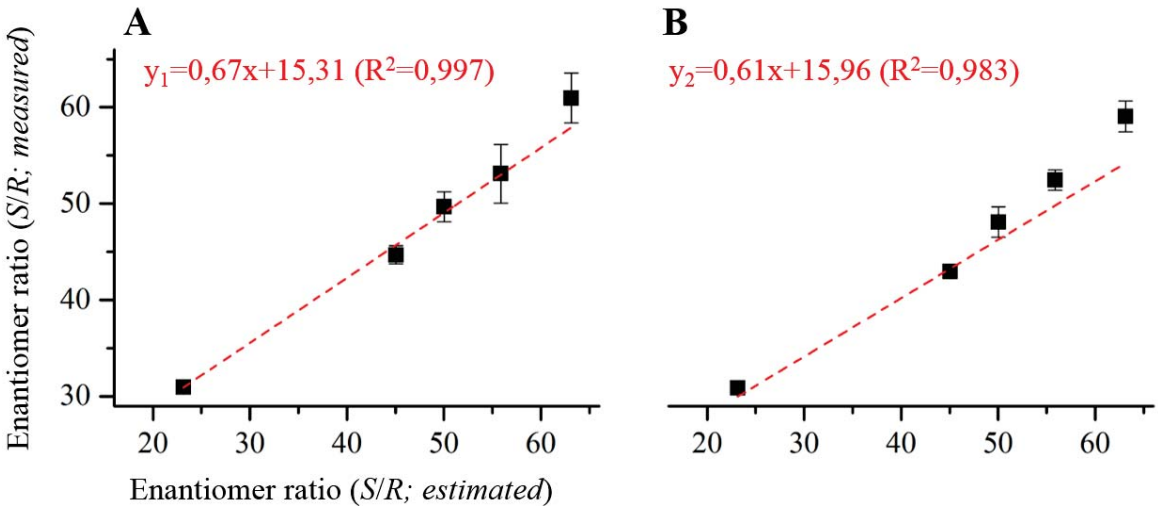

Fig. 61: Correlation of calculated enantiomer ratio with measured enantiomer ratio. Indication of linear fit (red lines). A and B are two mixtures, prepared independently, N=3.

In conclusion, the procedure was shown to be able to determine enantiomer ratios between about 20 and 70.

5.3.4.4 Metapleural gland compositions of several leaf-cutting ant species

In 2013 and 2014, only *Acromyrmex echinatior* from Dr. Wirth (University of Kaiserslautern) were used for preliminary experiments. Because of the small sample sizes (N=46 and 88), I additionally collected samples from other leaf-cutting ant species at the University of Würzburg in the lab of Prof. Dr. Roces. Herewith, I was able to compare six *Acromyrmex* and three *Atta* species.

Interestingly, the dominance of γ-octalactone varied significantly between *Acromyrmex* species. While single glands from *Acromyrmex echinatior* and *octospinosus* showed γ-octalactone with distinct dominance, only poor signal intensities were visible for *Acromyrmex lobicornis* and *lundii* (Fig. 62). The other tested *Acromyrmex* (two) and *Atta* (three) species showed no γ-octalactone signals for single gland measurements.

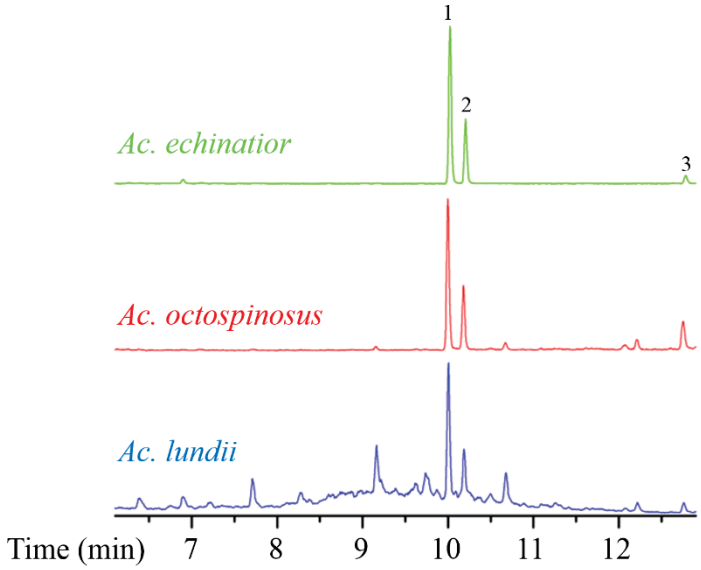

Fig. 62: Comparison of SPME-GC-MS spectra of metapleural gland measurements of individuals from different leaf-cutting ant species. 1: *S*-γ-octalactone; 2: *R*-γ-octalactone; 3: *S*-γ-decalactone.

After combination of ten metapleural glands, the signals for γ-octalactone enantiomers were visible for all six tested *Acromyrmex* species, but not for *Atta* (Tab. 7 and Fig. 63). In order to see other signals than γ-octalactone, the area was cut-out for *Acromyrmex echinatior* and *octospinosus*.

There are not only γ-octalactone signals present (*S*-γ-octalactone: R_t = 21,8 min and *R*-γ-octalactone: R_t = 22,3 min), but also *S*-γ-decalactone (R_t = 26,0 min) and *R*-γ-decalactone (R_t = 26,2 min). Previously, the presence of γ-nonalactone was observed (Prof. Dr. D. Spiteller, unpublished). If the signals at R_t =24,8 and 25,0 min belong to the γ-nonalactone enantiomers, then most of the tested *Acromyrmex* species and also *Atta* species would contain them (Fig. 63). There was no reference substance for γ-nonalactone measurements available, therefore the retention time could not be proven.

For the first time, comparative data sets of six *Acromyrmex* and three *Atta* species were analyzed using SPME-GC-MS. In conclusion, the dominance of γ-octalactone signals differed among *Acromyrmex* species with *Acromyrmex echinatior* and *octospinosus* with distinct dominance for single gland measurements. The enantiomer ratio of γ-octalactone from individual ants will be investigated in more detail.

Tab. 7: Presence and dominance of γ-octalactone for analyzed leaf-cutting ant species.

	Ant species	1 ant	10 ants
Acromyrmex	*ambiguus*	-	+
	echinatior	+	+
	heyeri	-	+
	lundii	~	+
	lobicornis	~	+
	octospinosus	+	+
Atta	*colombica*	-	-
	sexdens	-	-
	vollenweideri	-	-

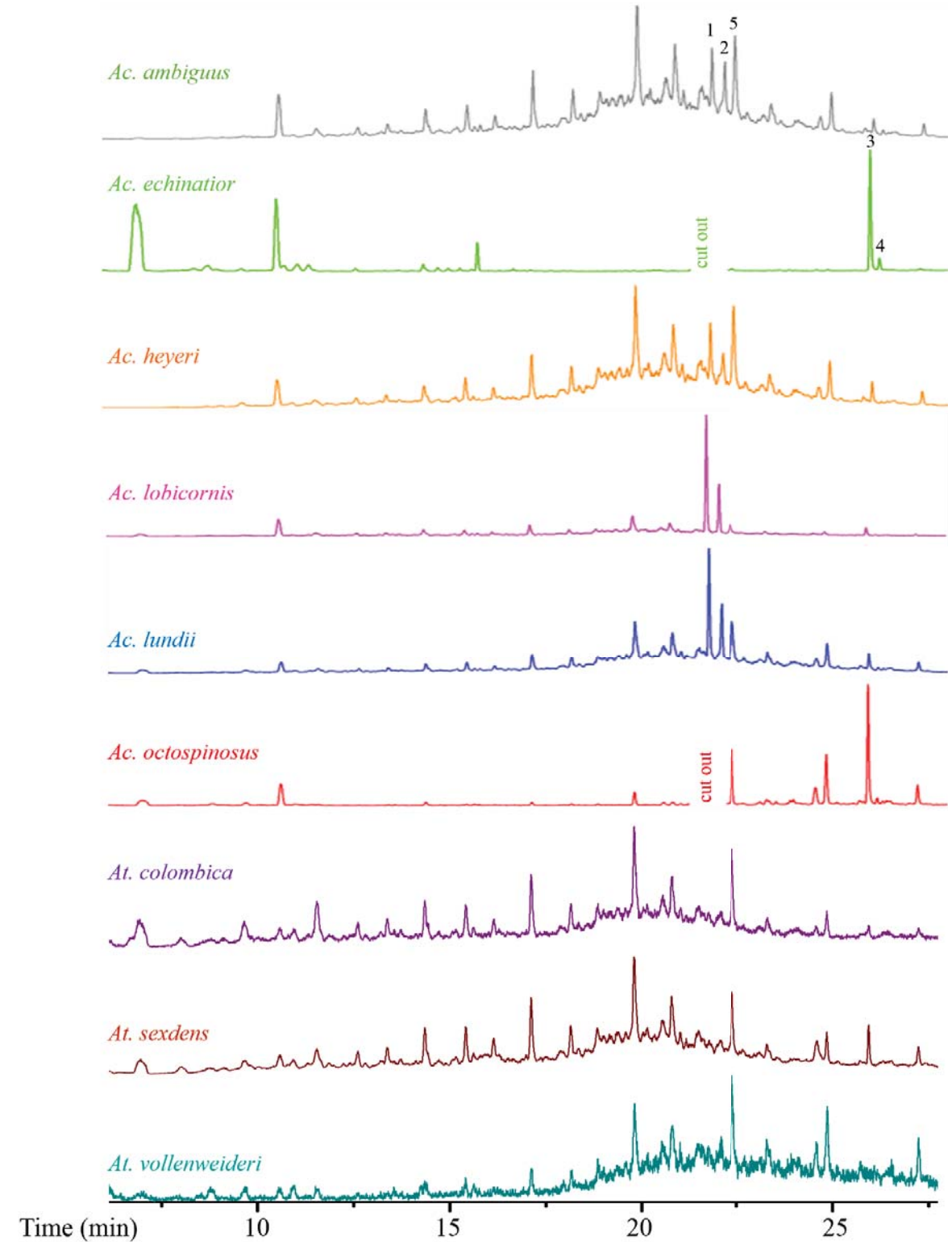

Fig. 63: Comparison of SPME-GC-MS spectra of 10 combined metapleural glands measured from different leaf-cutting ant species. 1: *S*-γ-octalactone; 2: *R*-γ-octalactone; 3: *S*-γ-decalactone; 4: *R*-γ-decalactone; 5: Heptadecane.

5.3.4.5 Presence of γ-octalactone on body parts of *Acromyrmex octospinosus*

To determine the distribution of γ-octalactone on the body of leaf-cutting ants, a comparative experiment was set up for *Acromyrmex octospinosus*. To increase γ-octalactone signals for other body parts than the thorax, body parts of twenty *Acromyrmex octospinosus* ants were combined.

As estimated, the fore and rear thorax parts showed the most dominant γ-octalactone signals (Fig. 64; indicated in dashed box; R_t =10,0 and 10,3 min). In contrast, MS spectra of heads, legs and gasters only showed minor amounts of γ-octalactone.

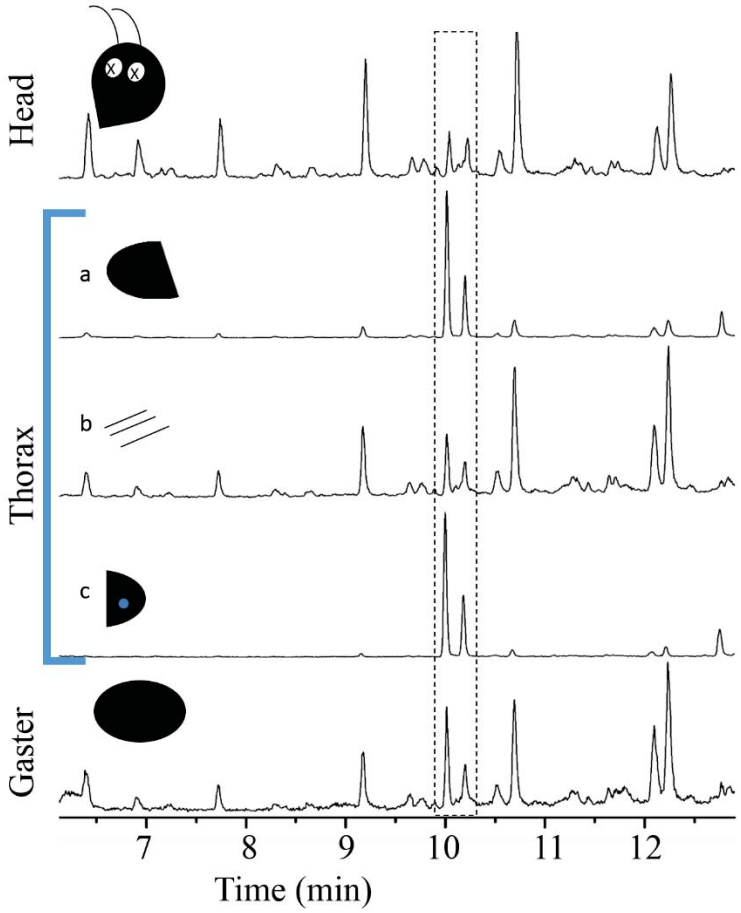

Fig. 64: Comparison of presence of γ-octalactone on body parts of 20 pooled *Acromyrmex octospinosus*. Indication of γ-octalactone with dashed box.

γ-Octalactone signals were only found in dominant proportions for front and rear thorax parts. In measurements of heads, legs and gasters, other compound signals were more dominant than γ-octalactone. The impact of this finding will be discussed later.

5.3.4.6 Enantiomer ratio of γ-octalactone with respect to collection location

To connect enantiomer ratios of γ-octalactone with other factors, the leaf cutting ants were collected from different nest chambers. As nests from leaf-cutting ants consist of three

obvious compartments (leaf, fungus and waste chamber), ants from all three compartments were collected separately.

Single glands of *Acromyrmex echinatior* and *octospinosus* were measured using the described and established protocol.

There was a variation of enantiomer ratio of γ-octalactone, but there was no correlation to the collection area (Fig. 65). While the variation ranged around an enantiomer ratio of 72,8±8,3, there was a minimum value of 25 and a maximum value of 97 observed for individual ants.

The enantiomer ratios of *Acromyrmex echinatior* showed higher variations for the first measurement (Fig. 65 A-C) than for the second measurement (Fig. 65 D-F). The data sets for *Acromyrmex octospinosus* are differentiated in their origin from Kaiserslautern (Fig. 65 G-I) and Würzburg (Fig. 65 J-L).

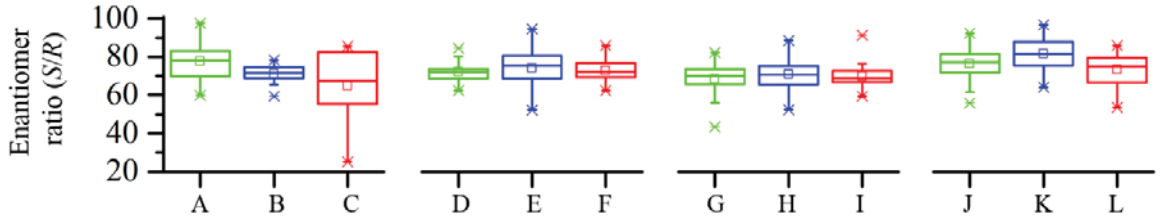

Fig. 65: Enantiomer ratio of γ-octalactone from *Acromyrmex echinatior* and *octospinosus* with respect to their collection area. A-C: *Acromyrmex echinatior* (set 1); D-F: *Acromyrmex echinatior* (set 2); G-I: *Acromyrmex octospinosus* (Kaiserslautern); J-L: *Acromyrmex octospinosus* (Würzburg); Green: leaf chamber; blue: fungus chamber; red: waste chamber.

The number of measurements and calculated enantiomer ratios were summarized (Tab. 8). In conclusion, there was no direct correlation between collection area and enantiomer ratio of γ-octalactone observed. The main differences were observed between leaf-cutting ants' nests. In case of *Acromyrmex octospinosus*, the overall enantiomer ratio of ants from Kaiserslautern was 69,7±7,4 (N=126) while ants from Würzburg resulted in 77,1±8,2 (N=104). The enantiomer ratio of *Acromyrmex echinatior* (Kaiserslautern) did not differ from 2015 (set 1) to 2016 (set 2). The enantiomer ratios of 71,2±11,0 (N=46; 2015) and 73,1±6,5 (N=88; 2016) are statistically equal.

Tab. 8: Compilation of data sets for enantiomer ratios of Acromyrmex echinatior and octospinosus.

	Chamber of origin			
	Leaf	**Fungus**	**Waste**	**Total**
***Acromyrmex echinatior* (set 1)**				
Number	20	16	10	46
Enantiomer ratio	77,6±9,6	71,2±4,9	64,8±18,5	71,2±11,0
***Acromyrmex echinatior* (set 2)**				
Number	29	30	29	88
Enantiomer ratio	72,0±4,8	74,5±8,8	72,7±5,8	73,1±6,5
***Acromymrex octospinosus* (Kaiserslautern)**				
Number	39	42	45	126
Enantiomer ratio	71,0±7,5	69,8±5,8	68,4±9,0	69,7±7,4
***Acromymrex octospinosus* (Würzburg)**				
Number	25	34	45	104
Enantiomer ratio	76,3±8,7	81,5±8,1	73,5±7,8	77,1±8,2

5.3.4.7 Enantiomer ratio of γ-octalactone with respect to head size

Determination of worker size was very often used in order to differentiate between specific tasks in leaf-cutting ants.[63-64] The head size of leaf-cutting ants was also linked to the size of metapleural glands and the number of secretory cells.[36, 54, 56, 65-66] In order to connect the enantiomer ratio of γ-octalactone with the worker size and the collection area, the eye distance of every individual ant was measured using a micrometer ruler.

There are no head sizes for *Acromyrmex echinatior* (set 1) because I purchased the micrometer ruler more than one year after their metapleural gland measurement and the heads were not stored any more.

Indeed, worker sizes differed like described in literature, with many minor workers in the fungal chamber, and comparatively more major workers in the leaf and waste chambers (Tab. 9 and Fig. 66).[63] The distribution of worker castes seemed not to be established yet for the young *Acromyrmex octospinosus* cultures from Kaiserslautern and Würzburg. The big variation in worker size compared to the *Acromyrmex echinatior* sample was assimilable with the described effect for young and old colonies.[64] Old, established leaf-cutting ant colonies showed a lower variety in worker size for several tasks than young colonies, where the size related worker task was less developed.

Tab. 9: Compilation of data sets for eye distances of Acromyrmex echinatior and octospinosus.

	Chamber of origin		
	Leaf	**Fungus**	**Waste**
***Acromyrmex echinatior* (set 2)**			
Number	29	30	29
Eye distance (mm)	1,9±0,2	1,2±0,2	1,6±0,2
***Acromyrmex octospinosus* (Kaiserslautern)**			
Number	39	42	45
Eye distance (mm)	1,8±0,3	1,1±0,3	1,8±0,2
***Acromyrmex octospinosus* (Würzburg)**			
Number	25	34	45
Eye distance (mm)	1,8±0,2	1,4±0,3	1,6±0,2

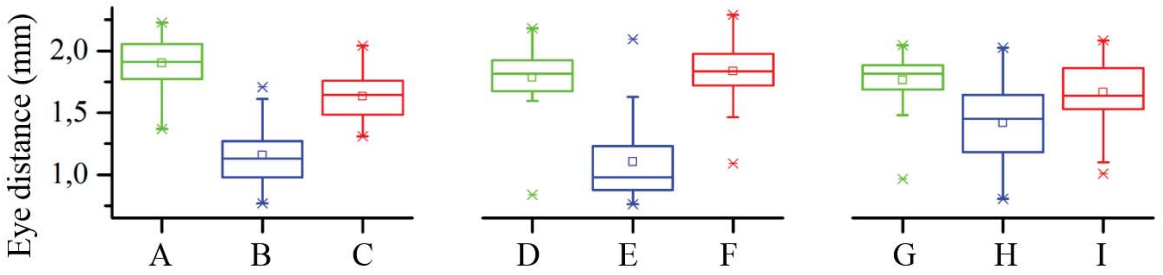

Fig. 66: Eye distance of *Acromyrmex echinatior* and *octospinosus* with respect to collection area. A-C: *Acromyrmex echinatior*; D-F: *Acromyrmex octospinosus* (Kaiserslautern); G-I: *Acromyrmex octospinosus* (Würzburg); Green: leaf chamber; blue: fungus chamber; red: waste chamber.

The correlation of eye distance with enantiomer ratio of γ-octalactone showed clear clouds for the established *Acromyrmex echinatior* colony (Fig. 67 A), but big variation for the young *Acromyrmex octospinosus* colonies (Fig. 67 B-C). It remains unclear, whether this is a difference between *Acromyrmex echinatior* and *octospinosus* or due to colony age.

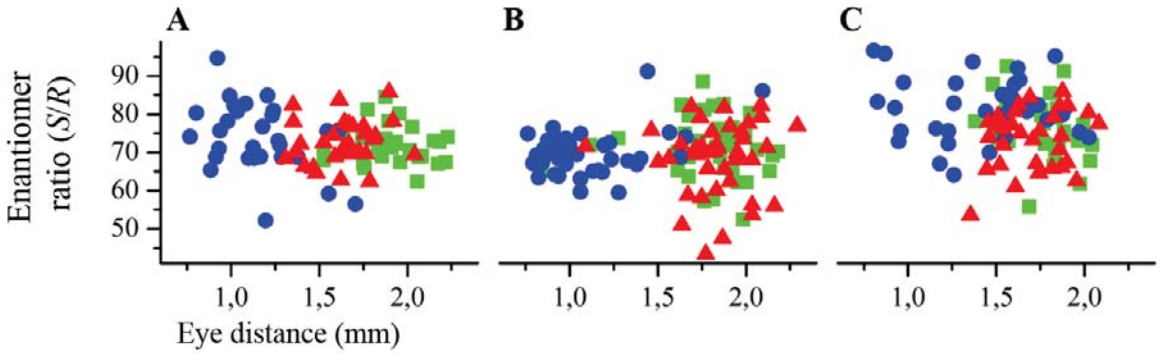

Fig. 67: Correlation of eye distance with enantiomer ratio. A: *Acromyrmex echinatior*; B: *Acromyrmex octospinosus* (Kaiserslautern); C: *Acromyrmex octospinosus* (Würzburg); Green square: leaf chamber; blue dots: fungus chamber; red triangles: waste chamber.

5.3.4.8 Enantiomer ratio of γ-octalactone with respect to signal intensity

To connect the amount of γ-octalactone, which is generally linked to peak area, with the collection area and enantiomer ratio, comparative measurements were combined. The body size of leaf-cutting ants was directly linked to metapleural gland size, where minor workers showed relatively increased metapleural glands compared to major workers.[54]

The peak areas were calculated by adding the peak areas of the signals from *R*- and *S*-γ-octalactone enantiomers.

Indeed, the signal intensities showed the lowest values for minor workers from the fungal chamber, while the highest values were reached by major workers from leaf chambers (Fig. 68).

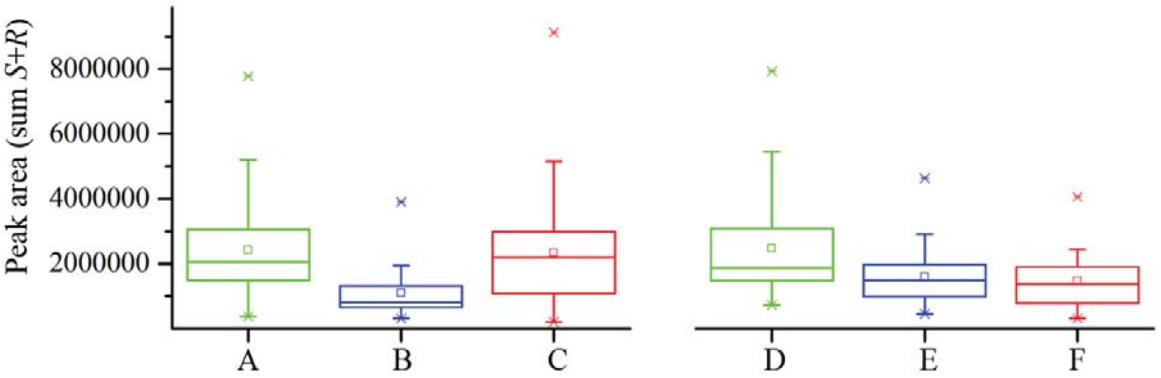

Fig. 68: Signal intensity of SPME-GC-MS measurements from *Acromyrmex octospinosus*. A-C: *Acromyrmex octospinosus* (Kaiserslautern); D-F: *Acromyrmex octospinosus* (Würzburg); Green: leaf chamber; blue: fungus chamber; red: waste chamber.

The direct correlation of peak intensity with eye distance of ants showed the same distribution, with increased peak areas especially for major workers (Fig. 69). Interestingly, not all major workers showed increased intensities, which means, that there is no direct correlation between size and intensity.

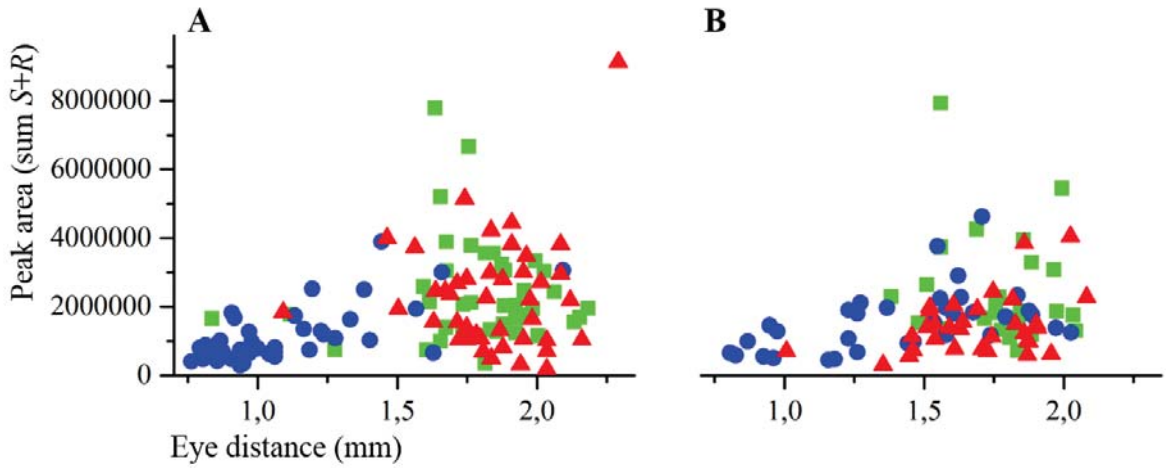

Fig. 69: Correlation of signal intensity of SPME-GC-MS measurements with eye distance from *Acromyrmex octospinosus*. A: *Acromyrmex octospinosus* (Kaiserslautern); B: *Acromyrmex octospinosus* (Würzburg); Green square: leaf chamber; blue dots: fungus chamber; red triangles: waste chamber.

Indeed, the combination of the signal intensities with head sizes of individual ants showed, that the relative signal intensity of γ-octalactone was similar when corrected with head size (Fig. 70). The highest relative levels were found for ants from the leaf chamber for both data sets (Fig. 70 A; D). This would indicate, that the overall content of γ-octalactone per individual ant is not dependent on body size or collection area but equal among nest mates. Again, this experiment needs to be repeated and brought into context of colony age and pathogen levels, as the levels of metapleural gland secretions were shown to correlate with pathogen treatment.[67]

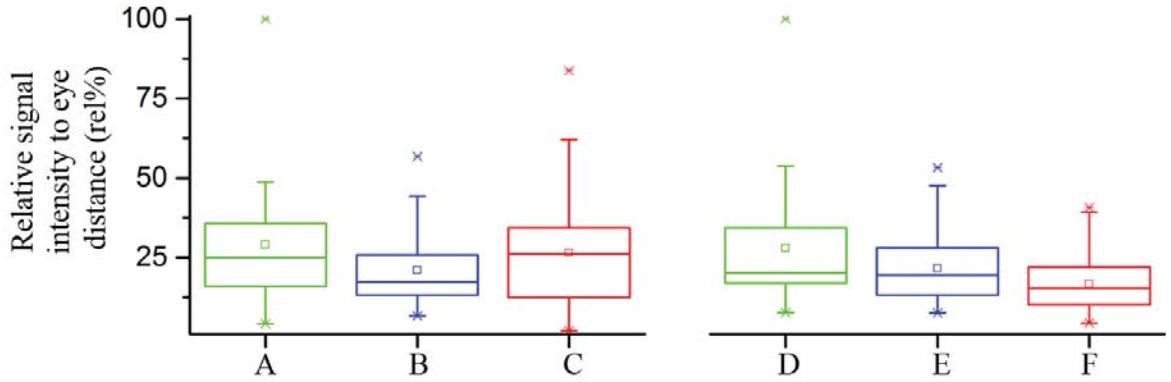

Fig. 70: Relative calculated correlation of signal intensity and eye distance. A-C: *Acromyrmex octospinosus* (Kaiserslautern); D-F: *Acromyrmex octospinosus* (Würzburg); Green: leaf chamber; blue: fungus chamber; red: waste chamber.

5.3.5 Discussion and Outlook

γ-Octalactone from metapleural glands of *Acromyrmex* and *Atta* leaf-cutting ants were shown to differ in dominance, enantiomer ratio and overall amount. Further experiments are necessary to prove possible influencing parameters:

- The **dominance** of γ-octalactone of *Acromyrmex echinatior* and *octospinosus* in contrast to *Acromyrmex ambiguus*, *heyeri*, *lundii* and *lobicornis* might be due to evolutionary changes. This can be investigated by comparison of SPME-GC-MS measurements of several species and estimation of their phylogenetic relations.
- Differences of **enantiomer ratios** can be investigated between species, between nests of the same species, between ant castes and between genetic differences (among patrilines within one nest). Investigations of expression levels of involved enzymes and influences like climate conditions would be advanced approaches.
- The **overall amount** of γ-octalactone might be influenced by genetic differences or external changes, for example the presence of pathogens. Experiments with different treatment groups might point towards possible triggers.

For all these approaches, I recommend to have direct access to several leaf-cutting ant colonies of relevant species. In my opinion, realistic planning together with sufficient material support and open-minded experimental setups will result in a wonderful topic for a PhD thesis with meaningful outcomes.

5.3.5.1 Enantiomer ratio of γ-octalactone

Stereoisomers have the same molecular formulas and bond connections, but differ in the three-dimensional orientation of their atoms in space. Stereochemical variation can influence the bioactivity of compounds, this is widely known in pharmacology, pheromone and pesticide sciences.[43, 68-70]

While alterations of enantiomer ratios were shown to influence herbivore resistance, antifeedant activity and therefore plant fitness,[71-72] there were several relevant observations for insects, too.[70, 73-74] For example, different enantiomer ratios of moth pheromones influenced mating preferences.[75-76] Determination of expression levels of involved enzymes showed, that there are genetic alterations and polymorphisms involved which might be due to evolutionary changes.[77]

The enantiomer ratios of γ-octalactone from metapleural glands in this project were investigated in more detail at least for one *Acromyrmex echinatior* nest and two *Acromyrmex octospinosus* nests. Previous investigations focusing on mating preferences and genetically

differences due to paternity showed, that there might be differences in sizes of metapleural glands.[65, 78-79] For patriline-specific differences of metapleural gland compositions from leaf-cutting ants, which did not focus on stereochemical differences but on overall variability, there were no clear results reported.[36]

While I predict the dominance of γ-octalactone for *Acromyrmex echinatior* and *octospinosus* in contrast to *Acromyrmex ambiguus*, *heyeri*, *lundii* and *lobicornis* and all tested *Atta* to evolutionary changes, which should be investigated with respect to their phylogenetic relations, the enantiomer ratio differed already within one nest. Due to genetic variations, the expression and effectiveness of involved enzymes might be influenced but the enantiomer ratio would be fixed during ant's lifetime. Whether there are external triggers, which influence the enantiomer ratio directly, is not known – this could be measured by comparison of changing expression levels of involved enzymes. The underlying biosynthetic pathways are still unknown, therefore one can only speculate about the possibilities.

Enantiomer ratios of γ-lactones play an important role for flavoring aspects, they were therefore investigated in more detail for description of food chemistry approaches. Different fruits, such as apricot, mango, peach, raspberry and strawberry, were analyzed and enantiomer ratios of γ-octalactone were determined.[80] For apricot, they found an enantiomeric excess of (*R*)-78,2%, while for example mango had (*R*)-6,8% and in contrast raspberry had (*S*)-20,2%. This example shows that enantiomer ratios of γ-octalactone alter not only for *Acromyrmex* leaf-cutting ants, but also for example among fruits. In other investigations, alterations of enantiomer ratios from plant derived products of different geographical origins were shown, which might be due to evolutionary changes or climatic influences.[81-82]

In conclusion, varying enantiomer ratios of γ-octalactone are not unique to leaf-cutting ants but already known as shown from fruits. Nevertheless, the circumstances for this effect within one nest are still unknown and need to be investigated.

5.3.5.2 Influence of *R*- and *S*-γ-octalactone on leaf-cutting ants' ecosystem

The metapleural gland of leaf-cutting ants was considered to play an important role for hygiene and disinfection, as the survival of leaf-cutting ants decreased with sealed metapleural glands.[50] The grooming behavior of leaf-cutting ants plays an unambiguous role for the survival of leaf cutting ants' colonies and is closely related to spreading of metapleural gland secretions.[29, 52]

Nevertheless, direct comparisons of bioactivity against direct pathogens of leaf-cutting ants showed only low efficiency for metapleural gland compositions.[35] Therefore, additional

alternative functions of metapleural gland secretions were discussed. The general function of defense against pathogens might be advanced in leaf-cutting ants compared to non-fungus growing ants.[55, 83] The mutualistic fungus needs to be maintained and kept free from encroaching fungal pathogens. Symbiotic bacteria were shown to assist leaf-cutting ants in keeping their bodies and nests in appropriate conditions.[28, 39, 84-85] The direct nutrient support and communication of leaf-cutting ants with their bacterial symbionts is still unknown.[86]

With our experiments, we found the *R*-enantiomer of γ-octalactone to be more bioactive against *Escovopsis weberi* than *S*-γ-octalactone. This conforms previous investigations for bioactivity of other γ-lactone enantiomers against fungal parasites.[62]

γ-Octalactone was found to be dominant in metapleural gland secretions from *Acromyrmex echinatior* and *octospinosus*, while it was less dominant for the other four tested *Acromyrmex* species and not detectable for all three tested *Atta* species.

The enantiomer ratio of γ-octalactone from *Acromyrmex echinatior* and *octospinosus* showed no direct correlation to collection area or worker size. The enantiomer ratio (*S*/*R*) ranged around 72,8±8,3 in average for all four data sets with both species combined. The absolute intensity of γ-octalactone showed only low variation in direct correlation to head size. The relative correlation after correction of signal intensity and head size showed, that even though the size of the metapleural glands and their secretory cells varies among head size, the relative levels of γ-octalactone remained constant.[54] Whether there is a variation in γ-octalactone levels when metapleural gland secretions are increased by fungal pathogen treatment remains unclear.[67] Whether the observed outbreak in enantiomer ratio of γ-octalactone from waste workers from *Acromyrmex echinatior* in the first data set was only an artefact or due to disinfection issues, is not known (Fig. 65 C). The data set contained only ten leaf-cutting ants, therefore the validity of this observation is very low. In order to study the impact of fungal contamination towards metapleural gland secretion - in particular γ-lactones and their enantiomer ratio - several sub-colonies need to be established and treated with spores of fungal pathogens like *Escovopsis weberi* or *Metarhizium anisopliae*.[29, 39] An increase of metapleural gland secretions or a shift of the enantiomer ratio towards higher bioactivity (more *R*-enantiomer) compared to an untreated control group would at least give a point towards a direct correlation of defense and γ-lactone production.

Another possible aspect to correlate the presence and dominance of γ-octalactone in *Acromyrmex* leaf-cutting ants with a function is communication with nest mates or bacterial symbionts.

There are nestmate recognition cues, mainly characterized as hydrocarbons, which allow rapid differentiation between nestmates and non-nestmates.[87-88] While most chemical cues

for recognition originate from the postpharyngeal or mandibular glands,[89-90] also dietary motifs were observed.[91-92] For *Acromyrmex octospinosus* there was no aggression against non-nestmates observed if supplied with the same forage materials.[93] Beside nestmate recognition, also territorial marking was described for metapleural gland secretions.[87] Whether the γ-lactones play a role for such recognition cues is not known and was not investigated yet.

Another communication pathway would be the marking of decontaminated material. In a short screening experiment at the University of Würzburg, waste particles of *Acromyrmex octospinosus* were treated with a racemate of γ-octalactone (gas phase) and offered in a behavioral experiment. Two waste piles were prepared, one treated one untreated, and the ants more often worked on the untreated pile and translocated the processed waste particles to the treated pile than the other way around. In order to prove this observation, more behavior experiments have to be prepared and compared to other leaf-cutting ant species, which do not produce γ-octalactone and therefore could not use them as a signal.

This observation can also be combined with a third possibility for chemical communication, which is the usage of γ-octalactone as signals for bacterial symbionts. The presence of symbiotic bacteria from the order Actinomycetales on bodies of *Acromyrmex* and their production of antibiotic compounds was investigated since 1999.[94] Mutualistic bacteria on the integument were not only found for *Acromyrmex*, but also for other fungus growing ants like *Cyphomyrmex* and *Trachymyrmex*.[95] Whether γ-octalactone is only present for fungus growing ants with visible biofilms was not investigated yet, but as *Atta* species did not show γ-octalactone and no biofilms, one could imagine a connection. For an experimental evidence, only ten combined thorax parts need to be measured with SPME-GC-MS.

Looking closer towards communication aspects, γ-lactones are known as signaling molecules at least for *Streptomyces* and *Aspergillus*.[96-97] Especially the impact of γ-butyrolactones for antibiotic production and morphological differentiation was investigated for Actinobacteria.[96, 98-99] There are some reports which contribute to this hypothesis. When the metapleural glands were sealed, the visible biofilms on the cuticle of leaf-cutting ants disappeared faster than without sealing.[100] Sealing of metapleural glands was furthermore connected to decreased survival of leaf-cutting ants treated with pathogens.[21, 50] This could be due to the direct disinfection patterns of metapleural gland secretions, but also due to lacking possibilities to induce antibiotic production from bacterial symbionts. While metapleural glands of ants in general were suspected to play an important role in defense, an additional function for fungus-growing ants with bacterial symbionts on their cuticle could be the production of quorum-sensing molecules.[66]

The induction of antibiotic production in lab experiments with isolated bacterial symbionts from leaf-cutting ants and addition of γ-octalactone might be influenced by nutrient rich agar media, which could overlie the effect of γ-octalactone by already contained similar compounds.

5.4 Acquisition of fluorescent bacteria by leaf-cutting ants

Contributions

This project was initially started in the Emmy Noether junior group of Prof. Dr. D. Spiteller at the Max Planck Institute for Chemical Ecology (MPI CE, Jena, Germany) associated with the group of Prof. Dr. Boland. Dr. Ilka Schoenian described the initial experiments and ideas in her PhD thesis (available online http://d-nb.info/1017079013; urn:nbn:de:gbv:27-20111109-142430-0). She modified plasmids and generated genetically modified organisms which were used in this work. Therefore, I will summarize her methods and results shortly and focus on my additional findings and plans.

I want to thank PD Dr. Bertolt Gust (University of Tübingen) for discussion and Dr. Wirth (University of Kaiserslautern) for leaf-cutting ant samples. Green fluorescent protein producing cells for control experiments were provided by Christoph Paone from the Hauck group (University of Konstanz).

Application of bacteria on leaves was one part of "Vertiefungskurs Chemische Ökologie 2014" with Yannik Altrichter and Michaela Holzem.

pRSETa mEos2 was a gift from Loren Looger (Addgene plasmid # 20341), tol2-mpx-Dendra2 was a gift from Anna Huttenlocher (Addgene plasmid # 29574).

5.4.1 Abstract

Leaf-cutting ants (tribe *Attini*) cultivate a fungal symbiont (*Leucoagaricus*) as their food source. However, the fungus garden is sensitive to infections by pathogenic fungi, such as *Escovopsis weberi*. Recently, antibiotic producing microbial symbionts associated with leaf-cutting ants were found to help defending their fungal-cultivar against infections. *Acromyrmex* leaf-cutting ants can have large microbial biofilms consisting mainly of *Pseudonocardia* and *Streptomyces* on their bodies.

The origin of the symbiotic bacteria remains unclear. While a co-evolutionary background is discussed, it is also conceivable that the bacterial symbionts are (non)specifically acquired from the environment. In order to study a possible - passive or active controlled - uptake of bacteria, we started an experiment with different isolated symbionts which were previously modified to constitutively express the fluorescent protein mCherry. Due to autofluorescence, photoconvertible fluorescent proteins such as Dendra2 and mEos2 replaced mCherry.

These mutated symbionts were used to inoculate several *Acromyrmex* leaf-cutting ants (some with their biofilms mechanically removed). The inoculated ants were reintroduced into their subcolony. After several months, the subcolony experiment was stopped and the ants were screened for fluorescence signals by fluorescence microscopy.

Unfortunately, the previously described findings at the MPI CE, Jena, could not be reproduced. Control experiments showed, in contrast to previously predicted results, that GFP could be an appropriate fluorescent protein. Genetically modified bacterial strains did not produce fluorescent proteins, the autofluorescent signals were as high as from unmodified strains. The procedure of previous plasmid modifications was verified and possible sources of problems were identified.

5.4.2 Introduction

The whitish biofilms on the bodies of *Acromyrmex* leaf-cutting ants consist of bacterial symbionts.[4]

In general, the origin of symbiotic bacteria associated with leaf-cutting ants remains unclear. While a co-evolutionary background is discussed, it is also conceivable that the established symbiotic strains could be exchanged.[5-6] Only a small variety of bacterial strains was described (mainly *Pseudonocardia* and *Streptomyces*), therefore all ants in one nest carry similar bacterial species.[7] This similarity might occur by chance due to high availability of these strains. Alternatively, ants might actively select for a favored strain because of bacterial features that would enhance ants' fitness.

Passing on of biofilm forming symbiotic bacteria from old leaf-cutting ants to young ants (genus *Acromyrmex*) is not completely understood. The accumulation of symbiotic bacteria, visible as whitish biofilm, is different between worker castes and status of contamination with pathogens in the nest.[8] Leaf-cutting ants (genus *Acromyrmex*) have no visible bacterial biofilm when they hatch, but they begin to accumulate bacteria during their first days. In comparison, the uptake of bacterial symbionts by beewolf digger wasps takes place through consuming of their cocoon after hatching. The cocoon was coated with bacteria by their mother to prevent the brood from infection by pathogens and is thereby passed from generation to generation.[101]

With this project, we aimed to establish a method to describe the uptake, exchange and distribution of (symbiotic) bacteria within a leaf-cutting ant colony.

Thus, bacteria associated with leaf-cutting ants will be isolated and genetically modified so that they produce fluorescent proteins when re-introduced into leaf-cutting ants' ecosystem. Their distribution will be investigated with the help of fluorescence microscopy and antibiotic assisted selective isolation of modified bacterial strains on agar plates (Fig. 71 A). Moreover, different possibilities for initial uptake will be compared in order to identify the mode of action in natural environments. The initial uptake could either start directly with the queen laying eggs coated with bacteria, as egg or larvae themselves or after hatching by

taking bacteria from nest mates (Fig. 71 B). By comparison of bacterial communities on egg/larvae/ant samples, the origin and composition of (symbiotic) bacteria could be described. Up to now, it is not known at which point the leaf-cutting ants are inoculated with bacteria and if they are able to actively exchange their bacterial community with nest mates. Thereafter, we want to find out, if the bacterial community can be altered by offering several mutated (symbiotic) bacteria at different locations in their nests (Fig. 71 C). When the offered modified bacterial strains are taken up, sub colonies could be monitored for several generations in order to find out, whether there is an active exchange and under which conditions or not.

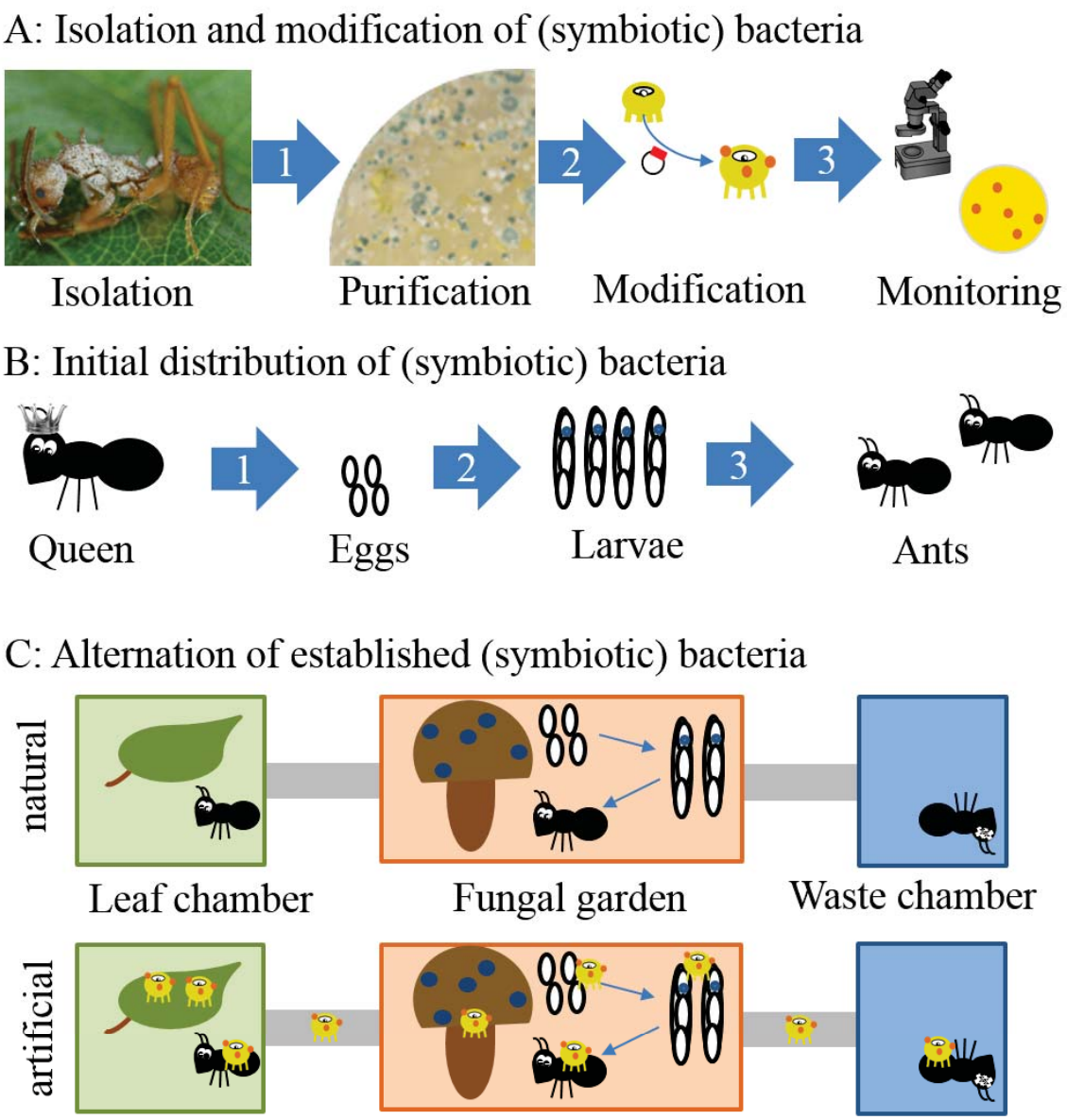

Fig. 71: Overview of modification of isolated strains (A), life cycle of leaf-cutting ants (B), and locations for manipulation to monitor bacterial exchange and a possible integration of modified bacterial strains into their biofilms (C).

5.4.3 Methods

5.4.3.1 Isolation of bacteria

The different isolation methods are described elsewhere (Ch. 7.2; p. 177ff). For this experiment, three different Actinomycetales strains were chosen due to their bioactivity in co-cultivation assays against *Escovopsis weberi* and their different colors on agar dishes in order to distinguish them after re-isolation.

AE1 (highly bioactive, whitish), AE4 (medium bioactive, whitish), ATV7 (medium bioactive, yellowish) and ATV9 (medium bioactive, grayish).

Furthermore, preliminary isolated strains (Ch. 5.4.3.3.1; Tab. 10) were grown and checked for their antifungal activities, but all of them showed no inhibition zones in bioassays.

5.4.3.2 Antibiotic sensitivity and resistance of selected bacteria from leaf-cutting ants

Isolated, modified or re-isolated bacteria were checked for their antibiotic resistances and sensitivities. Therefore, agar plates with different cultivation media and concentrations of antibiotics were prepared and aqueous suspensions were spread. To check one organism, the antibiotics were applied in holes and the organism was spread after diffusion, similar to agar diffusion assays.

Besides Actinomycetales, other bacteria and fungi from leaf-cutting ants grew on agar plates with apramycin and hygromycin. Growth of modified bacteria on SFM agar plates with more apramycin (25 to 250 µg/ml) or more hygromycin (10 to 50 µg/ml) or mixtures was monitored.

The number of unwanted resistant bacteria from leaf-cutting ants decreased, but unfortunately the modified bacteria showed similar sensitivity and resistance as resistant natural strains.

Growth of fungal contaminants was reduced by adding carbendazim (50 or 100 µg/ml).

5.4.3.3 Labelling of symbiotic bacteria with fluorescent proteins

5.4.3.3.1 Preliminary work

Initial experiments were performed by Dr. Schoenian (MPI CE, Jena, Germany).

The vector pIJ8655 (Sun, *et al.* [102]; see also for abbreviations) was used as backbone, the eGFP was replaced by mCherry (restriction enzymes NdeI and NotI). The promoter tipAP was replaced by the constitutive ermE promoter (ermE*p: 275 bp from pIJ4090 with restriction enzymes NdeI and EcoRV). In addition, this procedure cut out t0 (transcription terminator from phage k) and parts of ts^R (Thiostrepton resistance gene).

This plasmid was called ILS8655 and conjugated into selected Actinomycetes strains, isolated from different leaf-cutting ants (Tab. 10) following the attached protocol after Jon Thwaite 2002 and "Practical Streptomyces Genetics" (p. 249, 2000, ISBN 0-7084-0623-8).

Tab. 10: Name and origin of bacteria generated by Dr. Schoenian.

Name	Origin
Streptomyces Av25-6	*Acromyrmex volcanus*
Streptomyces Ae32-2	*Acromyrmex echinatior*
Streptomyces Ads	*unknown*
Pseudonocardia Ao1	*Acromyrmex octospinosus*

5.4.3.3.2 Microscope

The microscope of Prof. Dr. Kroth (University of Konstanz) was used for the following experiments. The Olympus BX51TF microscope was equipped with the filter cube U-MF2 (Olympus) and the filter AF F41-020 NB-EGFP for GFP, the filter AF F31-045 CFP for CFP and the filter AF F41-007 HQ-SET for red light. For surface light, I used a common light bulb. Samples were placed on standard coverslips (VWR), which were cleaned with 70% ethanol and reused for the same sample group.

5.4.3.3.3 Introduction of mEos2 and Dendra2 sequences into plasmid ILS8655

As the contrast between chitin-bodies, particles and fluorescent bacteria was very low, the fluorescent protein mCherry was exchanged with photoconvertible fluorescent proteins mEos2 or Dendra2 (same restriction enzyme recognition sites as mCherry, replacement with NdeI and NotI).

mEos2 and Dendra2 were purchased from Addgene, Cambridge. mEos2 was amplified using the designed primer set (Tab. 11) out of the plasmid "pRSETa mEos2" (ID20341; McKinney, *et al.* {McKinney, 2009 #8}) using PCR (Tab. 12 and Tab. 13). Unfortunately, the sequence of mEos2 contained a NdeI recognition site itself. The NdeI recognition side was removed using site directed mutagenesis (Ch. 5.4.3.3.7, p. 114).

Dendra2 was amplified using a designed primer set (Tab. 11) out of the plasmid "tol2-mpx-Dendra2" (ID29574; Yoo and Huttenlocher [103]) using PCR (Tab. 12 and Tab. 13). Tubes with master mixes were centrifuged shortly and placed into the PCR cycler with pre-heated lid (105°C). After finishing the temperature program (Tab. 13), tubes were taken out and stored in the fridge (4°C).

Tab. 11: Proposed primer sequences for amplification of fluorescent proteins and ermE promoter with restriction enzyme recognition sites (NN for nonsense tail; 3-5 bp).

Primer name	Primer sequence (without nonsense regions)
mCherry-NdeI-fw	NNCATATGGTGGTGAGCAAGGGCGAGGA
mCherry-NotI-rev	NNGCGGCCGCCTACTTGTACAGCTCGTCCA
mEos2-NdeI-fw	NNCATATGGTGAGTGCGATTAAGCCA
mEos2-NotI-rev	NNGCGGCCGCCTATTATCGTCTGGCATTGT
mEos2-MutaA	GGCATTTCCTTCAAGCAACAAAGCCATGT
mEos2-MutaB	AGTGCTGACGGGTGATATTCACATGGCTT
Dendra2-fw	NNCATATGGTGAACACCCCGGGAATTAACCTG
Dendra2-rev	NNGCGGCCGCCCTAGTACCTGGCTGGGCAGGGGGC

The purchased plasmids were received as plasmids in *E. coli*, therefore liquid cultures with LB medium were cultivated overnight (LB; liquid culture; 37°C), plasmids were isolated (Thermo Scientific Mini Preparation Kit) and dilutions (DNA concentration 0,1-10 ng/µl) were used for amplification by PCR. Master mixes were prepared in 0,2 ml reaction tubes on ice (Tab. 12).

Tab. 12: Master mixes for sequence amplification of fluorescent proteins.

Component	Volume (µl)
	mCherry, mEos2, Dendra2
5x Phusion GC buffer	6,0
$MgCl_2$ (25 mM)	3,0
DMSO	2,0
Primer-Mix (10 µM each)	0,8
dNTPs (10 µM each)	1,2
Phusion Hot Start II DNA Polymerase (2 U/µl)	0,2
adH_2O	5,8
DNA template	1,0
Final volume	20,0

Tubes with master mixes were centrifuged shortly and placed into the PCR cycler with preheated lid (105°C). After finishing the temperature program (Tab. 13), tubes were taken out and stored in the fridge (4°C).

Tab. 13: Temperature program for sequence amplification of fluorescent proteins, hygromycin resistance and ermE promoter.

Step		Temperature (°C)	Duration (sec)
Initial denaturation and activation of hot-start polymerase		98	30
Denaturation	30 cycles	98	10
Annealing	30 cycles	55	30
Elongation	30 cycles	72	60
Final elongation		72	300
Storage		4	unlimited

Alteration of $MgCl_2$ concentrations (0; 3; 6 µl/20 µl reaction mixture) and annealing temperatures (54,6°C; 56,9°C; 59,1°C; 62°C) resulted in no significant differences for the new primers; therefore, intermediate conditions were chosen (data not shown).

5.4.3.3.4 Densitometric measurements of DNA fragments and plasmids

Isolated plasmids and PCR mixtures were mixed with loading dye (6 times concentrated, Thermo Scientific) and separated using agarose gel electrophoresis (1,5% agarose in TAE buffer; Chamber filled with TAE buffer; Power supply 5 Volt per cm electrode distance; runtime 1 hour or until separation). DNA fragments were stained with ethidium bromide and compared to a DNA ladder (Fermentas gene ruler 1kb plus). The agaroses gels were photographed using an UV-chamber (Intas).

5.4.3.3.5 Cut out of DNA fragments and plasmids after agarose gel electrophoresis

After agarose gel electrophoresis, DNA fragments and plasmids were cut out of gels using a scalpel on the UV desk. The agarose pieces were transferred into one reaction tube and DNA was isolated using a purification kit (Thermo Scientific).

5.4.3.3.6 Cloning of DNA fragments and amplification of plasmids

Purified DNA fragments were ligated into the pJet-Vector using a cloning kit (Thermo Scientific; CloneJET PCR Cloning Kit; conditions as described in the protocol). The ligated vector or purified plasmids were transfected into chemically competent *E. coli* Top10 (Thermo Scientific) using a heat-shock protocol (attached; protocol of K. Bishop, Institute of Infections and Immunity). Cells were spread on LB-Agar dishes containing antibiotics (100 µg/ml ampicillin for pJet-Vector; 25-150 µg/ml apramycin for 8655; 5-50 µg/ml hygromycin for H8655). Cells were picked after 12-36 hours and transferred into liquid LB-medium, grown with the same antibiotic concentration for 12-36 hours and plasmids were isolated using a plasmid isolation kit (conditions as described in the protocol; Thermo Scientific Mini Preparation Kit).

5.4.3.3.7 Manipulation of the mEos2 sequence using site directed mutagenesis

The purchased mEos2 could not be used directly because it contained a NdeI recognition site inside of its sequence. The part of the sequence coded for a histamine, therefore one nucleotide was exchanged using site directed mutagenesis in a two step protocol.

At first, the original mEos2 was amplified using two primer mixes. Mix1 contained mEos2-fw and mEos2-MutaA. Mix2 contained mEos2-rev and mEos2-MutaB. The two reaction mixtures (Tab. 14) were amplified using the previously mentioned temperature program (Tab. 13).

Tab. 14: Master mixes for sequence amplification and manipulation of the photoconvertible fluorescent protein mEos2.

Component	Volume (µl)	Volume (µl)	Volume (µl)
	mEos2	EosMuta-A, EosMuta-B	EosMuta-AB
5x Phusion GC buffer	6,0	6,0	6,0
$MgCl_2$ (25 mM)	3,0	4,0	3,0
DMSO	2,0	2,0	2,0
Primer-Mix (10 µM each)	0,8	0,8	0,8
dNTPs (10 µM each)	1,2	0,8	1,2
Phusion Hot Start II DNA Polymerase (2 U/µl)	0,2	0,2	0,2
adH_2O	5,8	5,2	9,0
DNA template	1,0	1,0	0,3
Final volume	20,0	20,0	22,5

The DNA fragments were separated afterwards (Ch. 5.4.3.3.4), cut out and purified (Ch. 5.4.3.3.5). The two fragments were amplified together with a primer mixture containing mEos2-fw and mEos2-rev using the master mix EosMuta-AB (Tab. 14). The reaction tubes were placed into the PCR cycler after centrifugation and pre-heating of the lid (105°C; Tab. 15).

Tab. 15: Temperature program for connection of eosmuta-A and eosmuta-B.

Step		Temperature (°C)	Duration (sec)
Initial denaturation and activation of hot-start polymerase		98	30
Denaturation	6 cycles	98	10
Elongation		72	20
Denaturation	25 cycles	98	10
Annealing		55	30
Elongation		72	60
Final elongation		72	300
Storage		4	unlimited

The master mixes (concentrations of $MgCl_2$ and DNA template) and temperature programs (annealing temperature, durations and number of cycles) were altered, but the already described combination worked fine (data not shown).

The amplified DNA fragment was cut out of the agaroses gel after electrophoresis and transferred into the pJet Cloning vector.

5.4.3.3.8 Exchange of fluorescent proteins in the plasmid ILS8655

After cloning with the pJet-vector, DNA fragments containing sequences of modified Dendra2 or mutated mEos2 were cut out using restriction enzymes NdeI and NotI (conditions as described in the protocol, Thermo Scientific) and purified after separation with agarose gel electrophoresis (both around 700 bp).

The plasmid ILS8655 was digested using the restriction enzymes NdeI and NotI (conditions as described in the protocol, Thermo Scientific) and the backbone was purified after agarose gel electrophoresis (around 5.000 bp when linear).

The vector ILS8655v was ligated with the cut-off modified Dendra2 or mutated mEos2 and amplified using the cloning protocol (Ch. 5.4.3.3.6). Plasmids from picked *E. coli* strains were isolated and checked for their fluorescent protein sequence content using the previous described PCR protocols.

For nomenclature of generated plasmids see Ch. 5.4.3.3.11.

5.4.3.3.9 Introduction of hygromycin resistance sequence into plasmid ILS8655

The apramycin resistance was not selective enough in re-isolation experiments, therefore a hygromycin resistance gene was introduced (restriction enzyme ClaI).

The sequence of a hygromycin gene cluster was amplified out of an unknown plasmid provided by Prof. Dr. D. Spiteller using a mixture of designed primers (Tab. 16) and the previously described master mix (Tab. 12) and temperature program (Tab. 13).

Tab. 16: Sequences of primers for amplification of the hygromycin resistance gene cluster (NN for nonsense tail; 3-5 bp).

Primer name	Primer sequences
Hygr-ClaI-fw	NNATCGATGCGTTCTCGAAATCAGC
Hygr-ClaI-rev	NNATCGATCAACAGGTGCTCAGCCTA

The DNA fragment was cloned into the pJet vector (Ch. 5.4.3.3.8), after the cut out with the restriction enzyme ClaI, it was purified after separation with agarose gel electrophoresis. The fragment was then introduced into the ILS8655 backbone (Ch. 5.4.3.3.8) and amplified using the cloning protocol (Ch. 5.4.3.3.6) and hygromycin (5-50 µg/ml) together with apramycin (25-150 µg/ml) as antibiotics.

For nomenclature of generated plasmids see Ch. 5.4.3.3.11.

5.4.3.3.10 Sequencing of DNA

For sequencing, the samples were prepared as required in the protocol and sent to MWG Eurofins (Ebersberg, nearby München). Two samples with either the forward or the reverse primer were prepared in order to gain more information by aligning both pieces.

The received files were processed (remove unspecific signals) and both sequences from the forward and the reverse primer aligned using the software APE (A plasmid Editor; free; related to the University of Utah).

The sequences were blasted in the NCBI database (National Center for Biotechnology Information, U.S. National Library of Medicine; http://blast.ncbi.nlm.nih.gov/Blast.cgi) and aligned to known sequences in order to ensure their validity.

5.4.3.3.11 Generated plasmids replacing parts of pIJ8655

After generation of several DNA fragments containing sequences of fluorescent proteins or antibiotic resistances, they were combined to generate several versions (Tab. 17).

Tab. 17: Overview of generated plasmids with modifications.

Backbone	Inserted fragments	Restriction enzymes	Name of plasmid
Published original	TS^R, tipAp, Apr^R, eGFP	-	pIJ8655
pIJ8655	ermE Promoter, mcherry	NdeI, EcoRV; NdeI, NotI	ILS8655c
ILS8655c	Dendra2	NdeI + NotI	8655**d**
ILS8655c	mEos2m	NdeI + NotI	8655**e**
ILS8655c	Hyg^R	ClaI	**H**8655**c**
8655d	Hyg^R	ClaI	**H**8655d
8655e	Hyg^R	ClaI	**H**8655**e**

For a graphical overview of the sequence modifications see supplemented figures.

5.4.3.3.12 Generated modified bacterial strains

The generated plasmids were conjugated into selected *Actinomycetes* strains, isolated from different leaf-cutting ants (Tab. 18) following the attached protocol after Jon Thwaite 2002 and the book "Practical Streptomyces Genetics" (p. 249, 2000, ISBN 0-7084-0623-8).

For *Streptomyces* Ads and *Pseudonocardia* Ao1, I was not supported with the unmodified strains, therefore I was not able to modify them with my new plasmids. My isolates AE1, AE4, ATV7 and ATV9 were naturally apramycin resistant, therefore they were only modified with plasmids containing the sequence of the hygromycin resistance cluster. The

success of conjugation was checked by PCR using selective primers for sequences of fluorescent proteins or resistance clusters.

Tab. 18: Generated genetically modified bacterial strains isolated from leaf-cutting ants.

Name	Origin	Modifications
Streptomyces Av25_6	*Acromyrmex volcanus*	None, ILS8655, 8655d, 8655e, H8655c, H8655d, H8655e
Streptomyces Ae32_2	*Acromyrmex echinatior*	None, ILS8655, 8655d, 8655e, H8655c, H8655d, H8655e
Streptomyces Ads	*unknown*	ILS8655
Pseudonocardia Ao1	*Acromyrmex octospinosus*	ILS8655
AE1	*Acromyrmex echinatior*	None, H8655c, H8655d, H8655e
AE4	*Acromyrmex echinatior*	None, H8655c
ATV7	*Atta vollenveideri*	None, H8655d, H8655e
ATV9	*Atta vollenveideri*	None, H8655d, H8655e

In order to reduce the storage amount, useless modified strains were autoclaved after examination. For some strains, no defined fluorescent signal was seen between modified and not modified samples.

5.4.3.4 Cultivation of leaf-cutting ants

Sub colonies (without queens but all other castes) of *Acromyrmex echinatior* and *Atta colombica* were cultivated and used for research. These leaf-cutting ants were received from Dr. Wirth (University of Kaiserslautern, Germany).

To simulate the natural environment of leaf-cutting ants, they were kept in three plastic boxes which were connected with plastic pipes (nest). Their fungal-cultivar and their brood were placed in the middle box. Ants were supported with fresh bramble leaves and water, which were placed in the right box. The left box remained empty and was used as waste chamber. Cultivation of ants was improved by placing their nest into the climate room of Dr. Kleineidam (28°C, high humidity, University of Konstanz) instead of cultivation at room temperature (20-22°C, low humidity) or in an incubator.

If necessary, ants were paralyzed by placing them into the fridge (4°C) for a short time.

5.4.3.5 Inoculation of leaf-cutting ants with labelled Actinomycetes

Spores and mycelia of modified Actinomycetes were applied on dead ants' bodies in order to spot their contrast. Modified strains were grown on SFM agar plates for 3-5 days, dissolved in water, applied on ants using tooth sticks and fluorescence microscopy (Olympus

BX51; Olympus U-RFL-T; Zeiss Axio Cam MRc) was used with 4x magnification in order to take first pictures.

Modified bacterial strains were applied to living ants (paralyzed at 4°C). Application of dry spores on ants' bodies was not successful therefore spores were dissolved in water. Finally, a mixture of water and glycerol (3:2) showed best results to adhere modified bacteria on ants' bodies.

In order to mark treated ants, nail polish was used for recognition. Some nail polish colors showed fluorescence signals too, they were therefore replaced by other colors in order to prevent false positive results.

As mentioned before ants (genus *Acromyrmex*) have no bacterial biofilm when they hatch, but they somehow begin to accumulate bacteria in their first days. For that reason, established bacterial biofilms were reduced by scraping off these biofilms from some ants with wet toothpicks. These ants were marked with nail polish (color 1).

Some ants with reduced bacterial biofilms were treated with modified bacteria because if ants wanted to rebuild their bacterial biofilms actively, probably due to increased glandular secretions, the modified bacteria could have an advantage in conditions of growth. These ants were marked with nail polish (color 2).

The modified bacteria were applied alone or together in a mix. Treated ants were set back to their colonies. The colonies were cultured for several weeks, dependent on ants' fitnesses and remaining fungal cultivar.

5.4.3.6 Inoculation of leaf-cutting ants' ecosystem with labelled Actinomycetes

Spores and mycelia of labelled Actinomycetes were applied on bramble leaves or located in several areas in their nest.

We monitored, whether the ants stopped cutting leaves or preferred some application methods or strains. Results were documented as photo protocols.

Application of dry spores on bramble leaves was not successful therefore spores were dissolved in water. Finally, a mixture of water and glycerol (3:2) showed best results to adhere modified bacteria on bramble leaves without influencing ants' behavior.

5.4.3.7 Storage, sample preparation and screening of treated ant colonies

Dead ants were removed and stored at -20°C. Ants which were labeled with nail polish were stored in separate tubes in order to prevent contamination of untreated ants and false positive results. For visualization of modified bacteria, ants were placed onto a microscope slide and screened for fluorescence signals (4x or 10x magnification). Sometimes it was necessary to cut off legs or heads which covered other body parts.

Besides this, agar plates were used to cultivate modified bacteria which were isolated from ants' bodies. This should enhance recognition of modified bacteria on and in ants' bodies, which could not easily be visualized by fluorescence microscopy. The modified bacteria contain an apramycin and/or hygromycin resistance cluster and grow therefore on agar plates with apramycin and/or hygromycin as antibiotic. This was used for selective growth on agar plates. Especially *Atta colombica* ants were used for re-isolation experiments because they do not have visible bacterial biofilms on their bodies. Some ants were removed from the colony three weeks after treatment with modified bacteria. Ants were placed in tubes with water and vortexed for short time. After that they were transferred into another tube with water and were homogenized, vortexed and centrifuged.

Both solutions were spread on SFM agar plates containing apramycin (50 µg/ml). Plates were incubated for several days at 28°C.

5.4.4 Results and Discussion

This work was taken over from Dr. Schoenian (University of Jena), who prepared first plasmids and genetically modified organisms. She described initial observations in her PhD thesis. In the beginning, I performed some control experiments and had to face major difficulties. To overcome these problems, I modified the available plasmids with photoconvertible fluorescent proteins. Instead of solving problems, I discovered even more problems due to false estimations and lacking control experiments in the preliminary work. Herewith, I describe the control experiments and show results of my enhanced error analysis in more detail and microscope images.

5.4.4.1 Preliminary work

Dr. Ilka Schoenian described the initial experiments in her PhD thesis. She modified the plasmid pIJ8655[102] because the incorporated promotor was thiostrepton-induced and therefore not suitable for the ant experiment. The fluorescent proteins need to be expressed all the time, not only after incubation with thiostrepton. Therefore, the tipA promoter was replaced by the constitutive ermE* promoter.[104]

Furthermore, in order to enhance the fluorescence signal of modified bacteria compared to ants' chitinous exoskeleton, she replaced the gene sequence of the fluorescent protein eGFP (green) by the gene sequence of mCherry (red).

Actinomycetes, isolated from different leaf-cutting ants, were conjugated with the generated plasmids and placed in sub-colonies for one experiment (6 days).

Dr. Schoenian recommended her ermE*p-mCherry-plasmid and two bacterial strains (Streptomyces 25-6 and 32-2; both genetically modified) for further experiments.

5.4.4.2 Estimation of background signals with dead leaf-cutting ants' bodies

The modified bacteria should have been visualized on leaf-cutting ants' bodies. Therefore, leaf-cutting ants have to be viewed under a fluorescence microscope. Surfaces of ants' bodies were very rough and uneven. Therefore, no focus could be set to one distinct layer. The used microscope did not allow to produce stacked images; therefore, several pictures were taken in order to see all areas by comparing at least those images.

Unfortunately, solid particles and frozen droplets on ants' bodies showed strong fluorescence signals (Fig. 72). Chitinous bodies of leaf-cutting ants showed weaker auto-fluorescent signals than frozen particles (Fig. 72 A-C). Other particles like a greenish moss on the upside of nail polish also showed dominant fluorescent signals (Fig. 72 D).

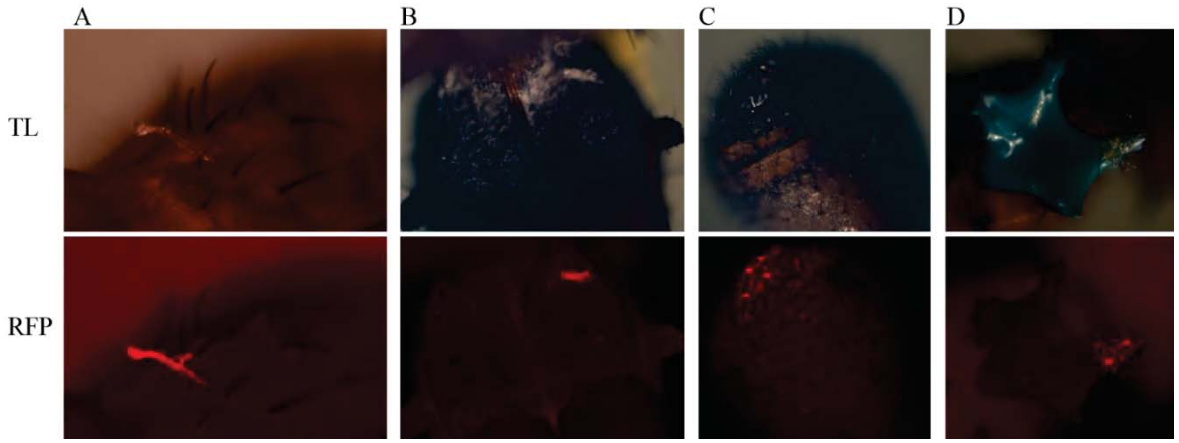

Fig. 72: Microscope pictures taken from bodies of *Acromyrmex echinatior* with transmitted light (TL), red light (RFP) and 4x magnification. A: Long iced particle causing RFP signal. B: Iced particle on ants' integument causing RFP signal. C: Iced particles on ants' gaster causing area of RFP signal. D: Waste particle causing RFP signal.

All bodies of leaf-cutting ants were shown to produce autofluorescent signals at 4x and 10x magnification, without application of labelled samples. The refraction of light has to be compared to real fluorescent signals of fluorescent proteins in order to estimate their relevance for further experiments.

Freezing of samples might be problematic, but also dirty ants collected from leaf-cutting ants' waste chamber showed autofluorescence signals because their bodies might be covered with waste particles (Fig. 73).

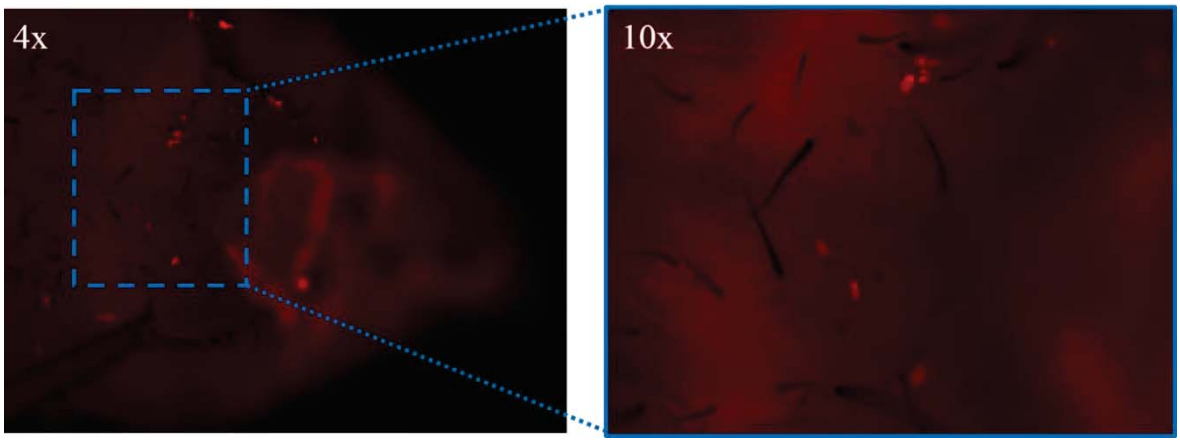

Fig. 73: Microscope pictures taken from a dead ant worker (*Acromyrmex echinatior*) with red light (RFP). Left picture: 4x magnification with zoom area. Right: Zoom area with 10x magnification.

As mentioned by Dr. Schoenian, the bodies of leaf-cutting ants were visible when fluorescence filter sets were applied. I observed further effects of particles, iced droplets and icicles. Therefore, the fluorescent labelling with mCherry should be substituted with photoconvertible fluorescent proteins in order to visualize a contrast between autofluorescent particles and green to red switchable fluorescent proteins.

5.4.4.3 Exchange of the fluorescent protein mCherry against photoconvertible proteins

The difficulties with ambiguous fluorescence signals by particles should be overcome by using photoconvertible fluorescent proteins. The fluorescence signals before and after photo conversion can be compared in order to identify modified bacteria (green to red conversion) in opposition to unchanged signals of particles (Fig. 74).

The sequence of mCherry within the transfection plasmid ILS8655ch was replaced with sequences of photoconvertible fluorescent proteins mEos2 or Dendra2 with the same restriction sites as used by Dr. Schoenian. mEos2 switches its fluorescence peak emission irreversibly from green (516 nm) to red (581 nm) after conversion with UV irradiation at 390 nm.[105] The conversion of Dendra2 is similar.[106]

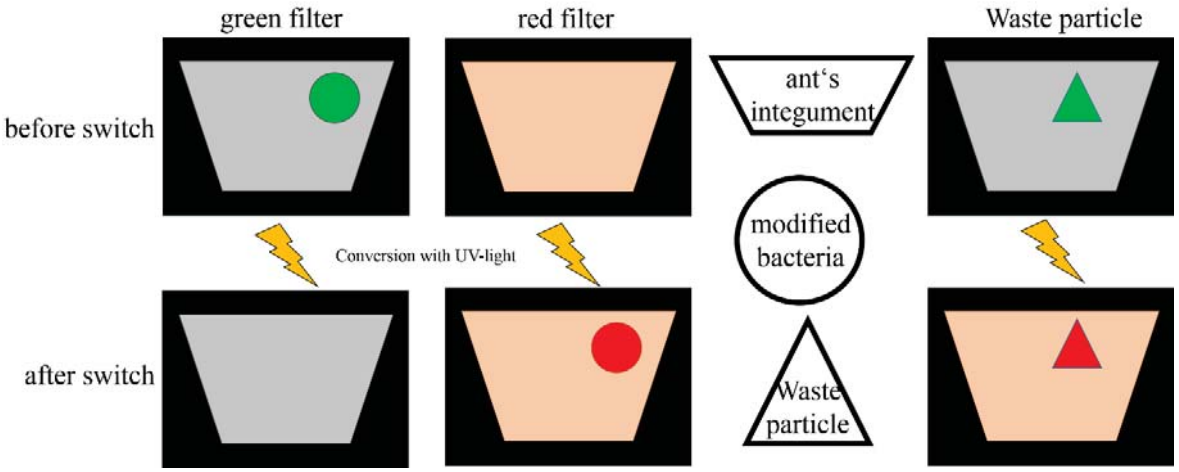

Fig. 74: Schematic overview of fluorescence signals before and after photo conversion as an example for mEos2/Dendra2 (left). Auto fluorescent signals of waste particles remain unchanged (right).

Within the sequence of mEos2, there was a NdeI recognition site which was removed using site directed mutagenesis with self-engineered primers (Fig. 76 A). Fortunately, the exchange of one base pair worked well in a two-step protocol with the developed primers (Fig. 75), which linked the PCR products together (Fig. 76 B). The amplification of Dendra2 and mEos2-original worked well with the developed primers, which introduced the restriction enzyme recognition sites (Fig. 75 C, E). The mutation of mEos2 worked well, as the products were nicely amplified (Fig. 75 A, D, F, G) and were connected thereafter with the help of another amplification using a PCR protocol (Fig. 75 H).

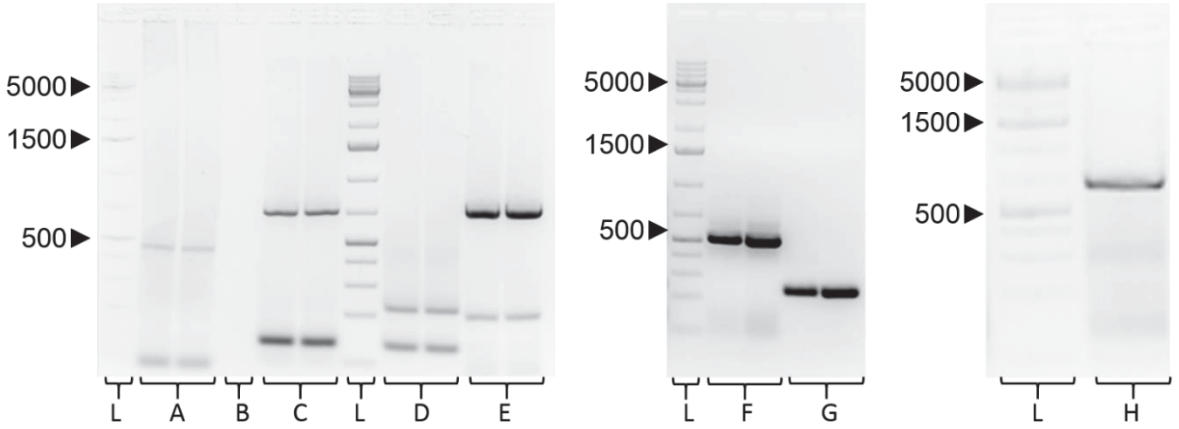

Fig. 75: Densitometric images of PCR products of fluorescent proteins. L: Ladder (Thermo scientific 1kb plus); A: mEos2-A; B: no template control; C: mEos2-original; D: mEos2-B; E: Dendra2; F: mEos2-A; G: mEos2-B; H: mEos2-muta; 2% agarose gel with ethidium bromide staining. 5V/cm in TAE-buffer.

The sequence of the generated oligonucleotide (mEos2-muta) was checked and compared to the amino acid sequence of published mEos2 sequences. Indeed, the amino acid sequence was the same (His) and the exchange of a C against a T was successful (Fig. 76 C).

Fig. 76: Generation of a mutated mEos2 sequence without a NdeI recognition site. A: The two initial PCR products to exchange one base pair. Blue and underlined: Recognition site to exchange a T against a C. B: Alignment of the two PCR products. C: Comparison of DNA sequence and amino acid sequence before and after mutation. Blue and underlined: Exchanged T against a C, but remaining His.

mEos2 and Dendra2 were ligated into the ILS8655ch plasmid replacing the sequence of mCherry. Thereafter, the same protocol and same unmodified Actinomycetes as used by Dr. Schoenian (25-6 and 32-2) were mutated and checked for their fluorescent abilities. Unfortunately, the microscope was not equipped with a suitable filter set for photo conversion, therefore the CFP filter set was used instead.[107]

If the conversion of mEos2 and Dendra2 would have worked, the fluorescence signal intensity should convert from green (GFP) to red (RFP) after irradiation with blue (CFP) light. The blue light could destroy the fluorescent proteins and cause bleaching. Therefore, several treatment durations were used (data not shown).

Indeed, there was no difference visible between treated and untreated bacterial strains (Fig. 77). Neither strain *Streptomyces* 25-6 showed fluorescent signals at all with any modification (mCherry, mEos2 or Dendra2), nor did strain *Streptomyces* 32-2. Additional, strain *Streptomyces* Ads from Dr. Schoenian with mCherry modification was tested, but showed no fluorescent signal.

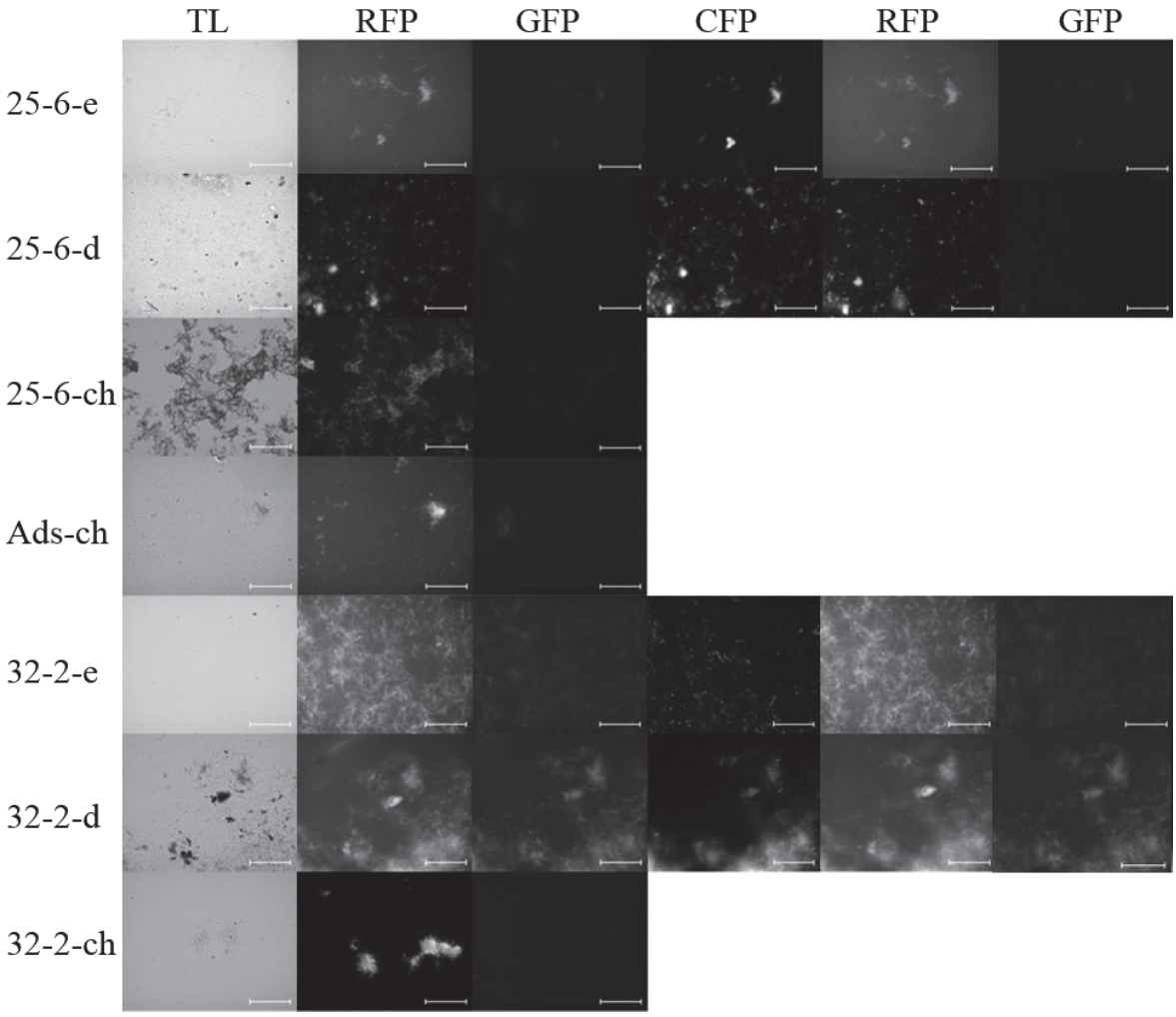

Fig. 77: Microscope pictures taken from *Streptomyces* 25-6, 32-2 and Ads which were genetically modified to produce mEos2 (e), Dendra2 (d) or mCherry (ch). All modified strains were radiated with transmitted light (TL), red light (RFP) and green (GFP) light. Modified strains producing mEos or Dendra2 were additional irradiated with blue light (CFP-filter) and again imaged under RFP and GFP filters. Scale bar: 50 µm.

Compared to untreated strains, no additional fluorescence intensities were obtained with the modified strains. These results indicated fundamental problems with the available strains or the equipment, which will be further investigated in the following chapters.

5.4.4.4 Application of fluorescent bacterial strains on dead leaf cutting ants' bodies

In order to estimate signal strength of fluorescent bacteria, modified bacterial strains of Dr. Schoenian were cultivated and visualized by fluorescence microscopy directly. Furthermore, I applied bacterial mycelium on dead ants' bodies in order to see the contrast of fluorescence signal compared to autofluorescence of untreated samples.

Indeed, no unambiguous differences were seen between fluorescent samples and non-fluorescent controls with the red filter set (data not shown; comparative with Fig. 81; Ch. 5.4.4.6; p. 130).

Therefore, control experiments with reference organisms were conducted. The reference organism (definitively fluorescent protein producing; provided by Christoph Paone from the Hauck group) were applied on bodies of leaf-cutting ants. Furthermore, the signals of reference strains were compared to modified strains from Dr. Schoenian.

The GFP-reference (pure cells in water) showed nice signals with the green filter set (Fig. 78 A). After application on body parts of leaf-cutting ants, the strong signals of green fluorescent protein were visible with much higher intensity than the chitinous exoskeleton of the ant (Fig. 78 B-D). In the overlay of white light and GFP images, the locations of the reference organism could have been easily estimated. The chitinous exoskeleton of the ant was very dominant in the red filter, this is most likely due to lacking reference signals.

Indeed, the statement of Dr. Schoenian to replace GFP with mCherry can not be legitimated with these observations. Unfortunately, Dr. Schoenian did not provide evidence pictures to retrace her findings and support her considerations. It remains unclear, if the equipment caused these problems for example because of a filter set applied in the microscope which has a wider wavelength range compared to our microscope?

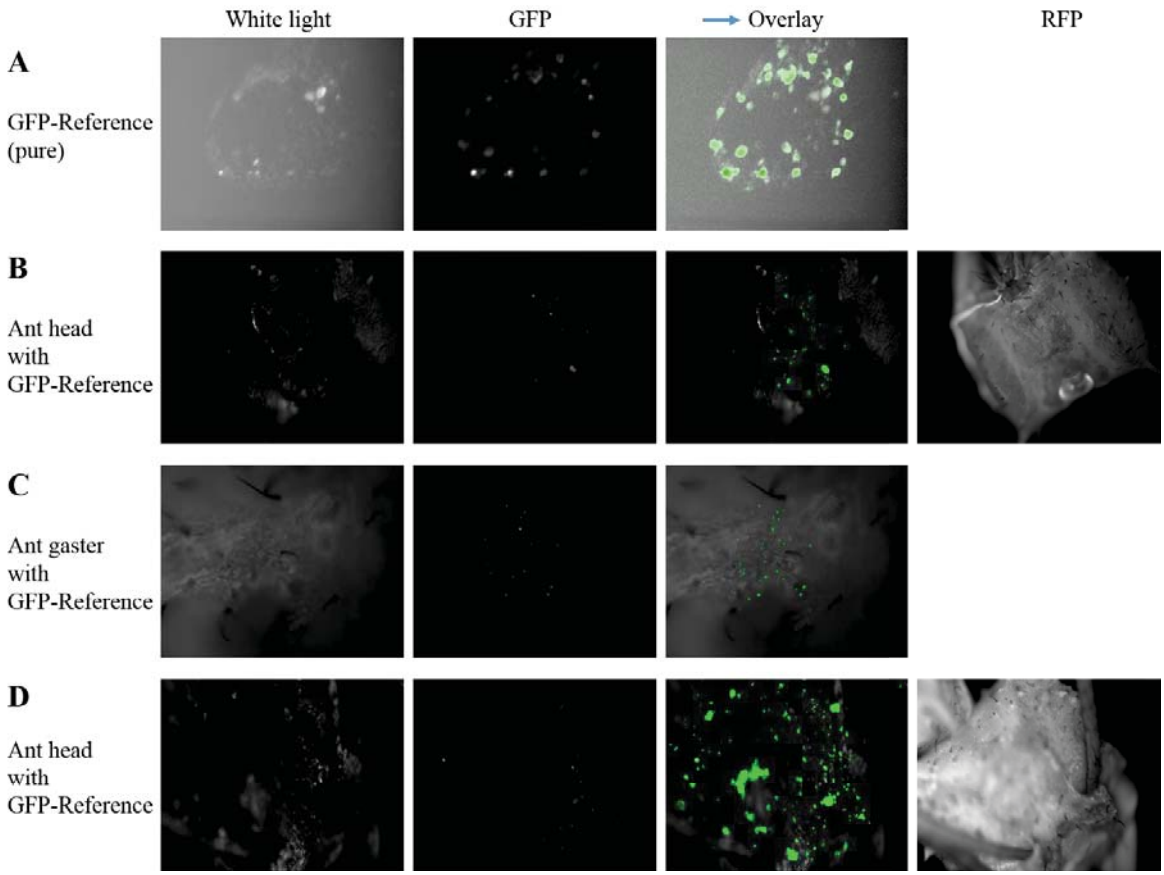

Fig. 78: Application of the GFP-reference organism on bodies of leaf-cutting ants. A: Pure GFP-reference organism in water. B: GFP-reference organism applied on ants' head. C: GFP-reference organism applied of ant's gaster. D: GFP-reference organism applied on ant's head.

The GFP-producing reference organism was compared with modified strains from Dr. Schoenian (mCherry) using the red filter set. If the modified bacteria would produce mCherry, a much higher fluorescence signal would be expected compared to the GFP-producing reference cells.

The GFP-producing reference organism showed the same autofluorescence like the modified bacteria. At first, the camera was tuned on the reference organisms with the red filter set (Fig. 79 A, blue box). The estimated signal should me much lower than the signal for a RPF producing bacterium. Nevertheless, the modified bacteria showed no increase in fluorescence signal (Fig. 79 B). The other way round, the camera was tuned on a modified bacterium (mCherry), where the GFP-producing organism should not show as high signals. The observed signal intensities did not differ at all (Fig. 79 B, blue box).

Recently generated strains with mEos2 and Dendra2 were compared with the same results (data not shown).

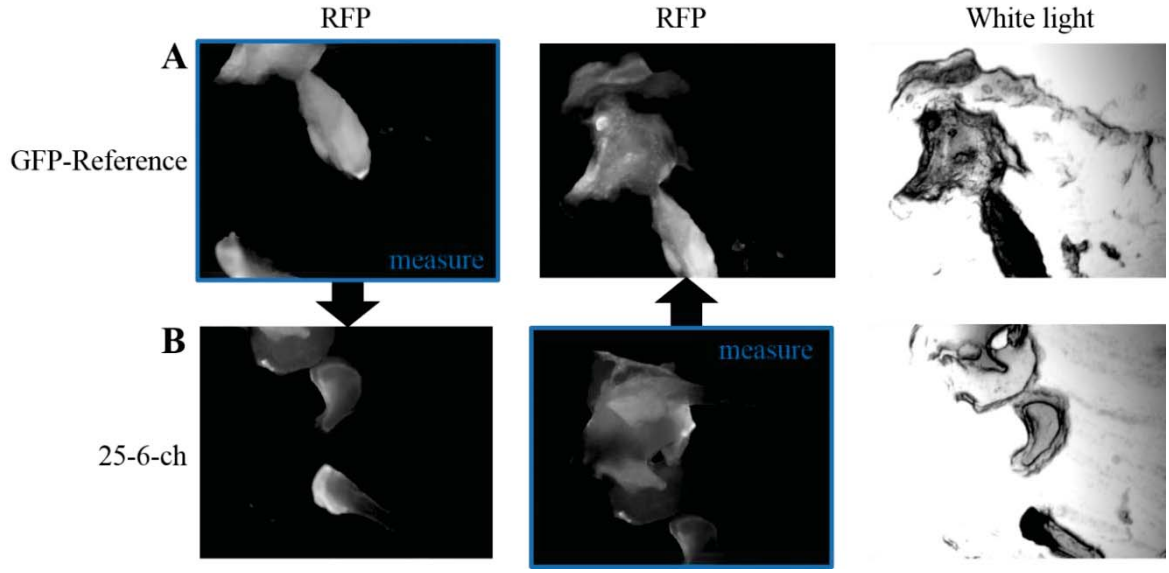

Fig. 79: Comparison of GFP-reference organisms with the modified strain *Streptomyces* 25-6 (mCherry). Blue box indicates the organism for tuning of camera A: GFP-reference organism. B: *Streptomyces* 25-6 with mCherry modification.

Consequently, the provided modified organisms did not produce fluorescent proteins. All my control experiments supported my observed effects (Ch. 5.4.4.3; p. 122) and the reasons needed to be further investigated. Therefore, the preliminary work was checked in more detail.

5.4.4.5 Verification of preliminary work

After unsuccessful repetition of previous observations from the preliminary work, especially concerning fluorescence signals, the complete material was checked.

Indeed, Dr. Schoenian described the problems of autofluorescence of the chitinous exoskeleton of ants. The influence of the exoskeleton was shown to be less relevant (Fig. 78 B-D) with GFP-producing cells as previously described.

Effects of hyphae, especially comparisons of fluorescence signals between modified and unmodified strains, were not described by Dr. Schoenian. In my opinion, the abilities of a modified strain has to be compared with the unmodified strain immediately after it was generated and before it is applied in ant experiments.

The production of fluorescent proteins in her modified strains was never proven by, for example, SDS-PAGE or heterologous expression in other host organisms which recognize her ermE* promoter. I did not perform such experiments, too, but they would help to find out whether fluorescent proteins are produced or not.

The usage of ΦC31 derived vectors was shown to integrate with high efficiency and standard protocols were used. I have shown the integration into the cells with PCR as a control, therefore these procedures were not challenged with further investigations.

Literature research of sequence modifications with primers and restriction enzyme recognition sites indicated some possible defective areas. The primer sets of Dr. Schoenian, which were used to incorporate suitable restriction enzyme recognition sites, may overlay required sequence areas of the promoter. In 1985, Bibb *et al.* described the ermE promoter for the first time in more detail, but they had some hints towards special conserved areas, which need to be present in order to promote transcription.[104] In 1994, they showed complete removal of promoter activity, when deletions are made nearby the -10 region of the promoter.[108] The promoter only worked without alteration of the -10 region and a distance of 7 base pairs to the start codon GTG.

Indeed, the primer sets of Dr. Schoenian (Fig. 80B) discriminated especially this fundamental DNA sequence in the -10 region (Fig. 80A, green hyphens). Therefore, the production of fluorescent proteins is questionable. As I found no additional fluorescence signals compared to unmodified strains, the observations made by Dr. Schoenian might all have been due to autofluorescence.

A

-35 region -10 region

Bibb (1994) gttgtgggctggacaatcgtgccggttggtaggatccagcggtg

Schoenian (2011) gttgtgggctggacaatcgtgccggttggt-----catatggtg

gtg: start codon (after ermEp1)
atg: rest of NdeI restriction site

B

Primers from Schoenian (2011)

ermE P-rev	TCGTGCCGGTTGGTCAT'ATG
mCherry-fw	CAT'ATGGTGAGCAAGGGCGAGGA

Fig. 80: Comparison of sequences of the ermE promoter published by Bibb (1994) and Schoenian (2011). A: Compiled sequences of ermE promoter until the start codon. Green and underlined: -35 and -10 areas of the promoter. Blue: Rest of NdeI recognition site. Red: Start codon of transcription. B: Primers used by Schoenian (2011) to introduce NdeI recognition sites. Blue: NdeI recognition site, position of cut marked by apostrophe.

Moreover, Dr. Schoenian performed an experiment for 6 days with a sub-colony of leaf-cutting ants and described a fluorescent strain after re-isolation on apramycin containing agar plates (p. 43 and picture no. 143 on p. 209)[32]. As I found several naturally apramycin resistant strains in the same *Acromyrmex echinatior* colony (Ch. 5.4.4.7; p. 131), the isolated strain should have been validated, for example by PCR, in order to prove the presence of modified sequences.

In conclusion, expression of fluorescent proteins with the available plasmids or in modified bacteria remains questionable. I recommend either to restart the project from scratch with a

suitable concept (do not forget to conduct control experiments) or to investigate possible problematic steps and solve mentioned discrepancies with experimental evidences (for example: recover -10 region of the ermE* promoter; use definitively fluorescent protein producing strains as references).

5.4.4.6 Application of modified bacterial strains on living leaf cutting ants

Modified bacterial strains were applied to living ants (paralyzed at 4°C). These ants have to survive the treatment and bacteria should be distributed in their nest and not been removed after grooming (hygienic behavior).

Application of dry spores on ants' bodies was not successful therefore spores were dissolved in mixtures with water. Finally, a mixture of water and glycerol (3:2) showed best results to adhere modified bacteria on ants' bodies. Glycerol acted like glue but high amounts killed ants because their limbs sticked together.

As artificially increased contamination with *Escovopsis weberi* led to increased bacterial distribution in ants' nests or on their bodies (genus *Acromyrmex*), the ants might have an influence on intensity of bacterial growth on their bodies. Following this theory, modified bacteria may have an advantage when growing on established bacterial biofilms than on "blank" ants, therefore the established biofilm was reduced by scraping parts off and inoculating the area with modified bacteria.

Finally, there were three treatment groups: those with only added modified bacteria, those with reduced biofilm and added modified bacteria and those with reduced bacterial biofilm and no further treatment. The groups were marked with different colored nail polish and set back to their sub-colony.

Dead ants with nail polish in the waste chamber were removed daily and stored frozen.

After eight weeks, the sub-colony was stopped and all ants were collected, stored frozen and monitored using the microscope. This workflow was only prepared two times because I lacked subcultures for further or longer experiments.

In the first experiment, only mCherry marked modified strains were used. In the second experiment, all available strains were used.

Comparison of collected ants showed no visible differences in the composition of biofilms on their bodies (Fig. 81). The conversion efforts for photoconvertible fluorescent proteins were not successful in control experiments (Ch. 5.4.4.2; p. 121), but were anyway repeated in this experiment. There were no visible differences.

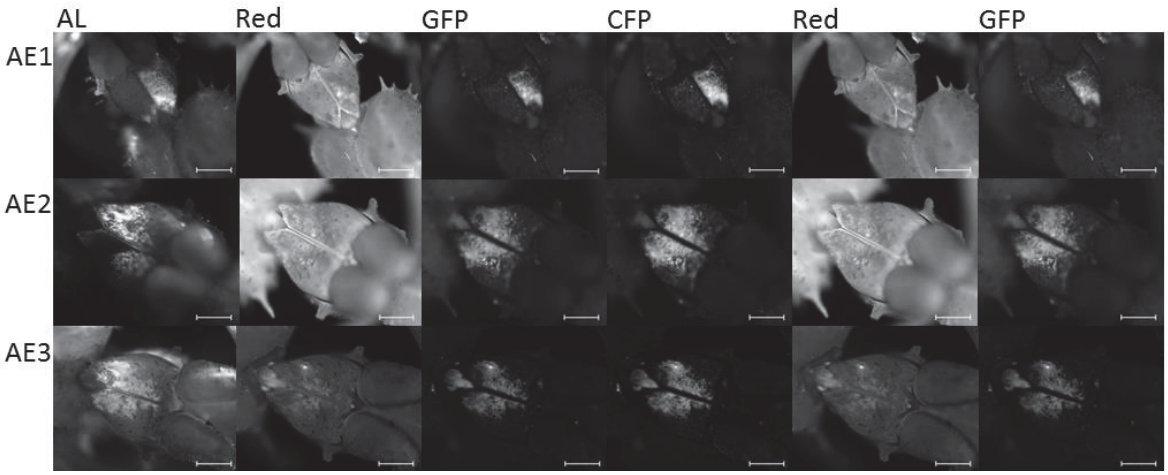

Fig. 81: Three ants (AE1-3) with visible biofilm on the ants' thorax. The ants were collected from the waste chamber and irradiated with reflected light (AL), red (RFP) and green (GFP) filter. The ants were afterwards irradiated with blue (CFP) light to convert the fluorescent proteins. Afterwards irradiation with red and green filter was performed again. Scale bar: 2 mm.

"Fluorescence" signals were also obtained on the back of fungal garden workers, whose bodies were completely covered with bacterial biofilms, but were not treated with fluorescent protein producing bacteria. Ants which were treated with modified bacteria directly showed no additional fluorescence intensity on their bodies. Modified bacteria did not grow in a visible layer on their bodies. Ants with completely removed bacterial biofilms did not recover the bacterial biofilms on their integuments and showed no additional fluorescence signals.

In conclusion, time and need to recover bacterial biofilms remain unclear. Probably more time will be needed to recover bacterial biofilms, or they are not able to recover removed biofilms during their lifetime. This effect may depend on worker caste, because workers in the fungal chamber show bigger bacterial biofilms than workers of other castes. In this experiment, ants from different castes were not treated separately, due to the limited number of ants in the sub-colony.

5.4.4.7 Application and re-isolation of modified bacterial strains

While the production of fluorescent proteins would be visible on the ants' bodies directly, re-isolation of antibiotic resistant bacterial strains from defined areas on their bodies would show their presence and distribution.

Using fluorescent proteins with those wavelengths and this equipment together with dirty environmental samples seemed to produce mayor difficulties because of autofluorescence. Another point, which was not considered yet is the half-life of fluorescence signals in the generated Actinomycetes. As growth rates of biofilm forming bacteria on leaf-cutting ants' bodies are unknown, the lifetime of once produced fluorescent proteins should be at least

days or weeks. The upper layer of the visible biofilms consists mainly of spores, therefore the fluorescent proteins have to be stable during sporulation and in the spores. As the visualization of the modifications is a nice gimmick, but not the crucial point in this research, the approach should have been supported with this second approach to describe the uptake and exchange of modified bacteria.

Bacteria were scraped off at defined points on ants' bodies using tooth picks or generally by washing or homogenizing ants' bodies and spreading supernatants on agar plates. Usage of antibiotic resistant modified bacterial strains simplifies the re-isolation, because by adding antibiotics into agar media, environmental contaminations were reduced. The growing isolates could be verified by PCR using selective primers of the modified sequence area.

First trials showed, that leaf-cutting ants (*Acromyrmex echinatior*) carry a lot of naturally apramycin resistant bacterial strains. Apramycin is therefore not selective for modified strains even at high concentrations. Basic concentration was 50 µg/ml apramycin, the highest tested concentration of 250 µg/ml showed only small differences.

As I was only offered the hygromycin resistance cluster as additional resistance, I cloned the hygromycin resistance gene sequence into the transfection plasmid and herewith modified the *Actinomycetes*. Maybe due to structural similarities with apramycin, the resistant natural strains were as strong as the resistant modified strains. Even a combination of apramycin and hygromycin in the media showed no difference in amount of unwanted bacterial growth.

In order to improve the efficacy of this approach, a screening of different antibiotics and their mixtures will show inhibition zones without growing organisms. Resistance clusters of these antibiotics can be inserted into the transfection plasmid. Furthermore, my approach of different colored Actinomycetes can be used to enhance the number of strains with similar mutation, as they can be distinguished fast and inexpensive by eye (white, yellow, grey) and genetically modified regions help to validate them by PCR amplification with available primers.

5.4.4.8 Application of modified bacterial strains on bramble leaves

In order to find out, whether the leaf-cutting ants differentiate between the modified bacterial strains, they were applied on bramble leaves. Bramble leaves were covered with (spore/mycelium) solutions in water-glycerol-mixtures. Every day, the remaining bramble leaves were taken out and monitored after preferences for a three-week period.

There was no discrimination between untreated, or water-glycerol treated leaves with or without bacteria. The ants showed no different behavior to the coated leaves compared to untreated leaves (data not shown). Furthermore, coating of bramble leaves with different

strains and markers showed no preferences of leaf-cutting ants towards any treatment (Fig. 82).

It remains unclear, if the provided organisms had any influence on ants' or fungus' fitness.

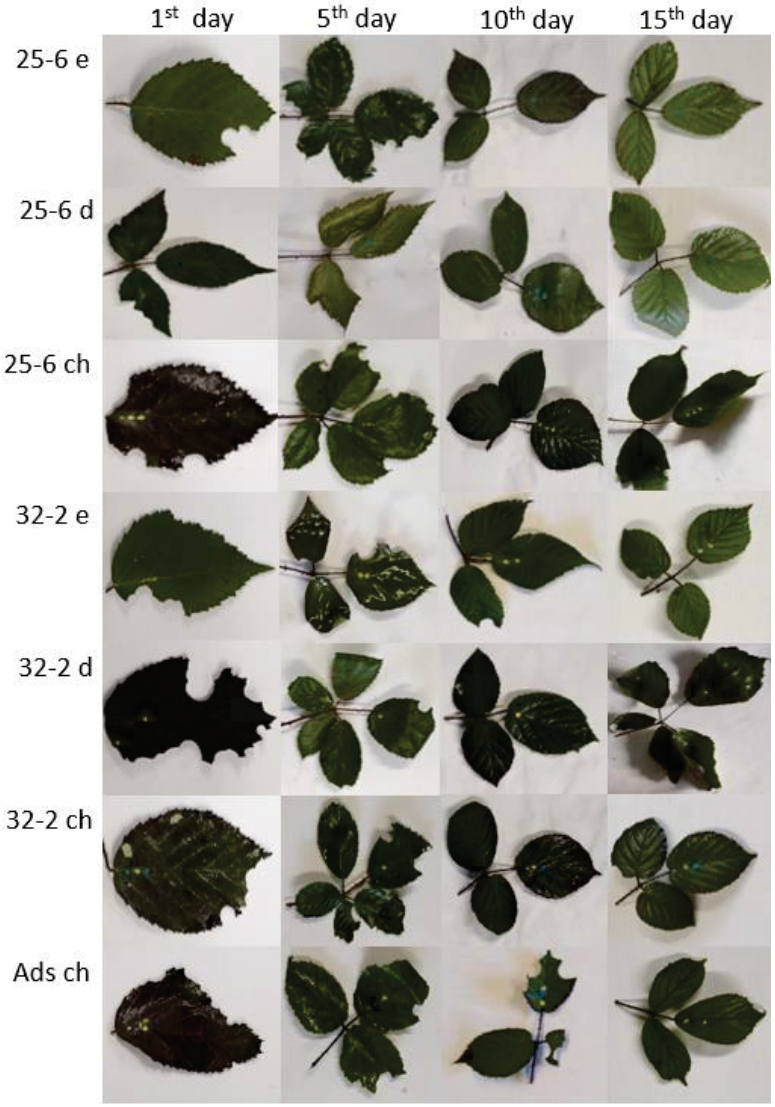

Fig. 82: Bramble leaves with coatings from the food chamber after one day. Four time points (day 1, 5, 10 and 15) were chosen exemplarily.

5.4.5 Conclusion and outlook

Bodies of leaf-cutting ants showed strong autofluorescence signals when monitored with the red filter set of the microscope. They are furthermore problematic samples as their surface is rough and uneven which hinders to focus on one layer. Particles or frozen water showed strong autofluorescence intensities, too.

The modified bacterial strains (mCherry, mEos or Dendra2) showed no additional fluorescence intensities compared to unmodified controls, neither dry nor suspended in water. In comparison to other cell lines, which definitely produce fluorescent proteins, the available and generated organisms showed no fluorescence signals.

The GFP producing cell lines showed strong fluorescence signals even on ants' bodies, which is contrary to Dr. Schoenian's thesis. Whether Dr. Schoenian has proven her statement to exchange GFP with mCherry to improve signal intensities with experimental setups or only speculated with no control experiments is not known.

Re-isolation of modified bacteria is possible, but appropriate antibiotics have to be identified and their resistance clusters need to be added to the transfection plasmid in order to speed up re-isolation. Apramycin was shown to be ineffective, as there have been already resistant strains in the controls. Differently colored strains enhance the number of possible experiments without generation of additional plasmids, as they can be distinguished by eye.

Application of modified strains on bramble leaves did not influence the cutting preferences of leaf-cutting ants in this experiment. None of the tested modified bacterial strain was preferred or discriminated.

Due to a lack of sub-colonies, specialized samples and support with material for further modifications of plasmids, this project was stopped. As there were no leaf-cutting ant colonies in our lab, this project was completely dependent on *Acromyrmex echinatior* leaf-cutting ants of Dr. Wirth (terminated in the end of 2015). Generous offers from Dr. Kleineidam and Prof. Dr. Roces to establish an own *Acromyrmex* colony in Konstanz were not recommended by Prof. Dr. D. Spiteller.

Nevertheless, I want to provide my thoughts and ideas in order to support other scientists following this approach. The provided ideas are usable for *Acromyrmex* and *Atta* colonies, because the techniques are suitable to observe changes in composition of bacterial communities (symbionts) even without visible biofilms.

5.4.5.1 Initial uptake of bacteria

The process of initial uptake of (symbiotic) bacteria is unknown, but could be answered by collection of material at defined sample points. It was discussed previously, whether the queen inoculates the eggs directly or eggs/larvae are inoculated by childcare nest mates or ants exchange after hatching (Fig. 83). A crucial point is to collect eggs/larvae in the different stages of growth, as they are stored within the fungal garden and disturbing them may influence the welfare of the colony.

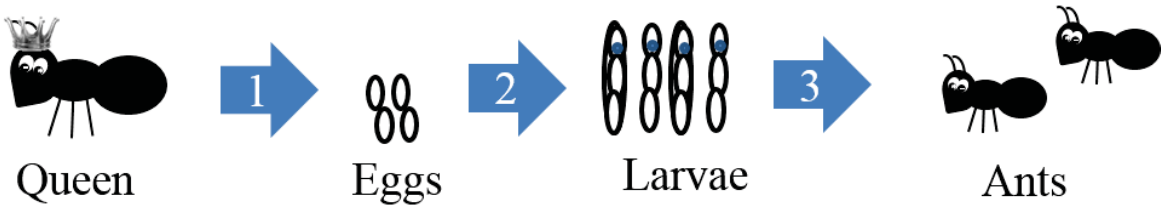

Fig. 83: Sample points to localize a suitable time point for initial inoculation with modified strains.

In order to find out, in which step of the life cycle the "inoculation" takes place, collected material has to be spread on agar plates. If the queen inoculates the eggs, the bacterial strains could be washed away from the surface and replaced by modified strains. If the larvae are fed by childcare nest mates and are inoculated herewith, the larvae and/or childcare nest mates have to be inoculated in order to successfully spread modified bacterial strains in the next generation. If there are no changes in the bacterial community, the spreading finally occurs between nest mates.

In order to reduce possible contrary effects, the modification of some established bacterial strains within the used colony may reduce uncertainties. This may improve the chance for uptake and distribution of modified bacteria because ants may prefer known symbionts and not recognize these bacterial strains as aliens.[42]

Dependent on which antibiotic resistance was used for the modification, the natural strain could be handicapped by application of the antibiotic within ants' nest.

5.4.5.2 Exchange of bacteria between mature nest mates

As soon as it is known, after which principle modified bacteria are selected, the bacterial community of mature ants can be manipulated.

It was discussed if the ants discriminate between abilities like production of chitinases (to stick to ants' bodies) or antibiotics (to enhance fitness) or if they just collect organisms by chance. Knowing the abilities of the modified strains, these questions could be addressed. If they discriminate after production of antibiotics, an antibiotic producing cluster can be inserted in one strain. After that, the distribution of the same strain with and without antibiotic producing cluster can be compared.

Any result of this effort will be a valuable addition to our current understanding.

5.4.5.3 Uptake of new environmental strains

This approach is very similar to the previous approach. Maybe there are additional influences of the application technique and worker caste which mediate the uptake of new bacterial strains. Modified bacterial strains could be applied on transport paths of leaves or waste, on bramble leaves or other places in ants' nests. Procedures to enhance the lifetime of ant (sub-)

colonies need to be established first because the uptake, acceptance and distribution of new bacterial strains with these methods may take longer time than the forced uptake.
Bacterial strains from other ant species with lower or higher ability than established bacteria to inhibit pathogens *in vitro* could be mutated and offered to ants. This may show preferences of ants' uptake behavior which depend on bacterial competencies or origin.

5.4.5.4 Advanced usage of modified bacterial strains

After knowing the uptake and distribution processes of modified bacteria in ants' nests, the generation of individual modified strains to study the expression of gene clusters of secondary metabolite producing proteins could be started. In order to show, which gene clusters play a relevant role in defense mechanisms against pathogens, their promoters could be added to modified bacterial strains producing recognition molecules. The recognition molecules, which are known and very sensitively detectable via LC-MS or GC-MS, will be searched for in the ants' nests.

6 Ecosystem of *Drosophila* fruit flies

6.1 Interactions of *Drosophila hydei* and *Pseudomonas* sp. D2p

Contributions

I started this project started in 2012. Structure elucidation of bioactive secondary metabolites was one of the topics of "Vertiefungskurs Chemische Ökologie 2014" with Yannik Altrichter and Michaela Holzem. Furthermore, Denis Maier wrote his bachelor thesis "Untersuchungen zur Attraktivität von *Pseudomonas* sp. D2p auf *Drosophila hydei*" (submitted in July 2015) and my DAAD RISE student Karolina Subko worked again on bioassay-guided fractionation to identify bioactive molecules (Jun-Aug 2015). Moreover, Laura Heinzelmann and Sabryna Broistedt tested selected pyrazines in behavior assays during "Vertiefungskurs Chemische Ökologie 2016".

MATLAB scripts were provided by Thomas Bochynek (Monash University; Melbourne, Australia).

Drosophila melanogaster and *hydei* were provided by Florian Schlusche (Animal collection of the University of Konstanz).

6.1.1 Abstract

Fruit flies evolved a great variety of mutualistic interactions with bacteria, located especially in their gut. Their principal food source is yeast growing on fermenting fruit. Therefore, they very often converge to overripe and contaminated food.

Attractiveness of bacteria to fruit flies has been investigated for about 60 years (Gow, 1954), but few of the specific chemicals responsible for this effect were identified yet. Recently, some olfactory cues for finding safe food were described. Geosmin, often produced by molds, was found to deter fruit flies from unsuitable feeding and breeding sites. Whereas volatile compounds produced by some *Lactobacillus* strains led to aggregation of fruit flies. Bacteria are also known to promote larval growth, protect against enteric infections and influence mating preferences.

I isolated the strain *Pseudomonas* sp. D2p from flightless *Drosophila hydei*. D2p inhibits the growth of pathogenous fungi, such as *Fusarium* spp.. Two bioactive substances were elucidated to be 4-hydroxy-3-nitro-benzoic acid and phenylacetic acid. Additionally, D2p produces volatile compounds smelling like fresh apricot when grown on SFG or TB agar plates. In novel developed behavioral assays, a strong attraction of fruit flies to bacterial cells of D2p was observed. In order to determine the chemical structures of attractive molecules, several methods like SPME-GC-MS and a cryo distillation apparatus were developed.

Substituted pyrazines were present in SPME-GC-MS profiles of D2p after 4 days, but not after 28 days of growth. Thus, methylated pyrazines were tested for their attractiveness, but the attractive compound(s) remained unknown.

6.1.2 Introduction

Drosophila fruit flies are widely used as model organisms in neurophysiological and genetic studies.[109] In recent years, interactions between fruit flies and microbes came into focus, because the microbiome of flies is less complex than the human microbiome.[110-112] Fruit flies like *Drosophila melanogaster* and *hydei* are easy to cultivate as they only require simple diets and climate conditions. They can be cultivated in a beaker glass together with their cultivation media and wood wool (Fig. 85A). Fruit flies have a short generation time; modifications can directly be monitored within one generation or over several generations if one wants to study long term influences.

Especially interactions with yeasts and bacteria were investigated, because both groups play an important role for their welfare (Fig. 85B). Yeasts and saprophytic flies evolved strong mutualistic associations, as yeasts serve as essential food sources for *Drosophila melanogaster* or *hydei* (Fig. 85B; green circle).[113] In return, fruit flies were shown to inoculate potential feeding areas for their larvae with yeasts and are herewith actively spreading strains.

Volatile organic compounds (VOCs) of yeasts were identified to attract *Drosophila* fruit flies, mixtures with defined ratios between acetic acid, acetoin, ethanol, 3-methyl-1-butanol and 2-phenyl ethanol were found to be as attractive as natural bouquets produced by *Saccharomyces cerevisiae*.[113] Recognition of several yeast strains by fruit flies were compared and showed huge differences, fruit flies seemed to discriminate or prefer certain yeast strains.[114-115]

An axenic fruit was less attractive than a fruit covered with yeast (Fig. 84; own experiment).

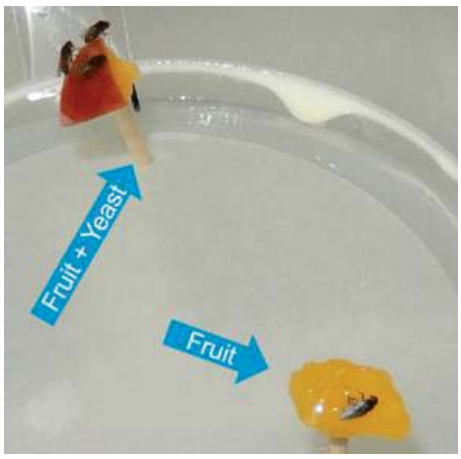

Fig. 84: Behavioral assay on a petri dish: Comparison of fruit fly attraction by pure fruit and with yeast inoculated fruit samples.

With the help of their olfactory sensory systems, fruit flies are able to distinguish between safe and potentially harmful feeding areas. Indeed, fruit flies have to face a lot of dangers concerning their diet, they very often consume overripe and contaminated food. VOCs of pathogenic fungi can be recognized as repellant, especially geosmin was shown to be a warning signal for fruit flies.[116] Geosmin is not only produced by fungi, but also by bacteria and cyanobacteria. Pathogenic fungi can harm fruit flies either by producing toxins or causing infections (Fig. 85B; red circle).

Interactions between fruit flies and bacteria were shown to help the growth of larvae and survival of adults.[117] It is widely accepted that bacteria have an impact on nutrition, immune function and other physiological systems of any host. Modifications of fruit flies' microbiota are easy to achieve and effects can be measured in simple setups.[110] Nevertheless, bacteria are also known to cause infections. Therefore, fruit flies need to distinguish between bouquets of "good" and "bad" bacteria (Fig. 85B; blue circle):

For example, in experiments with *Lactobacilli* it was shown that microbial volatiles attracted other fruit flies to join a feeding site.[118] Furthermore, bacterial communities were shown to have a direct impact on mating preferences of fruit flies.[119-120] These preferences changed either after direct inoculation of axenic individuals or were influenced by different nutrition of two groups, selecting for the survival of specific bacteria. Fruit flies from the same treatment groups preferred to mate with each other and discriminated fruit flies from other treatment groups. In concerns of host fitness, *Wolbachia* strains (α-proteobacteria) were shown to increase their natural host's fitness but decrease the fitness of hybrid fruit fly strains.[121] Therefore, bacteria have a direct impact on the welfare of their direct host.

For this project, I isolated a bacterial strain, named *Pseudomonas* sp. D2p, from flightless *Drosophila hydei*. *Pseudomonas* sp. D2p produces bioactive compounds which inhibit the growth of *Fusarium* spp.. These pathogenic fungi grow on fruits and crops and can produce

toxic compounds. The chemical structures of the bioactive compounds should be elucidated using bioassay-guided fractionation and NMR, combined with MS and IR.

Additionally, D2p produces a volatile compound or a mixture of compounds smelling like fresh apricot. In a novel developed behavior assay, *Drosophila hydei* was actively attracted by D2p's scent. Compound compositions of volatiles from D2p were analyzed by GC-MS to identify promising candidates for description of the observed attractiveness.

The direct influence of D2p on host's fitness was investigated by offering the bacterium to lab cultures of *Drosophila hydei*. The fitness of *Drosophila hydei* should be monitored to describe benefits or harms of this treatment in combination with the application of pathogenic fungi.

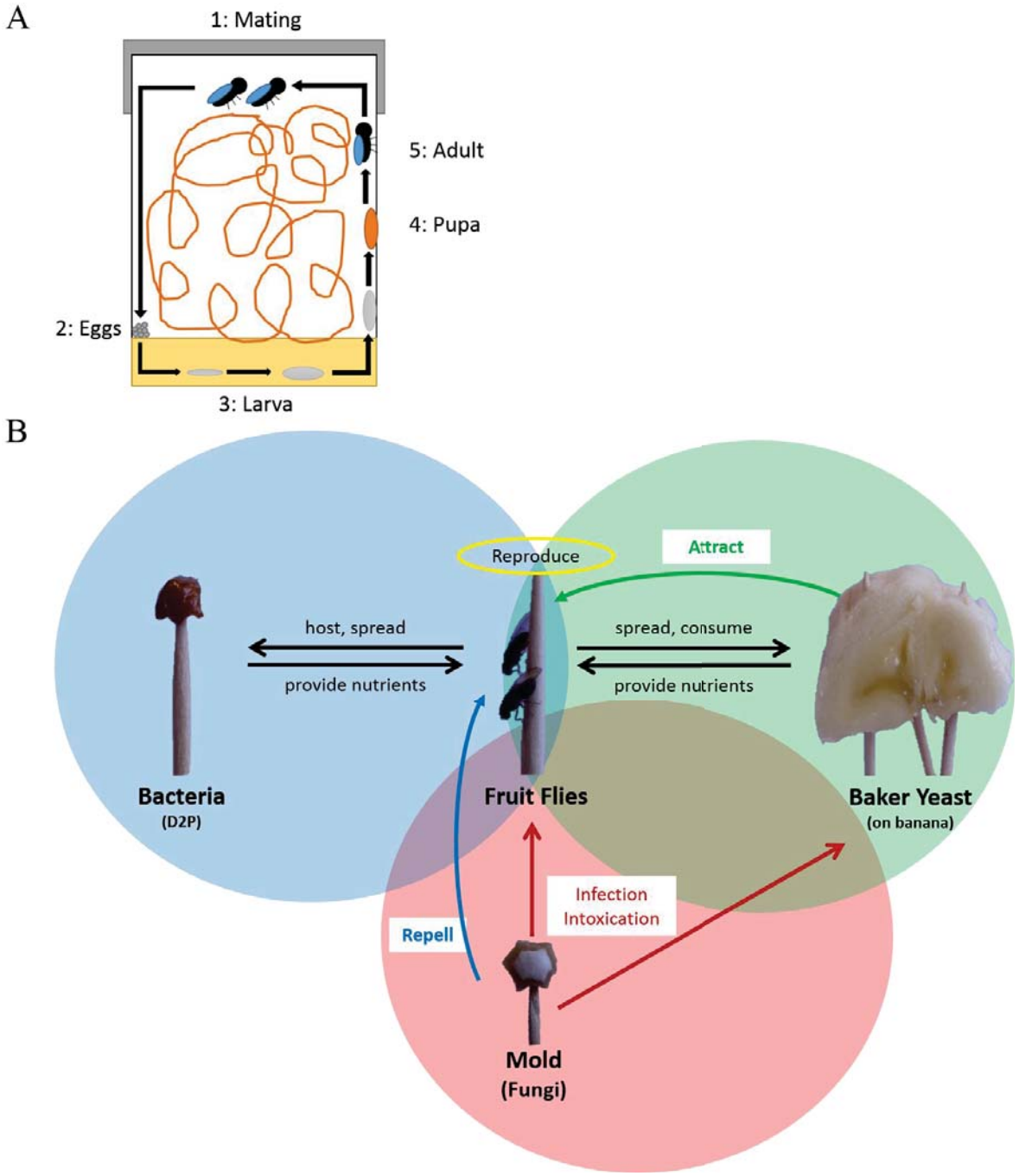

Fig. 85: Schematic overview of *Drosophila hydei* lab cultures. A: Lifecycle of fruit flies. B: Ecosystem of *Drosophila hydei*. Green circle: Interaction between fruit flies and yeasts. Blue circle: Interaction between fruit flies and bacteria. Red circle: Interaction between fruit flies and pathogenic fungi.

6.1.3 Methods

6.1.3.1 Isolation and growth parameters of *Pseudomonas sp.* D2p

Flightless *Drosophila hydei*, which were received from Florian Schlusche, technical assistant at the Zoo of the University Konstanz. The bacterium *Pseudomonas sp.* D2p was isolated in 2012 using an isolation agar medium (NO2-agar; Tab. 19).

Drosophila fruit flies were homogenated in a reaction tube, dissolved in adH_2O and spread on several growth media compositions (see Chap. 7.3; "Isolation of "; p. 180ff for details). D2p grew on NO2-agar at 28°C and was purified by picking and spreading several times in dilution.

D2p grows not only on NO2-agar, but also on SFG, TB and other media. D2p grows in yellow colonies, sometimes with a pleasant fruity smell (on SFG like apricot; TB has own dominant smell).

For the extraction of volatile compounds and GC-MS measurements, SFG and TB media were prepared with (+) or without (-) glycerol (Tab. 19).

Tab. 19: Media compositions for D2p cultivation.

Medium	*Components (g/l ddH_2O)*
SFG+	10 glycerol, 10 soy flour, 10 glucose, 15 Agar-Agar Kobe I
SFG-	10 soy flour, 10 glucose, 15 Agar-Agar Kobe I,
TB+	12 tryptone, 24 yeast extract, 4 glycerol, 2,3 potassium dihydrogen phosphate, 12,5 dipotassium hydrogen phosphate, 15 Agar-Agar Kobe I
TB-	12 tryptone, 24 yeast extract, 2,3 potassium dihydrogen phosphate, 12,5 dipotassium hydrogen phosphate, 15 Agar-Agar Kobe I
NO2	10 sucrose, 5 tryptone, 2 potassium dihydrogen phosphate, 2 sodium chloride, 0,01 ferrous sulfate, 15 Agar-Agar Kobe I

6.1.3.2 Antibiotic sensitivity and resistance of *Pseudomonas sp.* D2p

In order to speed up to select for or identify D2p, its sensitivity and resistance against antibiotic solutions was evaluated. Therefore, several antibiotic compounds and mixtures were applied in agar diffusion assays on NO2 and SFG agar dishes.

In the holes of the bioassay, 90 µl of the stock solutions with ampicillin (100 µg/ml), apramycin (100 µg/ml), hygromycin (50 µg/ml), kanamycin (25 µg/ml), thiostrepton (saturated) and adH_2O or methanol as solvent controls, were pipetted and D2p was spread all over the surface.

Inhibition zones were marked after 2-5 days incubation time (28°C).

6.1.3.3 Phylogenetic classification of *Pseudomonas sp.* D2p

After cultivation and DNA purification, the 16*S* rDNA was amplified using PCR. The DNA sequence was compared to database entries.

6.1.3.3.1 Cultivation and DNA extraction

D2p was cultivated for 2 days on SFM agar dishes. Bacterial cells (about 20 µl) were scraped off using a tooth stick and transferred into a 1,5 ml reaction tube. The cells were suspended with 250 µl STE buffer und 100 µl EDTA (0,5 M) and incubated for 5 min at 400 rpm and room temperature on a thermoshaker. The tube was centrifuged (6000 rpm for 10 sec), the supernatant was discarded.

Bacterial cells were suspended in 250 µl STE buffer and 10 µl EDTA (0,5 M). After adding 20 µl lysozyme (50 mg/ml), the tube was incubated at 37°C for 5 min. 20 µl proteinase K (20 mg/ml) and 120 µl SDS (10%) were added and incubated for 2 hours at 55°C (600 rpm on a thermoshaker).

Thereafter, 150 µl sodium chloride solution (5 M) was added and shaken until the solution became homogenous. After centrifugation at 13.000 rpm for 10 min, the supernatant was transferred to a clean tube, 500 µl of a chloroform-(3-methyl-1-butanol)-mixture (24:1) was added and the mixture was shaken. After centrifugation at 8.000 rpm for 2 min, the upper phase was transferred to a clean tube and the step was repeated, until there was no intermediate layer visible any more.

The cleaned upper phase was transferred without residual chloroform into a clean tube and twice the volume ice-cold (-20°C) isopropanol was added. The tube was shaken for 1 min and centrifuged at 13.000 rpm for 60 min (precooled centrifuge, 4°C).

The supernatant was discarded and the (often invisible) pellet was washed twice with 250 µl ethanol-water-mixture (7:3, ice-cold, -20°C), which was discarded after centrifugation at 8.000 rpm for 2 min. After evaporation of remaining ethanol, the pellet was dissolved in 15 µl autoclaved ddH_2O.

6.1.3.3.2 Amplification of the 16*S* rDNA using polymerase chain reaction

The concentration of the isolated DNA was measured using a nanophotometer (2 µl).

In a first run, several concentrations (1:1; 1:10; 1:100) of the DNA samples were screened. They were used in a final volume of 10 µl in order to find out, in which concentration the amplification works.

The published 8f and 1492r primers were used for PCR amplification.[122] The PCR-Kit of Phusion High-Fidelity DNA Polymerase (Thermo Scientific) with the developed mixture for the master mix (Tab. 20) and temperature program (Tab. 21) were used to amplify the 16*S* rDNA.

Tab. 20: Master mix for 16S rDNA amplification.

Component	Volume (µl)
5x Phusion GC buffer	30
$MgCl_2$ (25 mM)	24
DMSO	12
Primer-Mix (10 µM each)	6
dNTPs (10 µM each)	12
Phusion Hot Start II DNA Polymerase (2 U/µl)	2
adH_2O	49
DNA template dilution	15
Final volume	150

Tab. 21: Temperature program for 16S rDNA amplification.

Step		Temperature (°C)	Duration (sec)
Initial denaturation		93	30
Activation of hot-start polymerase		98	10
Denaturation	30 cycles	98	10
Annealing		55	30
Elongation		72	60
Final elongation		72	300
Storage		4	unlimited

The PCR mixtures were afterwards mixed with loading dye and separated using agarose gel electrophoresis (1,5% agarose in TAE buffer; chamber filled with TAE buffer; power supply 5 Volts per cm electrode distance; runtime 1 h or until separation). DNA fragments were stained with ethidium bromide and compared to a DNA ladder (Fermentas gene ruler 1 kb plus). The gels were recorded using an UV-chamber (Intas).

The DNA fragment with a length of around 1.500 bp was the target. The DNA template with the least unspecific fragments and the most dominant 1.500 bp signal was amplified again in 50 µl master mix. Herewith, the DNA fragment was either purified directly or separated first via gel electrophoresis, the target band was cut out and purified after that.

DNA purification was performed using a purification kit (Thermo Scientific).

6.1.3.3.3 DNA sequencing and database comparison

For sequencing, the samples were prepared as required in the protocol and sent to MWG Eurofins (Ebersberg, nearby München). Two samples with either the 8f or the 1492r primer were prepared in order to gain more information by annealing both sequenced pieces.

The received files were processed after trimming (remove unspecific signals) and both sequences from the 8f and the 1492r primer were combined using the software APE (A plasmid Editor; free software; related to the University of Utah).

This sequence was blasted using the nucleotide blast of the NCBI website (https://blast.ncbi.nlm.nih.gov/Blast.cgi?PAGE_TYPE=BlastSearch&BLAST_SPEC=TargLociBlast; National Center for Biotechnology Information, USA) and the database parameter "16*S* ribosomal RNA sequences (Bacteria and Archaea)" in order to receive only high quality results for bacterial samples.

Names of similar and related organisms were saved, sequences were searched in the NCBI database (National Center for Biotechnology Information, USA) and copied into the software MEGA 6 (Molecular Evolutionary Genetics Analysis; free license; related to the Tokyo Metropolitan University and the Arizona State University), which was then taken to calculate evolutionary trees.

6.1.3.4 Cultivation of *Drosophila* fruit flies

In order to have reproducible cultivation conditions for *Drosophila* fruit flies (*hydei* and *melanogaster*), a novel culture medium was developed. For co-cultivation experiments, the novel medium needs to allow growth not only for *Drosophila* fruit flies and baker yeast, but also for D2p. The presence of identified antibiotics should have been monitored in the culture media or fruit flies directly. Because our sources in the zoo used culture conditions with added antibiotics, we developed systems to cultivate *Drosophila* fruit flies without added antibiotics.

6.1.3.4.1 Composition of culture media and growth conditions

The initial medium was produced by Florian Schlusche (Animal collection of the University of Konstanz). The extreme usage of antibiotical compounds in the original medium hindered the GC-MS measurements, because added antibiotics (benzoic acid derivatives) dominated signals in chromatograms. Therefore, we developed alternatives without antibiotics. Thus alternative culture media were developed and parameters like nutritional composition, water content, pH and pre-incubation were optimized together with my bachelor student Denis Maier.

In the beginning, several compositions were tested. The most promising mixtures were used for further experiments (Tab. 22).

Tab. 22: Composition of sufficient media for Drosophila cultivation.

Components (g)	**N3**	**N4**	**N6**	**N46**	**Culture medium of Florian Schlusche**
Rice flour	69	69	69	69	69
Corn flour	79	79	79	79	79
Soy flour	-	-	-	-	33
Sucrose	-	25	25	25	50
Glycerol	13	-	-	-	-
Glucose	13	-	-	-	-
Tryptone	17	33	-	17	-
Yeast extract	-	-	33	17	-
Casein Natrium	17	-	-	-	-
Citric acid	-	-	-	-	2
Panel vinegar (5%)	-	-	-	-	50
H_2O	600	600	600	600	550

The mixtures were prepared and inoculated with 10 ml of a fresh yeast suspension (42 g yeast each 100 ml adH_2O; one yeast block from multideck cabinet in a German supermarket) per liter cultivation medium. The yeast was allowed to grow at 32°C overnight, CO_2 was removed by stirring.

After that, the medium was transferred to cultivation flasks and covered with wood wool. Every cultivation flask was inoculated with 10-20 fruit flies, covered with a tissue and placed in an incubator at 24°C and around 60-70% air humidity.

Denis Maier determined size and number of larvae and pupae, thereby a relation between growth and very dry conditions was observed. However, with a minimum water content of 1:1,5 (vol/vol), the fruit flies grow similar. Furthermore, we found no advantage in increasing or decreasing the native pH of the mixtures. A lower pH hinders the growth of contaminating fungi, but after inoculation with yeast, the fruit flies grew similar without contaminations. The most promising medium was N46: it is straight forward to prepare and comparatively cheap. D2p grew on medium N46, too. The developed medium N46 fulfilled all our requirements.

After 3-4 weeks cultivation in the incubator, the fruit flies were harvested. For behavioral assays, fruit flies were shaken out of the cultivation flasks or were allowed to come out

voluntarily. Collected fruit flies were placed into the fridge at 4°C, where they got paralyzed by temperature. Paralyzed fruit flies were only used on the same day.

6.1.3.4.2 Treatment of *Drosophila* fruit flies with antibiotics

In order to remove D2p, the influence of antibiotics on fruit flies was tested. D2p was found to be sensitive against kanamycin.

Dilutions of kanamycin (final concentration: 1; 10; 25; 50; 100; 200 µg/ml) were added to the fruit fly medium. Size and number of adult fruit flies and larvae were monitored and compared for several weeks. 50 to 100 µg/ml Kanamycin did not influence the growth of fruit flies.

To generate D2p-free fruit flies, two generations were treated with 50 µg/ml kanamycin before starting co-cultivation experiments.

6.1.3.4.3 Co-cultivation of *Drosophila* fruit flies and *Pseudomonas* sp. D2p

To evaluate the fitness of *Drosophila* fruit flies in relation to the presence of D2p and pathogenic contaminations, several experimental setups were prepared.

Size and number of untreated and kanamycin-treated fruit flies were compared. Both fruit fly groups were furthermore inoculated with D2p either in their cultivation medium (forced uptake) or as local spots (voluntary uptake). In another setup, both fruit fly groups were inoculated with fungi (*Fusarium* spp. and *Beauveria bassiana*) in order to challenge their welfare.

This part of the project was stopped because my private air humidifier broke, there was no prospect of replacement.

6.1.3.5 Behavioral assays with *Drosophila* fruit flies

6.1.3.5.1 Development of a cabinet for behavioral studies

Initially, we developed a three-dimensional system, where the fruit flies could run on tooth sticks. A filter paper was placed on an agar dish, where three tooth sticks were plugged in. On top of the sticks, the samples were presented.

After testing several volatile oils from the kitchen (like thyme), peppermint oil was found to deter fruit flies. We therefore took it as negative control. The three tooth sticks (or Q tips) were placed in the corners of an equilateral triangle, to have the same distance between every sample.

The edge of the agar dish was greased with peppermint oil containing lotion to hinder fruit flies from jumping out.

The agar dish was placed in a water bath (35°C) for constant temperature. After adding the paralyzed fruit flies in the middle of the filter paper, the water bath was covered with an open bucket (25 l). On top of the bucket, there were two holes. One for light supply (filtered after wave length) and one for a camera.

The best results were obtained without airflow and without the influence of moving shadows, which led to defending reactions like running away from predators. Moving shadows were for example caused by persons passing by or moving heads from observers in front of the experiment.

6.1.3.5.2 Development of a two-dimensional setup for behavioral studies

The previously developed three-dimensional setup had some drawbacks for automatic tracking and because of direct contact between fruit flies and samples on tooth sticks.

Therefore, a 2D-System should be developed to simplify automatic tracking. Furthermore, this system contained an airflow to blow volatile substances in one direction. The airflow prevented a saturation of airspace with volatiles and was placed in the hood.

There was no direct contact between fruit flies and samples, because they were separated by a net. Therefore, influences of feeding or attractant/repellant effects of taste instead of odor were removed.

Unfortunately, this setup could not be tempered. The airflow could not be controlled and the influence of light and shadows could not be removed in the hood.

Therefore, fruit flies did not act as usual, even without samples, there were struggling around like crazy. This part of the project was stopped because of lacking material. Most material was taken from the waste collection place in the university. We were not able to get rid of disturbing influences, but to describe them.

6.1.3.6 Chemical composition of volatiles from *Pseudomonas* sp. D2p

Chemical compositions were measured by GC-MS.

Volatile compounds were collected using cryo trap distillation (Fig. 86A), SPME fibers (solid phase micro extraction; Fig. 86B) or liquid extraction of bacterial cells. The application of closed loop stripping charcoal filters was tested, but neither attractive nor repellent effects were observed in behavioral assays (Fig. 86C). This method will therefore not be further discussed.

Sample collection with SPME

SPME-fibers (here most often polydimethylsiloxane fibers) were directly held inside of a petri dish with D2p cultures or D2p cells were scraped off and placed inside of a glass vial (Fig. 86B). SPME fibers do not collect the complete bouquet, but they provide a first hint to

identify some available volatiles in samples. D2p bacterial cells were measured after several days of growth; differences in GC-MS spectra were compared with results of the behavioral assay to prospectively identify the active substance.

Sample collection with liquid extracts

To produce a sample which could be used in the behavioral assay, the cultures were scraped off and extracted using solvents with different polarity (hexane, diethyl ether, acetone, acetonitrile, methanol, water).

Those extracts were applied on cotton and presented in behavioral assays.

In addition, the attractive extracts were fractionated using silica or RP SPE columns. The fractions were again used for behavioral assays. In consideration of dilution effects, the fractionation worked in small scales (500 µl each fraction, 100 µl in behavioral assay tested). Unfortunately, no volatile compounds were found in GC-MS chromatogram. Whether their concentration was too low or they were hidden by the solvent peak remained unclear.

Sample collection with cryo trap distillation

One method with reduced compound diversity compared to liquid extraction was a self-developed cryo trap distillation apparatus (Fig. 86A). Bacterial cells were collected, heated (40 or 60 or 80°C) and the gas phase was transferred into cooled organic solvents using an airflow. Solvents were cooled in steps, from ice water (0°C), sodium chloride-ice water mixtures (-20°C) over dry-ice (solid CO_2; -80°C) to liquid nitrogen ("-170°C"). Those liquids were subjected to behavioral assays and GC-MS analysis.

Furthermore, those liquid extracts were derivatized with TMSH or MSTFA for GC-MS measurements. Spectra were analyzed to determine the composition of D2p's volatiles.

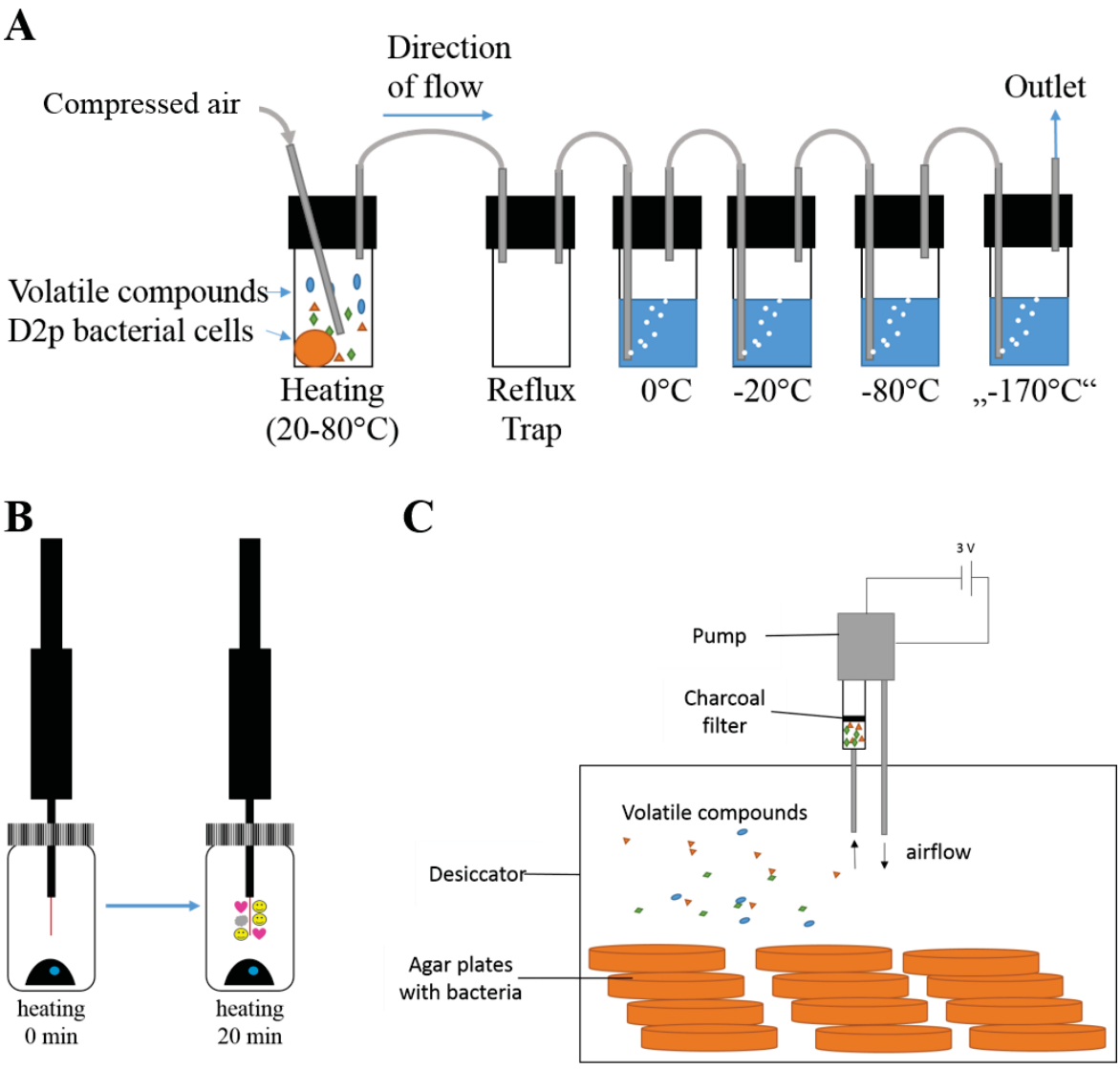

Fig. 86: Compilation of used collection methods for the analysis of volatile compounds from D2p. A: Cryo trap collection. B: SPME collection. C: Closed loop stripping charcoal filter.

A SPME fiber (Supelco; red; polydimethylsiloxane) together with a ISQ Single Quadrupole GC-MS Systems (Thermo Scientific) equipped with an Optima 5MS (25 m x 0,25 mm, 0,25 µm, Macherey Nagel, Düren) GC-column were used for analysis. Conditions were as described elsewhere (Tab. 5; p. 85) with variations for gradient screenings or solvent delay.

6.1.3.7 Purification and identification of antibiotic secondary metabolites from *Pseudomonas* sp. D2p

The ability of D2p to produce bioactive secondary metabolites was tested using co-cultivation diffusion assays against *Fusarium* spp. and *Beauveria bassiana* on SFM agar plates. The conditions for enhanced production of bioactive secondary metabolites was performed for D2p using several culture medium compositions (for more details see Ch. 7.3;

p. 180ff). The same protocol showed sufficient extraction solvents and conditions like pH, metal supplements and cultivation duration.

Cultures of D2p grew with a wide range of nutritients. The spent culture media very often exhibit a characteristic apricot-like smell.

Erlenmeyer flasks with culture media (m6/SFM/TB; composition Ch. 7.3; p. 180ff) were inoculated with D2p and incubated for 3-5 days at 28°C on a rotary shaker (280 rpm). After centrifugation (3000**g*; 10 min), the aqueous phase was acidified using hydrochloric acid (pH 2) and extracted with ethyl acetate (until year 2015) or with diethyl ether (since 2015). Efficiency was increased by application of counter-current exchange extraction.

The organic solvents were dried with sodium sulfate and evaporated. After evaporation, the solvents were reused.

Purification followed the described workflows (Ch. 7.4; p. 186ff) with silica filtration (bioactive: diethyl ether phase), methanol-hexane-separation (bioactive: methanol around 90%), silica chromatography (silica gel column; 60 mesh; 20x2,5 cm), eluted with petrol ether/diethyl ether mixtures (1:1; 1:2; 1:3; 1:4) and finally methanol in 5 fractions (120 ml each). The bioactive fraction was transferred to a RP-C_{18}-column (15x2,5 cm; Polygoprep C_{18} 60-50; Macherey-Nagel, Düren) eluted with methanol in ddH_2O (50%; 66%; 75%; 90%; 100%) in five fractions (120 ml each) followed by RP-HPLC fractionation.

For HPLC fractionation, an Agilent 1100 HPLC system was used. The bioactive residue was dissolved in ddH_2O/methanol (4:1) and several times (each maximum 30 µl) injected into an Agilent ZORBAX Eclipse XDB C_8 column (150x4,6 mm, particle size: 5 µm). A mixture of ddH_2O and methanol (each 0,1% acetic acid) was used at a flow rate of 0,6 ml/min (Tab. 23). The automatic fraction collector collected 27 fractions (1 tube/min) between 1 and 28 min of the runtime.

Tab. 23: HPLC gradient program used for fractionation.

Time (min)	%MeOH (in ddH_2O)
0	20
12	70
18	70
20	100
23	100
23,1	20
28	20

The collected fractions were lyophilized, residues were dissolved in methanol and tested for bioactivity in agar diffusion assays.

Bioactive fractions were measured by NMR (measured at 298 K on a Bruker Avance III 400 MHz spectrometer; dissolved in acetone-d_6 or Methanol-*d4* from Deutero, Kastellaun) or MS (Finnigan Mat LCQ; ESI probe).

6.1.4 Results and Discussion

Pseudomonas sp. D2p was isolated from flightless *Drosophila hydei* using NO2 isolation agar. D2p produces an apricot-like odor, when grown on SFG or TB agar plates and produces antifungal compounds against *Fusarium* spp..

At first, D2p was classified by comparison of 16*S* rDNA sequences with database entries of known bacterial strains. Moreover, the resistance and sensitivity towards available antibiotics was investigated.

As a second step, bioactive compounds against pathogenic fungi such as *Fusarium* spp. or *Beauveria bassiana* produced by D2p in liquid laboratory cultures were extracted, fractionated and identified.

As a third step, attractiveness of D2p bacterial cells towards *Drosophila* fruit flies (*hydei* and *melanogaster*) was investigated. Moreover, the attractive substances should have been identified using several methods for volatile analysis.

To combine all these steps, a co-culture experiment of *Drosophila* fruit flies and D2p was developed (Fig. 87). The fitness of natural and “axenic” (kanamycin-treated) fruit flies was compared with or without addition of D2p and pathogenic fungi such as *Fusarium* spp. or *Beauveria bassiana*. This experiment was intended to elucidate the biological role of D2p in the fruit fly ecosystem.

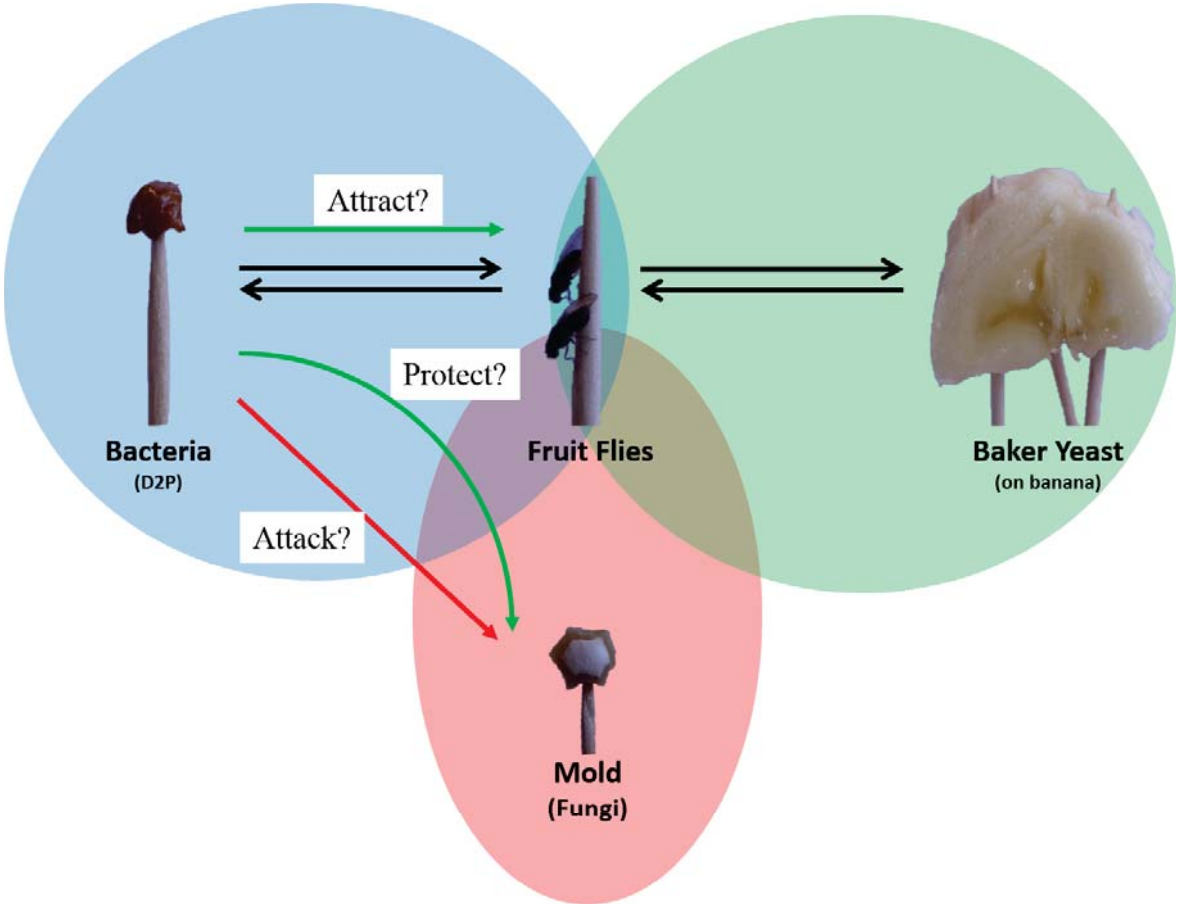

Fig. 87: Question to be answered: Is there a relation between D2p´s bioactivity against pathogenic microbes and attraction of fruit flies? (modified after Fig. 85)

6.1.4.1 Classification of *Pseudomonas* sp. D2p

6.1.4.1.1 Phylogenetic placement of *Pseudomonas* sp. D2p

The obtained sequence of the PCR product between the primers 8f and 1492r had an overlap of 499 bp, but only a length of 867 bp of total 1484 bp.

Comparison of the DNA sequences with the 16*S* rDNA database showed high similarity to *Pseudomonas genticula* (ATCC19374) and *Pseudomonas hibiscicola* (ATCC19867) with only 9 and 6 mismatches respectively in the 867 bp sequence. Thus the isolated bacterium was assigned to be a *Pseudomonas* strain, nevertheless, the sequence has to be longer for an unambiguous assignment. The length can be prolonged by cloning the PCR product into a vector and using the cloned plasmid with selective primers nearby the insert as sequencing sample.

Previously described *Lactobacillus* strains, which attracted fruit flies, are only distantly related to D2p (Fig. 88).[118] The commonly known pathogen *Pseudomonas aeruginosa* has been used for infection studies with fruit flies.[123] *Pseudomonas aeruginosa* is known for its fruity smell, but only distantly related to D2p (Fig. 88). *Bacillus subtilis* is an ubiquitous

bacterium, which was shown to produce attractive compounds for fruit flies too, but is only distantly related to D2p.[124]

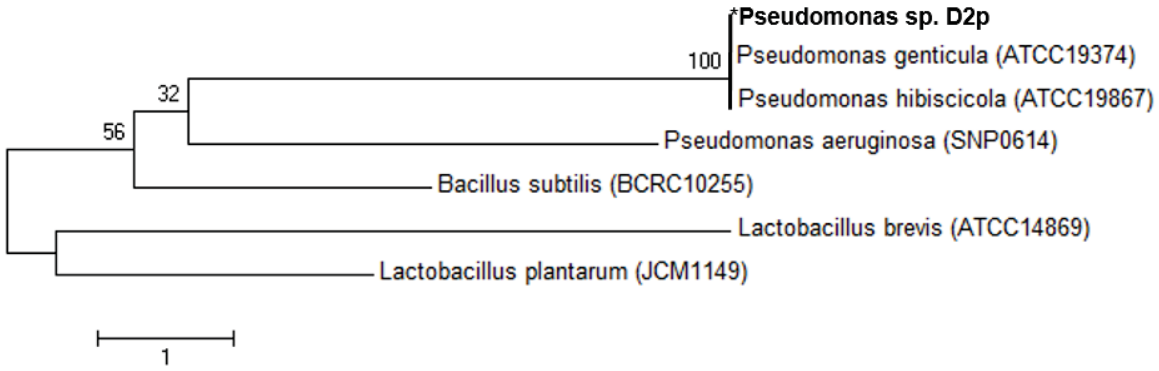

Fig. 88: Phylogenetic tree showing relation of *Pseudomonas* sp. D2p (most similar to *Pseudomonas genticula*) to previously described relevant bacterial strains.

6.1.4.1.2 Antibiotic sensitivity and resistance of *Pseudomonas sp.* D2p

Antibiotic sensitivity of D2p was tested using an agar diffusion assay. Antibiotic solutions were presented in holes, D2p was spread all over the agar plate. For co-cultivation experiments, D2p-free fruit flies should be generated by addition of antibiotics to the culture medium.

D2p was very sensitive to hygromycin (50 µg/ml; Fig. 89-2) and kanamycin (25 µg/ml; Fig. 89-4). Furthermore, ampicillin (100 µg/ml; Fig. 89-1) and apramycin (100 µg/ml; Fig. 89-3) caused weak inhibition zones, while thiostrepton (saturated; Fig. 89-5) and water (; Fig. 89-6) showed no inhibition.

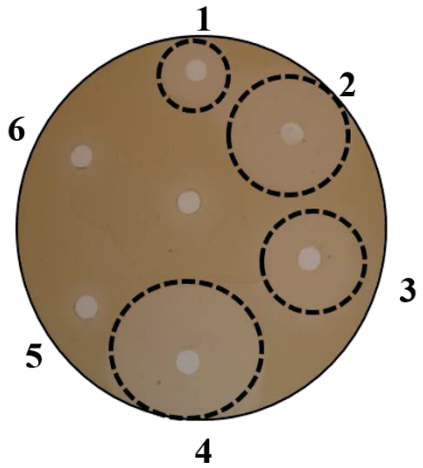

Fig. 89: Agar diffusion assay of antibiotic solutions against D2p. 1: ampicillin (100 µg/ml), 2: hygromycin (50 µg/ml), 3: apramycin (100 µg/ml), 4: kanamycin (25 µg/ml), 5: thiostrepton (saturated) 6: water.

Kanamycin was used for further co-cultivation experiments with *Drosophila* and D2p due to the strongest inhibition of D2p at the lowest concentration.

6.1.4.2 Antifungal compounds produced by *Pseudomonas* sp. D2p

Production of bioactive compounds was compared in screenings for beneficial media and growth conditions using several growth media and supplements (see Ch. 7.3, p. 180ff). The crude extracts showed dominant inhibition zones for m6, SFM and TB (Fig. 90).

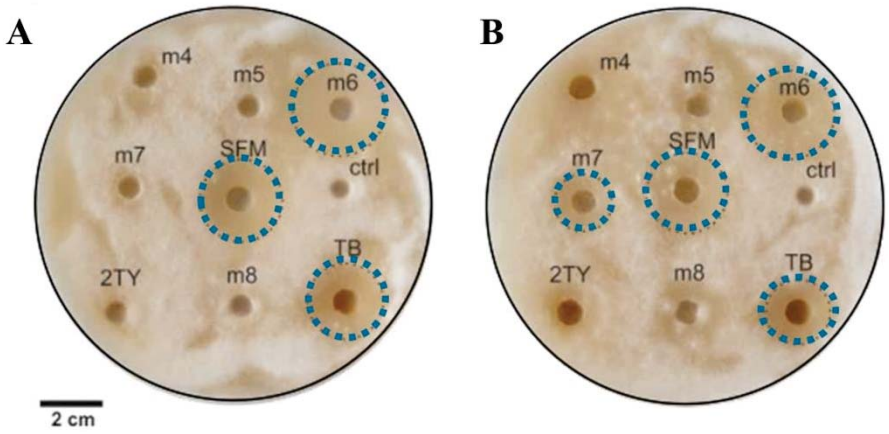

Fig. 90: Agar diffusion assays of D2p extracts against *Fusarium* spp. with native pH (A) and acidified pH (B; pH 2).

After growth for 4 days at 28°C on a rotary shaker, the spent culture media was acidified and extracted. Solvents were evaporated and bioactive substances were purified by bioassay-guided fractionation. The chemical structures were first elucidated by NMR spectroscopy.

After growth of D2p in medium m6, one purified bioactive compound seemed to be a substituted benzoic acid derivative. The substitutions were determined using IR spectroscopy, which resulted to be 4-hydroxy-3-nitro-benzoic acid (Fig. 91 A).

When D2p was grown in SFM or TB medium, one purified bioactive compound resulted to be phenylacetic acid (Fig. 91 B), which was visible already in the crude extract when measured with GC-MS.

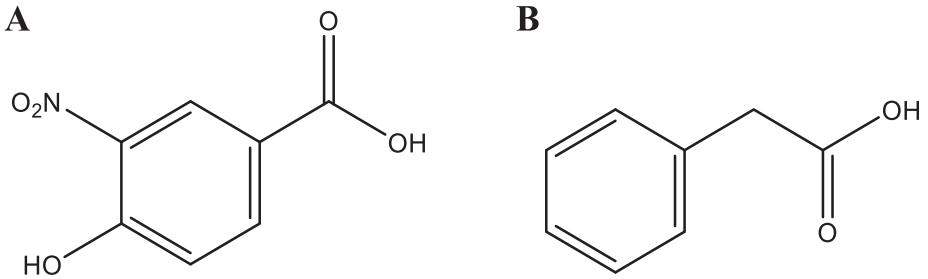

Fig. 91: Structures of bioactive compounds isolated from D2p extracts. A: 4-hydroxy-2-nitro-benzoic acid. B: phenylacetic acid.

Both substances are already known and commercially available. The catabolism of phenylacetic acid in *Pseudomonas* as well as its antifungal activity was already shown.[125-126]

4-Hydroxy-3-nitro-benzoic acid was previously described in supernatants of bacteria from artic ice. Several nitro-compounds as well as their bioactivities were investigated.[127-128]
The structures of the natural products were proven by comparison with reference substances. As I was not able to prove the presence of this compound in the aqueous supernatant, I have still some doubts about the origin of 4-hydroxy-3-nitro-benzoic acid as a natural product. To prove the presence of 4-hydroxy-3-nitro-benzoic acid in the aqueous supernatant of D2p cultures, a sensitive detection method needs to be developed. Measurements with LC-MS did not show 4-hydroxy-3-nitro-benzoic acid in the supernatant. The sensitivity of the Thermo scientific LCQ is limited, therefore the amount of the compound in the aqueous supernatant was maybe below the limit of detection.
Indeed, there were more bioactive compounds in the extracts which were not elucidated. Only small compounds were elucidated, because the number of signals received by NMR, IR and MS allowed an unquestionable assignment.

6.1.4.3 Behavioral assays with *Drosophila* fruit flies and *Pseudomonas* sp. D2p

To find out, whether volatiles from D2p attract *Drosophila* fruit flies, a behavioral assay was set up. As there was no material for a Y maze experiment in a wind channel, an alternative assay was established.
There will be no discussion about possible improvements of arrangements, methods and assays because most of the materials were taken from laboratories equipment, universities' waste disposal site or financed by myself.

6.1.4.3.1 Cultivation of *Drosophila* fruit flies

For this experiment, *Drosophila* fruit flies (*hydei* and *melanogaster*), which are unable to fly, were used. The original growth medium contained huge amounts of antimicrobial compounds (benzoic acid derivatives), which were dominant in GC-MS measurements, therefore elucidated bioactive compounds from D2p could not be found. To overcome these difficulties, we developed an optimized culture medium and described the conditions for culturing after scientific experiments.
Indeed, the addition of antibiotics or acidifying supplements was not necessary in an environment of established baker yeast. Denis Maier described the parameters in more detail in his bachelor thesis (July 2015).
The medium N46 was used for further experiments; fruit flies were cultivated in preserving jars, filled with 4 cm of media and wood wool. The jars were inoculated with up to 20 fruit flies, thereafter they were covered with paper towels and placed into an incubator at 24°C with an air humidifier (50-60%) for 4 weeks.

6.1.4.3.2 Attraction of *Drosophila* fruit flies to control samples

A novel behavioral assay was developed, to present the samples to the flightless fruit flies and readout the resulting distribution. The fruit flies were transferred in an experimental setup, where they had a choice to move to samples or stay at neutral places.

As the fruit flies were unable to fly, the assay was developed on a planar surface and samples were presented out of the horizontal plane (Fig. 92). The assay was optimized by some additional conditions. Denis Maier described assay conditions in more details in his bachelor thesis (July 2015).

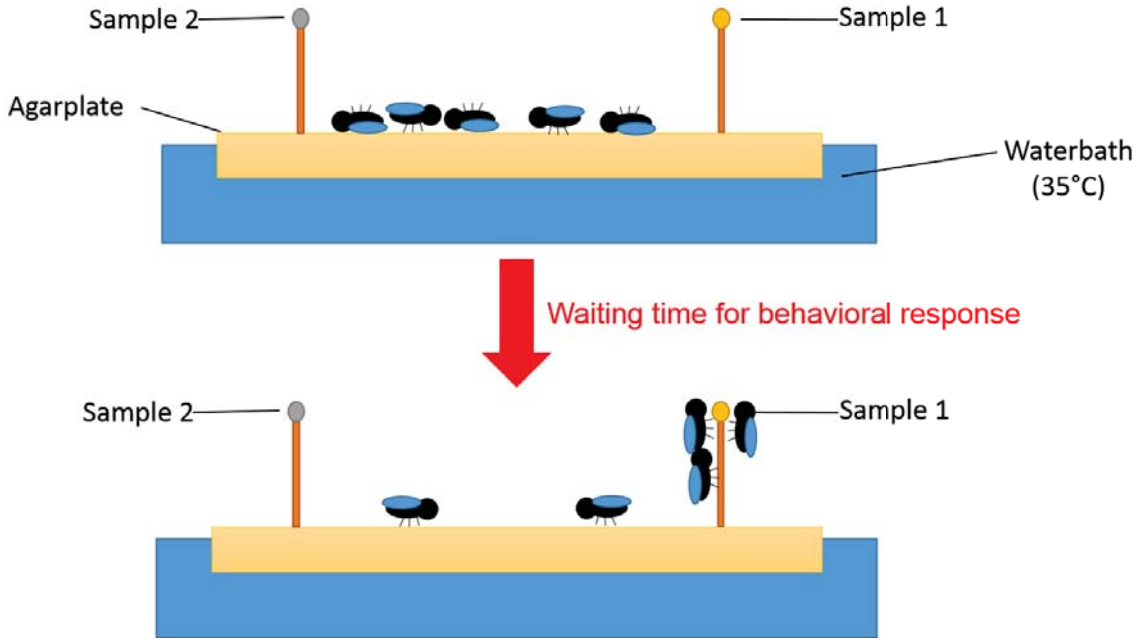

Fig. 92: Schematic setup of the established behavioral assay. Upside before and downside after behavioral response of fruit flies.

The assay was conducted in a covered water bath which provided not only constant temperature and humidity, but also eliminated influences of air and shadow movements (Fig. 93A). These movements, for example caused by persons passing by, led to escape behavior of the flies. Fruit flies tried to flee from predators, instead of staying at attractive samples.

An agar plate was covered with filter paper; tooth sticks or cotton swabs were used to apply substances of interest (Fig. 93B). Fruit flies were cold-paralyzed and deposited in the center of the filter paper.

The waiting time was set to 6 min by experimental comparison of time points (see ”Automated real-time tracking of *Drosophila* fruit flies”; Ch. 6.1.4.3.4). Fruit flies needed some time to wake up after paralyzation. Thereafter, they needed some time for orientation. These observations were monitored with cameras as well as by replicated end point determinations.

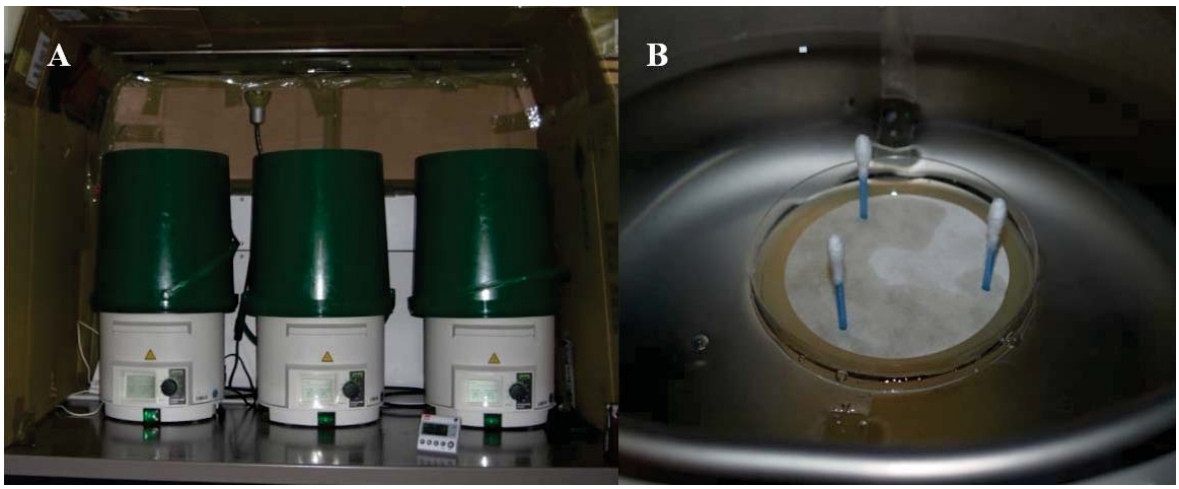

Fig. 93: Setup of measurement cabinet. A: Water bath in the dark, covered with a open plastic bucket. B: An agar plate used as arena in the water bath with filter paper and cotton swabs.

At first, attractive and repellent substances were applied to have samples for control experiments. Pepper mint oil with menthol as main component repelled fruit flies. Fresh fruits (banana, apple, peach, apricot, strawberry) seemed to be unattractive, while grown yeast either in sugar water or on fruits attracted fruit flies (80%). The rate of 80% was set as upper dimension for "attraction". On empty sticks, the average rate of fruit flies was between 15-20%, therefore that rate was set as "neutral". For repellent compounds, the rate of fruit flies was around 0-5%. Those thresholds were used for further experiments.

The attraction rates of several fruits, as well as bacterial and fungal strains were determined. In comparison, fresh cultures of baker's yeast were most attractive, followed by D2p bacterial cells followed by fruits. Other microbes such as *Bacillus subtilis*, *Streptomyces* spp. or *Fusarium* spp. showed no explicit attraction (exemplarily in Fig. 94).

Like that, a ranking of attractiveness could be developed. If there are several attractive microbes, they can be compared with each other.

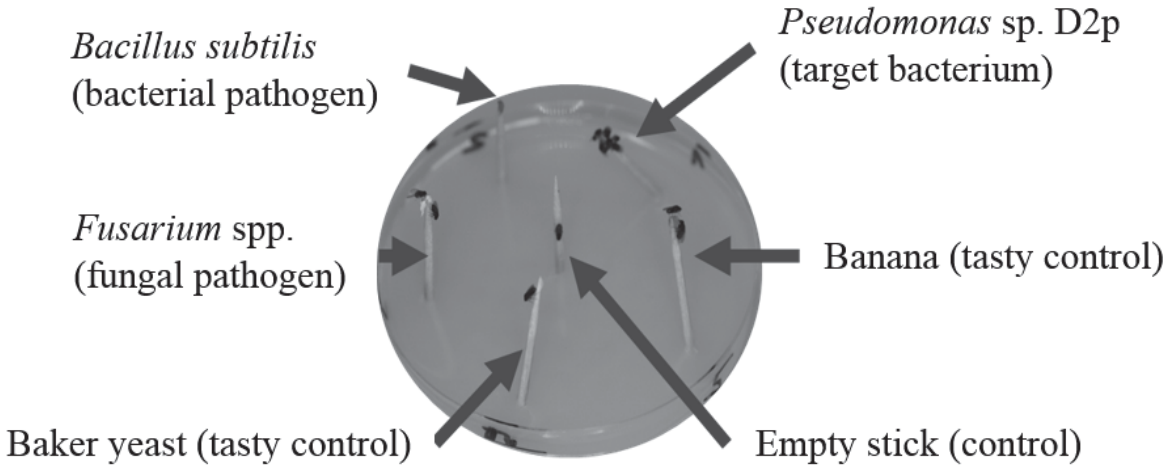

Fig. 94: Direct comparison how some samples attracted fruit flies. Aggregation of fruit flies on the D2p sample clearly visible.

In conclusion, the developed assay showed attraction rates and preferred samples as estimated by literature. We therefore applied the novel behavioral assay to assess if fruit flies are attracted by volatiles from D2p.

6.1.4.3.3 Attraction of *Drosophila* fruit flies to bacterial cells of *Pseudomonas* sp. D2p

The attraction of D2p to *Drosophila* fruit flies was tested in the developed assay. At first, bacterial cells were offered directly on a tooth pick. Depending on duration of growth and cultivation medium, the fruit flies were attracted by the presented D2p samples.

D2p showed attraction rates around 80% (Fig. 95 B), whereas for example fresh fruits only showed 25% with most fruit flies staying on the ground (Fig. 95 A; 65%).

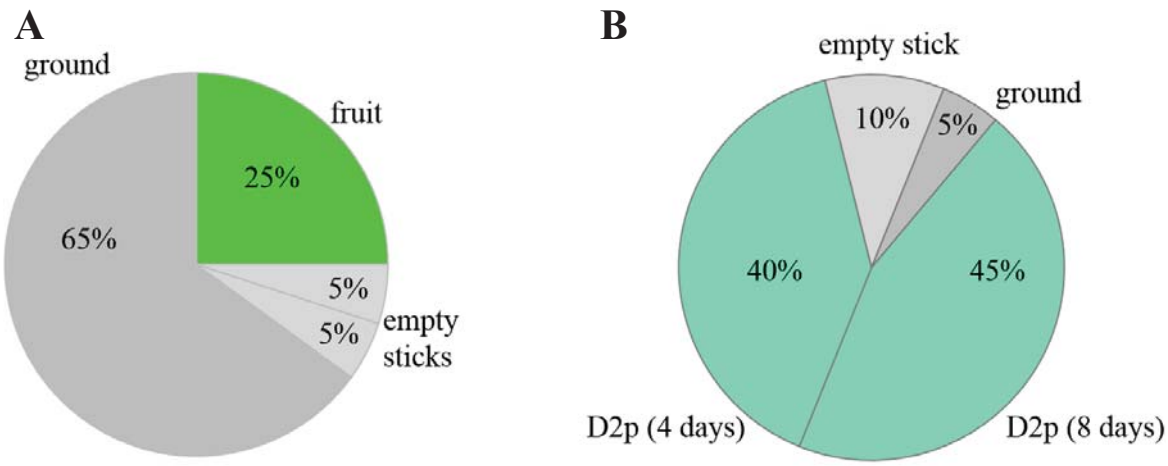

Fig. 95: Comparison of attraction rates of fruit and D2p. A: Attraction modulated by fruit (apricot). B: Attraction modulated by D2p.

When cultivated for 4 to 10 days on SFG or TB media, the D2p samples were attractive for *Drosophila* fruit flies. Comparison of growth durations from 4 and 8 days old cultures showed no significant difference (Fig. 96 A). The D2p bacterial cells lost their attractiveness

after growth durations of more than 14 days. As an example, the number of fruit flies on D2p bacterial cells after 8 days of growth were compared to 21 days of growth. The sample after 8 days of growth showed the previously observed attraction, whereas after 21 days of growth there was no difference to the empty stick (Fig. 96 B).

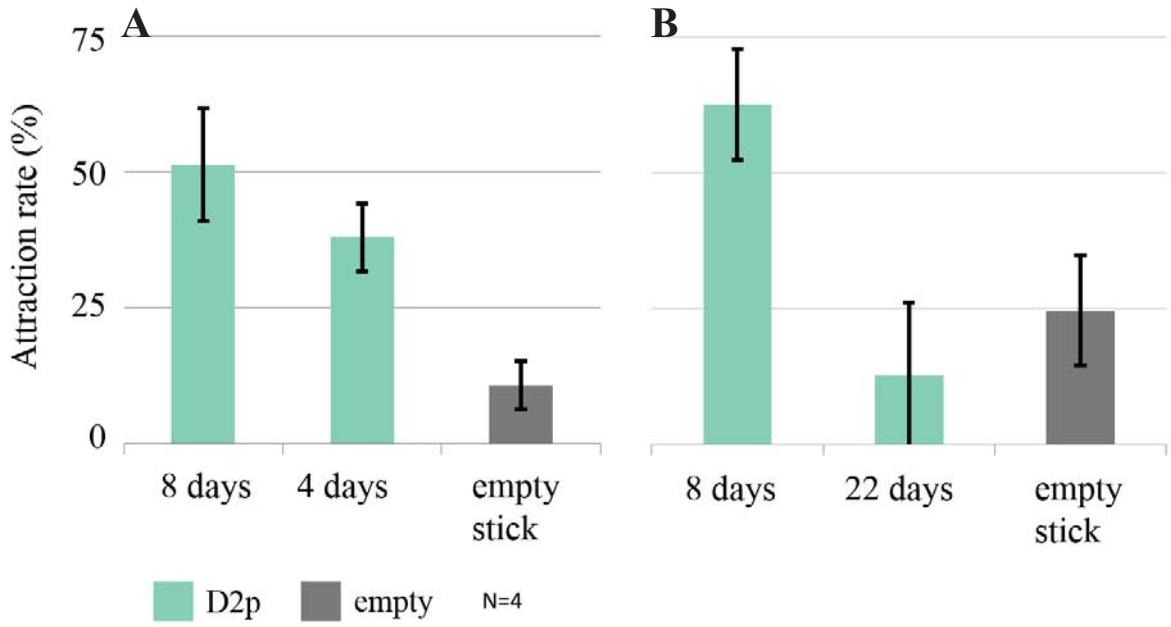

Fig. 96: Behavioral assay to correlate D2p's attractiveness with duration of cultivation time. A: Comparison of 4 and 8 days. B: Comparison of 8 and 22 days.

In order to exclude influences of D2p as food source, the bacterial cells were washed and compared to the feeding and attraction activities of other bacteria (*Bacillus subtilis*, *Streptomyces* sp.). Cell material and extracts were presented in the behavior assay as samples on cotton swabs. Attraction of fruit flies by D2p bacterial cells was based on extractable compounds (water-acetonitrile 1:1), not cell material. Separation of the extracted bioactive substances was possible, but likely due to the volatility of the compounds, there were no useful signals after measurement with GC-MS (see Ch. 6.1.4.4.1 for more detail).

6.1.4.3.4 Automated real-time tracking of *Drosophila* fruit flies

In order to monitor the behavior of fruit flies not only at the endpoint of the behavioral assay but also during the measurement time, a setup for real-time tracking was developed.

As the fruit flies could have been confused by light sources, because they showed a tendency to run towards light, several filters were applied in order to divide the spectrum of visible light (data not shown). The light source was applied in the center of the measurement arena. On top of the setup, cameras were applied in order to record movies of the behavioral assay. The numbers of fruit flies on the samples could have been noticed by hand, but Thomas Bochynek from the Monash University (Melbourne, Australia) applied his Matlab scripts for tracking fruit flies in those movies.

The area of interest (agar plate) was marked by a yellow circle. The sample sticks were marked as areas of counting with blue circles. Every fruit fly was marked with a red circle. The distribution of fruit flies in the area of interest or the samples were given in tabulators and were visualized in graphs (Fig. 97).

After 0 min, all the fruit flies were laying in the middle of the filter paper, still cold paralyzed (Fig. 97A). After 1 min, most fruit flies started to move around and orientate on the filter paper (Fig. 97B). After 3 min, there was already a preference for the D2p sample visible, but still some fruit flies moved around on the agar plate (Fig. 97C). After 6 min, already 80% of the fruit flies were sitting on the D2p sample stick, whereas 10% were sitting on the ground and 10% were sitting on the empty stick (Fig. 97D).

This result completely correlated to the previous observations. With the help of those Matlab scripts, the distribution over time as well as the final distribution can be estimated automatically.

The movies of the behavioral assay for *Drosophila* fruit flies contributed to the application of Thomas Bochynek's Matlab scripts on relevant experimental setups.

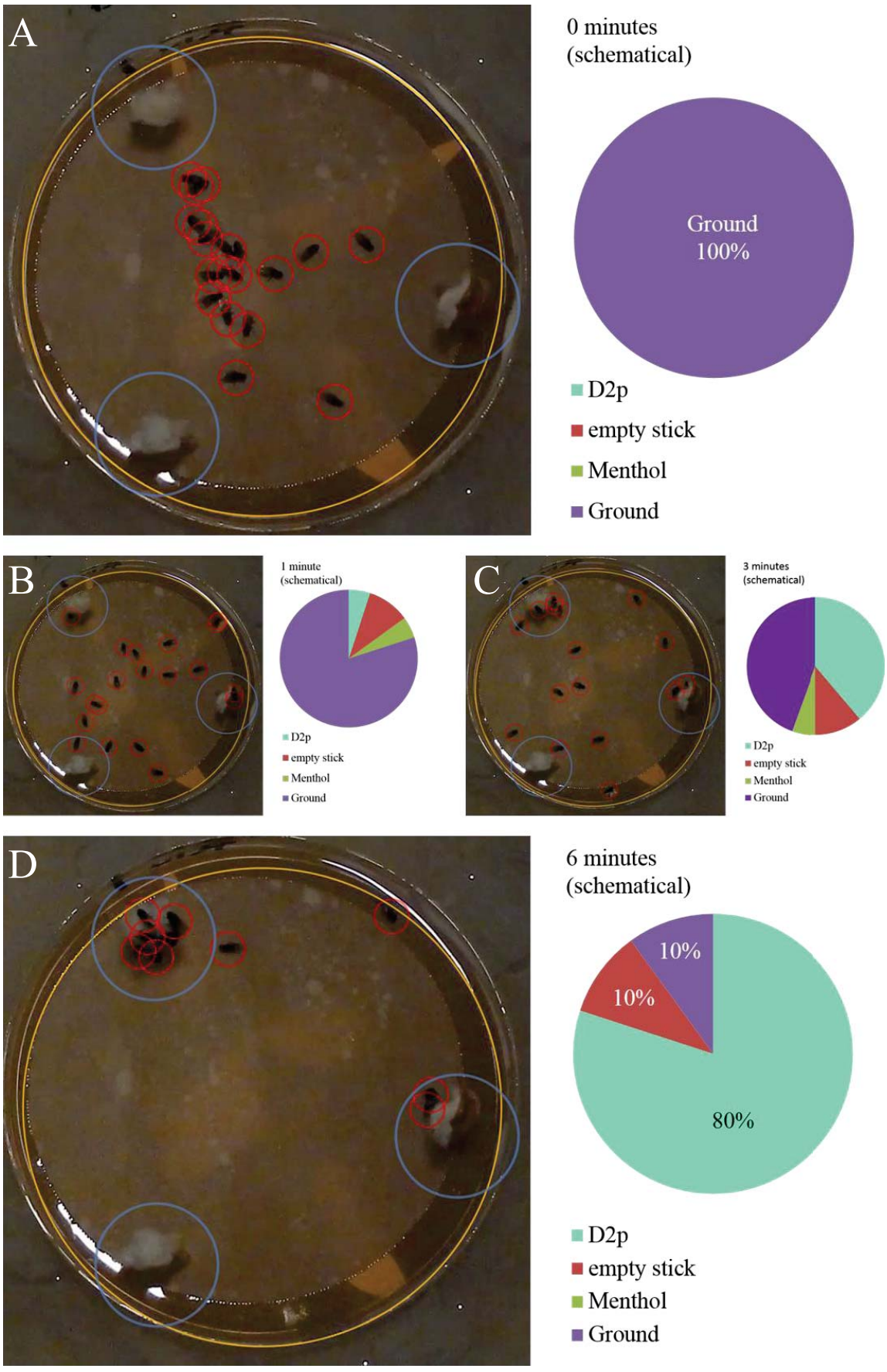

Fig. 97: Overview of real-time tracking after 0 min (A), 1 min (B), 3 min (C) and 6 min (D) measurement time. Yellow: Circle of interest. Blue: Sample sticks. Red: Fruit flies.

6.1.4.4 Chemical composition of volatile compounds from *Pseudomonas* sp. D2p

Volatile compounds from bacteria can be collected using SPME fibers and directly analyzed by GC-MS. Therefore, small volatile compounds are not hidden by a solvent peak. Unfortunately, coating material of SPME fibers discriminates between several functional groups, this hinders a reliable answer of the complete bouquet of the volatiles. Measurements with head-space-GC-MS could provide additional substances to complete a full bouquet of D2p.

The main disadvantage of these methods is, that they cannot be combined with the behavioral assay.

Indeed, extraction of volatile compounds using a cryo trap distillation allowed to test and fractionate promising compounds. After fractionation, some compounds can be excluded to play a role for attraction. The fractions can be applied in the behavioral assay – pure or mixed.

In fact, several million mixtures with thousands of combinations could be tested to identify the responsible volatile compound or the mixture of compounds determined by SPME-GC-MS measurements. Another way to determine the attractive compound(s) is to use the bouquet of D2p directly or after fractionation.

6.1.4.4.1 GC-MS measurements of liquid extracts from *Pseudomonas* sp. D2p bacterial cells

Bacterial cells of D2p were transferred into a glass vial after 4 days of growth. The bacterial cells were vortexed with several solvents. Extracts with a mixture of ddH_2O and acetronitrile (1:1) were found to be attractive for fruit flies in the behavioral assay. In order to get rid of water, the extract was subjected to a C_{18}-SPE column and eluted with pure acetonitrile. Extracts and fractions were directly injected into GC-MS. There were no substance peaks visible in the spectra (only siloxane background). Derivatization with TMSH for methylation of functional groups like hydroxy-, amino- or carboxylic acid-groups, resulted in several MS signals (Fig. 98A). Selections for characteristic mass to charge ratios (m/z) showed especially alkanes, terpenes or carboxylic acids (methylated by TMSH). Spectra of several compounds are shown exemplarily (Fig. 98B). Library search did not point towards certain compounds; therefore, commercially available reference substances will be necessary to identify the compounds behind the signals with retention time and fragmentation pattern.

The main advantage of this method was, that extracts could be fractionated and tested in the behavioral assay. Airspace collections with SPME do not allow an application in the behavioral assay and GC-MS.

The main drawback of this "liquid extraction"-method is, that not only volatile compounds, but also cell material is extracted by solvents. Furthermore, very volatile compounds are hidden behind the solvent peak. Collection methods like SPME do not require solvent delays and are able to collect substances which are only present in the airspace. Thus, SPME collection of volatile compounds in the airspace above D2p bacterial cells was conducted next.

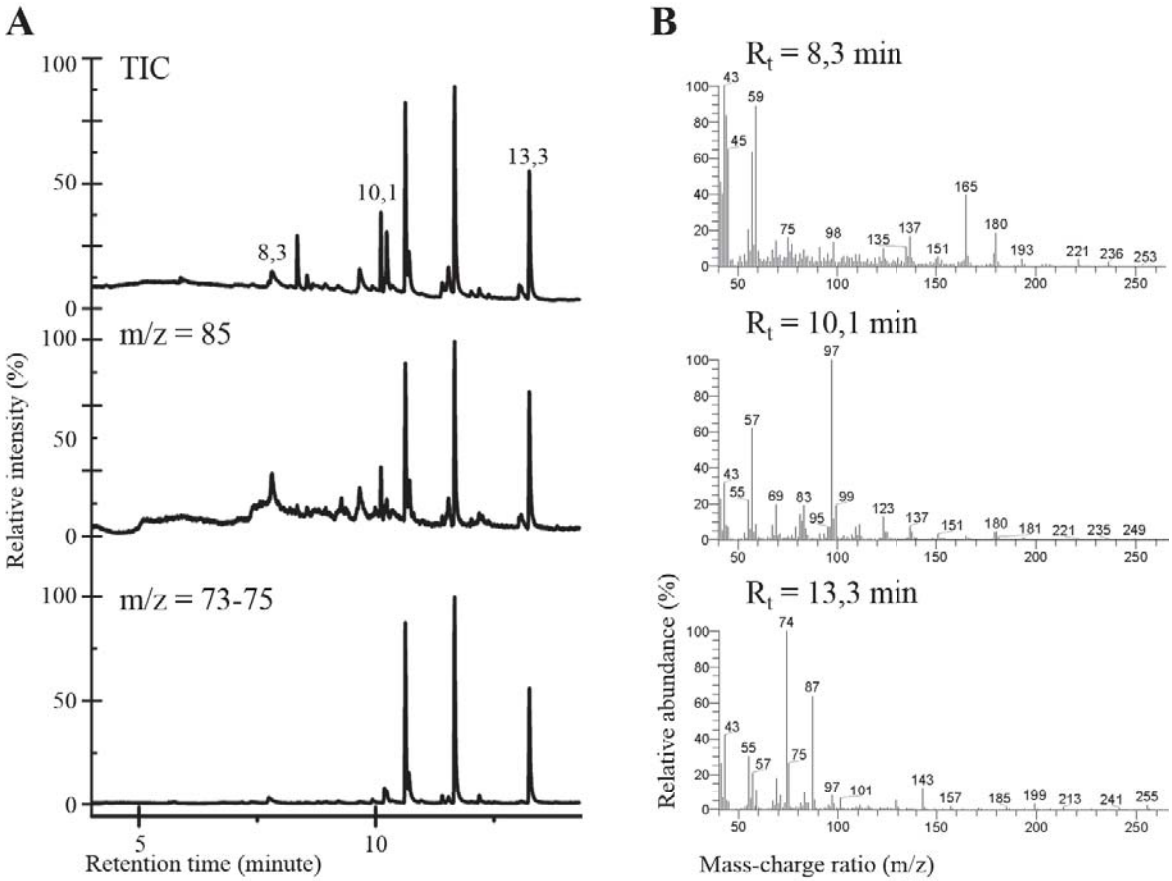

Fig. 98: GC-MS analysis of attractive extracts from D2p (bacterial cells). A: Chromatogram with total ion count (TIC) and mass range filters of m/z=85 and m/z=73-75. B: Mass spectra of selected retention times with different fragmentation patterns.

6.1.4.4.2 SPME-GC-MS measurements of *Pseudomonas* sp. D2p bacterial cells

Bacterial cells of D2p were transferred into a glass vial after 4 and 28 days of growth. The vial was heated to 70-80°C and volatiles in the airspace of the vial were collected by SPME for 20 min and directly injected into GC-MS.

Previously, D2p bacterial cells were shown to be attractive after 4 days of growth, but not after 22 days of growth (Fig. 96; p. 160). Furthermore, two cultivation media were shown to be suitable for bacterial growth and production of attractive volatiles, therefore bacterial cells grown on TB and SFG agar plates were compared. The GC-MS profiles after 4 and 28 days of growth were compiled.

Indeed, there are similar and different substance peaks visible. No matter, whether D2p grew on SFG or TB medium (Fig. 99A), the observed GC-MS profiles were very similar. Especially the higher molecular lactones, ketones and carboxylic acids (Fig. 99B c,d) stayed in the cultures, whereas for example some substituted pyrazines (Fig. 99B a) disappeared. The indicated boxes (a-d) are similar for TB medium (Fig. 99C), where another additional unknown substance disappeared (Fig. 99C e). The intensity of some peaks decreased relative to neighboring peaks (Fig. 99B b).

There are several possibilities for the loss of attractiveness of D2p in the behavioral assay. Either the attractive substances disappeared over time or additional repellent substances were produced, which overwhelmed the attractive effect.

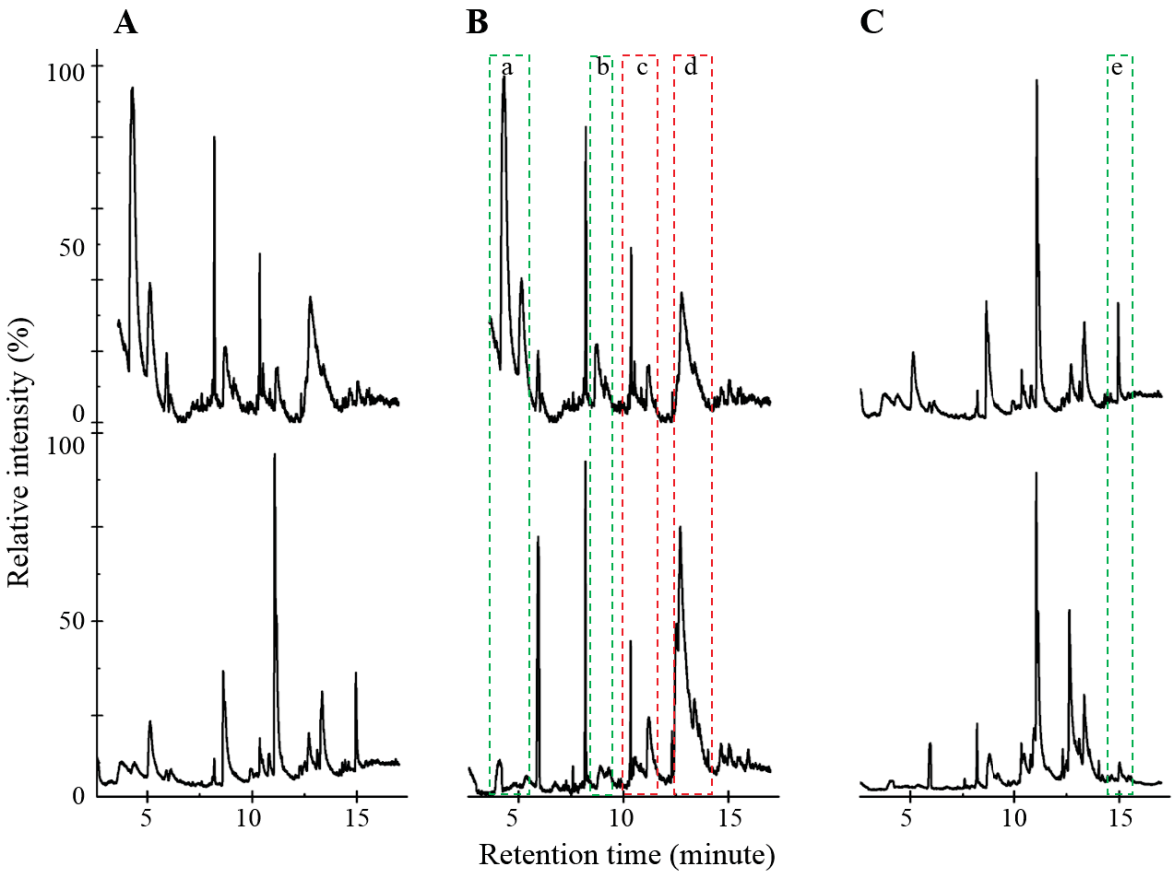

Fig. 99: Comparison of SPME-GC-MS chromatograms (TIC) of D2p samples after 4 and 28 days of growth on TB or SFG medium. Green boxes: only after 4 days of growth. Red boxes: after 4 and 28 days of growth. A: SFG and TB after 4 days of growth. B: SFG after 4 days and 28 days of growth. C: TB after 4 days and 28 days of growth.

At early retention times, there were several substituted pyrazines in the chromatogram, which were not present in samples after 28 days of growth (Fig. 99B a). The substitution patterns of pyrazines can not be elucidated by fragmentation patterns definitely, therefore both retention times and fragmentation patterns have to be compared to commercially available standards.

The fragmentation patterns of some compounds were compared using mass range filters. Indeed, the presence of differently substituted pyrazines in the airspace above D2p bacterial cells was shown after around 5 min (Fig. 100). The pattern of pyrazines will be discussed in more detail. Furthermore, several alkane or terpene fragmentation patterns were observed after 8 and 11 min. Fragments such as m/z=85 pointed towards the presence of lactones / carboxylic acid groups and were observed at 12 and 13 min.

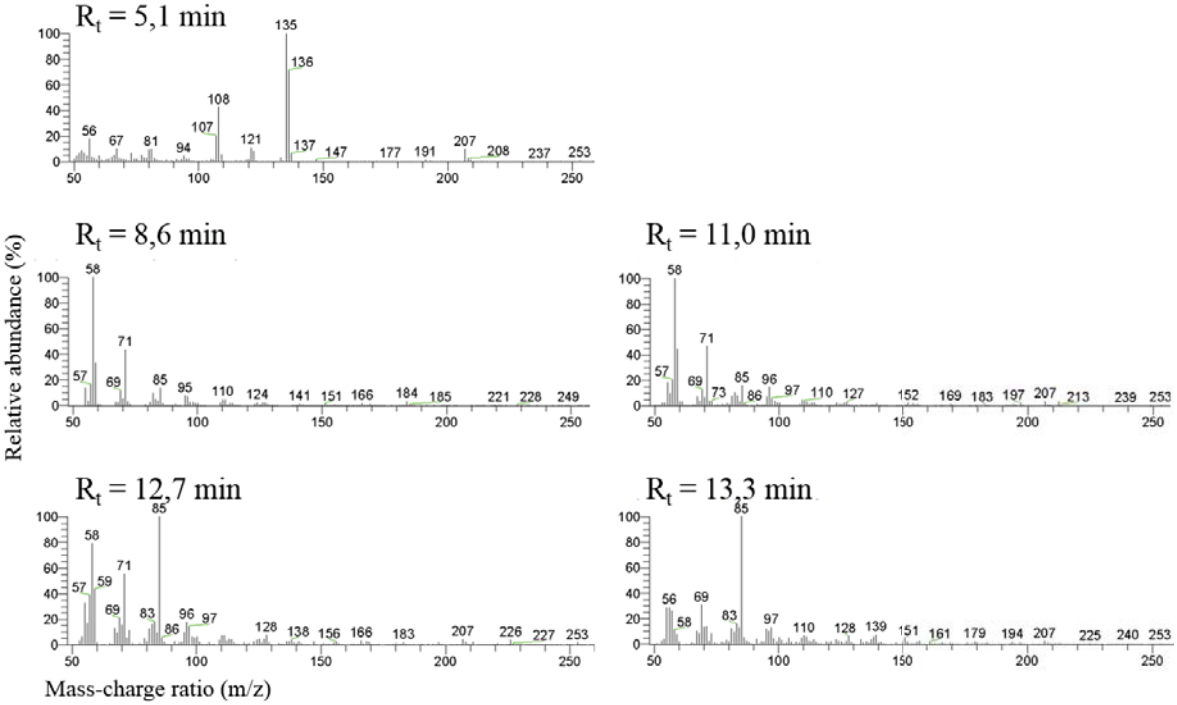

Fig. 100: Compilation of MS spectra after several retention times. Substituted pyrazines after around 5 min. Alkanes and terpenes around 8-11 min. Carboxylic acids and lactones after around 12-14 min.

Pyrazines in the airspace of D2p bacterial cells were investigated in more detail. Indeed, there were several differently substituted pyrazines present (Fig. 101).

There was no signal for 2-methylpyrazine because of the delay of GC-MS measurements (3,5 min). It is therefore not known, if 2-methylpyrazine is present in the bouquet of D2p or not. Pyrazines with higher molecular weights were detected with the help of mass range filters (m/z= 108 or 122 for pyrazine backbone with alkane substitution). Substitution patterns were selected separately with addition of methylene groups, resulting each in a m/z increase of 14 (m/z=108 for $C_5H_6N_2$; 122 for $C_6H_8N_2$; 136 for $C_7H_{10}N_2$; 150 for $C_8H_{12}N_2$).

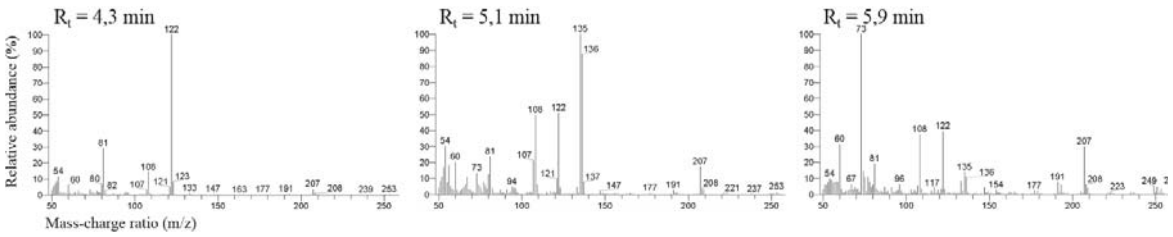

Fig. 101: Mass spectra of substituted pyrazines in D2p samples after 4 days of growth on SFG media. R_t=4,3 min with mass range m/z=122. R_t=5,1 min with mass range m/z=136. R_t=5,9 min with mass range m/z=150.

In order to assign molecular masses to chemical structures, the structures of modified pyrazines were compared (Fig. 102). For behavioral experiments, several methyl substituted pyrazines were purchased by Prof. Dr. D. Spiteller. There were no tests with other modified pyrazines (with ethyl or propyl side chains) or other compounds like lactones or terpenes performed yet.

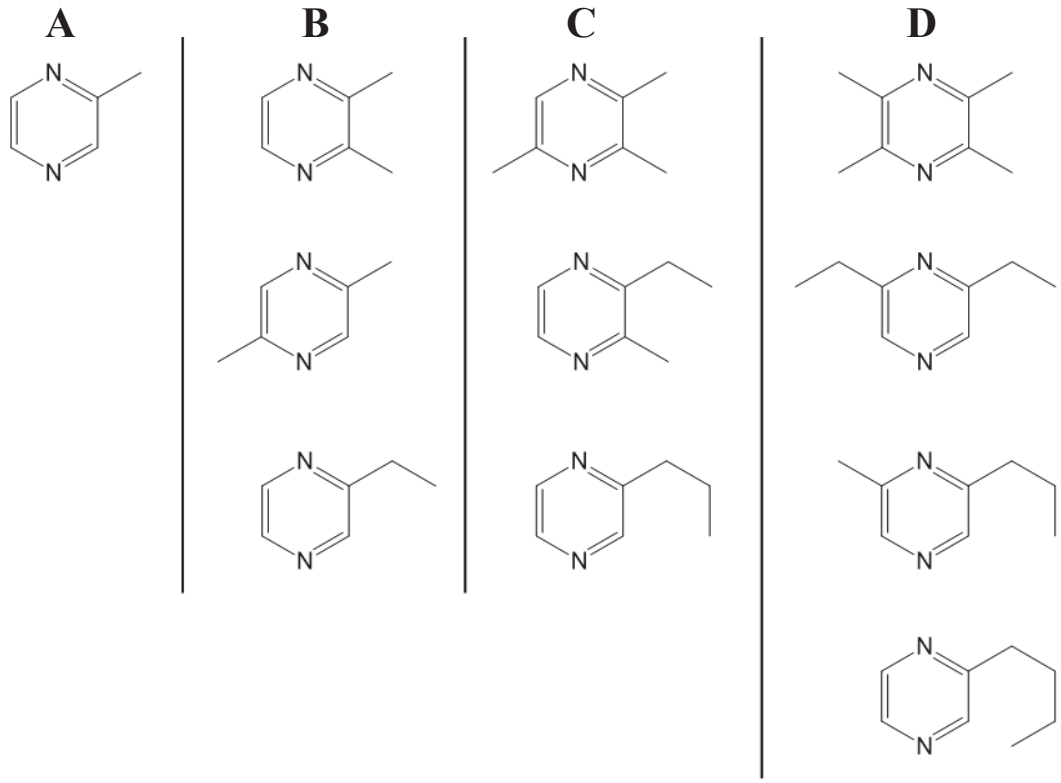

Fig. 102: Examples for chemical structures of proposed pyrazines. A: Pyrazine with formula $C_5H_6N_2$. B: Pyrazines with formula $C_6H_8N_2$. C: Pyrazines with formula $C_7H_{10}N_2$. D: Pyrazines with formula $C_8H_{12}N_2$.

Furthermore, even more volatile compounds should be considered for analysis and behavioral tests. In literature, several small compounds such as acetic acid or 2-propanol were described to be present in bacterial bouquets and attractive for fruit flies.[129] The impact of volatile compounds from yeast such as acetic acid, acetoin, ethanol, 3-methyl-1-butanol and 2-phenyl ethanol was described before.[113, 130] In order to identify these compounds, the

GC separation protocol has to be changed and the separability with the applied GC-column has to be shown by mixtures of reference substances.

6.1.4.4.3 Attraction of *Drosophila* fruit flies to selected pyrazines

Components of bouquets from yeasts were previously analyzed by GC-MS and several hundred volatile compounds were identified.[130-131] In yeast bouquets, methyl substituted pyrazines but also more complex substituted pyrazines were identified. Behavioral experiments with fruit fly larvae showed different attraction rates of 2-methylpyrazine compared to 2-ethylpyrazine.[132] Fruit flies were attracted more by dilutions of 2-ethylpyrazine than 2-methylpyrazine.

The following five methyl substituted pyrazines were used for behavioral experiments (Fig. 103). Their retention times were not evaluated with SPME-GC-MS because after the waiting time for reference compounds, the same measurement conditions were not available any more. It is not known, whether these compounds have an attractive, repellent or no effect on fruit flies. For other bouquets related to fruit fly attraction, it was shown that several compounds in a defined ratio are responsible for attractiveness.[113] Including all possibilities, like concentrations, ratios and mixtures, several thousand experiments with those compounds would be necessary to either having seen attraction or having no increase of knowledge at all, because there might have been missing components in the mixture.

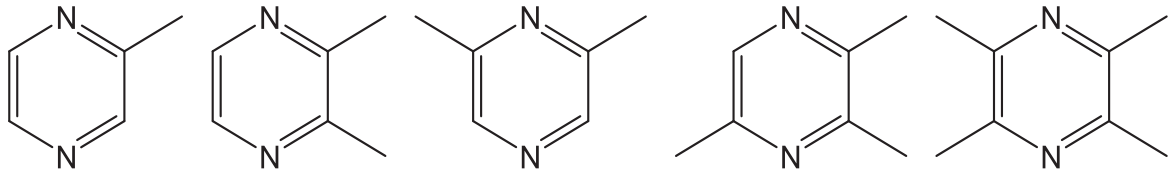

(1) (2) (3) (4) (5)

Fig. 103: Chemical structures of available pyrazines as reference compounds. (1): 2-methylpyrazine. (2): 2,3-dimethylpyrazine. (3): 2,5-dimethylpyrazine. (4): 2,3,5-trimethylpyrazine. (5): tetramethylpyrazine.

Hypothetically, if there is a mixture of three methylated pyrazines, two attractive in a ratio 2:1 at dilutions around 10^{-4} and one strong repellent at dilutions down to 10^{-7}, no effect would be visible in 1:1:1 mixture. If the pyrazines are tested one after the other, attractiveness could be seen or overlooked due to synergistic effects of the two attractants. The avoidance of the repellent would be invisible. If thereafter mixtures of only two pyrazines at once are monitored, the two attractive pyrazines could maybe be spotted. If the attraction is only present in ratios between 7:3 and 9:1, there would be no visible attractiveness in the 1:1 mixture.

In order to improve the effectiveness of this gambling, mixtures of pyrazines and attractive material (honey-vinegar or D2p bacterial cells) were prepared in order to identify repellent

compounds or concentrations. Of course, those compounds could be anyway attractive in defined mixtures.

Samples, which attracted more than 50% of the Drosophila fruit flies in the behavioral experiments were counted as “attractive”. In contrast, samples with attraction rates below 15% were counted as “not attractive”, which means either repellent or neutral (Fig. 104A). Attraction rates between 15 and 50% were counted as “undefined”, which for example might be modulated by loss of attractiveness due to higher dilution.

Dilutions of 2-methylpyrazine, 2,3-dimethylpyrazine and 2,3,5-trimethylpyrazine were used in behavioral assays in mixture with honey-vinegar (1:2). Pure honey-vinegar (1:2) showed attraction rates of 66±15%. The mixtures indicated, that this attraction was regained with dilutions of 10^{-1} for 2-methylpyrazine, 10^{-3} for 2,3-dimethylpyrazine and 10^{-2} for 2,3,5-trimethylpyrazine (Fig. 104B).

Indeed, the effects of behavioral responses are complex. For attractants, there are at least two possibilities. For example, attractant (A) might be repellent in high concentrations, become attractive with dilutions between 10^{-3} and 10^{-5} and lose attraction thereafter because of too low concentration (Fig. 104C). Another attractant (B) might be attractive in pure application and thereafter loses attractiveness due to dilution.

For repellents and undefined responses, there are only two possibilities. Repellents are avoided by fruit flies, but in low concentrations the repellent effect might disappear. Undefined responses might be fluctuating; this was not observed.

There are already some obvious pitfalls: if attractants are tested in too low concentrations, their attractiveness might be overseen. In case of attractant (A), only a defined concentration range causes attraction, the other dilutions might be misinterpreted as repellent.

In conclusion, if there is attraction, it counts as attraction. If there is no attraction, it remains unclear, if this is due to wrong concentration, mixture, ratio, and so on.

To overcome this problem, the sample of interest was mixed with attractants like D2p bacterial cells. Attractants should stay attractive or might increase D2p’s attractiveness (Fig. 104C; Attractant+D2p). The main point is, that repellents lose their effects with higher dilutions and D2p regains its attractiveness (Fig. 104C; Repellent+D2p).

Herewith, repellent and neutral effects can be differentiated.

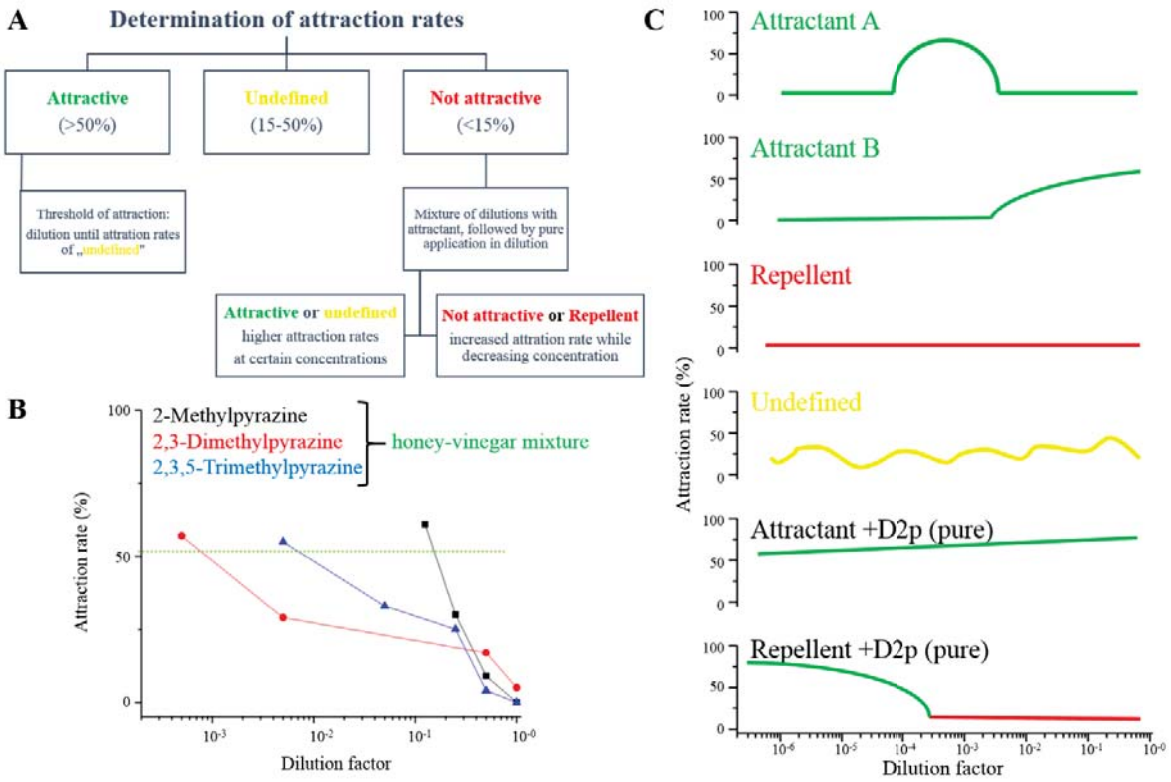

Fig. 104: Schematic compilation of determination principle for behavioral experiments with pyrazines. A: Criteria to distinguish between fruit flies' responses. B: Attraction rates of methylated pyrazines to show regaining of attractiveness with dilution of pyrazines. C: Schematic overview to distinguish between behavioral responses.

All five available methylated pyrazines were applied in behavioral experiments. They were either tested alone or in mixture with D2p bacterial cells (1:1). These results are preliminary, as there were no triplicates. After stopping my own cultivation of fruit flies, I was limited in fruit fly supply.

None of the samples showed clear indications for attraction (Fig. 105). Without dilution, all samples showed attraction rates of 0%, pure tetramethylpyrazine even caused death of *Drosophila* fruit flies. Mixtures of pyrazine references with D2p bacterial cells regained attractiveness for dilutions less than 10^{-2} of 2-methylpyrazine or 2,3,5-trimethylpyrazine. The observations of these experiments were pointing towards repellent effects of the tested pyrazines.

Tests with dilutions of pure methylated pyrazines did not show clear attraction rates >50%. In conclusion, none of the tested dilutions exhibited clear attraction for any of the applied methylated pyrazine. It remains unclear, whether the purchased methylated pyrazines are present in the bouquet or not.

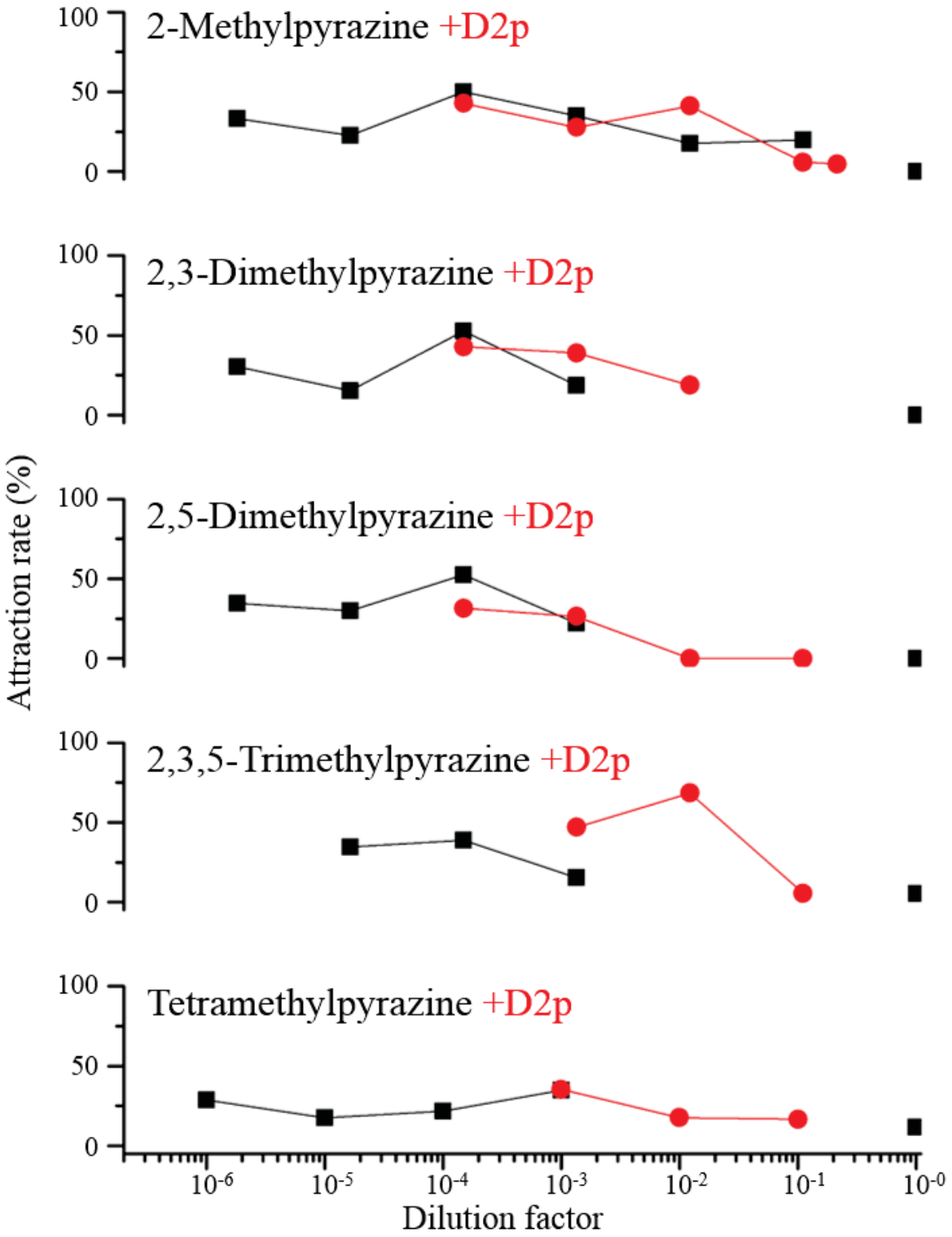

Fig. 105: Attraction rates of tested methylated pyrazines with (red) and without (black) addition of D2p bacterial cells.

In order to avoid an intransparent experimental nightmare with mixtures of the methylated pyrazines, this approach was never started. Hundreds of experiments would have been necessary in order to have preliminary representative results. I suggest to go for GC-MS analysis of the whole bouquet first and look for more promising compounds.

6.1.4.4.4 Attraction of *Drosophila* fruit flies to cryo trap distillates

A cryo-distillation apparatus was developed to collect the volatiles from Pseudomonas sp. D2p. The sampled volatiles were investigated in behavioral assays as well as analyzed by GC-MS. The advantages and disadvantages of simultaneous distillation-extractions compared to SPME are known from literature.[133-135]

The apparatus consisted of 5 ml screw cap vials, which were connected by cannulas and Teflon tubes. The volatiles were evaporated with the help of heat, forced in the direction of the traps with pressured air and condensed in cooled organic solvents (Fig. 106).

The chosen organic solvents differed in their abilities to dissolve compound classes, which allowed a first separation. The solvents were chosen along the eluotropic series, ranging from hexane to water. The chosen temperatures decreased from room temperature for a reflux trap, ice water, sodium chloride freezing mixture, dry ice (solid CO_2) down to liquid nitrogen ("-170°C").

The setup could have been changed to a dry trap without solvents, but in this case the surfaces should have been enlarged. Otherwise the airflow would not be cooled down appropriately and volatile compounds would fly away through the outlet. The dry setup has the advantage to not contain solvents, which is advantageous for SPME-GC-MS measurements. Nevertheless, the increased surface may lead to increased air volume, which dilutes concentrations of volatile compounds in air space.

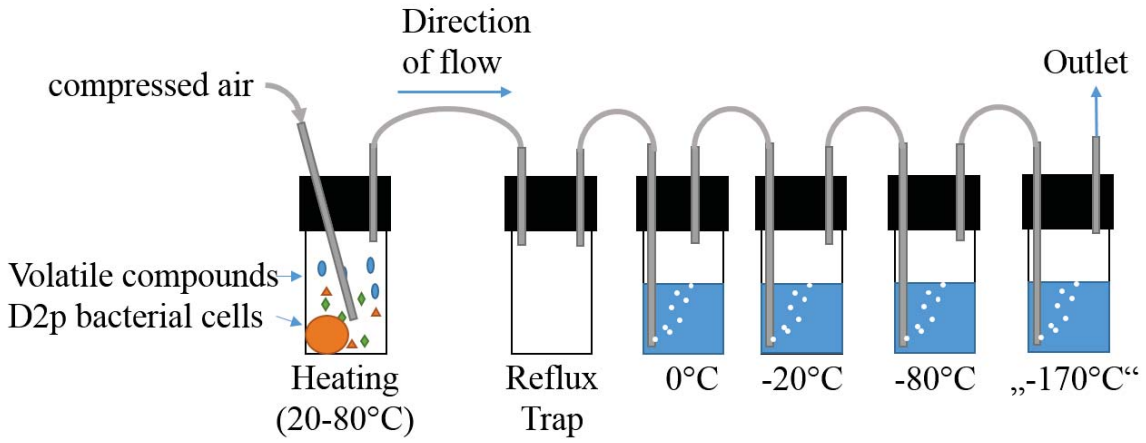

Fig. 106: Schematic setup of the developed cryo trap distillation apparatus.

The tubes or cannulas were never blocked by frozen water. Obviously, the apparatus was more complex as it needed to be. If the volatile compound of interest would have been trapped in a hypothetical solvent at a certain temperature, it would be enough to apply these conditions to trap the compound. However, stepwise cooling of heated airflow combined with trapping of uninteresting compounds may help to pre-purify the compound of interest.

Trapping volatile compounds in solvents with different polarities allowed to mix several distilled fractions.

The distillates and their mixtures were applied to behavioral assays. So far, the conditions for trapping the compound of interest are unknown. Some solvents have been shown to be ineffective, as they attract fruit flies themselves or kill fruit flies (diethyl ether, chloroform, acetone). Most likely the amount of D2p bacterial cells in the heated vial needs to be increased, as the volatiles might be diluted in the solvent or cooling traps.

Nevertheless, using this method helped to have only volatile compounds in the trapping solvents instead of e.g. cell membrane particles in case of extraction from complete bacterial cells, which cause irrelevant signal peaks in GC-MS analysis and might contribute to false positive results because of feeding behavior.

In a second step, the solvent traps could be used for another cryo distillation, where volatiles are separated from the solvent reflux and frozen-out on glass surfaces.

6.1.4.5 Influence of *Pseudomonas* sp. D2p on the fitness of *Drosophila* fruit flies

In order to find out, whether D2p has a positive, negative or none effect on the fitness of *Drosophila* fruit flies (*hydei* and *melanogaster*), the influences were compared between native, "axenic" (kanamycin treated) and inoculated fruit flies.

Kanamycin was effective against D2p, moreover *Drosophila* fruit flies survived treatments with kanamycin, too. Therefore, *Drosophila* fruit flies were treated with kanamycin in their cultivation medium for two generations in order to remove potentially present D2p from the system. Untreated and treated fruit flies were then cultivated as usual, inoculated with D2p or both even contaminated with a pathogenic fungus (*Fusarium* spp.).

D2p and *Fusarium* spp. were either mixed in the culture media, pre-grown on agar and added as a piece of agar or smeared on the wall of the glass beaker.

The influences of the treatments were measured by comparison of number and size of fruit flies and larvae after days of growth (several time points) between the treatment groups in triplicates. Those criteria were already successfully applied in preliminary experiments to determine pH and water content of culture media.

Unfortunately, my air humidifier broke down and I declined to buy myself a second one. As the air humidity in the cultivation room was below 30%, I had to stop this part of the project. The preliminary experiments were not finished, therefore the results are not representative and were not repeated yet. The idea of the approach is described to allow a repetition with sufficient material in future.

6.1.5 Outlook

SPME-GC-MS measurements of D2p bacterial cells should be repeated with another gradient and column, in order to be able to identify more volatile compounds in the bouquet. Reference substances like acetic acid, 2-propanol and phenylethanol are available and can be used for evaluation of the conditions.

The approach with substituted pyrazines could be continued with differently substituted pyrazines, for example containing ethyl and propyl groups.

In order to identify attractive compound(s) in the bouquet of D2p bacterial cells, the complete bouquet needs to be fractionated and fractions need to be applied in behavioral assays. The fractionation can be performed with GC, equipped with a preparative fraction collector.[136-137] Herewith the bouquet of D2p could be redesigned and the attractive fractions can be identified. After identification of the mixture of attractants, these mixtures could have been recreated with commercially available reference substances in order to prove and describe their influences.

A preparative fraction collector for application with GC is available in the lab of Prof. Dr. D. Spiteller (Brechbühler Prep9000), financed by the Graduate School Chemical Biology in October 2015. The project for behavioral assays with D2p was part of the application proposal. Unfortunately, the instrument was not ready to use (Mai 2016).

6.1.6 Conclusion

A nutrient medium without added antibiotics for cultivation of *Saccharomyces cerevisiae* as well as for *Pseudomonas* sp. D2p and *Drosophila hydei* was developed. The medium N46 was applied for co-cultivation to study insect-microbe interactions.

Two bioactive compounds against *Fusarium* spp. were identified to be 4-hydroxy-2-nitro-benzoic acid and phenylacetic acid. Both substances are already known and commercially available.

A novel behavioral assay for flightless *Drosophila hydei* was developed. D2p bacterial cells were shown to be attractive in the behavioral assay. Cultivation conditions for D2p were studied, to enhance production of attractive compounds.

Real-time tracking of the distribution of fruit flies was achieved by analyzing recorded movies with Matlab scripts.

Volatile compounds of *Pseudomonas* sp. D2p were analysed by GC-MS either with liquid extracts or SPME. Five commercially available methylated pyrazines were applied in the behavioral assays, but no attraction was observed in various dilutions. Mixtures of

methylated pyrazines or differently substituted pyrazines (ethyl-, propyl-) were not tested so far but might be good prospects after SPME-GC-MS measurements.

A cryo trap distillation apparatus was developed. Application of fractions in the behavioral assay showed no preferences, which might be due to dilution effects. Separation by GC and fractionation might deliver representative results in order to narrow the complete bouquet down to fractions or their mixtures.

Unfortunately, required instruments broke and with stopping cultivation of *Drosophila hydei*, also co-cultivation to study insect-microbe interactions had to be stopped. Several assays for determination of the influence of *Pseudomonas* sp. D2p on the fitness of *Drosophila hydei* were established, but need to be continued.

7 Method development for chemical analysis of secondary metabolites

Prolog

Within this chapter, I will summarize my developments to inform about basic ideas and support following projects with my obtained knowledge.

I will not present data of not yet elucidated and characterized bioactive compounds here. Specific spectra of elucidated compounds will be shown in the corresponding chapters (such as Ch. 6.1 p. 137 or Ch. 8.2; p. 197 and their Annexes p. xxxviiiff).

7.1 Overview

Relations between partners in ecosystems are most often investigated using simplified models. To set up such models, the partners need to be discovered, their interactions need to be studied and involved modulation signals and substances need to be elucidated.

For insect-microbe interactions, which for example examine protection of the insect by bacteria against pathogenic fungi, pathogenic fungi and bioactive bacteria have to be identified at first. Thereafter, the bioactive substance(s) of one bacterium has/have to be elucidated. To accomplish that, growth conditions and bioassay-guided purification workflows need to be developed. The chemical structure of a pure compound will be elucidated using NMR, IR, MS and other techniques, if necessary. Meanwhile, the presence and influence of the bacterium in the ecosystem has to be confirmed. Third, the bioactive substance has to be found in the ecosystem in order to verify its presence in the natural environment and not only under laboratory conditions.

In principle, these steps are comprehensible and the workflow seems to be straight forward to follow. However, there are plenty of pitfalls, such as arbitrary claims which are misguiding. Therefore, I developed a set of methods, which can be combined and exchanged to a widely applicable fast workflow. The following chapters will explain how to isolate microorganisms, screen them for their ability to produce bioactive secondary metabolites, purify these metabolites and elucidate their structures.

7.2 Isolation of microorganisms

7.2.1 Abstract

Pharmaceutical antibiotics derived from microbes are widely known to cure infections. Besides the anthropogenic use of bioactive molecules, they are obviously essential in their producers' ecosystem and play an important role in the rise and fall of competing organisms. Microbial communities can be studied regarding synergistic or antagonistic effects with common materials in the lab.[138] Especially antagonistic effects can be easily described using inhibition zones in agar diffusion assays. Only two microbes are necessary for such investigations. For the combined study of synergistic and antagonistic effects, two cooperating microorganisms can be combined to defeat against a third microbe.

To start investigations, microbes must be isolated and purified.[139-141] The isolation can take place specifically or nonspecifically, for example with a toothpick from a small area or with aqueous extracts. Furthermore, several isolation conditions have to be chosen because growth of microorganisms depends on nutrient composition and culturing conditions.[142] The major part of microorganisms are presumed to be uncultivable under lab conditions.

For this chapter, different isolation techniques were combined with several media compositions and supplements. There was no problem to isolate hundreds of strains, which were purified and tested for their possible interaction with other strains.

7.2.2 Methods

Different techniques were used for the isolation of bacteria from leaf-cutting ants or fruit flies. Several liquid and solid cultivation media were used in order to obtain different bacterial strains (Tab. 24). The compositions can be combined with the addition of antibiotics, complex nutrients (for example chitin) or in-/organic supplements (not discussed here).

Agar plates were incubated at 28°C for several days, depending on the individual multiplying time of bacteria. Liquid media was incubated at 28°C on a shaker (220 rpm). Incubation time was one to seven days and depended on the medium. Nutrient rich media were incubated overnight. To separate bacterial strains, the liquid culture was centrifuged and the pellet was dissolved in water. This solution was spread, diluted or undiluted, on agar plates.

Isolation technique 1: Living ants from different worker castes were placed on agar plates and incubated directly.

Isolation technique 2: The whitish biofilm from the integument of leaf-cutting ants was scraped off with a sterile toothpick. The toothpick was either used to

spread bacteria directly on agar plates or vortexed with water. Diluted or undiluted solutions were then spread on agar plates or transferred into liquid media.

Isolation technique 3: For isolation of inward living bacteria, the surface of the ant's body was sterilized. First, the ant was put into sodium hypochlorite (12%, 30-90 seconds), thereafter ethanol (70%, 30-90 seconds) and after that into water to wash away chemicals. Second, the ant's body was placed into water and homogenized. In addition, the solution was vortexed, centrifuged and/or placed into ultrasonic bath before spreading it on agar plates or transferring it into liquid media.

Tab. 24: Compositions of some used isolation media.

medium	composition (per l^{-1} ddH_2O; for solid media add Agar-Agar 15 g)
2TY[a]	NaCl 5 g, tryptone 10 g, yeast extract 10 g
TB[a]	Tryptone 12 g, yeast extract 24 g, glycerol 4 ml, 2,3 g KH_2PO_4, 12,5 g K_2HPO_4
SFM[b]	Mannitol 20 g, soy flour 20 g
SIA[b]	Na-caseinate 2 g, Na-propionate 4 g, KH_2PO_4 0,5 g, asparagine 0,1 g, glycerol 5 g, $MgSO_4*7H_2O$ 0,1 g, $FeSO_4*7H_2O$ 0,001 g
SFG[c]	Glucose 10 g, soy powder 10 g
gSFG[c]	Glucose 10 g, soy powder 10 g, glycerol 5 g
m4[d]	Mannitol or glucose 10 g, soy powder* 10 g, Na-caseinate 10 g
m5[d]	Mannitol or glucose 10 g, soy powder 1 g, $NaNO_3$ 10 g
m6[d]	Mannitol or glucose 10 g, soy powder 10 g, starch 10 g, $NaNO_3$ 10 g
m7[d]	Mannitol or glucose 10 g, soy powder 0,1 g, starch 5 g, $NaNO_3$ 5 g, NH_4Cl 5 g, KH_2PO_4 2 g, K_2HPO_4 12 g
m8[d]	Mannitol or glucose 10 g, soy powder 1 g, $NaNO_3$ 10 g, NH_4Cl 3 g

a: Commonly used bacterial *E. coli* growth media. b: Taken from "Practical Streptomyces Genetics"[143]. c: Modified after "Practical Streptomyces Genetics"[143]. d: Examples of promising self-developed media compositions.

7.2.3 Conclusion

The isolation of random microbes is not the crucial point, but the reproducible isolation and linkage to interactions between microbes or influences on insects.

Following the proposed isolation techniques with samples from leaf-cutting ants, the same aqueous extract can be spread on different media compositions. Sometimes, inhibition zones are already visible during the isolation procedure.

Nutrient rich agar media like SFM/SFG can be used for isolation, but the great variety of microorganisms complicates the isolation of slow growing microbes, because they are already overgrown. After addition of antibiotics, there is more selection and therefore less growth at all (Fig. 107 A), but there are still more microbes visible than in comparison to less nutrient rich media (Fig. 107 B-D).

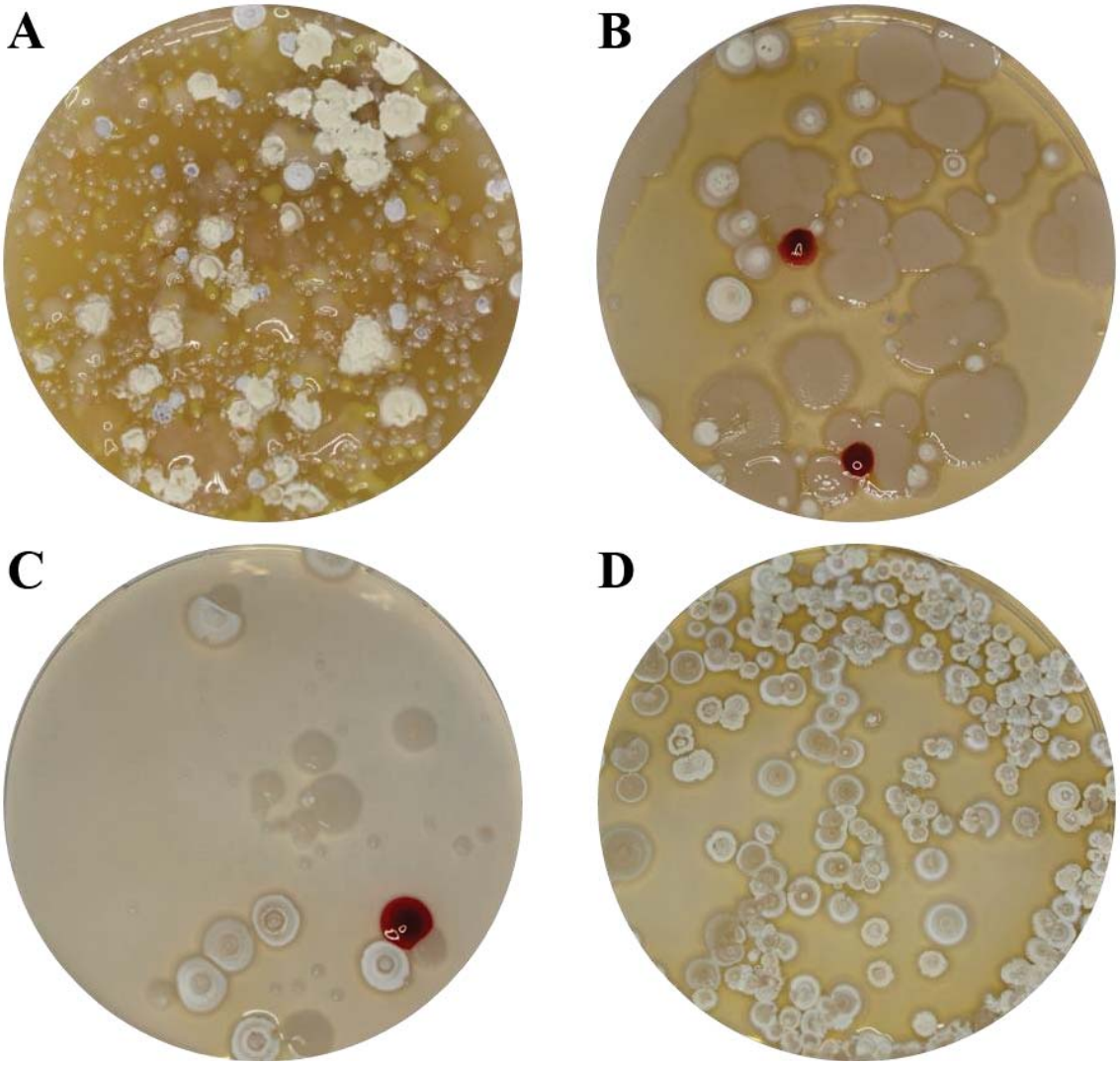

Fig. 107: Comparison of microorganisms isolated from leaf-cutting ants. A: SFM medium with 50 µg/ml apramycin. B: No2 (composition see Ch. 6.1.3.1, p. 142). C/D: SIA with pH 7,5 and unspecific (C) or specific (D) isolation method.

7.3 Induce and enhance the production of secondary metabolites

Prolog

Results were combined on a poster, awarded for the best poster at the KoRS-CB Retreat 2014.

7.3.1 Abstract

The discovery of bioactive secondary metabolites under laboratory conditions is - more or less - still a matter of luck. Besides the need of performing a convenient bioassay with an appropriate competitor to detect present antibiotics,[138] the production of bioactive compounds could be silenced due to growth conditions and absent elicitors.[144] Activation of silent gene clusters by application of stress factors or signaling molecules[145] and imitation of natural growth conditions[146] leaded to remarkable discoveries of bioactive molecules in recent years.

There are innumerable possibilities to set up growth and detection assays to spot bioactive molecules.[147] Once a working process was found, little variations could increase or decrease its efficiency. Indeed, not all options can be applied and no one wants to spend a long time on screening for "optimal" conditions.

However, the preparation of some simple mixtures and monitoring of caused effects normally guide to a setup with enhanced production of bioactive molecules. With the hereby developed methods, bacteria can be screened for bioactivity against other microbes directly (Fig. 108 A) and influences of media compositions can be easily compared (Fig. 108 B).

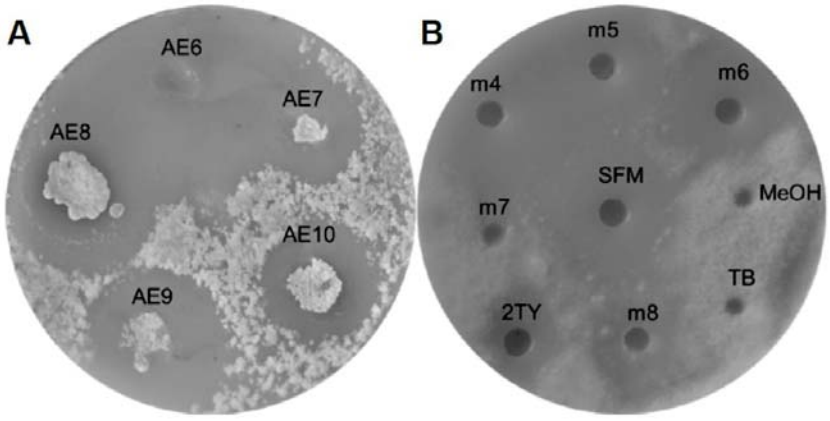

Fig. 108: A: Co-cultivation assay of bacteria (isolated from *Acromyrmex echinatior*; AE6-10) against the pathogenic fungus *Escovopsis weberi*. B: Bioactivity of extracts (ethyl acetate) of a bacterial strain, grown in custom media, against *Fusarium* spp..

7.3.2 Methods

The isolated and purified microbe has to be cultivated in an appropriate medium in order to grow and produce bioactive secondary metabolites. One main part to reach this goal are nutrients.

For a first screening, one microbe was spread all over an agar plate, while the antagonist was filled into indentions (Fig. 108 A). With this setup, both microbes have to use the same spectrum of nutrients and supplements. Therefore, another setup was developed in order to check growth conditions for the bioactive substance producing strain, while the attacked microbe could be cultivated without supplements. The bioactive substance producing strain was inoculated in liquid media with or without supplements and incubated in a rotary shaker in culture tubes. The culture tubes were only half filled, therefore extraction at native or acidified pH could be prepared directly in the culture tube. This approach was found to be very time saving for screening issues. The extracts were thereafter evaporated and dissolved in solvent. This liquid was applied in holes in the agar plates and screened for bioactivity (Fig. 108 B).

Several liquid media were used, at first those which were already published in books and thereafter self-developed media (Tab. 25). Mannitol was again exchanged by glucose due to no visible benefit but 5-10 times higher costs.

Tab. 25: Compositions of some used cultivation media.

medium	composition (per l^{-1} ddH_2O; for solid media add Agar-Agar 15 g)
2TY[a]	NaCl 5 g, tryptone 10 g, yeast extract 10 g
TB[a]	Tryptone 12 g, yeast extract 24 g, glycerol 4 ml, 2,3 g KH_2PO_4, 12,5 g K_2HPO_4
SFM[b]	Mannitol 20 g, soy flour 20 g
SFG[c]	Glucose 10 g, soy flour 10 g
gSFG[c]	Glucose 10 g, soy flour 10 g, glycerol 5 g
m4[d]	Mannitol or glucose 10 g, soy flour * 10 g, Na-caseinate 10 g
m5[d]	Mannitol or glucose 10 g, soy flour 1 g, $NaNO_3$ 10 g
m6[d]	Mannitol or glucose 10 g, soy flour 10 g, starch 10 g, $NaNO_3$ 10 g
m7[d]	Mannitol or glucose 10 g, soy flour 0,1 g, starch 5 g, $NaNO_3$ 5 g, NH_4Cl 5 g, KH_2PO_4 2 g, K_2HPO_4 12 g
m8[d]	Mannitol or glucose 20 g, soy flour 1 g, $NaNO_3$ 10 g, NH_4Cl 3 g

a: Commonly used bacterial *E. coli* growth media. b: Taken from "Practical Streptomyces Genetics"[143]. c: Modified after "Practical Streptomyces Genetics"[143]. d: Examples of promising self-developed media compositions.

In order to describe growth parameters, also pH, oxygen and temperature influences were investigated. These parameters are microbe specific and generalized assumptions should not be made and are not mentioned here.

For some microbes, signaling molecules were isolated and added to fresh cultures. One example is shown on the poster, but was not investigated in more details.

Inorganic supplements, such as heavy metal ions, were claimed to be advantageous for secondary metabolite production. In order to test this statement, several compositions and microbes were cultivated and evaluated. The addition of supplements influenced morphology, growth and metabolite production of the microbes.

Tab. 26: Compositions of some used inorganic supplements.

Name	**Composition (exemplarily in different amounts)**
Trace	$FeCl_3$, $MnCl_2$, $ZnSO_4$, $CuSO_4$
Al-Mix1	$Al_2(SO_4)_3$, $NiSO_4$, $CuSO_4$
Al-Mix2	$Al_2(SO_4)_3$, LiBr, $MnCl_2$
Al-10	$Al_2(SO_4)_3$, NaOH (pH 10)

Cultivation was thereafter carried out in bigger flasks (250-2000 ml), sometimes even in self-developed systems in 10 liter buckets.

For some strains, it was shown, that in different media there were different metabolites produced. Therefore, with only one screening, a complete set of information is generated.

7.3.3 Poster

Main aims of this project

- Find antibiotics to cure infectious diseases
- Study interactions in ecological systems

Example: **Ecosystem of leaf-cutting ants**
Antibiotic producing microbial symbionts associated with leaf-cutting ants were found to help defending their fungal-cultivar against infections, such as *Escovopsis weberi*. *Acromyrmex* leaf-cutting ants can have large microbial biofilms consisting mainly of *Pseudonocardia* and *Streptomyces* on their bodies.

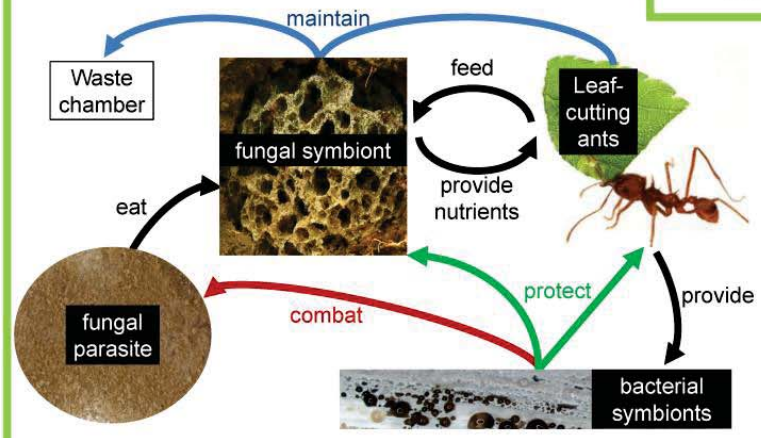

ChemicalBiology
University of Konstanz

How to induce
of bioactive seco

Ralf Schlesiger, Dieter Spiteller. Chemical Ecology, Univers

Microbial biofilms on *Acromyrmex echinatior* leaf-cutting ants.

Intr

The disco
or less –
detection
decrease
„optimal"
Here we
monitorin
bioactive

Co

It was sh
and inorg
These eff
of a bacte
from your
Do not for

Strategies to enhance/induce the produc

Nutrition

Some bacterial genera are known to be able to digest complex molecules (e.g. by production of α- or β-amylases), while others are not. This can be used to select for bacterial species, but also to provide essential nutrients for antibiotic production.

- **Carbon-sources**
  - Monomeric sources (Glucose, Mannose, Glycerol)
  - Complex sources (Sucrose, Starch, Cellulose, Chitin)
- **Nitrogen-sources**
  - Monomeric sources (Amino acids, Ammonium/Nitrate ions)
  - Complex sources (Protein, Tryptone, Casein, Chitin)
- **Essential ions**

Growth conditions

Bacteria which are isolated from different sources, such as black smokers in deep sea or arctic ice, need obviously different conditions to grow.

- **Temperature**
  - Cold and hot temperatures can inhibit/enhance antibiotic production
- **Incubation time**
  - Production of antibiotics can take place after different time periods
  - Antibiotics can be digested/modified after several time, this can lead to a loss/enhancement of activity

Signaling m

The production of bioactive com
diffusible molecules which allow
They can either induce (Quorum
quenching) a signal cascade.

- **Autoinducers**
  - Oligopeptides (often Gram-p
  - N-Acyl homoserine lactones
    bacteria)
- **Analogues to autoinducers**

Besides bioactivity, Strain L stair
color, when its population reache

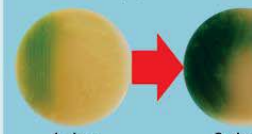

Bioassays with an extract from
to inhibited growth, followed by
green compound. Lower c
production of the green compou
(data not shown).

Example: **Culture media tests with Strain L**

Strain L was grown in several media. Extracts were prepared after 10 days of growth with ethyl acetate at native and pH 2.
The extracts were tested against *Fusarium spp.*

Results:
Strain L shows acitivity when grown in m4, m5, m6, SFM and TB. Extraction at pH 2 was more efficient.

Composition of custom media	
m4	Mannitol, Casein, Soy
m5	Mannitol, $NaNO_3$, Soy
m6	Mannitol, Starch, $NaNO_3$, Soy
m7	Mannitol, Starch, $NaNO_3$, NH_4Cl, KH_2PO_4, K_2HPO_4, Soy
m8	Mannitol, $NaNO_3$, NH_4Cl, Soy
2TY	Tryptone, Yeast extract, NaCl
TB	Yeast extract, Tryptone, Glycerol, KH_2PO_4, K_2HPO_4
SFM	Mannitol, Soy

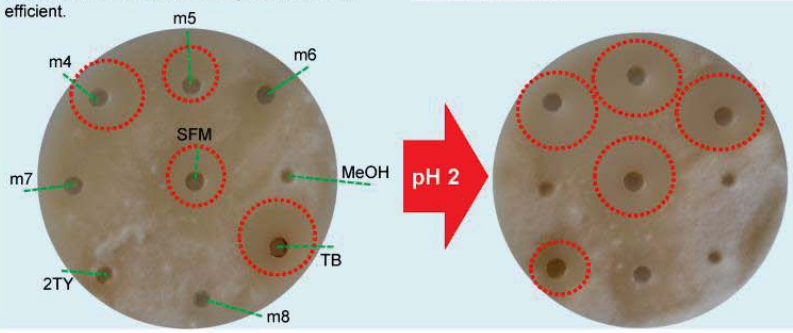

Universität Konstanz

e the production
ndary metabolites?

ität Konstanz. Germany. Mai 2014. Ralf.Schlesiger@Uni-Konstanz.de

roduction

very of bioactive secondary metabolites under laboratory conditions is – more still a gambling game. There are plenty of possibilities to set up growth and assays to identify bioactive molecules. Little variations may increase or the assay's efficiency, but it is impossible to vary all possible parameters to find conditions.
show that the preparation of selected mixtures with several compositions and of caused effects normally guide to a setup with enhanced production of molecules.

nclusion

own that little variations in media compositions, especially nutritional elements anic supplements, increase or decrease the production of bioactive molecules. ects can not be predicted, whenever you want to evaluate the growth conditions rial strain, you have to try different conditions and **piece together the puzzle** results.
get to run appropriate controls for all your experiments!

Workflow of bioactive compound discovery

- Isolation of microbes
- Antagonistic growth assay: bacteria and parasite on agar

- Enhancement/induction of compound production
  - Culture conditions/addition of supplements in tubes
  - Extraction of culture media
  - Agar diffusion assay (bacterial extract and parasite)

ction of bioactive secondary metabolites

olecules

pounds can be mediated by cell-to-cell communication. n sensing) or stop (Quorum

positive bacteria)
(often Gram-negative

s agar plates with a green s a certain cell density.

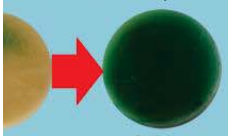

ys 6 days

6 days old agar plates lead inhibited production of the oncentrations induce the d even at lower cell density

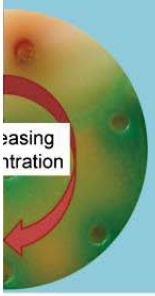

Inorganic supplements

Addition of certain supplements can induce/inhibit the production of secondary metabolites. Sometimes they are even essential for bacterial growth.

- **Trace elements**
  - Environmental stimuli (Activation of signalling cascades)
- **Stress factors**
  - heavy metal ions (Production of siderophores)

Inorganic supplement solutions	
Trace	$FeCl_3$, $MnCl_2$, $ZnSO_4$, $CuSO_4$
Al-Mix1	$Al_2(SO_4)_3$, $NiSO_4$, $CuSO_4$
Al-Mix2	$Al_2(SO_4)_3$, LiBr, $MnCl_2$
Al-10	$Al_2(SO_4)_3$, NaOH (pH 10)

Example 1: **Supplement tests with Strain L**

Strain L was grown in several media with several supplement solutions. Extracts were prepared after 10 days of growth with ethyl acetate at native and pH 2 (mixed).
The extracts were tested against *Escovopsis weberi*.

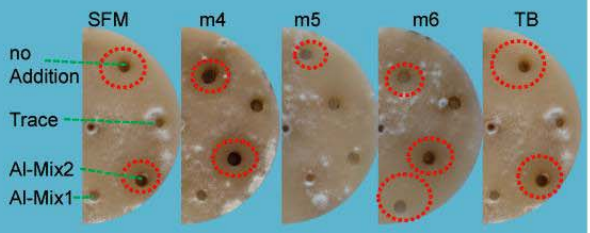

Results:
Strain L shows increased acitivity when grown in m4 supplemented with Al-Mix2 and in m6 supplemented with Al-Mix1 and Al-Mix2.

Example 2: **Supplement tests with Strain A6, which shows no activity in unsupplemented media**

Strain A6 was grown in numerous media with several supplement solutions. Extracts were prepared after 10 days of growth with ethyl acetate at native and pH 2 (mixed). The extracts were tested against *Escovopsis weberi*.

Results:
Strain A6 shows acitivity when grown in m4 supplemented with Trace, m6 supplemented with Al-Mix2 and TB supplemented with Trace or Al-Mix2.

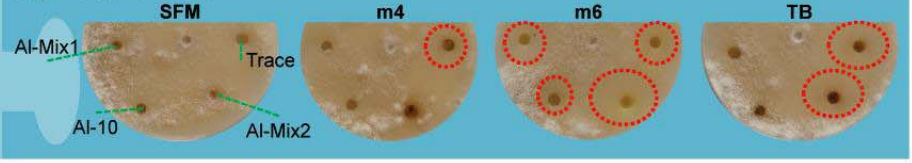

7.3.4 Conclusion

With this project, I aimed to show the importance of screenings to optimize cultivation conditions beforehand and not only to use one standard medium for all approaches. Indeed, it was shown that small variations of growth conditions might result in major changes of bioactive secondary metabolite production.

Starting with nutrition, the amount of soy flour should be decreased because soy was found to contain a complex mix of unwanted substances. This will play a role in the next chapter, because "soy compounds" have to be removed from bacterial culture extracts in order to identify bioactive secondary metabolites. This was one reason, why media compositions were developed with simple combinations for energy and nitrogen sources and tested for their ability to allow microorganisms to grow.

Alterations of mannitol to glucose had no measurable effects on the tested strains, but mannitol was 5 times more expensive than glucose. Therefore, mannitol was replaced by glucose. Furthermore, media with starch or cellulose were used, which do not allow growth for all organisms and are therefore more challenging for the microbes than freely available glycerol. As nitrogen sources, some salts (NH_4Cl or $NaNO_3$) or amino acid mixtures (sodium caseinate, tryptone, yeast extract) were used.

Growth conditions like pH and temperature play an important role, but are most of the time not considered to be changed by scientists. The application of metal helices, together with fill height and rotation speed in the shaker were shown to influence oxygen intake and biofilm formation. All these parameters influenced the production of bioactive secondary metabolites.

The addition of isolated signaling molecules can cause two effects, either the growth and/or production stopped or was increased. There were effects like morphological changes, cell proliferation and antibiotic production which might have been linked to signaling molecules in extracts.[148] I proposed to look at this effects in more detail.

For the supplements, I showed examples for all three possibilities: the production of bioactive secondary metabolites was either increased, decreased or unaffected. Therefore, no generalized statement should be made concerning supplements. Already in 1951, the production of streptomycin was shown to be only possible when zinc and copper ions are present in the culture medium.[144] Another aspect might be the activation of silent gene clusters, which produce a different set of metabolites in modified conditions.[149]

These effects can only be investigated by screenings with different combinations of culture media and supplement solutions.

7.4 Secondary metabolite purification workflows

7.4.1 Introduction

Bioactive secondary metabolites are produced by many organisms. There are several points of action for antibiotics, which can be specific or unspecific. Consequently, the chemical structures of metabolites are enormously diverse, too.

In the past, especially colorful metabolites with chromophore structures were identified, because they can be spotted by eye even on TLC plates or with UV-Vis techniques.[150-151] Handling of crude extracts can be crucial, especially when bioactive secondary metabolites are instable or when extracts are very rich of unwanted compounds, which have to be removed. The choice of extraction solvents or resins together with conditions like pH and temperature play an important role for the following purification process. When the extract is rich of lipids and carbohydrates, they can be removed within min. Thereafter, purification protocols with flash chromatography with several resins can be applied, until the residual bioactive fraction is pure or the amount is small enough to be applied in HPLC fractionation.

7.4.2 Methods

Extraction

For a first screening, several solvents (hexane, petrol ether, ethyl acetate, dichloromethane, diethyl ether) were used at native or acidified pH in order to evaluate their extraction abilities. Solid resins like XAD16 (Amberlite) can be applied in spent culture media in tea bags, and thereafter bound substances can be eluted with organic solvents (hexane, petrol ether, ethyl acetate, dichloromethane, diethyl ether, acetone, methanol).

Removal of polar compounds

The mostly viscous, tarlike extracts were pre-purified using silica filtration through a silica plug. Sand and silica powder (60 mesh) were added to the crude extract, solvent such as diethyl ether was evaporated and the sand mixture was homogenated. A silica plug with a minimum of ten times the sand mixture volume was prepared with diethyl ether. The material was filtered into two fractions, first diethyl ether and afterwards methanol. Both fractions were evaporated and checked in bioassays.

Removal of very unpolar compounds (lipids)

If the diethyl ether fraction was bioactive, it was used for a methanol-hexane-separation in a 100 ml bottle. The hexane layer (upper) was exchanged until it remained clear. Both phases were evaporated and checked in bioassays.

Please note: This step was very important because liquid unpolar compounds influence fractionation on silica gel and lead to smearing.

Chromatography

Several chromatography workflows were investigated to identify effective solvent mixtures.

Please note: Separation in much more fractions did not make sense, because if the process was at all ineffective, the compound of interest might be hidden. If you only have 5 fractions, every fraction would contain 20% of your compound in the worst case. You will be able to spot the difficulty and go further. If you have 30 fractions, every fraction contains only 3% of your compound and you have to find out, where the compound is.

A reasonable amount of solvent for dilutions of fractions can be calculated, but if the best and the worst case scenario are too different, it will be absolutely unpredictable.

The methanol phase (when bioactive) was further purified by flash chromatography on a silica gel column (20x2,5 cm), eluted with petrol ether/diethyl ether (4:1; 2:1; 1:1; 1:2) and final methanol in 5 fractions (120 ml each).

The bioactive fraction was subjected to a RP-C_{18}-Column (15x2,5 cm; Polygoprep C_{18} 60-50; Macherey-Nagel, Düren) eluted with methanol in ddH_2O (30%; 50%; 70%; 90%; 100%) in 5 fractions (120 ml each) followed by RP-HPLC fractionation of the bioactive fraction.

For HPLC fractionation, an Agilent 1100 HPLC system was used. The bioactive residue was dissolved in ddH_2O/methanol and several times (each maximum 30 µl) injected into an Agilent ZORBAX Eclipse XDB C_8 column (150x4,6 mm, particle size: 5 µm). A mixture of ddH_2O and methanol (each 0,1% acetic acid) was used at a flow rate of 0,6 ml/min and a gradient from 30 to 100% methanol. The automatic fraction collector collected 27 fractions (1 tube/min) between 1 and 28 min of the runtime.

Thereafter, suitable column materials for the separation of compounds in the fraction (modified with C_{18} or aminopropyl or ether-linked phenyl groups) should be identified. Different conditions like pH or additives should be tested.

7.4.3 Conclusion

Comparative screenings for extraction conditions were shown to be helpful, as the efforts for extraction or the amount of hindering unwanted compounds could be lowered right in the beginning of the purification process. Again, no generalized statement can be made concerning extraction or fractionation procedures.

I used the principle of counter-current extraction to increase the efficiency of every extraction step. Solvents were redistilled, hereby the amount of necessary organic solvents was reduced dramatically.

It is very important to know a wide set of methods, to be able to apply suitable steps for observed difficulties. I will discuss one very demonstrative effect in another chapter, where antibacterial compounds were extracted by methanol and antifungal compounds were extracted using ethyl acetate (Ch. 5.2.3; p. 76).

The procedures of filtration through a silica plug and hexane-methanol-separation are two very simple, but effective and reliable methods. In contrast to chromatographic separations, they can be conducted within min and remove up to 95% of extract weight containing only unwanted compounds. To prevent blocking of the column, also freezing was suitable but needed more time (dissolve residue in methanol and store overnight in freezer; -81°C; lipids precipitated and liquid was transferred).

For chromatographic separation, the knowledge of the bacterial strain might be helpful. If there is a suspected substance class, similar procedures might guide towards suitable methods and conditions.[152-154] If not, one must play around for example with polar or reverse phase, ion exchange or size exclusion.

7.5 Potential and restrictions of ESI-LC-MS in mass determination of unknown secondary metabolites

Prolog

This project was started during the "Vertiefungskurs Chemische Ökologie 2016", because the previously obtained masses from bioactive extracts with unknown secondary metabolites were not usable and therefore non-satisfying. Herewith, my student Nils Glücklich and I, we compared the measurement parameters of known antibiotic compounds to describe the difficulties for following measurements of unknown secondary metabolites.

7.5.1 Introduction

Mass spectrometry is an analytical technique that provides qualitative (structure) and quantitative (molecular mass or concentration) information.

Liquid chromatography - electrospray ionization - mass spectrometry (LC-ESI-MS) has become a powerful technique capable of analyzing both, small and large molecules of various polarities in complex biological samples, for example in proteomics and metabolomics. Nevertheless, its usability for detection and identification of unknown natural products remains challenging.[155] The structural diversity of bioactive natural products requires several tunes with compounds of different substance classes, in order to decrease the detection threshold and obtain reliable results for mass determination.[156]

For this study, a HPLC-ESI-MS system (Finnigan LCQ) was used. We compared spectra of selected antibiotics from different substance classes and optimized several MS parameters (lenses, quadrupols) by using the auto-tune software.

Influences of capillary voltage and temperature to the detection sensitivity were compared for erythromycin as an example (Fig. 109). Furthermore, the solvent composition, HPLC flow rate, as well as the nebulizer and sheath gas flows influenced the results dramatically.[157]

The effects of acidic or alkaline conditions were tested via supplementation of the solvent mixture with different amounts of acetic acid or triethylamine. According to the substance class and functional groups, the beneficial amount of supplements was different.

The resulting spectra of an antibiotic mixture with several tunings and conditions were compared; massive differences in sensitivity and specificity were obtained.

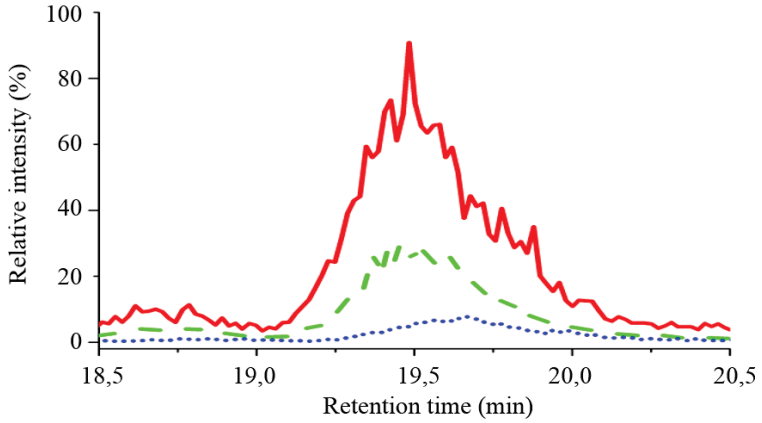

Fig. 109: Spectra for the same amount of Erythromycin with tunes of different compounds (positive mode; erythromycin tune - solid line; apramycin tune - dashed line; vancomycin tune - dotted line).

7.5.2 Methods

Ampicillin (β-lactame), apramycin (aminoglycoside), erythromycin (macrolide) and vancomycin (glycopeptide) were selected as reference antibiotics for a first comparison. The reference solutions were analyzed with liquid chromatography - electrospray ionization - mass spectrometry (LC-ESI-MS).

Several MS parameters (lenses, quadrupoles) were optimized by using the auto-tune software, whereas not auto-tuned settings (like gas flows, capillary temperature and capillary voltage) were tuned by hand with erythromycin as an example. Furthermore, advanced parameters such as solvent composition (water, methanol), HPLC flow rates (0,1-0,6 ml/min) and concentrations of acidic/alkaline supplements (acetic acid, triethylamine; 0-1 %vol) were changed and spectra of up to four selected antibiotics were compared.

Comparisons were made either by relative intensity, if only one compound was screened (in most cases erythromycin), while the relative area was calculated for every compound and the maximum was set to 100%. In order to compare different compounds, the relative area per mmol was calculated and the highest value was set to 100% for every single figure. Thereby, the detectability of substances could be compared with each other, while for instrument parameters the effect of setting changes was nicely visualized.

ChemicalBiology
University of Konstanz

Universität Konstanz

University of Konstanz, Chemical Ecology, Universitätsstraße 10, 78457 Konstanz, Germany.

Capabilities and restrictions of LC-ESI-MS in mass determination of unknown bioactive natural products

Nils Glücklich, **Ralf Schlesiger**, D. Spiteller. Feb 2016

Introduction

- LC-ESI-MS is a common used technique, especially for proteomic and metabolomic researches.
- Every substance class needs specific conditions and parameters for accurate measurements and high sensitivity.
- Some instrument parameters cannot be changed fast, they are fixed but need complementary conditions.[1]
- Addition of acidic or basic supplements influences the sensitivity.

► Consequently, for unknown samples one needs several reference tunes with altering instrument parameters.

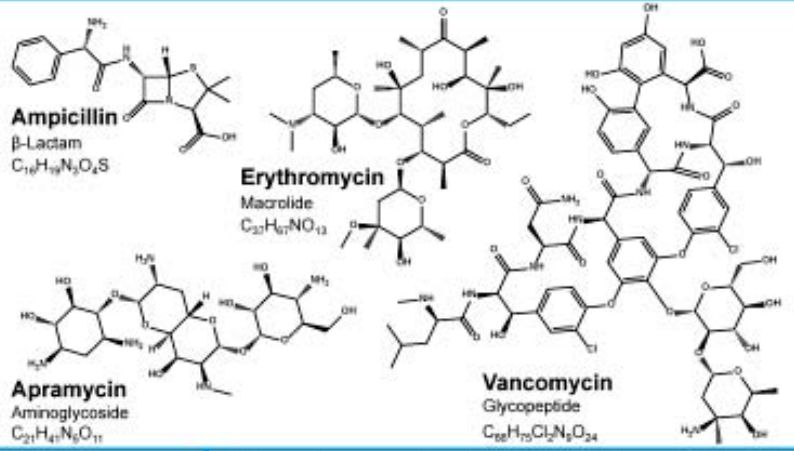

Principle of ESI-MS

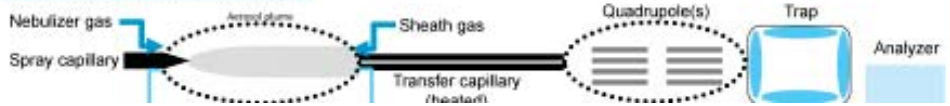

Supplements: Donor / Acceptor

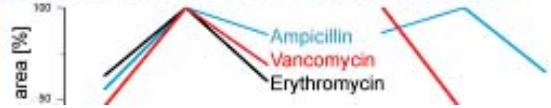

Transfer capillary: Temperature and Voltage

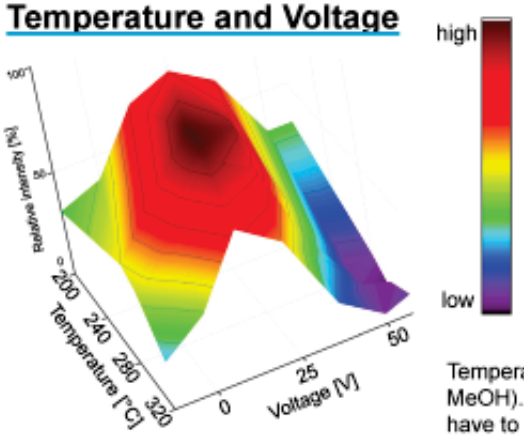

Correlation of HPLC flow and gas flow

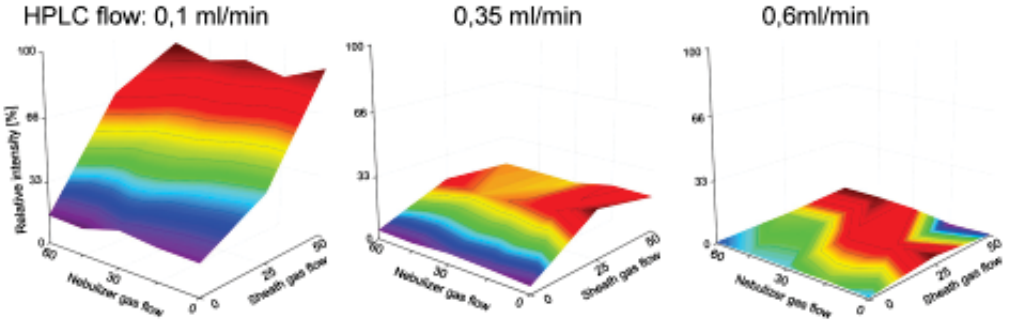

Temperature and voltage of the transfer capillary effected the sensitivity of MS measurements (0,1 ml/min; 50% MeOH). HPLC flow rate and gradient influenced the obtained results. Nebulizer and sheath gas flow of the MS have to be adjusted according to every change (gradient not shown; all Erythromycin stock solution). [2]

Comparison of tunings

Positive mode; tune for Ampicillin (upside) and Erythromycin (downside)

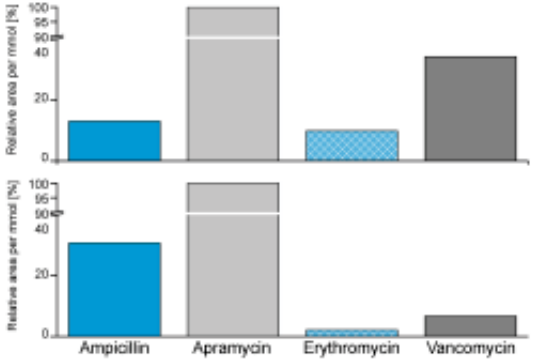

Negative mode; tune for Ampicillin (left) and Vancomycin (right)

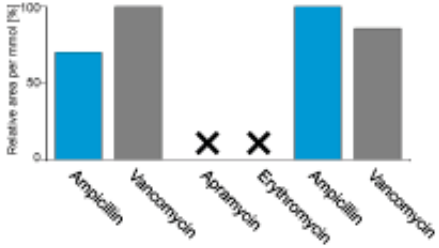

Sample detection varies between tunes and modes. In some tunes, no sample was detected (negative mode, no signals for Apramycin and Erythromycin).

Conclusion / Outlook

- Instrument parameters have to be adjusted manually.
- Gas flows (nebulizer; sheath) have to be adjusted according to HPLC flow rates.
- ► Elucidation of "unknown" samples with optimized set of tunes.
- ► Pitfalls for quantification efforts.

References

[1] J Am Soc Mass Spectrom. 2009; 20(4); 682–688.
[2] J Chrom A. 1996;755(2); 189-204.

7.5.4 Conclusion

With our project, we wanted to describe the influences of measurement parameters with known antibiotics to allow the measurement of unknown bioactive substances. While parameters like the positive and negative mode had an obvious and expected influence on the overall detectability of compounds, there were numerous further parameters found to be considered.

Comparisons of auto-tunes for ampicillin and erythromycin were used for measurements of all four antibiotics in positive mode. While the relative intensity (area per mmol) for apramycin was the highest in both cases, ampicillin was better detectable in erythromycin tunes than in ampicillin tunes. For vancomycin, the effect was the other way around. The relative intensity for erythromycin ranged in both cases below 15%, therefore the detectability of erythromycin was weak even for the specific erythromycin tune.

For the negative tune, ampicillin and vancomycin were used. There were no signals for apramycin or erythromycin, only ampicillin and vancomycin were detected. Indeed, free carboxylic acid groups contributed to their detectability.

The addition of supplements increased the signal intensity, but there was no generalized beneficial supplement or amount of supplement. The addition of acetic acid increased signal intensity compared to no addition, but the effect turned back when adding more than 1%. The addition of triethylamine had the same effect for signal intensities of ampicillin. In contrast, addition of triethylamine decreased signal intensities of vancomycin compared to no supplement.

In conclusion, all three parameters (mode, tune and supplement) influenced the overall detectability of reference substances. While these influences can be altered easily, the HPLC flow rates should match to the column diameter and particle size.

In contrast, instrument parameters like capillary temperature and voltage showed a clear maximum for the erythromycin tune. The maximum region ranged from +1 to +10 volts and between 250 and 300°C in positive mode for erythromycin.

In conclusion, alteration of HPLC and gas flow parameters helped to increase relative intensities. The influence of the nebulizer gas flow was negligible, while changing HPLC flow rates as well as the sheath gas flow led to differences up to 100% in peak areas.

For future approaches, a set of tune files has to be developed in order to cover a wide range of substance classes and functional groups. Herewith, the possibility to detect unknown secondary metabolites will be increased and simplified, as you can screen a fresh prepared bioactive fraction with those tunes and thereafter evaluate obtained masses.

8 Side projects of interest

8.1 Setup and administration of a computer network after DFG guidelines and good scientific practice

Prolog

This project was privately financed with the aim to create an IT infrastructure which was DFG and GSP compliant. In addition, I solved the problem with overaged software which is incompatible with recent operation systems (Windows XP only) by setting up virtual operation systems on a server. Using this approach, data analysis was possible with office computers.

I want to thank the Microsoft Dreamspark/Imagine program, from where I received the licenses for Windows Server 2012R2, Windows 7 and Windows XP. Pictures were taken from pixabay.com and are licensed after Creative Commons (CC0).

Please get informed about backup possibilities and redundant storage. Fault rates of hard disk drives are an underestimated danger for data security.

8.1.1 Initial state

Data of lab computers were only stored on their internal hard disk drives (HDDs). Sometimes, these unprotected Windows XP computers were connected to the internet, even though the IT service of the university advised against doing this because it opens the door for external attacks.

Some data was transferred to office computers with USB devices, which again stored data only on internal HDDs with no external backup routine.

In case of hardware defects, overvoltage or hacker attacks, raw data would get lost and experiments need to be repeated. The DFG guidelines advice to backup raw data in order not to cause additional costs for redundant analysis and measurements.

Some overaged software products only operate with Windows XP, but not with recent operation systems. Therefore, for interpretation of data, one must use Windows XP. This was only possible at lab computers, which is time consuming and inefficient for example while writing a proposal at an office computer. Furthermore, when interpretation of data caused blue screens on lab computers, operating analyses were stopped unexpectedly.

8.1.2 Backup of data

To solve all spotted problems with one solution, a Windows Server 2012R2 system was established. The Windows server was only connected to the intranet of the University Konstanz, which can be externally accessed with a VPN client after login. A hacker would have needed login data from the University of Konstanz. Data of the Windows server were mirrored on a Linux server, which was connected to the internet directly. Both servers were protected against overvoltage and even though one system is hacked or destroyed, data is still secure on the other system or on lab computers.

Furthermore, data was stored on external HDDs periodically (3-6 months).

Lab computers with Windows XP were connected to a subnet of the Windows server, which allowed to backup raw data from measurements automatically. Data were available for office computers directly.

Data from office computers were also stored on the server systems. Hereby, also proposals and scans from lab notebooks were protected against defects.

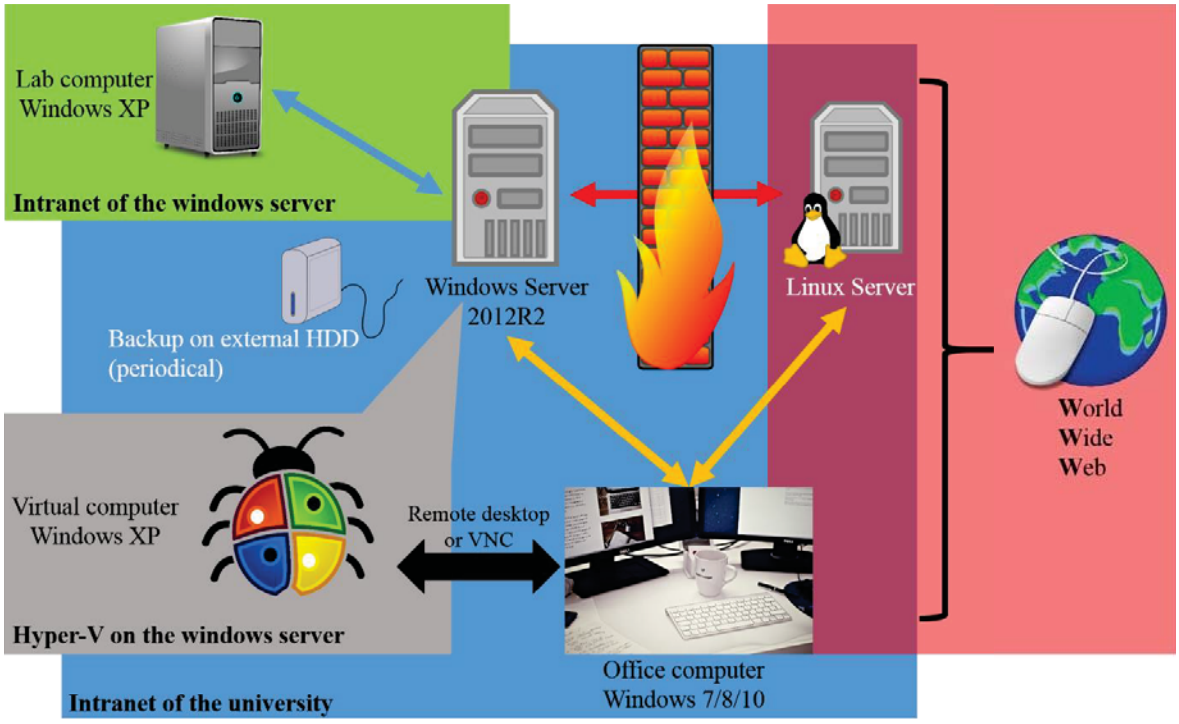

Fig. 110: Overview of the developed IT infrastructure. Green box: Intranet for lab computers. Blue box: Intranet of the University Konstanz. Grey box: Virtual computer on the Windows server. Red box: Internet connection.

8.1.3 Virtual operation systems

In order to interpret and process raw data using office computers while writing proposals, virtual computers were built. Unfortunately, the office computers were slow. Therefore, virtual operation systems were processed on the Windows server and accessed via remote desktop or VNC software.

The virtual systems were equipped with Windows XP and analysis software. With this approach, data could be exported and directly copy-pasted into research documents prepared with office computer.

8.2 Structure elucidation of degradation products after anaerobic desulfonation of 3-(4'-sulfophenyl) butyrate and *p*-toluene sulfonate by *Clostridium* sp. EV4

Contributions

This projects continued the efforts of Prof. em. A. Cook.

One project during "Vertiefungskurs Chemische Ökologie 2013", our biological technician Karin Denger and her students Anna Gorenflo and Eva Oechsle reproduced the growth parameters. I performed chemical separation and structure elucidation of liquid cultures. Prof. Dr. D. Spiteller and our chemical technician Daniela Starke started several synthesis routes in 2013 and 2014. My synthesis approach was successful in 2014, thereafter Daniela Starke synthesized three stereoisomers in 2015.

Separation of stereoisomers was accomplished by Phenomenex Ltd. Deutschland (Aschaffenburg), with their free column screening program.

I want to thank Prof. Dr. Harald Groß (Department of Pharmaceutical Biology; University of Tübingen) for his generous support with HR-MS measurements.

This project was topic of my 18-month proposal for the graduate school and two poster sessions.

8.2.1 Abstract

The anaerobic bacterium *Clostridium* sp. EV4 (DSM8245) is able to desulfonate 3-(4'-sulfophenyl) butanoic acid, when supplied with this intermediate of linear alkylbenzene sulfonate degradation as sole source of sulfur.

The products of the anaerobic desulfonation of 3-(4'-sulfophenyl) butanoic acid and *p*-toluene sulfonate were identified by metabolic profiling using LC-DAD-MS of the *Clostridium* sp. EV4 supernatant. After purification of these products, they were characterized by high resolution mass spectrometry, tandem mass spectrometry, 1D and 2D NMR spectroscopy.

3-(4'-sulfophenyl) butanoic acid is converted to 3-(4'-(5''-deoxy-D-ribofuranos-5''-yl)phenyl) butanoic acid. The structurally related *p*-toluene sulfonate is converted to 5-deoxy-5-tol-4'-yl-D-ribofuranose. In order to acquire essential sulfur, *Clostridium* sp. EV4 performs a remarkable reaction that yields a 5-aryl-5-deoxy-glycoside.

8.2.2 Introduction

Linear alkylbenzene sulfonates (LAS, **1**, Fig. 111) are used worldwide as synthetic surfactants. LAS were introduced in the 1960s to replace branched alkylbenzene sulfonates

which caused severe pollution due to their slow biodegradability. Instead, LAS are rapidly degraded by aerobic bacteria, with sulfophenyl carboxylic acids (SPC) as intermediates.

For a long time, no evidence for anaerobic microbial degradation of LAS or SPC was found, the biodegradation of LAS/SPC was thought to occur only under aerobic conditions.[158-159] Therefore, an accumulation of LAS and SPC in anoxic soil layers and sediments was assumed. However, some researchers observed that anoxic bacteria dissimilate alkylbenzene or SPC as carbon [160] or sulfur [161-163] source.

Since 2003, more and more evidences for anaerobic degradation of LAS/SPC were shown using laboratory reactors,[164] also bacterial species were identified which were present in the reactors and could be involved in LAS/SPC degradation.[165-166] While the aerobic degradation of LAS in waste water treatment plants is very fast (<7 days) and effective (>95%), the anaerobic degradation was shown to reach about 80% in 165 days.[167]

In 2010, Lara-Martín *et al.*[168] proposed an anaerobic degradation pathway for LAS, starting with the addition of fumarate and leading in their experiment to small SPC molecules such as 3-(4'-sulfophenyl) butyrate (3-C_4SPC, **2**, Fig. 111) and 1-(4-sulfophenyl)ethanol (SPEt, **3**, Fig. 111). Further degradation products were not described, but a discrepancy between supplied LAS and formed SPC was observed leading to the question how 3-C_4SPC is further degraded.

In our experiment, we took the previously described *Clostridium* sp. strain EV4,[161-162] which desulfonates several *para*-sulfophenyl compounds under sulfur-restricted conditions within 48 hours. For the first time, we present the chemical characterization of products of the anaerobic desulfonation of 3-C_4SPC and *p*-toluene sulfonate (TS, **4**, Fig. 111). Furthermore, a synthesis route was developed to identify the stereochemistry of the degradation product and to allow continuative degradation experiments.

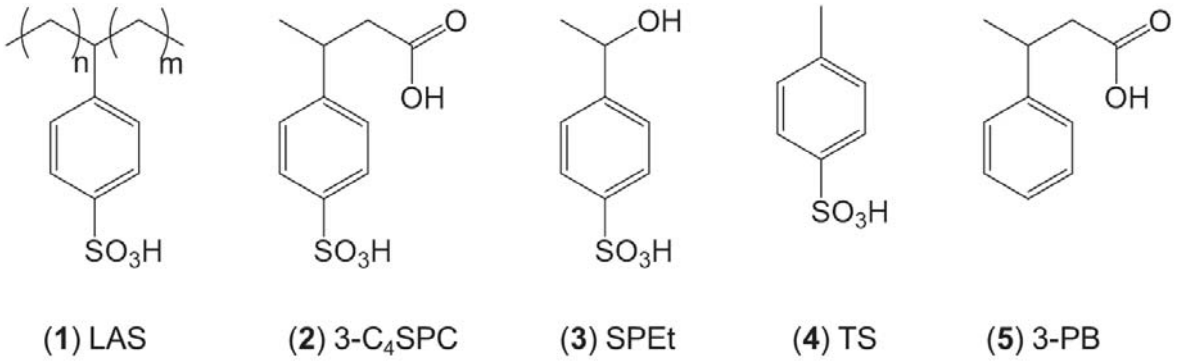

Fig. 111: Chemical structures of linear alkylbenzene sulfonates (**1**; with n+m<13), 3-(4'-sulfophenyl)butanoic acid (**2**), 2-(4'-sulfophenyl)ethanol (**3**), *para*-toluene sulfonate (**4**) and 3-phenyl butanoic acid (**5**).

8.2.3 Methods

8.2.3.1 Cultivation conditions

Clostridium sp. strain EV4 (DSM8245) was cultivated as described before in detail.[161] The liquid mineral salts medium was buffered with 50 mM $NaHCO_3$ adjusted to pH 7, containing 1 mM titan(III)nitrilotriacetate, 2 µM resazurin as indicator for anoxic conditions and 10 mM glucose as carbon source.

50 µM 3-(4'-sulfophenyl)butyrate, toluene sulfonate or Na_2SO_4 as a control were used as sole sulfur source. Cultures were incubated in sealed bottles under an atmosphere of N_2:CO_2 (80:20) at 30°C for 36 hours without shaking.

The culture broths of the different cultivations were centrifuged at 6000**g* for 10 min and the aqueous supernatants were used for analysis.

8.2.3.2 Analysis of degradation products by LC-DAD-MS

The supernatants were extracted three times with an equal volume of ethyl acetate (freshly distilled) at native pH (around 6,5). The ethyl acetate extract was concentrated *in vacuo* and dissolved in methanol (VWR; HPLC-grade).

The obtained samples were analyzed with an Agilent 1100 HPLC-DAD-System with an Agilent Eclipse XDB-C18 HPLC column (150x4,6 mm, 5,0 µm) in 2013 and 2014. In 2015, the Agilent column was replaced with a Phenomenex Aqua C18 column (250x4,6 mm, 5,0 µm). HPLC-conditions: Solvent A double-distilled water, 0,1% acetic acid (Roth; Rotipuran p.a.), solvent B methanol (VWR; HPLC-grade) supplied with 0,1% acetic acid (Roth; Rotipuran p.a.), flow rate 0,8 ml/min. Gradient elution was used to analyze SPC, TS and their degradation products (Tab. 27).

Tab. 27: HPLC gradient to separate SPC, TS and their degradation products.

Time (min)	Eluent B (%)
0	5
3	5
3,5	30
6,5	30
15	55
20	55
23	100
28	100
28,5	5
35	5

For mass spectrometric detection, a Thermo Scientific™ LCQ ion trap mass spectrometer was fitted with an electrospray ionization source (ESI-MS). The instrument was tuned using

3-phenyl butyrate (3-PB, **5**, Fig. 111) in methanol (0,1% acetic acid). Measurement in negative mode furnished m/z=163 as molecular ion ($[M-H]^-$).

The degradation product of 3-C_4SPC as sulfur source for EV4 furnished a peak at 14,8 min with an UV characteristic for aromatic compounds and a quasi-molecular ion $[M\ H]^-$ at m/z=295. In case of toluene sulfonate as sulfur source for EV4, a peak at 14,2 min with an UV characteristic for aromatic compounds but no mass was observed. In the corresponding control samples using sulfate as sulfur source for EV4, no signals for the suspected degradation products were observed.

8.2.3.3 Characterization of the desulfonated metabolites

Semi-preparative HPLC fractionation was performed in reaction tubes (28 ml) collecting for a first screening one min each tube and later 0,33 min each tube.

The collected fractions were evaporated using a freeze dryer. The purified samples corresponding to retention times of suspected target structures were analyzed by HR-ESI-MS and NMR spectroscopy.

8.2.3.4 Conditions for nuclear magnetic resonance spectroscopy

NMR spectra were acquired either on Bruker Avance III 400 MHz or Bruker Avance III 600 MHz (TCI-H/C/N triple resonance cryoprobe) at a temperature of 300 K. Samples were dissolved in deuterated methanol (methanol-d_4; Deutero; 99,8% purity) or deuterated water (D_2O; Deutero; 99,95% purity) or deuterated chloroform ($CDCl_3$; Deutero; 99,8% purity) and measured in Rototec RS-3-4E (diameter 3 mm; length 100 mm) or Norell 502/509 (diameter 5 mm; length 177,8 mm) tubes.

8.2.3.5 Reference substances and modified pentoses

Compounds were purchased from the following sources:

- 3-Phenyl butyrate (Sigma Aldrich, Germany)
- 5-Deoxy-L-arabinose (Carbosynth, UK)
- 5-Phospho-D-ribose (Sigma Aldrich, Germany)
- 5-Deoxy-L-ribose (Carbosynth, UK)

Further substances were purchased from Sigma Aldrich or obtained from other work groups with unknown origin.

8.2.3.6 Synthesis of the *p*-toluene sulfonate degradation product

The following synthesis route can be applied to pentoses such as ribose and lyxose, with syn orientation of hydroxyl groups in C2 and C3.

The synthesis route is shown in Fig. 123; p. 213.

8.2.3.6.1 Protection and iodation of pentoses

One pentose was suspended in a 1:1 mixture of acetone and methanol (1 g pentose each 100 ml solvent). Concentrated hydrochloric acid (3 ml each 1 g pentose) was added dropwise at room temperature, thereafter the mixture was refluxed for 1 h. After cooling to room temperature, the mixture was neutralized with pyridine and separated between an aqueous and diethyl ether phase (1:1; 300 ml). The aqueous phase was extracted two times more with diethyl ether (100 ml each). All diethyl ether phases were combined and washed once with equal volumes of saturated copper sulfate solution, water and saturated sodium chloride. Thereafter, the diethyl ether phase was dried over sodium sulfate and solvent was removed *in vacuo*.

For iodation, the oily protected pentose was suspended in a toluene-acetonitrile mixture (5:1; 100 ml each 5 g protected pentose), containing imidazole (2 g each 5 g protected pentose) and triphenyl phosphine (6,5 g each 5 g protected pentose). Iodine was dissolved in a toluene-acetonitrile mixture (5:1; 6,5 g in 5 ml each 5 g protected pentose) and added dropwise at room temperature. The mixture was refluxed for 5 min and dissolved iodine was added until the mixture remained light brown.

After cooling to room temperature, double volume of diethyl ether was added and the organic phase was washed several times with an equal volume of 10% sodium thiosulfate solution until colorless. Thereafter, the organic phase was washed with equal volumes of water and saturated sodium chloride. The organic phase was dried with sodium sulfate and solvent was removed *in vacuo*.

The oily residue was filtered through a plug of silica with a hexane-ethyl acetate mixture (95:5). The solvent was removed *in vacuo*. The oily residue was used for further coupling.

8.2.3.6.2 Suzuki cross-coupling of protected iodated pentoses with *p*-tolylboronic acid

We adapted a Suzuki cross-coupling of primary alkyl iodides with boronic acids, which was described by Gonzalez-Bobes and Fu in 2006.[169] The Suzuki cross-coupling was catalyzed with NiI_2 and trans-2-aminocyclohexanol under nitrogen atmosphere. All instruments and chemicals were water-free; air was exchanged with shielding gas (nitrogen) beforehand.

The oily protected and iodated pentose was dissolved in an isopropanol-toluene mixture (2:1; 5 g each 100 ml), containing solid NiI_2 (6%; treated with ultrasonic to increase surface) and NaHMDS (2 g each 5 g protected iodated pentose) and 2-aminocyclohexanol (6%). The mixture was heated to 110°C.

p-Tolylboronic acid (2 g each 5 g protected iodated pentose) was dissolved in an isopropanol-toluene mixture (1:1; 10 ml) and added dropwise to the reaction mixture. Thereafter, small amounts of NaHDMS (2 g) were added stepwise.

An excess of NaHMDS caused the formation of *p*-triphenylboroxines, therefore the initial amount of NaHMDS (published: 2 equivalents) was decreased and re-adjusted during the reaction by dropwise addition until formation of *p*-triphenylboroxines (monitored with TLC or GC-MS).

After completion of the chemical reaction, the components were purified with a silica flash chromatography using a hexane-ethyl acetate mixture (1:1). The fraction containing the protected 5-deoxy-5-tolyl-pentose was dried *in vacuo*.

The protection groups were removed using a water:tetrahydrofurane mixture, containing 1 %vol sulfuric acid. The mixture was refluxed for 1 h, thereafter equal volumes of water and ethyl acetate were added. The organic phase was collected and extraction was repeated twice. After evaporation, the residue was dissolved in methanol and separated using HPLC with the previously described separation method.

8.2.3.6.3 Yields and optimizations

The protection and iodation of pentoses worked with nearly quantitative yields.

The conditions of the Suzuki cross-coupling were optimized by using a toluene/isopropanol mixture and reduced initial NaHMDS usage. With the published protocol, the borate condensed and was not available for cross-coupling. NaHMDS as well as the borate were added after heating the reaction mixture to 110°C. The addition was conducted in two equal portions one after the other.

With this optimized protocol, the reaction was finished after 30 min with higher yields from initially 3% up to around 70%.

The cross-coupling worked well for D/L-Ribose with yields around 70%, but with D-Lyxose the yields were only around 25%. This might be due to sterical hindrance of protection groups.

The deprotection process yielded around 90% of pure products.

8.2.4 Results and Discussion

The anaerobic desulfonation of a degradation product of LAS, 3-C_4SPC, was investigated by growing *Clostridium* sp. EV4 under anoxic conditions with 3-C_4SPC as sole source of sulfur. The growth of EV4 under these conditions was already described by Denger and Cook (1996, 1997).[161-162]

8.2.4.1 Characterization of reference substances

3-C_4SPC, TS and 3-phenyl butyrate (Fig. 111) were characterized as references using HPLC-DAD-MS and NMR. Spectra will be discussed in comparison to the degradation products of 3-C_4SPC and TS.

8.2.4.2 Structure elucidation of degradation products of 3-(4'-sulfophenyl) butyrate and *p*-toluene sulfonate

8.2.4.2.1 Purification and determination of chemical structure

After 0 and 36 hours of incubation, small portions of the culture were harvested and centrifuged. In order to study the metabolism of 3-C_4SPC, we subjected the supernatant directly to LC-DAD-MS analysis.

Comparison of culture broth at 0 hours and after 36 hours of growth of EV4 prepared with 3-C_4SPC showed a decreasing peak at 8,4 min (3-C_4SPC; m/z=243) and an increasing peak at 14,8 min in the DAD-Detector at 256 nm and a $[M-H]^-$ ion at m/z 295 in ESI-MS.

For a first screening, one liter of culture medium was extracted with ethyl acetate, following semi-preparative HPLC fractionation. The respective fraction (around 14,8 min) was measured using NMR, the ^{1}H-NMR spectrum of the suspected degradation product of 3-C_4SPC still contained signals of the butyrate side chain and aromatic protons, but additional proton signals were found (Fig. 112, A, desulfonated product of 3-C_4SPC called 3-C_4PDDR). Then, three liters of culture media were purified to generate a sufficient amount of the unknown substance for structure elucidation.

3-C_4PDDR was analyzed by 1D and 2D NMR spectroscopy. The ^{1}H-NMR spectrum and the ^{1}H-^{1}H-COSY verified a 3-substituted butanoic acid moiety and a *para*-substituted benzene ring like in 3-C_4SPC. In addition, at 5,09 and 5,17 ppm, characteristic anomeric proton signals corresponding to a carbohydrate were observed.[170-171] The α and β anomers were present in a ratio 2:1. Proton signals between 3,7 and 4,3 ppm that matched to two datasets in 2:1 ratio of 3 protons attached to a C-OH moiety each. Additionally, a double dataset of proton signals was observed at 2,7-3,0 ppm corresponding to two methylene units not

attached to oxygen. We suspected a 5-deoxy pentose motif to be added to our target structure at carbon number 5 of the pentose.

The deduced core structure of 3-C_4PDDR was confirmed by analysis of the ^{1}H-^{13}C-HSQC$_{ed}$ and ^{1}H-^{13}C-HMBC spectra (see supplementary). In particular, ^{1}H-^{13}C-HMBC showed correlations of the benzene protons 2' and 6' to carbon number 5 of the 5-deoxy pentose moiety and backwards (Fig. 112, B).

It turned out, that the sulfonate moiety was exchanged against a 5-deoxy pentose, coupled at atom number 5 of the deoxy sugar to the aromatic ring, in case of 3-C_4SPC or TS (desulfonated product called TDDR) as sole sulfur source for strain EV4.

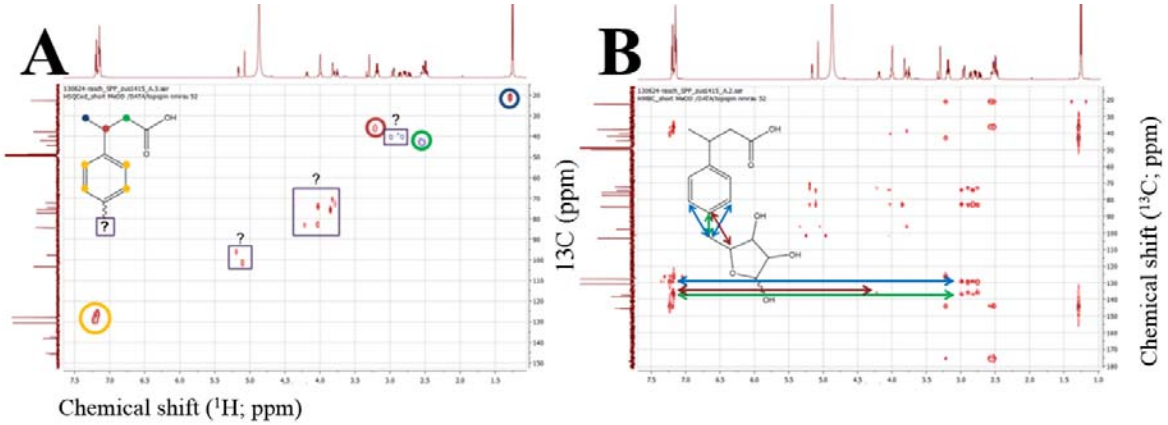

Fig. 112: NMR spectra of 3-C_4PDDR. A: Comparison of ^{1}H-^{13}C-HSQC$_{ed}$ spectra of 3-C_4SPC and 3-C_4PDDR. Unknown signals marked with "?". B: Alignment of unknown ^{1}H-^{13}C-HMBC signals of 3-C_4PDDR to the aromatic ring system. (Bruker, 600 MHz, accumulated scans).

HR-ESI-MS analysis revealed an $[M+NH_4]^+$ ion at m/z 314,16019 corresponding to the molecular formula $C_{15}H_{20}O_6$, containing six double bond equivalents.

Tandem mass spectrometry of the $[M-H]^-$ resulted in the loss of CO_2, which suggests that the carboxylic acid moiety of the butanoic acid side chain is likely present in 3-C_4PDDR. The elimination of two times water and $C_2H_4O_2$ as well as $C_3H_6O_3$ pointed to the addition of a sugar-like moiety ($C_5H_9O_4$) to the phenyl-3-butanoate core (Fig. 113).

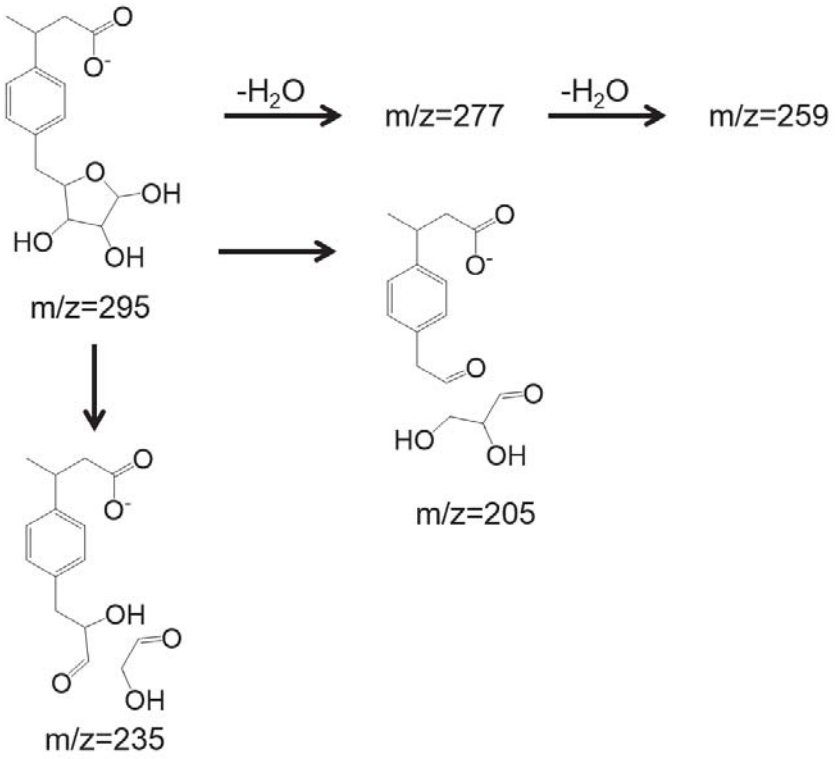

Fig. 113: ESI-MS/MS of the quasimolecular ion $[M-H]^-$ of 3-C_4PDDR with m/z=295 and its suggested fragmentation.

8.2.4.2.2 Assignment of the relative stereochemistry in aldopentose references

There are four aldopentoses to be considered to have the same relative configuration compared to the target structure (Fig. 114). Additionally, there are D/L conformations and mutarotation, which play a role in stereochemical analysis. Mutarotation takes place by formation of intramolecular hemiacetals, resulting in α/β anomers. This is caused by a free exchange of protons with the solvent (at least in D_2O and MeOD) and was already observed in ^{1}H-NMR-spectra of 3-C_4PDDR. The presence of the two signals from the α and β anomer are no factor to select appropriate aldopentoses, but it is important to consider mutarotation during interpretation of NMR spectra.

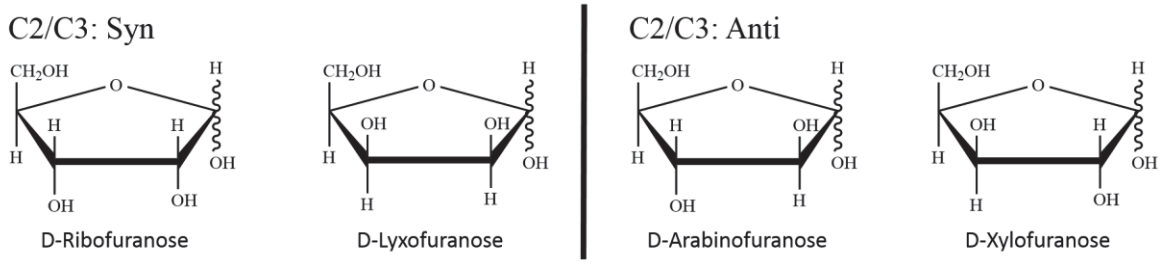

Fig. 114: Haworth projection of relevant D-pentofuranoses, separation for C2/C3 in syn- and anti-orientation. Wave lines indicate the α anomer.

A ^{1}H-^{1}H-NOESY experiment was performed to determine the relative stereochemistry of the chiral centers in position C2 and C3 of the aldopentoses. The ^{1}H-^{1}H-NOESY shows

correlations through-space and provides positional information over small distances, in opposite to through-bond coupling of, for example, ^{1}H-^{1}H-COSY.

Three inexpensive commercially available references were chosen for measurements. 5-deoxy-L-arabinose (Carbosynth, UK), 5-phospho-D-ribose (Sigma Aldrich, Germany) and 5-deoxy-L-ribose (Carbosynth, UK) were characterized as references using NMR spectroscopy, acquiring especially ^{1}H-^{1}H-COSY and ^{1}H-^{1}H-NOESY spectra. Because of their substituents in position C5, they only form furanoses. Therefore, they are more comparable to the structures of interest, because unmodified pentoses form furanoses and pyranoses.

5-Deoxy-L-arabinose was chosen as an example for arabinofuranose and xylofuranose, which have an anti-conformation in C2 and C3. In contrast, ribofuranose and lyxofuranose have a syn-conformation in C2 and C3.

The ^{1}H-^{1}H-COSY and ^{1}H-^{1}H-NOESY were overlaid to differentiate between neighboring protons (both spectra) and correlations through space (only NOESY). This means, when correlations are blue and red, they are due to through-bond couplings. If they are only blue, they are through-space couplings.

It was not possible to distinguish between all proton signals of 5-deoxy-L-ribose. Several signals like C2, C3, C4 of the α state have similar chemical shifts (3,95 ppm). Therefore, the ^{1}H-^{1}H-NOESY resulted only in two helpful correlations, indicating C3-C5 and C5-C1 couplings through space (Fig. 115 A; 1-2).

Proton signals of 5-deoxy-L-arabinose were assigned, at least the estimated C5-C3 through-space correlation was clearly visible (Fig. 115 B; 4). There was no signal for a C5-C2 trough-space correlation, this corresponds to the stereochemical arrangement (Fig. 115 B; 3).

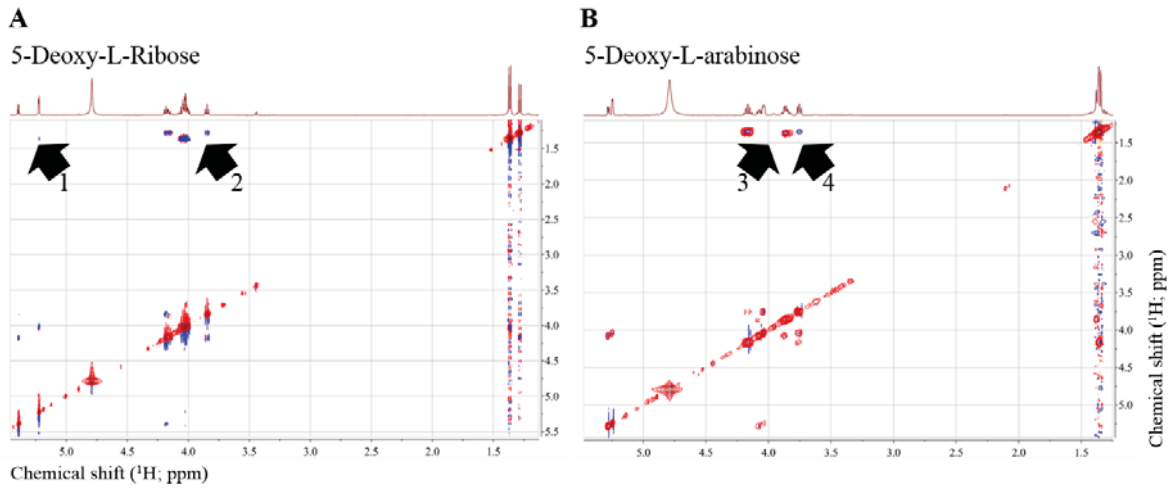

Fig. 115: NMR spectra of 5-deoxy-L-ribose (A) and 5-deoxy-L-arabinose (B). Upside: ^{1}H spectra. Downside: ^{1}H-^{1}H-NOESY-COSY overlay. Arrows indicate discussed signals. 1: C5-C1 correlation; 2: C3-C5 correlation; 3: missing C2-C5 correlation as expected; 4: C3-C5 correlation.

In contrast to 5-deoxy-D-ribose, the ^{1}H-^{1}H-COSY of 5-phospho-D-ribose showed the relation of the protons clearly. The chemical shift of the protons was influenced by the phosphate modification in position C5, whose influence decreased with distance through bonds. The correlations in the ^{1}H-^{1}H-NOESY-COSY overlay will be discussed in more detail.

The proton signals were assigned according to the ^{1}H-^{1}H-COSY pattern (Fig. 117 A). Anomeric protons were assigned using ^{3}J couplings (equivalent to Fig. 118; p. 209).[170]

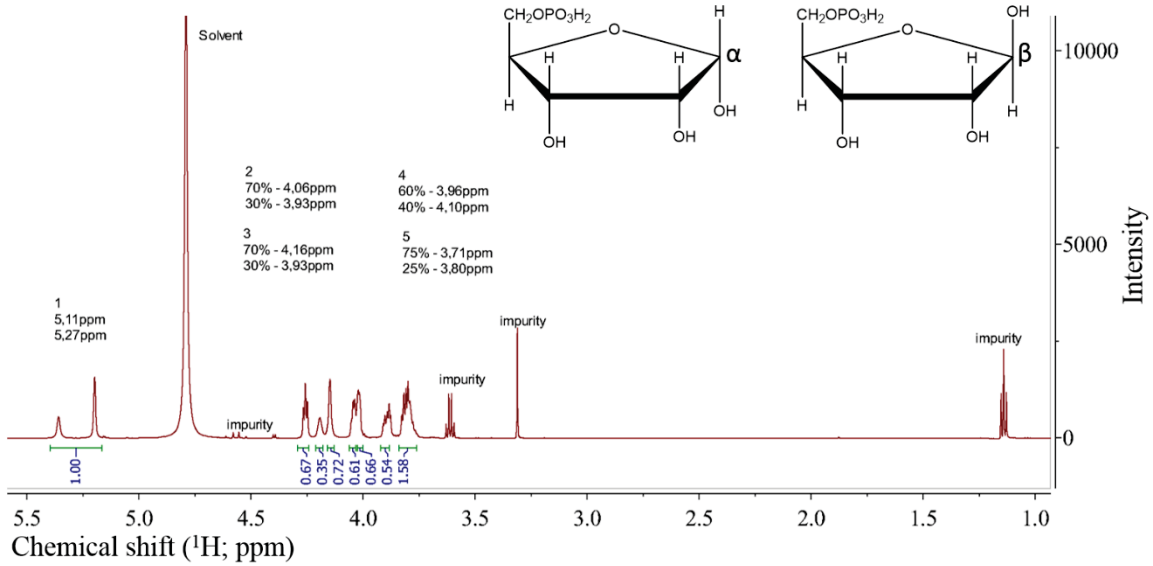

Fig. 116: Proton NMR spectrum of 5-phospho-D-ribose with assignments.

In the ^{1}H-^{1}H-NOESY-COSY overlay, the through-space correlations were assigned considering α/β states.

Indeed, all through-space interactions could be allocated (Fig. 117).

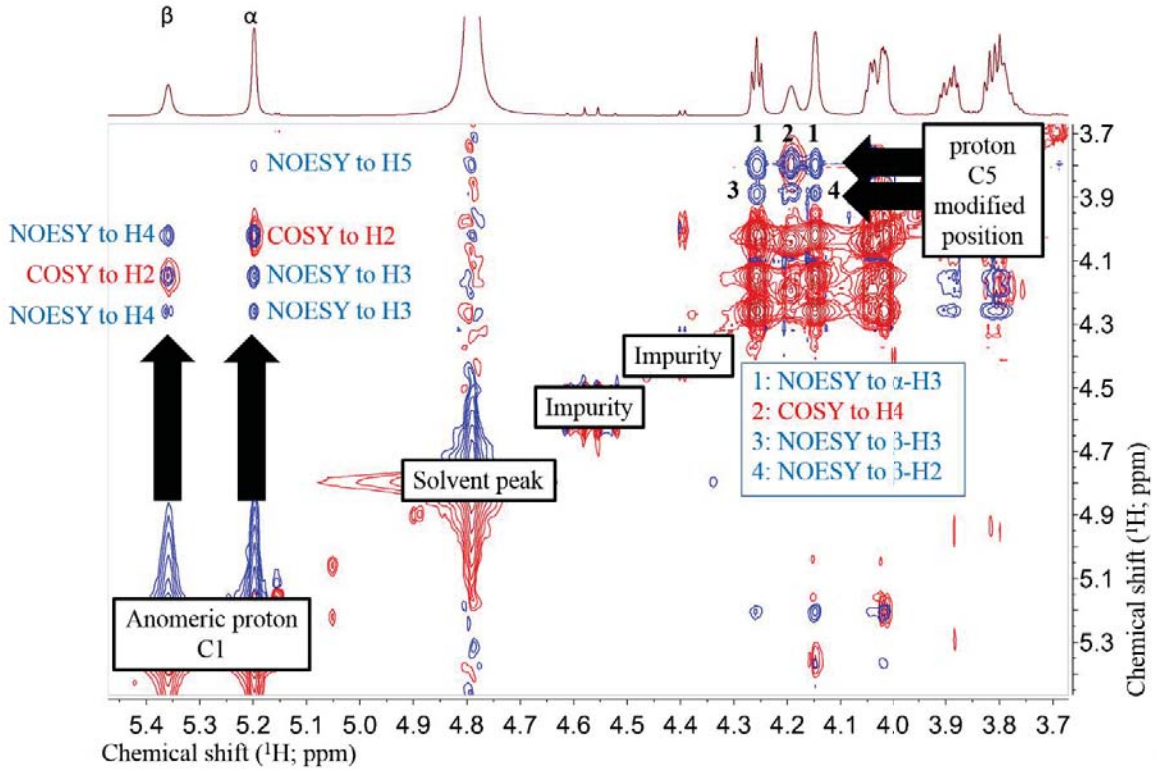

Fig. 117: ^{1}H-^{1}H-NOESY-COSY overlay of 5-phosphate-D-ribofuranose with correlations of protons from C1 and C5 (Bruker, 600MHz, D_2O).

In conclusion, the syn orientation of protons at C2 and C3 of pentofuranoses were distinguished from anti oriented protons. This principle will be applied to the desulfonated product of TS (called TDDR) in a next step.

8.2.4.2.3 Assignment of relative stereochemistry for 5-deoxy-5-tol-4'-yl-D-ribofuranose

For further experiments, TDDR was chosen due to the lack of the side chain compared to 3-C_4PDDR, which would cause confusion due to unessential signals for the determination of the stereochemistry.

Fortunately, the ^{3}J-coupling of the protons allow an unambiguous assignment of the α and β states (Fig. 118).

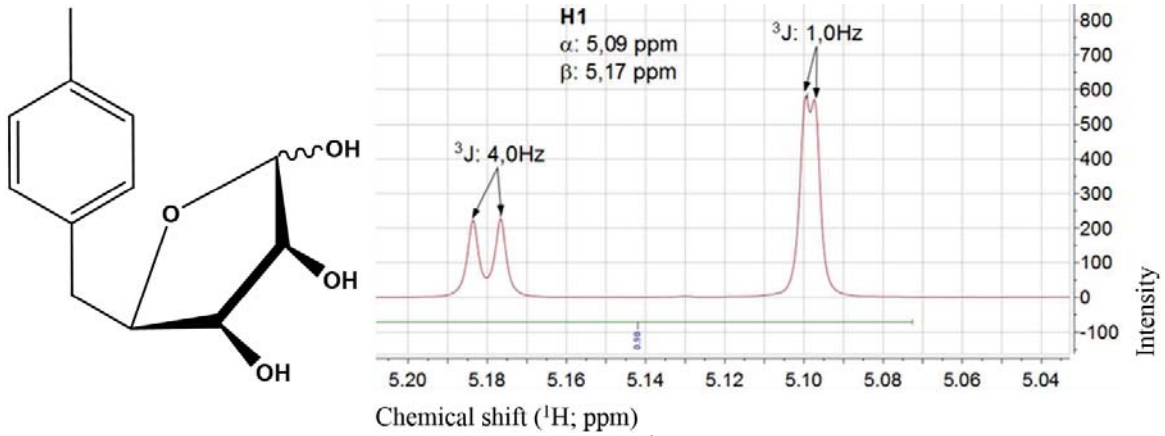

Fig. 118: Detail of anomeric proton signals in a ^{1}H-NMR spectrum of TDDR in order to determine the ratio of its α and β states.

The proton signals were assigned according to the ^{1}H-^{1}H-COSY pattern (Fig. 119). The signals of the proton β-C3 and β-C2 overlapped (3,7 ppm). The signals of α-C3 and α-C4 overlapped as well, this might cause problems in ^{1}H-^{1}H-NOESY assignments later. The other signals have different chemical shifts, which allowed to assign correlations.

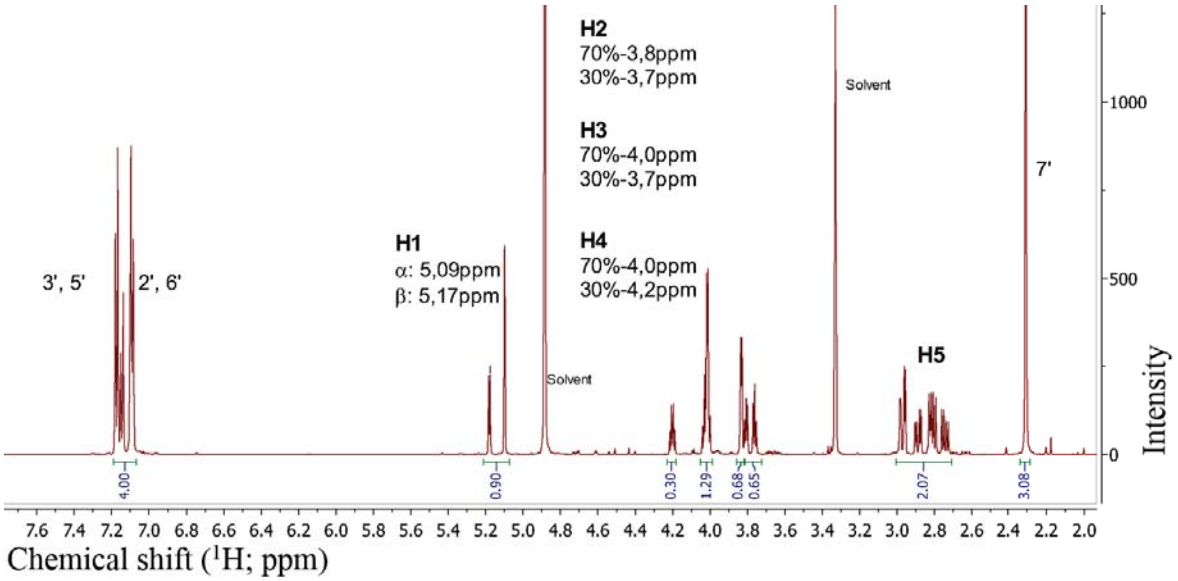

Fig. 119: ^{1}H-NMR spectrum of TDDR with assignments and integrated peaks.

The ^{1}H-^{1}H-COSY and ^{1}H-^{1}H-NOESY were overlaid to differentiate between neighboring protons (both spectra) and correlations through space (only NOESY). All expected correlations were assigned except the correlation through space of α-C3 and α-C5 (Fig. 120). This was due to the overlap with the ^{1}H-^{1}H-COSY signal of proton α-C4 (4,0 ppm).

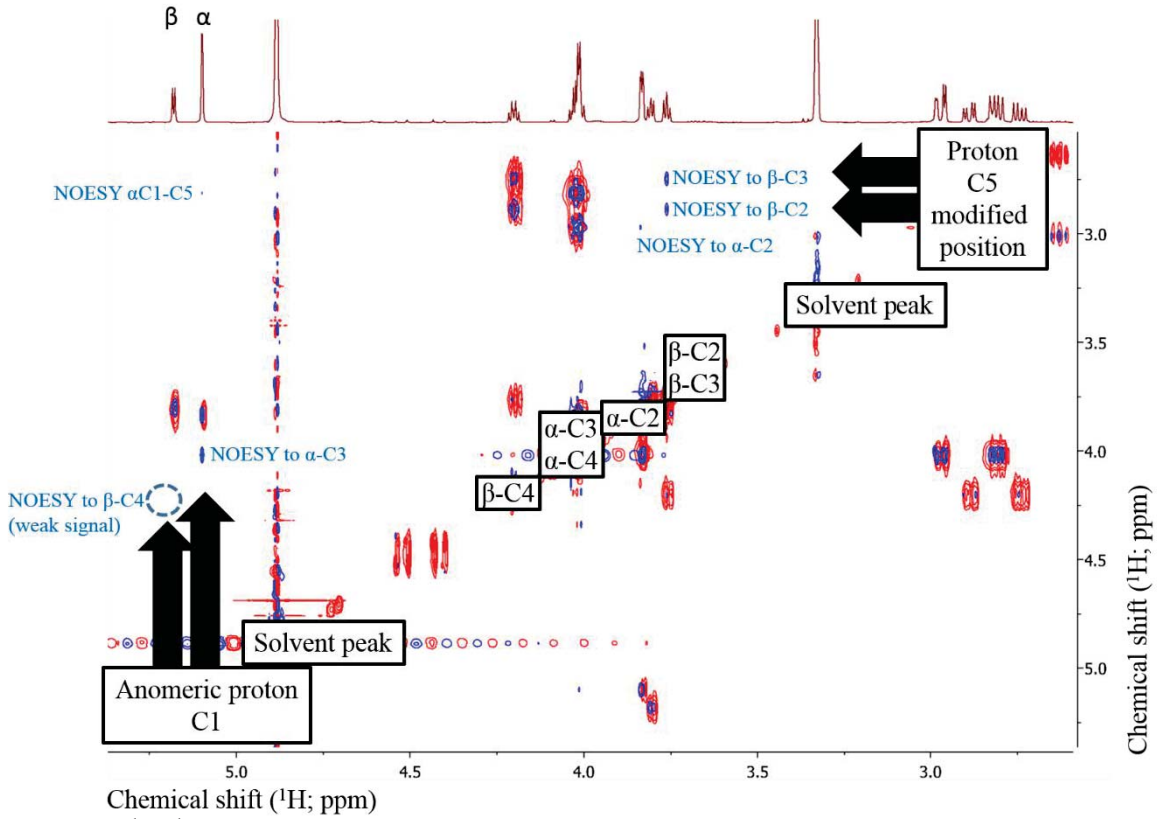

Fig. 120: ^{1}H-^{1}H-NOESY-COSY overlay of TDDR with assignments of important through-space correlations (Bruker, 600 MHz, MeOD).

The observed and expected correlations through space were compiled in three dimensional models for TDDR (Fig. 121). Only one correlation is missing due to an overlapping signal. Nevertheless, these results pointed towards Ribose as target pentose backbone.

To verify these results, synthesized compounds with Ribose and Lyxose backbones will be compared with each other and with the target compound.

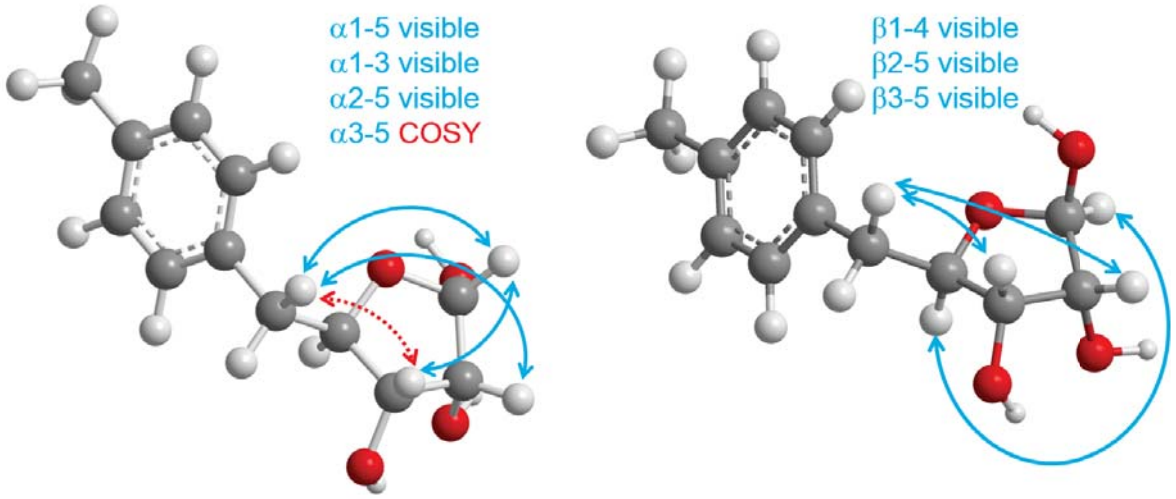

Fig. 121: Transfer of results from ^{1}H-^{1}H-NOESY-COSY overlay of TDDR on three dimensional chemical structures in α and β state.

8.2.4.3 Synthesis of 5-deoxy-5-tolylpentoses

Initial attempts for synthesis were started in 2013 with synthesis routes planned by Prof. Dr. Spiteller and executed by our chemical technician Daniela Starke.

All synthesis routes started with pentoses, as they exhibited the needed differences in stereochemistry. The pentoses needed to be protected at their hydroxyl groups in position C1 to C4, while the position at C5 needed to be an active center for coupling. The active center should be a good leaving group, as the aromatic ring must be activated in a way to form a new C-C-bond.

Unfortunately, all their synthesis routes failed. I want to summarize some of these attempts. Moreover, Daniela and I evaluated some of these failed synthesis efforts retrospectively to understand their difficulties.

As the synthesis of different stereoisomers was one of the key elements, I took over developing another synthesis route. I succeeded with my approach after initial problems were solved. Thereafter, Daniela Starke synthesized three stereoisomers with D/L-ribose and D-lyxose in 2015.

8.2.4.3.1 Unsuccessful synthesis routes

The initial steps of protecting hydroxyl groups of pentoses and activating the C5 position made no obvious problems. For most approaches, the C5 position was halogenated, triflated or tosylated to have good leaving groups (Fig. 122).

The coupling of the protected pentose with an aromatic system was tested at first with phenyl magnesium bromide. Those Grignard reactions resulted in formation of biphenyl, when no, ferrum, nickel or copper catalysts were used. Changes to cuprate reactions with

phenyllithium and copper catalysts resulted in formation of biphenyl compounds, too. Cross-couplings with p-tolylboronic acid and catalysis by copper or palladium/silver ions failed. These conditions were close to the later used successful synthesis route.

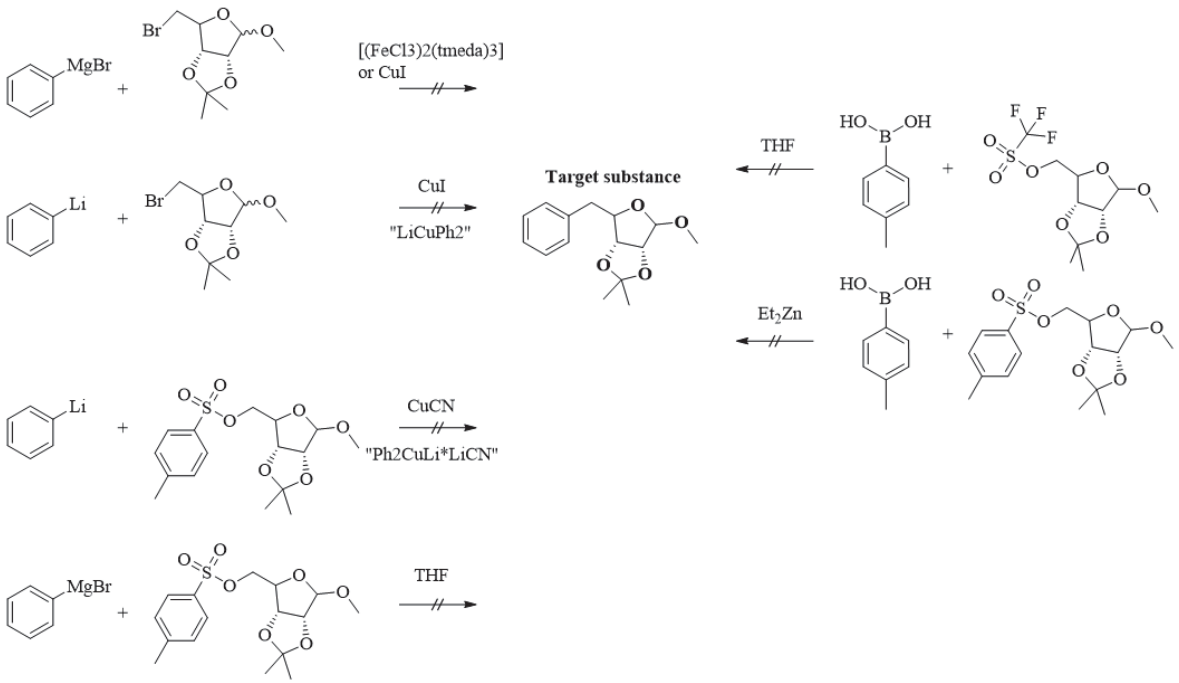

Fig. 122: Examples for tested synthesis routes, such as Grignard, cuprate and Suzuki reactions.

For unsuccessful Suzuki cross-couplings, the used copper or palladium/silver catalysts seemed to cause severe problems. During evaluation, we again observed polymerization of starting material. Furthermore, some instruments were not sufficiently dried and degassed (I prefer common methods like storing glassware overnight in desiccators over silica or using a heat gun with evacuated gas phase).

In conclusion, it remains unclear, whether the reactions would have worked with optimizations.

8.2.4.3.2 Successful synthesis route using Suzuki Cross-coupling

After Prof. Dr. D. Spiteller decided to stop his synthesis approaches, I discussed with synthesis experts from the Marx group after literature search. Indeed, a cheap and uncomplicated synthesis route was developed. Unfortunately, I had to organize some reagents for initial tests by myself.

The initial protection of the pentoses and iodation at the C5 position worked with nearly quantitative yields.[172] After protection and iodation of the pentoses, they were cross-coupled with *p*-tolylboronic acid. The cross-coupling was catalyzed by NiI_2 and 2-aminocyclohexanol. Especially the base NaHMDS caused problems, because *p*-tolylboronic acid polymerized to *p*-triphenyl boroxines. The addition of NaHMDS in portions and *p*-

tolylboronic acid after heating to the reaction temperature (110°C) led to coupling yields of around 70% for D/L-Ribose as starting material.

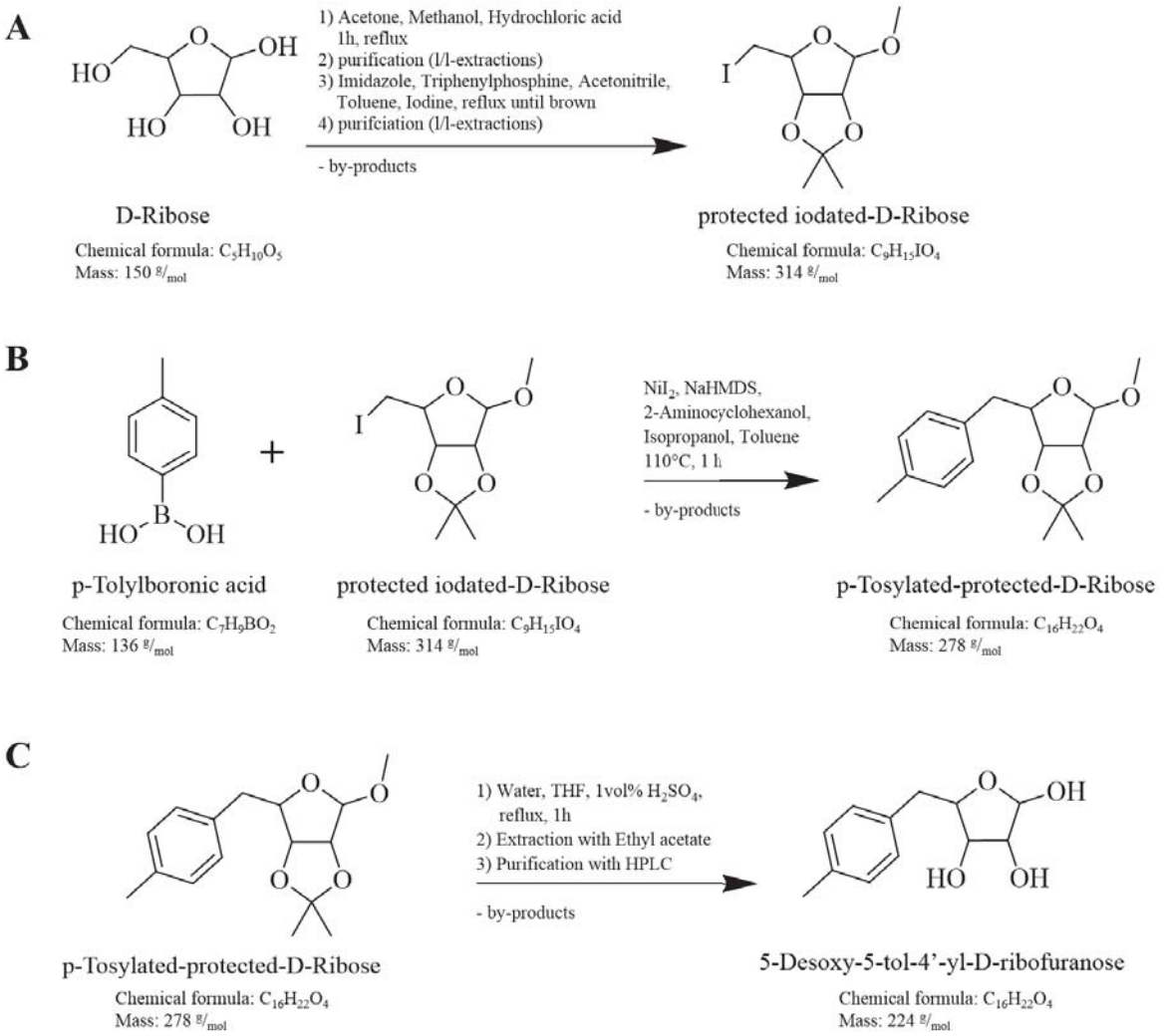

Fig. 123: Established synthesis route to generate 5-(4'-tolyl)-5-deoxy-pentoses. A: Protection and iodination. B: Suzuki cross-coupling. C: Deprotection.

The following synthesis was processed with D-/L-ribose and D-lyxose as examples for relevant pentoses. Yields with D-lyxose were smaller, only around 25%, which might be due to sterical hindrance. The deprotection after coupling was not a critical step and worked with nearly quantitative yields.

The intermediates as well as the reaction products were evaluated by NMR and GC-MS or HR-MS.

8.2.4.4 Comparison of spectra from 5-deoxy-5-tol-4'-yl-D-ribofuranose with synthesis products

To assign the natural product TDDR with synthesized references, MS and NMR spectra were compared.

Indeed, ^{1}H NMR spectra of 5-(4'-tolyl)-5-deoxy-L-ribose and 5-(4'-tolyl)-5-deoxy-D-ribose showed no differences in chemical shifts (Fig. 124 B-C). Compared to 5-(4'-tolyl)-5-deoxy-D-lyxose, there were two obvious differences. The peak ratio of the anomeric proton was turned around (Fig. 124 A1). While all anomeric centers of ribose derivatives showed a 2:1 ratio (5,09 to 5,17 ppm), the lyxose derivate showed a 1:2 ratio. Furthermore, at the chemical shift of Ribose-β-C2 and β-C3 (3,7 ppm), there was no signal in the lyxose spectrum (Fig. 124 A2).

Comparison of ^{1}H-^{1}H-NOESY spectra of the four compounds resulted in equal findings.

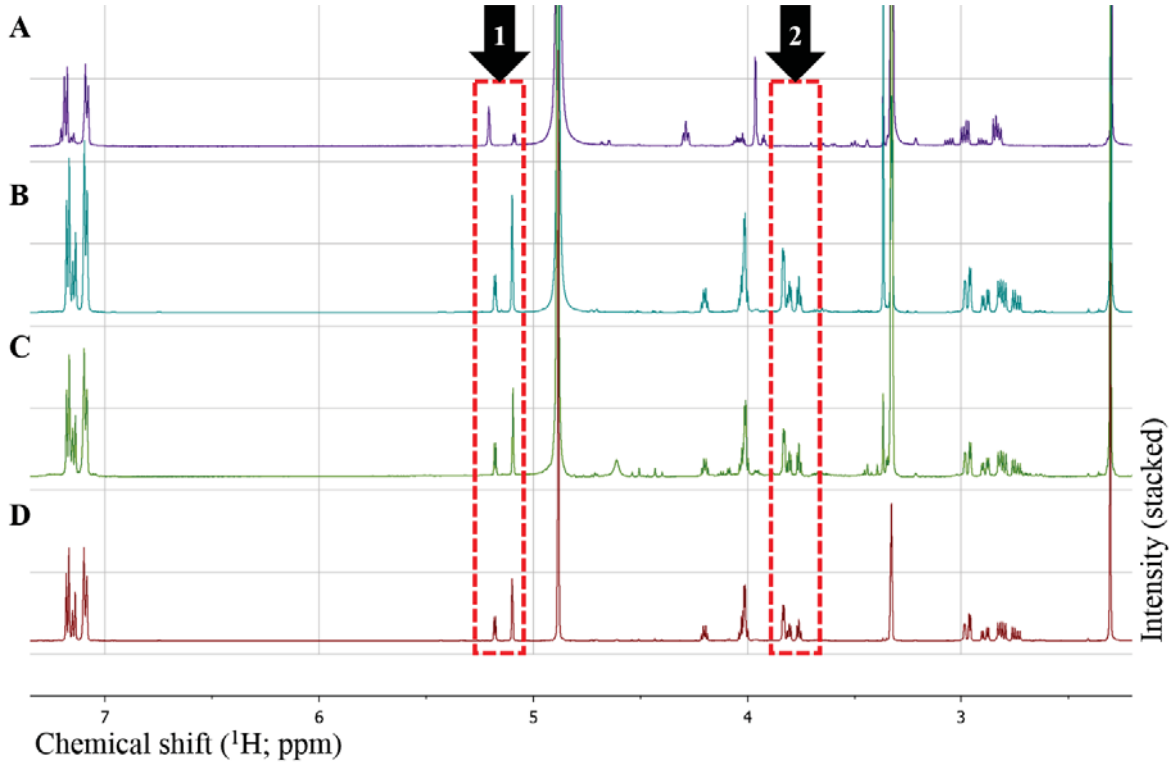

Fig. 124: Comparison of ^{1}H-NMR spectra of the natural product TDDR with synthesized references. Red rectangles indicate main differences. A: 5-(4'-tolyl)-5-deoxy-D-lyxose. B: 5-(4'-tolyl)-5-deoxy-L-ribose. C: 5-(4'-tolyl)-5-deoxy-D-ribose. D: natural product TDDR.

In conclusion, TDDR was shown to be either 5-(4'-tolyl)-5-deoxy-D-ribose or 5-(4'-tolyl)-5-deoxy-L-ribose. The absolute stereochemistry of TDDR cannot be elucidated by NMR without modifications.

I tried to separate the stereoisomers with our available chiral HPLC columns under normal and reverse phase conditions. We did not have a column with appropriate modifications (this was confirmed with measurements from Phenomenex).

Separation of stereoisomers was accomplished by Phenomenex (Aschaffenburg), with their free column screening program. They tested several of their HPLC columns to separate chiral compounds and separated the three synthesized compounds under following conditions:

- Phenomenex Lux Cellulose-3 column (250x4,6mm; 5 µm)
- water:acetonitrile:TFA (80:20:0.1); 1 ml/min

Retention times were reported as follows:

- 5-(4'-tolyl)-5-deoxy-D-lyxose 4,8 min
- 5-(4'-tolyl)-5-deoxy-D-ribose 5,4 min
- 5-(4'-tolyl)-5-deoxy-L-ribose 6,1 min
- ✓ TDDR (natural product) 5,4 min

These results have to be reevaluated after purchasing the column. This was not possible until I left the lab, therefore I present it here as a preliminary result (spectra available upon request).

p-Toluene sulfonate is converted to 5-deoxy-5-tol-4'-yl-D-ribofuranose (TDDR, Fig. 125 B). The structurally related 3-(4'-sulfophenyl)butanoic acid was assumed to be converted following the same degradation pathway to 3-(4'-(5''-deoxy-D-ribofuranos-5''-yl)phenyl)butanoic acid (3-C_4PDDR, Fig. 125 A).

In summary, *Clostridium* sp. EV4 performs a remarkable reaction under anoxic conditions in order to acquire essential sulfur which yields a 5-aryl-5-deoxy-glycoside.

We described the formation of a novel anaerobic degradation intermediate, which may fit into the pathway of LAS degradation in sediments. 3-C_4PDDR may also be present in anaerobic reactors, available for other bacteria to be further metabolized.

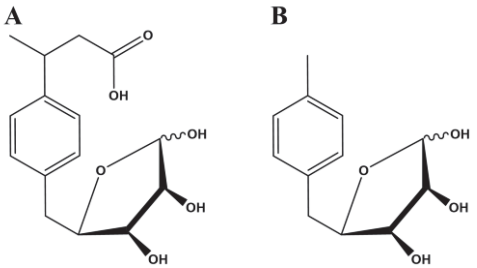

Fig. 125: Chemical structures of 3-(4'-(5''-deoxy-D-ribofuranos-5''-yl)phenyl)butanoic acid (A) and 5-deoxy-5-tol-4'-yl-D-ribofuranose (B).

8.2.4.5 Preliminary results for prospective experiments

The anaerobic degradation of SPC and TS is interesting, but nothing is known about the biochemical pathway. It is not known, which enzymes are involved in the process and whether there are intermediates or further degradation products.

To answer some of these questions, I started to test more sulfonated aromatic compounds similar to 3-C_4-SPC and TS. The choice of bigger chromophores and side chains or functional groups would be helpful for analysis. For example, the carboxylic acid group of 3-C_4-SPC allowed its analysis with LC-MS (LCQ) in negative mode, while TS could not be detected by LC-MS.

Influences of side groups may help to slow down degradation enzymes, catch intermediates or even allow further degradation. I will show some preliminary results; experiments were not continued and most tests were limited to a volume of 50 ml.

Several compounds were tested from the repertoire of Dr. David Schleheck. There were no aromatic sulfonates available which would have fulfilled all recommendations. Compounds such as azophloxin (Fig. 126 A) or acid orange II contained an azo group, which was cleaved during incubation with EV4. Stilbenes, such as 4,4'-dinitrostilbene-2,2'-disulfonic acid (Fig. 126 B; DNS) and 4,4′-diamino-stilbene-2,2′-disulfonic acid (Fig. 126 C; DAS) were stable. They contained two sulfonate groups and the chromophore was not altered during incubation with EV4.

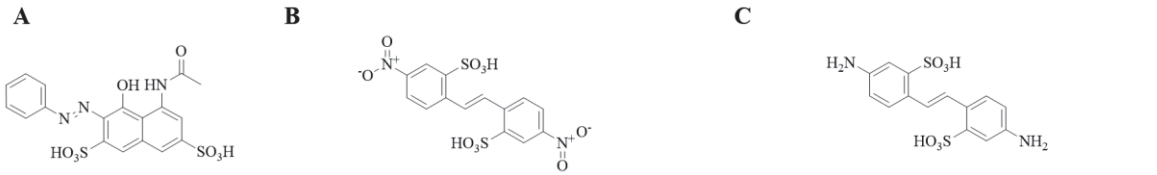

Azophloxin
Acid red 1
CAS: 3734-67-6

4,4'-Dinitrostilbene-2,2'-disulfonic acid
DNS
CAS: 3709-43-1

4,4′-Diamino-stilbene-2,2′-disulfonic acid
DAS
CAS: 81-11-8

Fig. 126: Chemical structures of Acid red I (A), DNS (B) and DAS (C).

The mass spectrometer was tuned with reference substances (starting material such as azophloxin, DNS or DAS). For 3-C_4-SPC, mass detection was possible after tuning the mass spectrometer with 3-phenyl butanoic acid (Fig. 111 structure 5), but not with the starting material itself. The same might be true for these additional reference substances.

For NMR assignment, a bigger amount is needed (at least 1 mg of each compound). I will therefore mainly focus on UV-Vis data.

Azophloxin was visible by eye and UV-Vis in culture supernatants because of its chromophore (Fig. 127 A). After incubation for two days with EV4, several peaks were visible in HPLC-DAD spectra with smaller chromophores (Fig. 127 B). The azo group was

cleaved during incubation and modified the compound in a way that is not relevant for the investigation of desulfonation.

For stilbenes, degradation products were present in HPLC-DAD spectra. Because of the extended chromophore, they could be spotted with UV-Vis (Fig. 127 C; λ_{max} between 300 and 400 nm). In contrast to completely degraded samples of DNS/DAS, one sample was taken which still contained the stilbene core of DNS. The sample was enriched by rotavap (mild conditions; stopping at 5% of initial volume) and injected into HPLC. There were several polar compounds visible (UV-Vis) with a similar chromophore as DNS and its possible degradation product (Fig. 127 D; Arrows: more polar compounds at 7 min; main possible degradation product around 11 min). These more polar compounds were suspected to be intermediates or side products of the anaerobic desulfonation.

There were no noteworthy MS or NMR spectra obtained, therefore, the identity of the compounds remains unknown. This part of the project was not continued.

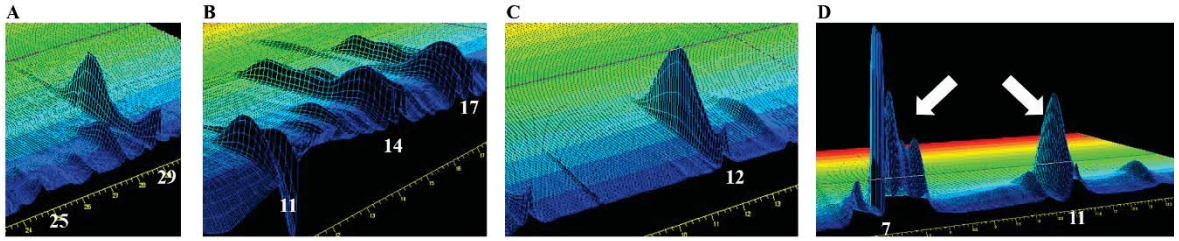

Fig. 127: UV-Vis chromatogram of first screenings after separation with HPLC; three-dimensional DAD screenshots with retention time on x-, wavelength on z- and intensity on y-axis (not indicated). A: Sample with azophloxin before degradation with EV4 (03061444-ex-ev4-t0-azophlox). B: Sample with azophloxin after degradation with EV4 (03061432-ev4-azoph-wass). C: Sample with DNS after degradation with EV4 (07061420-ev4-dns-wass). D: Enriched sample of DNS during degradation with EV4, λ_{max} between 300 and 400 nm (07061405-ev4-dns-rowa).

Another part of the project was prepared by co-workers. They performed enzyme assays *in vitro* and tried to identify degradation proteins by peptide mass fingerprinting. Hereby, proteins were isolated from EV4, grown with sulfate or TS as sole source of sulfur. Comparison of two-dimensional SDS-PAGE gels should have shown differences and promising candidates should have been identified with the help of proteomics.

Unfortunately, protein isolation was performed from outgrown cultures with the statement of maximum concentration for total protein during that time range (Fig. 128 A arrow).

In my opinion, the time point of interest is reached, when most of the TS is degraded. As an example, I correlated the TS concentration with sampling time. For my calculations, I took the growth curves published by Denger *et al.*[161] The TS concentration decreased over time (Fig. 128 B) and I calculated the degrading speeds after certain time points. The degrading

speed increased from 0,2 µM per hour up to 3,2 µM per hour and decreased thereafter (Fig. 128 C). The maximum speed was reached only in a small time frame of about 2,5 hours.

This time frame can be shifted, depending of initial growth rates of EV4 spore cultures (personal communication with Karin Denger). For this example, the optimal time point of cell harvest would have been 20-22,5 hours after inoculation (Fig. 128 D arrow). The protein yield would have been only around 50% compared to outgrown cultures. Nevertheless, the protein(s) of interest is/are present in this time frame in large number, proven by their maximum degradation rate. It is not known, whether the protein(s) is/are present outgrown cultures at all.

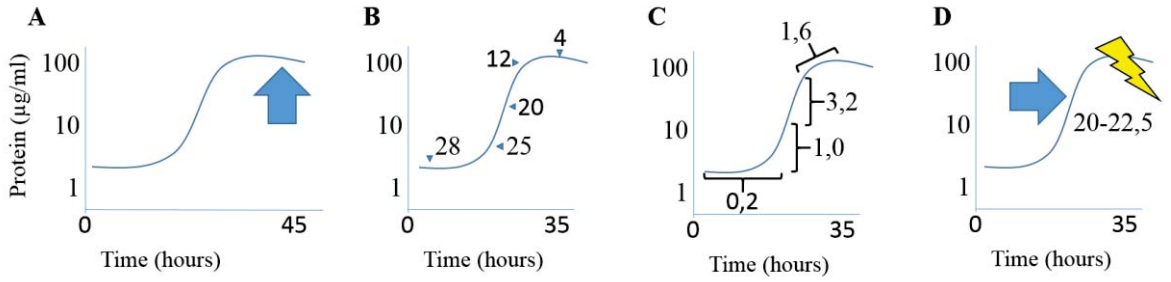

Fig. 128: Estimation for cell harvesting for enzymatic tests. A: Time point with highest protein yield (arrow). B: TS concentration after Denger *et al.*[161] C: Calculated degradation speed in µM per hour. D: Suggested point for cell harvest at maximum slope (arrow). Difference to highest protein yield indicated as thunder.

I would suggest an experimental approach with several modified compounds to generate more information. There is the chance to identify possible intermediates or further degraded products. Even when compounds are not degraded, this delivers information about the degradation process.

The herewith generated data would contribute to enzyme assays. It remains unknown, whether TS is degraded to TDDR in a concerted reaction or if there are intermediates. If TDDR is generated in the fifth step after TS (hypothetical), the process of desulfonation would maybe require completely different shaped compounds for tests *in vitro*. They would be thereafter exchanged in four steps against "5-deoxy-D-ribose", which was the only part of conducted experiments.

ChemicalBiology
University of Konstanz

Universität Konstanz

Anaerobic desulfonation of the commercial surfactant degradation product 3-(4'-sulfophenyl)-butanoic acid by *Clostridium* sp. EV4

Ralf Schlesiger, Karin Denger, Daniela Starke, and Dieter Spiteller
University of Konstanz, Chemical Ecology, Universitätsstraße 10, D-78457 Konstanz, Germany.

Introduction

- Linear alkylbenzene sulfonates (LAS; **1**) are used worldwide as synthetic surfactants.
- LAS are degraded via sulfophenyl carboxylic acids (SPC) as intermediates.[1]
- Anaerobic bacteria degrade LAS/SPC[2] to 3-(4'-sulfophenyl)-butanoic acid (3-C_4SPC; **2**).[3]
- Further breakdown products of 3-C_4SPC (**2**) have not been identified so far.
- Anaerobic bacteria use *p*-toluenesulfonic acid (TS, **3**) as sulfur source in the same way.

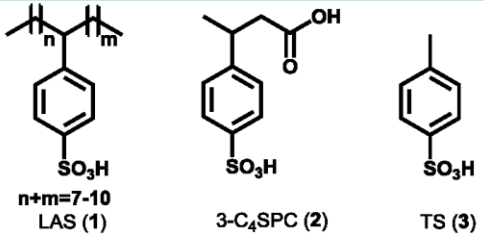

How does *Clostridium* sp. EV4 desulfonate 3-C_4SPC (2) and TS (3)?[4]

Structure elucidation: 3-C_4SPC degradation product

HR-MS $[M+NH_4]^+$ 314,16019 ($C_{15}H_{24}NO_6^+$; Δppm = 1.2)

ESI-MS/MS $[M-H]^-$

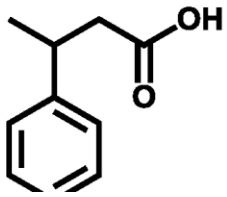

Synthesis: TS degradation product

Protection and Iodination[5]

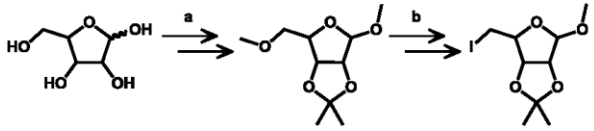

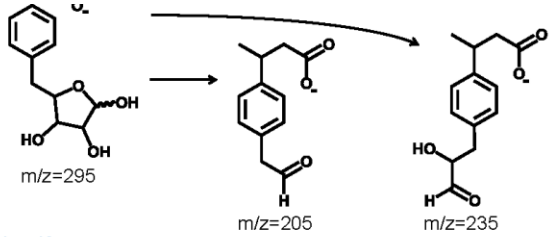

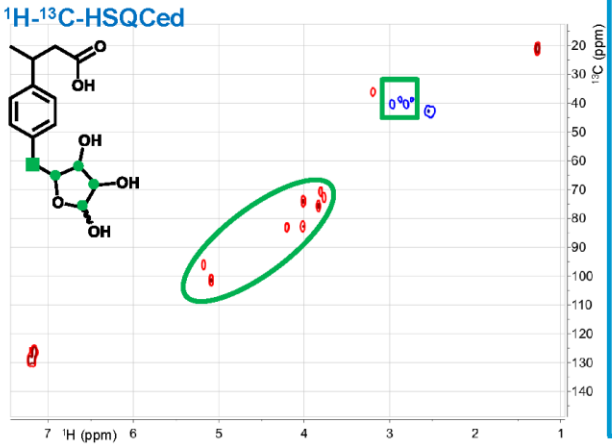

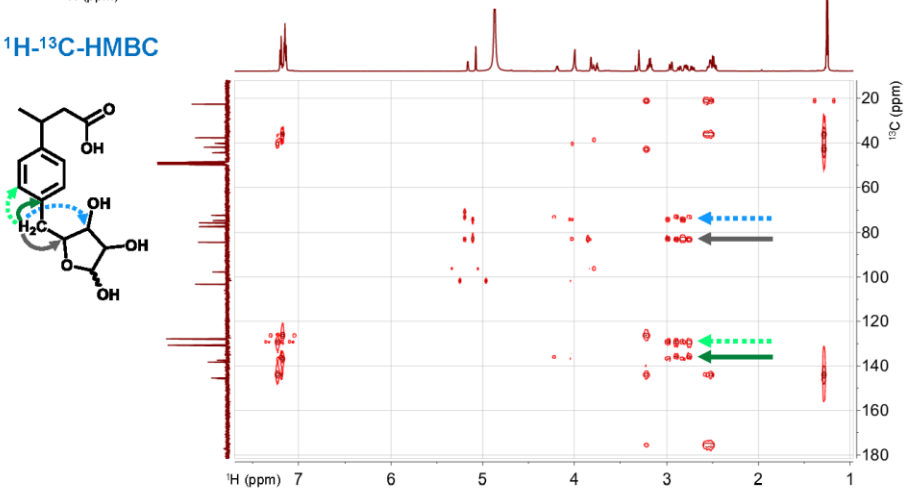

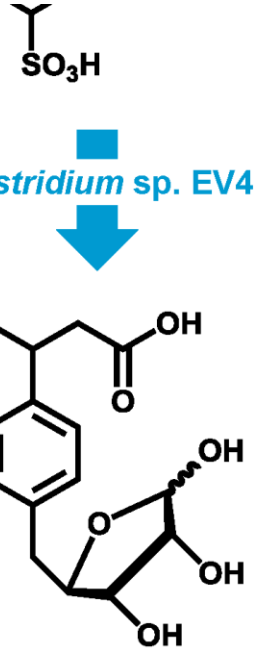

a) Acetone, methanol, HCl; 1h, reflux (yield ≥ 95%)
b) Imidazole, acetonitrile, triphenylphosphine, toluene, iodine (yield ≥ 95%)

Nickel-catalyzed Suzuki Reaction[6]

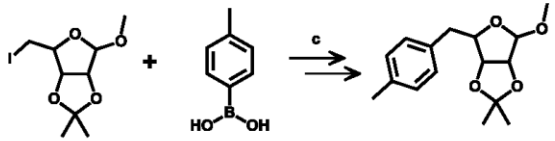

c) NiI_2, NaHMDS, 2-aminocyclohexanol, isopropanol, toluene; 60°C, 6h (yield ≥ 80%)
Caution: Add NaHMDS only until borate polymerizes.

Deprotection

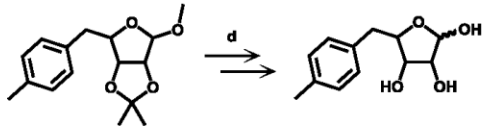

d) Water, 1,4-dioxane, H_2SO_4; reflux, 1h (yield ≥ 95%)

Conclusions/Outlook

- Desulfonation by formation of a unique C-glycoside
- Proof of the stereochemistry of the sugar moiety by synthesis
- Biosynthetic pathway still unknown

References

[1] D. C. McAvoy, *et al. Environmental Toxicology and Chemistry*, **1998**, *17*, 1705-1711.
[2] S. Mogensen, *et al. Environmental Toxicology and Chemistry*, **2003**, *22*, 706-711.
[3] P. A. Lara-Martin, *et al. Environmental Science and Technology*, **2010**, *44*, 1670-1676.
[4] K. Denger, *et al. Applied and Environmental Microbiology*,**1996**, *62*, 1526-1530.
[5] F. González-Bobes and G. C. Fu. *Journal of the American Chem.Society*, **2006**, *128*, 5360–61.
[6] L. A. Paquette and S. Bailey. *Journal of Organic Chemistry*, **1995**, *60*, 7849–7856.

9 References

1. *Mueller, U. G.; Gerardo, N., Fungus-farming insects: Multiple origins and diverse evolutionary histories. Proceedings of the National Academy of Sciences 2002, 99 (24), 15247-15249.*
2. *Schultz, T. R.; Brady, S. G., Major evolutionary transitions in ant agriculture. Proceedings of the National Academy of Sciences of the United States of America 2008, 105 (14), 5435-5440.*
3. *Hart, A. G.; Ratnieks, F. L. W., Waste management in the leaf-cutting ant Atta colombica. Behavioral Ecology* ***2002,*** *13 (2), 224-231.*
4. *Currie, C. R.; Scott, J. A.; Summerbell, R. C.; Malloch, D., Fungus-growing ants use antibiotic-producing bacteria to control garden parasites. Nature* ***1999,*** *398 (6729), 701-704.*
5. *Poulsen, M.; Currie, C. R., Symbiont interactions in a tripartite mutualism: exploring the presence and impact of antagonism between two fungus-growing ant mutualists. PLoS One* ***2010,*** *5 (1), e8748.*
6. *Mueller, U. G., Symbiont recruitment versus ant-symbiont co-evolution in the attine ant-microbe symbiosis. Current opinion in microbiology* ***2012,*** *15 (3), 269-277.*
7. *Cafaro, M. J.; Currie, C. R., Phylogenetic analysis of mutualistic filamentous bacteria associated with fungus-growing ants. Canadian Journal of Microbiology* ***2005,*** *51 (6), 441-446.*
8. *Currie, C. R.; Bot, A. N.; Boomsma, J. J., Experimental evidence of a tripartite mutualism: bacteria protect ant fungus gardens from specialized parasites. Oikos* ***2003,*** *101 (1), 91-102.*
9. *Currie, C. R.; Mueller, U. G.; Malloch, D., The agricultural pathology of ant fungus gardens. Proceedings of the National Academy of Sciences of the United States of America* ***1999,*** *96 (14), 7998-8002.*
10. *Little, A. E. F.; Murakami, T.; Mueller, U. G.; Currie, C. R., Defending against parasites: fungus-growing ants combine specialized behaviours and microbial symbionts to protect their fungus gardens. Biology Letters* ***2006,*** *2 (1), 12-16.*
11. *Seipke, R. F.; Barke, J.; Brearley, C.; Hill, L.; Yu, D. W.; Goss, R. J.; Hutchings, M. I., A single Streptomyces symbiont makes multiple antifungals to support the fungus farming ant Acromyrmex octospinosus. PLoS One* ***2011,*** *6 (8), e22028.*

12. *Schoenian, I.; Spiteller, M.; Ghaste, M.; Wirth, R.; Herz, H.; Spiteller, D., Chemical basis of the synergism and antagonism in microbial communities in the nests of leaf-cutting ants. Proceedings of the National Academy of Sciences* ***2011,*** *108 (5), 1955-1960.*
13. *Adam, G. H.; Francis, L. W. R., Task Partitioning, Division of Labour and Nest Compartmentalisation Collectively Isolate Hazardous Waste in the Leafcutting Ant Atta cephalotes. Behavioral Ecology and Sociobiology* ***2001,*** *49 (5), 387-392.*
14. *Bot, A.; Currie, C.; Hart, A.; Boomsma, J. J., Waste management in leaf-cutting ants. Ethology Ecology & Evolution* ***2001,*** *13 (3), 225-237.*
15. *Farji-Brener, A. G.; Elizalde, L.; Fernández-Marín, H.; Amador-Vargas, S., Social life and sanitary risks: evolutionary and current ecological conditions determine waste management in leaf-cutting ants. Proceedings of the Royal Society B: Biological Sciences* ***2016,*** *283 (1831).*
16. *Hölldobler, B.; Wilson, E. O., The leafcutter ants: civilization by instinct. WW Norton & Company: 2010.*
17. *Weber, N. A., Gardening Ants, the Attines. American Philosophical Society: 1972.*
18. *Rodrigues, A.; Bacci Jr, M.; Mueller, U. G.; Ortiz, A.; Pagnocca, F. C., Microfungal "Weeds" in the Leafcutter Ant Symbiosis. Microbial Ecology* ***2008,*** *56 (4), 604-614.*
19. *Scott, J. J.; Budsberg, K. J.; Suen, G.; Wixon, D. L.; Balser, T. C.; Currie, C. R., Microbial Community Structure of Leaf-Cutter Ant Fungus Gardens and Refuse Dumps. PLOS ONE* ***2010,*** *5 (3), e9922.*
20. *Hart, A. G.; Bot, A.; Brown, M. J., A colony-level response to disease control in a leaf-cutting ant. Naturwissenschaften* ***2002,*** *89 (6), 275-277.*
21. *Poulsen, M.; Bot, A. N.; Nielsen, M. G.; Boomsma, J. J., Experimental evidence for the costs and hygienic significance of the antibiotic metapleural gland secretion in leaf-cutting ants. Behavioral Ecology and Sociobiology* ***2002,*** *52 (2), 151-157.*
22. *Römer, D. Where and how to build? Influence of social and environmental cues on nest building behavior in leaf-cutting ants*

Wo und wie Bauen? Der Einfluss von sozialen und Umwelt-Hinweisen auf das Nestbauverhalten von Blattschneiderameisen. 2014.

23. *Ribeiro, L. P.; Navas, A. C., The Leaf-Cutting ant Atta Sexdens rubropilosa, FOREL, 1908 Prefers Drier Chambers for Garbage Disposal. Journal of Insect Behavior* ***2007,*** *20 (1), 19-24.*
24. *Currie, C. R.; Mueller, U. G.; Malloch, D., The agricultural pathology of ant fungus gardens. Proceedings of the National Academy of Sciences* ***1999,*** *96 (14), 7998-8002.*
25. *Carreiro, S. C.; Pagnocca, F. C.; Bueno, O. C.; Júnior, M. B.; Hebling, M. J. A.; da Silva, O. A., Yeasts associated with nests of the leaf-cutting ant Atta sexdens rubropilosa Forel, 1908. Antonie van Leeuwenhoek* ***1997,*** *71 (3), 243-248.*
26. *Rodrigues, A.; Pagnocca, F.; Bacci, M.; Hebling, M.; Bueno, O.; Pfenning, L., Variability of non-mutualistic filamentous fungi associated withAtta sexdens rubropilosa nests. Folia microbiologica* ***2005,*** *50 (5), 421-425.*
27. *Pinto-Tomás, A. A.; Anderson, M. A.; Suen, G.; Stevenson, D. M.; Chu, F. S. T.; Cleland, W. W.; Weimer, P. J.; Currie, C. R., Symbiotic Nitrogen Fixation in the Fungus Gardens of Leaf-Cutter Ants. Science* ***2009,*** *326 (5956), 1120.*
28. *Baer, B.; Krug, A.; Boomsma, J. J.; Hughes, W. O. H., Examination of the immune responses of males and workers of the leaf-cutting ant Acromyrmex echinatior and the effect of infection. Insectes Sociaux* ***2005,*** *52 (3), 298-303.*
29. *Reber, A.; Purcell, J.; Buechel, S. D.; Buri, P.; Chapuisat, M., The expression and impact of antifungal grooming in ants. J Evolution Biol* ***2011,*** *24 (5), 954-964.*
30. *Santos, A. V.; Dillon, R. J.; Dillon, V. M.; Reynolds, S. E.; Samuels, R. I., Ocurrence of the antibiotic producing bacterium Burkholderia sp. in colonies of the leaf-cutting ant Atta sexdens rubropilosa. FEMS Microbiology Letters* ***2004,*** *239 (2), 319-323.*
31. *Waddington, S. J.; Hughes, W. O., Waste management in the leaf-cutting ant Acromyrmex echinatior: the role of worker size, age and plasticity. Behavioral ecology and sociobiology* ***2010,*** *64 (8), 1219-1228.*

32. *Schoenian, I. Untersuchungen zur Vielfalt und Funktion von Antibiotika im Ökosystem der Blattschneiderameisen. University of Jena, 2011.*
33. *Little, A. E.; Murakami, T.; Mueller, U. G.; Currie, C. R., The infrabuccal pellet piles of fungus-growing ants. Naturwissenschaften* ***2003,*** *90 (12), 558-62.*
34. *Ortius-Lechner, D.; Maile, R.; Morgan, E. D.; Boomsma, J. J., Metapleural gland secretion of the leaf-cutter ant Acromyrmex octospinosus: new compounds and their functional significance. Journal of chemical ecology* ***2000,*** *26 (7), 1667-1683.*
35. *Bot, A.; Ortius-Lechner, D.; Finster, K.; Maile, R.; Boomsma, J. J., Variable sensitivity of fungi and bacteria to compounds produced by the metapleural glands of leaf-cutting ants. Insectes Sociaux* ***2002,*** *49 (4), 363-370.*
36. *Ortius-Lechner, D.; Maile, R.; Morgan, E. D.; Petersen, H. C.; Boomsma, J. J., Lack of patriline-specific differences in chemical composition of the metapleural gland secretion in Acromyrmex octospinosus. Insectes Sociaux* ***2003,*** *50 (2), 113-119.*
37. *Poulsen, M.; Cafaro, M. J.; Erhardt, D. P.; Little, A. E.; Gerardo, N. M.; Tebbets, B.; Klein, B. S.; Currie, C. R., Variation in Pseudonocardia antibiotic defence helps govern parasite-induced morbidity in Acromyrmex leaf-cutting ants. Environmental microbiology reports* ***2010,*** *2 (4), 534-540.*
38. *Wang, Y.; Mueller, U. G.; Clardy, J., Antifungal diketopiperazines from symbiotic fungus of fungus-growing ant Cyphomyrmex minutus. Journal of chemical ecology* ***1999,*** *25 (4), 935-941.*
39. *Poulsen, M.; Bot, A.; Currie, C.; Boomsma, J. J., Mutualistic bacteria and a possible trade-off between alternative defence mechanisms in Acromyrmex leaf-cutting ants. Insectes Sociaux* ***2002,*** *49 (1), 15-19.*
40. *Seipke, R. F.; Barke, J.; Brearley, C.; Hill, L.; Douglas, W. Y.; Goss, R. J.; Hutchings, M. I., A single Streptomyces symbiont makes multiple antifungals to support the fungus farming ant Acromyrmex octospinosus. PLoS One* ***2011,*** *6 (8), e22028.*
41. *Poulsen, M.; Hughes, W. O. H.; Boomsma, J. J., Differential resistance and the importance of antibiotic production in Acromyrmex echinatior leaf-cutting ant castes towards the*

entomopathogenic fungus Aspergillus nomius. Insectes Sociaux ***2006,*** *53 (3), 349-355.*

42. *Zhang, M. M.; Poulsen, M.; Currie, C. R., Symbiont recognition of mutualistic bacteria by Acromyrmex leaf-cutting ants. The ISME journal* ***2007,*** *1 (4), 313-20.*
43. *Patel, A. V.; Rojas-Vera, J.; Dacke, C. G., Therapeutic constituents and actions of Rubus species. Current medicinal chemistry* ***2004,*** *11 (11), 1501-12.*
44. *Ali, L.; Alsanius, B. W.; Rosberg, A. K.; Svensson, B.; Nielsen, T.; Olsson, M. E., Effects of nutrition strategy on the levels of nutrients and bioactive compounds in blackberries. European Food Research and Technology* ***2012,*** *234 (1), 33-44.*
45. *Krisch, J.; Galgóczy, L.; Tölgyesi, M.; Papp, T.; Vágvölgyi, C., Effect of fruit juices and pomace extracts on the growth of Gram-positive and Gram-negative bacteria. Acta Biologica Szegediensis* ***2008,*** *52 (2), 267-270.*
46. *Riaz, M.; Ahmad, M.; Rahman, N., Antimicrobial screening offruit, leaves, root and stem of Rubus fruticosus. Journal of Medicinal Plants Research* ***2011,*** *5 (24), 5920-5924.*
47. *Zia-Ul-Haq, M.; Riaz, M.; De Feo, V.; Jaafar, H. Z.; Moga, M., Rubus fruticosus L.: constituents, biological activities and health related uses. Molecules* ***2014,*** *19 (8), 10998-11029.*
48. *Hölldobler, B.; Wilson, E. O., The ants. Harvard University Press: 1990.*
49. *Fernandez-Marin, H.; Zimmerman, J. K.; Nash, D. R.; Boomsma, J. J.; Wcislo, W. T., Reduced biological control and enhanced chemical pest management in the evolution of fungus farming in ants. P R Soc B* ***2009,*** *276 (1665), 2263-2269.*
50. *Fernández-Marín, H.; Zimmerman, J. K.; Rehner, S. A.; Wcislo, W. T., Active use of the metapleural glands by ants in controlling fungal infection. Proceedings of the Royal Society B: Biological Sciences* ***2006,*** *273 (1594), 1689-1695.*
51. *Do Nascimento, R. R.; Schoeters, E.; Morgan, E. D.; Billen, J.; Stradling, D. J., Chemistry of metapleural gland secretions of three attine ants,Atta sexdens rubropilosa, Atta cephalotes, andAcromyrmex octospinosus (Hymenoptera: Formicidae). Journal of chemical ecology* ***1996,*** *22 (5), 987-1000.*
52. *Fernández-Marín, H.; Nash, D. R.; Higginbotham, S.; Estrada, C.; van Zweden, J. S.; d'Ettorre, P.; Wcislo, W. T.; Boomsma, J.*

J., Functional role of phenylacetic acid from metapleural gland secretions in controlling fungal pathogens in evolutionarily derived leaf-cutting ants. Proceedings of the Royal Society B: Biological Sciences ***2015,*** *282 (1807).*

53. *North, R. D.; Jackson, C. W.; Howse, P. E., Evolutionary aspects of ant-fungus interactions in leaf-cutting ants. Trends Ecol Evol* ***1997,*** *12 (10), 386-389.*
54. *Bot, A.; Obermayer, M.; Hölldobler, B.; Boomsma, J. J., Functional morphology of the metapleural gland in the leaf-cutting ant Acromyrmex octospinosus. Insectes Sociaux* ***2001,*** *48 (1), 63-66.*
55. *Vieira, A. S.; Bueno, O. C.; Camargo-Mathias, M. I., Morphophysiological Differences between the Metapleural Glands of Fungus-Growing and Non–Fungus-Growing Ants (Hymenoptera, Formicidae). PLoS ONE* ***2012,*** *7 (8), e43570.*
56. *Vieira, A. S.; Bueno, O. C.; Camargo-Mathias, M. I., The functional morphology of the metapleural gland of the leaf-cutting ant Atta laevigata (Formicidae: Attini). Micron (Oxford, England : 1993)* ***2010,*** *41 (2), 149-57.*
57. *Borchert, J. Untersuchungen flüchtiger Inhaltsstoffe brasilianischer Blattschneiderameisen der Gattungen Atta und Acromyrmex. University of Hamburg, 1987.*
58. *Welsch, T., W. A. König, Gas Chromatographic Enantiomer Separation with Modified Cyclodextrins. 168 S., 132 Abb., 15 Tab., Hüthig Buch Verlag, Heidelberg 1992. (Chromatographic Methods, Hrsg. W. Bertsch, H. Frank, W. G. Jennings, P. Sandra). Leinen, DM 138,–.ISBN 3-7785-2026-1. Journal für Praktische Chemie/Chemiker-Zeitung* ***1993,*** *335 (5), 486-486.*
59. *Habel, A.; Boland, W., Efficient and flexible synthesis of chiral [gamma]- and [small delta]-lactones. Organic & Biomolecular Chemistry* ***2008,*** *6 (9), 1601-1604.*
60. *Gawley, R. E., Do the Terms "%ee" and "%de" Make Sense as Expressions of Stereoisomer Composition or Stereoselectivity? The Journal of organic chemistry* ***2006,*** *71 (6), 2411-2416.*
61. *Liu, W.-w.; Mu, W.; Zhu, B.-y.; Du, Y.-c.; Liu, F., Antagonistic Activities of Volatiles from Four Strains of Bacillus spp. and Paenibacillus spp. Against Soil-Borne Plant Pathogens. Agricultural Sciences in China* ***2008,*** *7 (9), 1104-1114.*

62. *Kishimoto, N.; Sugihara, S.; Mochida, K. Y. O.; Fujita, T., In Vitro Antifungal and Antiviral Activities of γ-and δ-Lactone Analogs Utilized as Food Flavoring. Biocontrol Science* ***2005,*** *10 (1-2), 31-36.*
63. *Muscedere, M. L.; Berglund, J. L.; Traniello, J. F., Polymorphism and division of labor during foraging cycles in the leaf-cutting ant Acromyrmex octospinosus (Formicidae; Attini). Journal of insect behavior* ***2011,*** *24 (2), 94-105.*
64. *Wetterer, J., The Ecology and Evolution of Worker Size-Distribution in Leaf-Cutting Ants (Hymenoptera: Formicidae. Sociobiology* ***1999,*** *34, 119-144.*
65. *Hughes, W. O. H.; Bot, A. N. M.; Boomsma, J. J., Caste-specific expression of genetic variation in the size of antibiotic-producing glands of leaf-cutting ants. Proceedings of the Royal Society B: Biological Sciences* ***2010,*** *277 (1681), 609.*
66. *Yek, S. H.; Mueller, U. G., The metapleural gland of ants. Biological reviews of the Cambridge Philosophical Society* ***2011,*** *86 (4), 774-91.*
67. *Yek, S. H.; Nash, D. R.; Jensen, A. B.; Boomsma, J. J., Regulation and specificity of antifungal metapleural gland secretion in leaf-cutting ants. Proceedings of the Royal Society B: Biological Sciences* ***2012,*** *279 (1745), 4215-4222.*
68. *Magrans, J. O.; Alonso-Prados, J. L.; García-Baudín, J. M., Importance of considering pesticide stereoisomerism—proposal of a scheme to apply Directive 91/414/EEC framework to pesticide active substances manufactured as isomeric mixtures. Chemosphere* ***2002,*** *49 (5), 461-469.*
69. *Ye, J.; Zhao, M.; Liu, J.; Liu, W., Enantioselectivity in environmental risk assessment of modern chiral pesticides. Environmental Pollution* ***2010,*** *158 (7), 2371-2383.*
70. *Leal, W. S., Chemical Communication in Scarab Beetles: Reciprocal Behavioral Agonist-Antagonist Activities of Chiral Pheromones. Proceedings of the National Academy of Sciences of the United States of America* ***1996,*** *93 (22), 12112-12115.*
71. *Ahern, J. R.; Whitney, K. D., Sesquiterpene lactone stereochemistry influences herbivore resistance and plant fitness in the field. Annals of Botany* ***2014,*** *113 (4), 731-740.*
72. *Tabanca, N.; Demirci, F.; Demirci, B.; Wedge, D. E.; Baser, K. H. C., Composition, enantiomeric distribution, and*

antimicrobial activity of Tanacetum argenteum subsp. flabellifolium essential oil. Journal of Pharmaceutical and Biomedical Analysis ***2007,*** *45 (5), 714-719.*

73. *Motais de Narbonne, M.; van Zweden, J. S.; Bello, J. E.; Wenseleers, T.; Millar, J. G.; d'Ettorre, P., Biological activity of the enantiomers of 3-methylhentriacontane, a queen pheromone of the ant Lasius niger. J Exp Biol* ***2016,*** *219 (Pt 11), 1632-8.*
74. *Szczepanik, M.; Dams, I.; Wawrzeńczyk, C., Feeding Deterrent Activity of Terpenoid Lactones with the p-Menthane System Against the Colorado Potato Beetle (Coleoptera: Chrysomelidae). Environmental Entomology* ***2005,*** *34 (6), 1433-1440.*
75. *Dotterl, S.; Burkhardt, D.; Weissbecker, B.; Jurgens, A.; Schutz, S.; Mosandl, A., Linalool and lilac aldehyde/alcohol in flower scents. Electrophysiological detection of lilac aldehyde stereoisomers by a moth. Journal of chromatography. A* ***2006,*** *1113 (1-2), 231-8.*
76. *Ulland, S.; Ian, E.; Borg-Karlson, A.-K.; Mustaparta, H., Discrimination between Enantiomers of Linalool by Olfactory Receptor Neurons in the Cabbage Moth Mamestra brassicae (L.). Chemical Senses* ***2006,*** *31 (4), 325-334.*
77. *Groot, A. T.; Schöfl, G.; Inglis, O.; Donnerhacke, S.; Classen, A.; Schmalz, A.; Santangelo, R. G.; Emerson, J.; Gould, F.; Schal, C.; Heckel, D. G., Within-population variability in a moth sex pheromone blend: genetic basis and behavioural consequences. Proceedings of the Royal Society of London B: Biological Sciences* ***2014,*** *281 (1779).*
78. *Bekkevold, D.; Frydenberg, J.; Boomsma, J. J., Multiple mating and facultative polygyny in the Panamanian leafcutter ant Acromyrmex echinatior. Behavioral Ecology and Sociobiology* ***1999,*** *46 (2), 103-109.*
79. *Boomsma, J. J.; Fjerdingstad, E. J.; Frydenberg, J., Multiple paternity, relatedness and genetic diversity in Acromyrmex leaf-cutter ants. Proceedings of the Royal Society B: Biological Sciences* ***1999,*** *266 (1416), 249-249.*
80. *Bernreuther, A.; Christoph, N.; Schreier, P., Determination of the enantiomeric composition of γ-lactones in complex natural matrices using multidimensional capillary gas chromatography. Journal of Chromatography A* ***1989,*** *481, 363-367.*

81. *Ruiz del Castillo, M. L.; Gómez Caballero, E.; Blanch, G. P.; Herraiz, M., Enantiomeric composition of filbertone in hazelnuts and hazelnut oils from different geographical origins. Journal of the American Oil Chemists' Society* ***2002,*** *79 (6), 589-592.*
82. *Spanik, I.; Pazitna, A.; Siska, P.; Szolcsanyi, P., The determination of botanical origin of honeys based on enantiomer distribution of chiral volatile organic compounds. Food chemistry* ***2014,*** *158, 497-503.*
83. *Hughes, W. O.; Pagliarini, R.; Madsen, H. B.; Dijkstra, M. B.; Boomsma, J. J., Antimicrobial defense shows an abrupt evolutionary transition in the fungus-growing ants. Evolution* ***2008,*** *62 (5), 1252-7.*
84. *Fernandez-Marin, H.; Zimmerman, J. K.; Nash, D. R.; Boomsma, J. J.; Wcislo, W. T., Reduced biological control and enhanced chemical pest management in the evolution of fungus farming in ants. Proceedings. Biological sciences / The Royal Society* ***2009,*** *276 (1665), 2263-9.*
85. *Mattoso, T. C.; Moreira, D. D. O.; Samuels, R. I., Symbiotic bacteria on the cuticle of the leaf-cutting ant Acromyrmex subterraneus subterraneusprotect workers from attack by entomopathogenic fungi. Biology Letters* ***2012,*** *8 (3), 461-464.*
86. *Poulsen, M.; Bot, A. N. M.; Currie, C. R.; Nielsen, M. G.; Boomsma, J. J., Within-colony transmission and the cost of a mutualistic bacterium in the leaf-cutting ant Acromyrmex octospinosus. Functional Ecology* ***2003,*** *17 (2), 260-269.*
87. *Jaffe, K.; Puche, H., Colony-specific territorial marking with the metapleural gland secretion in the ant Solenopsis geminata (Fabr). Journal of insect physiology* ***1984,*** *30 (4), 265-270.*
88. *van Zweden, J. S.; d'Ettorre, P., Nestmate recognition in social insects and the role of hydrocarbons. Insect hydrocarbons: biology, biochemistry and chemical ecology* ***2010,*** *11, 222-243.*
89. *Akino, T.; Yamamura, K.; Wakamura, S.; Yamaoka, R., Direct behavioral evidence for hydrocarbons as nestmate recognition cues in Formica japonica (Hymenoptera: Formicidae). Applied Entomology and Zoology* ***2004,*** *39 (3), 381-387.*
90. *Hernández, J. V.; Goitía, W.; Osio, A.; Cabrera, A.; Lopez, H.; Sainz, C.; Jaffe, K., Leaf-cutter ant species (Hymenoptera: Atta) differ in the types of cues used to differentiate between self and others. Anim Behav* ***2006,*** *71 (4), 945-952.*

91. *Liang, D.; Silverman, J., "You are what you eat": diet modifies cuticular hydrocarbons and nestmate recognition in the Argentine ant, Linepithema humile. Naturwissenschaften* ***2000,*** *87 (9), 412-416.*
92. *Hernández, J. V.; López, H.; Jaffe, K., Nestmate recognition signals of the leaf-cutting ant Atta laevigata. Journal of Insect Physiology* ***2002,*** *48 (3), 287-295.*
93. *Jutsum, A. R.; Saunders, T. S.; Cherrett, J. M., Intraspecific aggression is the leaf-cutting ant Acromyrmex octospinosus. Anim Behav* ***1979,*** *27, Part 3, 839-844.*
94. *Currie, C. R.; Scott, J. A.; Summerbell, R. C.; Malloch, D., Fungus-growing ants use antibiotic-producing bacteria to control garden parasites. Nature* ***1999,*** *398.*
95. *Currie, C. R.; Poulsen, M.; Mendenhall, J.; Boomsma, J. J.; Billen, J., Coevolved Crypts and Exocrine Glands Support Mutualistic Bacteria in Fungus-Growing Ants. Science* ***2006,*** *311 (5757), 81-83.*
96. *Takano, E., Gamma-butyrolactones: Streptomyces signalling molecules regulating antibiotic production and differentiation. Curr Opin Microbiol* ***2006,*** *9 (3), 287-94.*
97. *Williams, H. E.; Steele, J. C. P.; Clements, M. O.; Keshavarz, T., γ-Heptalactone is an endogenously produced quorum-sensing molecule regulating growth and secondary metabolite production by Aspergillus nidulans. Appl Microbiol Biot* ***2012,*** *96 (3), 773-781.*
98. *Liu, G.; Chater, K. F.; Chandra, G.; Niu, G.; Tan, H., Molecular regulation of antibiotic biosynthesis in Streptomyces. Microbiology and Molecular Biology Reviews* ***2013,*** *77 (1), 112-143.*
99. *Zhu, H.; Sandiford, S. K.; van Wezel, G. P., Triggers and cues that activate antibiotic production by actinomycetes. Journal of Industrial Microbiology & Biotechnology* ***2014,*** *41 (2), 371-386.*
100. *Poulsen, M.; Bot, A. N.; Boomsma, J. J., The effect of metapleural gland secretion on the growth of a mutualistic bacterium on the cuticle of leaf-cutting ants. Naturwissenschaften* ***2003,*** *90 (9), 406-409.*
101. *Kroiss, J.; Kaltenpoth, M.; Schneider, B.; Schwinger, M. G.; Hertweck, C.; Maddula, R. K.; Strohm, E.; Svatos, A., Symbiotic*

Streptomycetes provide antibiotic combination prophylaxis for wasp offspring. Nature chemical biology ***2010,*** *6 (4), 261-3.*

102. *Sun, J.; Kelemen, G. H.; Fernandez-Abalos, J. M.; Bibb, M. J., Green fluorescent protein as a reporter for spatial and temporal gene expression in Streptomyces coelicolor A3(2). Microbiology (Reading, England)* ***1999,*** *145 (Pt 9), 2221-7.*
103. *Yoo, S. K.; Huttenlocher, A., Spatiotemporal photolabeling of neutrophil trafficking during inflammation in live zebrafish. J Leukoc Biol* ***2011,*** *89 (5), 661-7.*
104. *Bibb, M. J.; Janssen, G. R.; Ward, J. M., Cloning and Analysis of the Promoter Region of the Erythromycin Resistance Gene (Erme) of Streptomyces-Erythraeus. Gene* ***1985,*** *38 (1-3), 215-226.*
105. *Lukyanov, K. A.; Chudakov, D. M.; Lukyanov, S.; Verkhusha, V. V., Photoactivatable fluorescent proteins. Nat Rev Mol Cell Biol* ***2005,*** *6 (11), 885-890.*
106. *Gurskaya, N. G.; Verkhusha, V. V.; Shcheglov, A. S.; Staroverov, D. B.; Chepurnykh, T. V.; Fradkov, A. F.; Lukyanov, S.; Lukyanov, K. A., Engineering of a monomeric green-to-red photoactivatable fluorescent protein induced by blue light. Nat Biotech* ***2006,*** *24 (4), 461-465.*
107. *Chudakov, D. M.; Lukyanov, S.; Lukyanov, K. A., Using photoactivatable fluorescent protein Dendra2 to track protein movement. BioTechniques* ***2007,*** *42 (5), 553, 555, 557 passim.*
108. *Bibb, M. J.; White, J.; Ward, J. M.; Janssen, G. R., The mRNA for the 23S rRNA methylase encoded by the ermE gene of Saccharopolyspora erythraea is translated in the absence of a conventional ribosome-binding site. Molecular microbiology* ***1994,*** *14 (3), 533-45.*
109. *Rosay, P.; Kaiser, K.; Armstrong, J. D., A novel approach to Drosophila neurophysiology: the targeted expression of aequorin. In Handbook of Molecular-Genetic Techniques for Brain and Behavior Research, Elsevier: 1999; pp 487-495.*
110. *Shin, S. C.; Kim, S. H.; You, H.; Kim, B.; Kim, A. C.; Lee, K. A.; Yoon, J. H.; Ryu, J. H.; Lee, W. J., Drosophila microbiome modulates host developmental and metabolic homeostasis via insulin signaling. Science* ***2011,*** *334 (6056), 670-4.*

111. *Chaston, J. M.; Dobson, A. J.; Newell, P. D.; Douglas, A. E., Host genetic control of the microbiota mediates Drosophila nutritional phenotype. Appl Environ Microb* ***2015****.*
112. *Huang, J.-H.; Douglas, A. E., Consumption of dietary sugar by gut bacteria determines Drosophila lipid content. Biology letters* ***2015,*** *11 (9), 20150469.*
113. *Becher, P. G.; Flick, G.; Rozpędowska, E.; Schmidt, A.; Hagman, A.; Lebreton, S.; Larsson, M. C.; Hansson, B. S.; Piškur, J.; Witzgall, P.; Bengtsson, M., Yeast, not fruit volatiles mediate Drosophila melanogaster attraction, oviposition and development. Functional Ecology* ***2012,*** *26 (4), 822-828.*
114. *Palanca, L.; Gaskett, A. C.; Günther, C. S.; Newcomb, R. D.; Goddard, M. R., Quantifying Variation in the Ability of Yeasts to Attract <italic>Drosophila melanogaster</italic>. PLoS ONE* ***2013,*** *8 (9), e75332.*
115. *Hoang, D.; Kopp, A.; Chandler, J. A., Interactions between Drosophila and its natural yeast symbionts—Is Saccharomyces cerevisiae a good model for studying the fly-yeast relationship? PeerJ* ***2015,*** *3, e1116.*
116. *Stensmyr, M. C.; Dweck, H. K.; Farhan, A.; Ibba, I.; Strutz, A.; Mukunda, L.; Linz, J.; Grabe, V.; Steck, K.; Lavista-Llanos, S.; Wicher, D.; Sachse, S.; Knaden, M.; Becher, P. G.; Seki, Y.; Hansson, B. S., A conserved dedicated olfactory circuit for detecting harmful microbes in Drosophila. Cell* ***2012,*** *151 (6), 1345-57.*
117. *Ridley, E. V.; Wong, A. C. N.; Westmiller, S.; Douglas, A. E., Impact of the Resident Microbiota on the Nutritional Phenotype of <italic>Drosophila melanogaster</italic>. PLoS ONE* ***2012,*** *7 (5), e36765.*
118. *Venu, I.; Durisko, Z.; Xu, J.; Dukas, R., Social attraction mediated by fruit flies' microbiome. J Exp Biol* ***2014,*** *217 (8), 1346-1352.*
119. *Najarro, M. A.; Sumethasorn, M.; Lamoureux, A.; Turner, T. L., Choosing mates based on the diet of your ancestors: replication of non-genetic assortative mating in Drosophila melanogaster. PeerJ* ***2015,*** *3, e1173.*
120. *Sharon, G.; Segal, D.; Ringo, J. M.; Hefetz, A.; Zilber-Rosenberg, I.; Rosenberg, E., Commensal bacteria play a role in*

mating preference of Drosophila melanogaster. Proceedings of the National Academy of Sciences ***2010,*** *107 (46), 20051-20056.*

121. *Miller, W. J.; Ehrman, L.; Schneider, D., Infectious Speciation Revisited: Impact of Symbiont-Depletion on Female Fitness and Mating Behavior of Drosophila paulistorum. PLoS Pathogens* ***2010,*** *6 (12), e1001214.*
122. *Eden, P. A.; Schmidt, T. M.; Blakemore, R. P.; Pace, N. R., Phylogenetic analysis of Aquaspirillum magnetotacticum using polymerase chain reaction-amplified 16S rRNA-specific DNA. Int J Syst Bacteriol* ***1991,*** *41 (2), 324-5.*
123. *D'Argenio, D. A.; Gallagher, L. A.; Berg, C. A.; Manoil, C., Drosophila as a Model Host forPseudomonas aeruginosa Infection. Journal of bacteriology* ***2001,*** *183 (4), 1466-1471.*
124. *Ng, W., Odourous volatile compounds as mediators in possible interkingdom communication between Bacillus subtilis and flies. PeerJ* ***2015****.*
125. *Schleissner, C.; Olivera, E. R.; Fernandez-Valverde, M.; Luengo, J. M., Aerobic catabolism of phenylacetic acid in Pseudomonas putida U: biochemical characterization of a specific phenylacetic acid transport system and formal demonstration that phenylacetyl-coenzyme A is a catabolic intermediate. Journal of bacteriology* ***1994,*** *176 (24), 7667-76.*
126. *Hwang, B. K.; Lim, S. W.; Kim, B. S.; Lee, J. Y.; Moon, S. S., Isolation and In Vivo and In Vitro Antifungal Activity of Phenylacetic Acid and Sodium Phenylacetate fromStreptomyces humidus. Appl Environ Microb* ***2001,*** *67 (8), 3739-3745.*
127. *Al-Zereini, W.; Schuhmann, I.; Laatsch, H.; Helmke, E.; Anke, H., New Aromatic Nitro Compounds from Salegentibacter sp. T436, an Arctic Sea Ice Bacterium: Taxonomy, Fermentation, Isolation and Biological Activities. J Antibiot* ***2007,*** *60 (5), 301-308.*
128. *Schuhmann, I.; Yao, C. B. F.-F.; Al-Zereini, W.; Anke, H.; Helmke, E.; Laatsch, H., Nitro derivatives from the Arctic ice bacterium Salegentibacter sp. isolate T436[ast]. J Antibiot* ***2009,*** *62 (8), 453-460.*
129. *Mazzetto, F.; Gonella, E.; Crotti, E.; Vacchini, V.; Syrpas, M.; Pontini, M.; Mangelinckx, S.; Daffonchio, D.; Alma, A., Olfactory attraction of Drosophila suzukii by symbiotic acetic acid bacteria. Journal of Pest Science* ***2016,*** *89 (3), 783-792.*

130. *Ames, J. M.; Elmore, J. S., Aroma components of yeast extracts. Flavour Frag J* ***1992,*** *7 (2), 89-103.*
131. *Lin, M.; Liu, X.; Xu, Q.; Song, H.; Li, P.; Yao, J., Aroma-active components of yeast extract pastes with a basic and characteristic meaty flavour. Journal of the science of food and agriculture* ***2014,*** *94 (5), 882-9.*
132. *Montague, S. A.; Mathew, D.; Carlson, J. R., Similar odorants elicit different behavioral and physiological responses, some supersustained. The Journal of Neuroscience* ***2011,*** *31 (21), 7891-7899.*
133. *De Frutos, M.; Sanz, J.; Martinez-Castro, I., Simultaneous distillation-extraction (SDE) method in the qualitative and quantitative GC analysis of cheese volatile components. Chromatographia* ***1988,*** *25 (10), 861-864.*
134. *Chaintreau, A., Simultaneous distillation–extraction: from birth to maturity—review. Flavour Frag J* ***2001,*** *16 (2), 136-148.*
135. *Lin, P.-C., COMPARISON OF SIMULTANEOUS DISTILLATION AND EXTRACTION (SDE) AND HEADSPACE SOLID PHASE MICROEXTRACTION (SPME) FOR DETERMINATION OF VOLATILES OF MUSCADINE GRAPES (Vitis rotundifolia). All Theses* ***2014,*** *Paper 1947.*
136. *Zuo, H. L.; Yang, F. Q.; Huang, W. H.; Xia, Z. N., Preparative gas chromatography and its applications. Journal of chromatographic science* ***2013,*** *51 (7), 704-15.*
137. *Pieke, E.; Heus, F.; Kamstra, J. H.; Mladic, M.; van Velzen, M.; Kamminga, D.; Lamoree, M. H.; Hamers, T.; Leonards, P.; Niessen, W. M.; Kool, J., High-resolution fractionation after gas chromatography for effect-directed analysis. Analytical chemistry* ***2013,*** *85 (17), 8204-11.*
138. *Kerr, J. R., Bacterial inhibition of fungal growth and pathogenicity. Microbial ecology in health and disease* ***1999,*** *11 (3), 129-142.*
139. *Bakken, L. R., Separation and Purification of Bacteria from Soil. Appl Environ Microb* ***1985,*** *49 (6), 1482-1487.*
140. *Williams, S. T.; Locci, R.; Beswick, A.; Kurtboke, D. I.; Kuznetsov, V. D.; Le Monnier, F. J.; Long, P. F.; Maycroft, K. A.; Palma, R. A.; Petrolini, B.; et al., Detection and identification of novel actinomycetes. Res Microbiol* ***1993,*** *144 (8), 653-6.*

141. *Lindahl, V.; Bakken, L. R., Evaluation of methods for extraction of bacteria from soil. FEMS Microbiology Ecology* ***1995,*** *16 (2), 135-142.*
142. *Stewart, E. J., Growing Unculturable Bacteria. Journal of bacteriology* ***2012,*** *194 (16), 4151-4160.*
143. *Kieser, T.; Foundation, J. I., Practical Streptomyces Genetics. John Innes Foundation: 2010.*
144. *Chesters, C.; Rolinson, G., Trace elements and streptomycin production. Microbiology (Reading, England)* ***1951,*** *5 (3), 559-565.*
145. *Murphy, T.; Roy, I.; Harrop, A.; Dixon, K.; Keshavarz, T., Effect of oligosaccharide elicitors on bacitracin A production and evidence of transcriptional level control. Journal of biotechnology* ***2007,*** *131 (4), 397-403.*
146. *Lincke, T.; Behnken, S.; Ishida, K.; Roth, M.; Hertweck, C., Closthioamide: an unprecedented polythioamide antibiotic from the strictly anaerobic bacterium Clostridium cellulolyticum. Angewandte Chemie (International ed. in English)* ***2010,*** *49 (11), 2011-3.*
147. *Nair, R.; Murphy, T.; Roy, I.; Keshavarz, T., Optimization studies on multiple elicitor addition in microbial systems: P. chrysogenum and B. Licheniformis. Chem Eng Trans* ***2008****.*
148. *Waters, C. M.; Bassler, B. L., QUORUM SENSING: Cell-to-Cell Communication in Bacteria. Annual Review of Cell and Developmental Biology* ***2005,*** *21 (1), 319-346.*
149. *Lim, F. Y.; Sanchez, J. F.; Wang, C. C. C.; Keller, N. P., Toward Awakening Cryptic Secondary Metabolite Gene Clusters in Filamentous Fungi. Methods in enzymology* ***2012,*** *517, 303-324.*
150. *Thomas, A., Analysis and assay of polyene antifungal antibiotics. A review. Analyst* ***1976,*** *101 (1202), 321-340.*
151. *Waksman, S. A.; Lechevalier, H. A.; Schaffner, C. P., Candicidin and other polyenic antifungal antibiotics: A review. Bulletin of the World Health Organization* ***1965,*** *33 (2), 219.*
152. *Leisinger, T.; Margraff, R., Secondary metabolites of the fluorescent pseudomonads. Microbiological Reviews* ***1979,*** *43 (3), 422.*
153. *Jensen, P. R.; Fenical, W., Strategies for the discovery of secondary metabolites from marine bacteria: ecological*

perspectives. Annual Reviews in Microbiology ***1994,*** *48 (1), 559-584.*

154. *Jůzlová, P.; Martínková, L.; Křen, V., Secondary metabolites of the fungusMonascus: A review. Journal of Industrial Microbiology* ***1996,*** *16 (3), 163-170.*

155. *Cheng, K. W.; Wong, C. C.; Wang, M.; He, Q. Y.; Chen, F., Identification and characterization of molecular targets of natural products by mass spectrometry. Mass spectrometry reviews* ***2010,*** *29 (1), 126-55.*

156. *Vaidyanathan, S.; Kell, D. B.; Goodacre, R., Selective Detection of Proteins in Mixtures Using Electrospray Ionization Mass Spectrometry: Influence of Instrumental Settings and Implications for Proteomics. Analytical chemistry* ***2004,*** *76 (17), 5024-5032.*

157. *Amad, M. H.; Cech, N. B.; Jackson, G. S.; Enke, C. G., Importance of gas-phase proton affinities in determining the electrospray ionization response for analytes and solvents. Journal of mass spectrometry : JMS* ***2000,*** *35 (7), 784-9.*

158. *Garcia, M. T.; Campos, E.; Ribosa, I.; Latorre, A.; Sanchez-Leal, J., Anaerobic digestion of linear alkyl benzene sulfonates: biodegradation kinetics and metabolite analysis. Chemosphere* ***2005,*** *60 (11), 1636-43.*

159. *Federle, T. W.; Schwab, B. S., Mineralization of Surfactants by Microbiota of Aquatic Plants. Appl Environ Microbiol* ***1989,*** *55 (8), 2092-2094.*

160. *Rooney-Varga, J. N.; Anderson, R. T.; Fraga, J. L.; Ringelberg, D.; Lovley, D. R., Microbial communities associated with anaerobic benzene degradation in a petroleum-contaminated aquifer. Appl Environ Microbiol* ***1999,*** *65 (7), 3056-63.*

161. *Denger, K.; Kertesz, M. A.; Vock, E. H.; Schon, R.; Magli, A.; Cook, A. M., Anaerobic Desulfonation of 4-Tolylsulfonate and 2-(4-Sulfophenyl) Butyrate by a Clostridium sp. Appl Environ Microbiol* ***1996,*** *62 (5), 1526-30.*

162. *Denger, K.; Cook, A. M., Assimilation of sulfur from alkyl- and arylsulfonates by Clostridium spp. Archives of microbiology* ***1997,*** *167 (2-3), 177-81.*

163. *Chien, C. C., Arylsulfonates as sole source of sulfur for Clostridium pasteurianum DSM 12136. J Basic Microbiol* ***2005,*** *45 (4), 274-8.*

164. *Mogensen, A. S.; Haagensen, F.; Ahring, B. K., Anaerobic degradation of linear alkylbenzene sulfonate. Environmental toxicology and chemistry / SETAC* ***2003,*** *22 (4), 706-11.*
165. *de Oliveira, L. L.; Costa, R. B.; Okada, D. Y.; Vich, D. V.; Duarte, I. C.; Silva, E. L.; Varesche, M. B., Anaerobic degradation of linear alkylbenzene sulfonate (LAS) in fluidized bed reactor by microbial consortia in different support materials. Bioresource technology* ***2010,*** *101 (14), 5112-22.*
166. *Lara-Martin, P. A.; Gomez-Parra, A.; Kochling, T. K.; Sanz, J. L.; Amils, R.; Gonzalez-Mazo, E., Anaerobic degradation of linear alkylbenzene sulfonates in coastal marine sediments. Environmental science & technology* ***2007,*** *41 (10), 3573-9.*
167. *McAvoy, D. C.; Dyer, S. D.; Fendinger, N. J.; Eckhoff, W. S.; Lawrence, D. L.; Begley, W. M., Removal of alcohol ethoxylates, alkyl ethoxylate sulfates, and linear alkylbenzene sulfonates in wastewater treatment. Environmental Toxicology and Chemistry* ***1998,*** *17 (9), 1705-1711.*
168. *Lara-Martin, P. A.; Gomez-Parra, A.; Sanz, J. L.; Gonzalez-Mazo, E., Anaerobic degradation pathway of linear Alkylbenzene sulfonates (LAS) in sulfate-reducing marine sediments. Environmental science & technology* ***2010,*** *44 (5), 1670-6.*
169. *González-Bobes, F.; Fu, G. C., Amino Alcohols as Ligands for Nickel-Catalyzed Suzuki Reactions of Unactivated Alkyl Halides, Including Secondary Alkyl Chlorides, with Arylboronic Acids. Journal of the American Chemical Society* ***2006,*** *128 (16), 5360-5361.*
170. *Bubb, W. A., NMR spectroscopy in the study of carbohydrates: Characterizing the structural complexity. Concepts in Magnetic Resonance Part A* ***2003,*** *19 (1), 1-19.*
171. *Chu, C. K.; El-kabbani, F. M.; Thompson, B. B., Determination of the Anomeric Configuration of C-Nucleosides by 1H and 13C NMR Spectroscopy. Nucleosides and Nucleotides* ***1984,*** *3 (1), 1-31.*
172. *Paquette, L. A.; Bailey, S., Evaluation of D-Ribose as an Enantiopure Building Block for Construction of the C-Ring of Taxol and Its Congeners. The Journal of Organic Chemistry* ***1995,*** *60 (24), 7849-7856.*

10 List of figures

11 List of tables

12 Annexes

Supplementary material for Ch. 5.2 Waste management of leaf-cutting ants

5.2.1 Ant behavior assists complete decomposition in waste chambers of *Atta vollenweideri*, *Atta laevigata* and *Acromyrmex lundii*

Example videos are available on DVD

6.1 Interactions of *Drosophila hydei* and *Pseudomonas* sp. D2p

Video file on Disk:

- Fruit-fly-video.mp4
    - Makro view of fruit flies on tooth sticks
    - Real-time tracking using MATLAB scripts

16*S* rDNA sequence of *Pseudomonas* sp. D2p

```
d2p-zusammen.str from 1 to 867
Alignment to
1492r-t5-modlang.str--  Matches:499; Mismatches:0; Gaps:368; Unattempted:0
8f-d2p-tii1_premix.ab1 basecalls--  Matches:520; Mismatches:0; Gaps:347; Unattempted:0

                *         *         *         *         *         *         *         *         *         *
  1>TGGGGAATATTGGACAATGGGCGCACGCCTGATCCAGCCATACCGCGTGGGTGAAGAAGGCCTTCGGGTTGTAAAGCCCTTTTGTTGGGAAAGAAATCCA>100
500<~~~~~~~~~~~~~~~~~~~~~~~~~~~~~~~~~~~~~~~~~~~~~~~~~~~~~~~~~~~~~~~~~~~~~~~~~~~~~~~~~~~~~~~~~~~~~~~~~~~<500
  1>TGGGGAATATTGGACAATGGGCGCACGCCTGATCCAGCCATACCGCGTGGGTGAAGAAGGCCTTCGGGTTGTAAAGCCCTTTTGTTGGGAAAGAAATCCA>100

                *         *         *         *         *         *         *         *         *         *
101>GCTGGTTAATACCCGGTTGGGATGACGGTACCCAAAGAATAAGCACCGGCTAACTTCGTGCCAGCAGCCGCGGTAATACGAAGGGTGCAAGCGTTACTCG>200
500<~~~~~~~~~~~~~~~~~~~~~~~~~~~~~~~~~~~~~~~~~~~~~~~~~~~~~~~~~~~~~~~~~~~~~~~~~~~~~~~~~~~~~~~~~~~~~~~~~~~<500
101>GCTGGTTAATACCCGGTTGGGATGACGGTACCCAAAGAATAAGCACCGGCTAACTTCGTGCCAGCAGCCGCGGTAATACGAAGGGTGCAAGCGTTACTCG>200

                *         *         *         *         *         *         *         *         *         *
201>GAATTACTGGGCGTAAAGCGTGCGTAGGTGGTCGTTTAAGTCCGTTGTGAAAGCCCTGGGCTCAACCTGGGAACTGCAGTGGATACTGGGCGACTAGAAT>300
500<~~~~~~~~~~~~~~~~~~~~~~~~~~~~~~~~~~~~~~~~~~~~~~~~~~~~~~~~~~~~~~~~~~~~~~~~~~~~~~~~~~~~~~~~~~~~~~~~~~~<500
201>GAATTACTGGGCGTAAAGCGTGCGTAGGTGGTCGTTTAAGTCCGTTGTGAAAGCCCTGGGCTCAACCTGGGAACTGCAGTGGATACTGGGCGACTAGAAT>300

                *         *         *         *         *         *         *         *         *         *
301>GTGGTAGAGGGTAGCGGAATTCCTGGTGTAGCAGTGAAATGCGTAGAGATCAGGAGGAACATCCATGGCGAAGGCAGCTACCTGGACCAACATTGACACT>400
499<~~~~~~~~~~~~~~~~~~~~~~~~~~~~~~~~~~~~~~~~~~~~~~~~~~~~~~~~~~~~~~~~~~~~~~~~~~~~~~~~~~~~~~~~~~~~~~~~~~~CGAAGGCAGCTACCTGGACCAACATTGACACT<468
301>GTGGTAGAGGGTAGCGGAATTCCTGGTGTAGCAGTGAAATGCGTAGAGATCAGGAGGAACATCCATGGCGAAGGCAGCTACCTGGACCAACATTGACACT>400

                *         *         *         *         *         *         *         *         *         *
401>GAGGCACGAAAGCGTGGGGAGCAAACAGGATTAGATACCCTGGTAGTCCACGCCCTAAACGATGCGAACTGGATGTTGGGTGCAATTTGGCACGCAGTAT>500
467<GAGGCACGAAAGCGTGGGGAGCAAACAGGATTAGATACCCTGGTAGTCCACGCCCTAAACGATGCGAACTGGATGTTGGGTGCAATTTGGCACGCAGTAT<368
401>GAGGCACGAAAGCGTGGGGAGCAAACAGGATTAGATACCCTGGTAGTCCACGCCCTAAACGATGCGAACTGGATGTTGGGTGCAATTTGGCACGCAGTAT>500

                *         *         *         *         *         *         *         *         *         *
501>CGAAGCTAACGCGTTAAGTTCGCCGCCTGGGGAGTACGGTCGCAAGACTGAAACTCAAAGGAATTGACGGGGGCCCGCACAAGCGGTGGAGTATGTGGTT>600
367<CGAAGCTAACGCGTTAAGTTCGCCGCCTGGGGAGTACGGTCGCAAGACTGAAACTCAAAGGAATTGACGGGGGCCCGCACAAGCGGTGGAGTATGTGGTT<268
501>CGAAGCTAACGCGTTAAGTT~~~~~~~~~~~~~~~~~~~~~~~~~~~~~~~~~~~~~~~~~~~~~~~~~~~~~~~~~~~~~~~~~~~~~~~~~~~~~~>520

                *         *         *         *         *         *         *         *         *         *
601>TAATTCGATGCAACGCGAAGAACCTTACCTGGCCTTGACATGTCGAGAACTTTCCAGAGATGGATTGGTGCCTTCGGGAACTCGAACACAGGTGCTGCAT>700
267<TAATTCGATGCAACGCGAAGAACCTTACCTGGCCTTGACATGTCGAGAACTTTCCAGAGATGGATTGGTGCCTTCGGGAACTCGAACACAGGTGCTGCAT<168
520>~~~~~~~~~~~~~~~~~~~~~~~~~~~~~~~~~~~~~~~~~~~~~~~~~~~~~~~~~~~~~~~~~~~~~~~~~~~~~~~~~~~~~~~~~~~~~~~~~~~>520

                *         *         *         *         *         *         *         *         *         *
701>GGCGGTCGTCAGCTCGTGTCGTGAGATGTTGGGTTAAGTCCCGCAACGAGCGCAACCCTTGTCCTTAGTTGCCAGCACGTAATGGTGGGAACTTTAAGGA>800
167<GGCGGTCGTCAGCTCGTGTCGTGAGATGTTGGGTTAAGTCCCGCAACGAGCGCAACCCTTGTCCTTAGTTGCCAGCACGTAATGGTGGGAACTTTAAGGA<68
520>~~~~~~~~~~~~~~~~~~~~~~~~~~~~~~~~~~~~~~~~~~~~~~~~~~~~~~~~~~~~~~~~~~~~~~~~~~~~~~~~~~~~~~~~~~~~~~~~~~~>520

                *         *         *         *         *         *
801>GACCGCCGGTGACAAACCGGAGGAAGGTGGGGATGACTTCAAGTCATCATGGCCCTTACGGCCAGGG>867
 67<GACCGCCGGTGACAAACCGGAGGAAGGTGGGGATGACTTCAAGTCATCATGGCCCTTACGGCCAGGG<1
520>~~~~~~~~~~~~~~~~~~~~~~~~~~~~~~~~~~~~~~~~~~~~~~~~~~~~~~~~~~~~~~~~~~~>520
```

16*S* rDNA sequence of *Pseudomonas* sp. D2p (first line) compared with the sequence of *Pseudomonas genticula* (ATCC19374; second line) and *Pseudomonas hibiscicola* (ATCC19867; third line).

Differences indicated in boxes/red

```
d2p-zusammen.str from 1 to 867
Alignment to
pseudo-gen-atcc19374.str--  Matches:858; Mismatches:9; Gaps:630; Unattempted:0
Pseudo-hibiscicola-ATCC 19867.str--  Matches:861; Mismatches:6; Gaps:652; Unattempted:0

                *         *         *         *         *         *         *         *         *         *
      0>~~~~~~~~~~~~~~~~~~~~~~~~~~~~~~~~~~~~~~~~~~~~~~~~~~~~~~~~~~~~~~~~~~~~~~~~~~~~~~~~~~~~~~~~~~~~~~~~~>0
      1>tggctcagagtgaacgctggcggtaggcctnanacatgcaagtcgaacggcagcacagaggagcttgctccttgggtggcgagtggcggacgggtgagga>100
      1>tggctcagagtgaacgctggcggtaggcctaacacatgcaagtcgaacggcagcacagaggagcttgctccttgggtggcgagtggcggacgggtgagga>100

                *         *         *         *         *         *         *         *         *         *
      0>~~~~~~~~~~~~~~~~~~~~~~~~~~~~~~~~~~~~~~~~~~~~~~~~~~~~~~~~~~~~~~~~~~~~~~~~~~~~~~~~~~~~~~~~~~~~~~~~~>0
    101>atacatcggaatctantctgtcgtgggggataacgtaggganacttacgctaataccgcatacgacctacgggtgaaagcagggnaccttcgggccttgc>200
    101>atacatcggaatctacttttttcgtgggggataacgtagggaaacttacgctaataccgcatacgacctacgggtgaaagcaggggatcttcggaccttgc>200

                *         *         *         *         *         *         *         *         *         *
      0>~~~~~~~~~~~~~~~~~~~~~~~~~~~~~~~~~~~~~~~~~~~~~~~~~~~~~~~~~~~~~~~~~~~~~~~~~~~~~~~~~~~~~~~~~~~~~~~~~>0
    201>gcgattgaatgagccgatgtcggattagctagttggcggggtaaaggcccaccaaggcgacgatccgtagctggtctgagaggatgatcagccacactgg>300
    201>gcgattgaatgagccgatgtcggattagctagttggcggggtaaaggcccaccaaggcgacgatccgtagctnntctgngaggatgatcagccacactgg>300

                *         *         *         *         *         *         *         *         *         *
      1>~~~~~~~~~~~~~~~~~~~~~~~~~~~~~~~~~~~~~TGGGGAATATTGGACAATGGGCGCACGCCTGATCCAGCCATACCGCGTGGGTGAAGAAGGCC>62
    301>aactgagacacggtccagactcctacgggaggcagcagtggggaatattggacaatgggcgcaagcctgatccagccataccgcgtgggtgaagaaggcc>400
    301>aactgagacacggtccagactcctacgggaggcagcagtggggaatattggacaatgggcgcaagcctgatccagccataccgcgtgggtgaagaaggcc>400

                *         *         *         *         *         *         *         *         *         *
     63>TTCGGGTTGTAAAGCCCTTTTGTTGGGAAAGAAATCCAGCTGGTTAATACCCGGTTGGGATGACGGTACCCAAAGAATAAGCACCGGCTAACTTCGTGCC>162
    401>ttcgggttgtaaagccctttttgttgggaaagaaatccagctggctaatacccggttgggatgacggtacccaaagaataagcaccggctaacttcgtgcc>500
    401>ttcgggttgtaaagccctttttgttgggaaagaaatccagctggctaatacccggttgggatgacggtacccaaagaataagcaccggctaacttcgtgcc>500

                *         *         *         *         *         *         *         *         *         *
    163>AGCAGCCGCGGTAATACGAAGGGTGCAAGCGTTACTCGGAATTACTGGGCGTAAAGCGTGCGTAGGTGGTCGTTTAAGTCCGTTGTGAAAGCCCTGGGCT>262
    501>agcagccgcggtaatacgaagggtgcaagcgttactcggaattactgggcgtaaagcgtgcgtaggtggtcgtttaagtccgttgtgaaagccctgggct>600
    501>agcagccgcggtaatacgaagggtgcaagcgttactcggaattactgggcgtaaagcgtgcgtaggtggtcgtttaagtccgttgtgaaagccctgggct>600

                *         *         *         *         *         *         *         *         *         *
    263>CAACCTGGGAACTGCAGTGGATACTGGGCGACTAGAATGTGGTAGAGGGTAGCGGAATTCCTGGTGTAGCAGTGAAATGCGTAGAGATCAGGAGGAACAT>362
    601>caacctgggaactgcagtggatactgggcgactagaatgtggtagagggtagcggaattcctggtgtagcagtgaaatgcgtagagatcaggaggaacat>700
    601>caacctgggaactgcagtggatactgggcgactagaatgtggtagagggtagcggaattcctggtgtagcagtgaaatgcgtagagatcaggaggaacat>700

                *         *         *         *         *         *         *         *         *         *
    363>CCATGGCGAAGGCAGCTACCTGGACCAACATTGACACTGAGGCACGAAAGCGTGGGGAGCAAACAGGATTAGATACCCTGGTAGTCCACGCCCTAAACGA>462
    701>ccatggcgaaggcagctacctggaccaacactgacactgaggcacgaaagcgtggggagcaaacaggattagataccctggtagtccacgccctaaacga>800
    701>ccatggcgaaggcagctacctggaccaacattgacactgaggcacgaaagcgtggggagcaaacaggattagataccctggtagtccacgccctaaacga>800

                *         *         *         *         *         *         *         *         *         *
    463>TGCGAACTGGATGTTGGGTGCAATTTGGCACGCAGTATCGAAGCTAACGCGTTAAGTTCGCCGCCTGGGGAGTACGGTCGCAAGACTGAAACTCAAAGGA>562
    801>tgcgaactggatgttgggtgcaatttggcacgcagtatcgaancntaacgcgttaagttcgccgcctggggagtacggtcgcaagactgaaactcaaagga>900
    801>tgcgaactggatgttgggtgcaatttggcacgcagtatcgaagctaacgcgttaagttcgccgcctggggagtacggtcgcaagactgaaactcaaagga>900

                *         *         *         *         *         *         *         *         *         *
    563>ATTGACGGGGGCCCGCACAAGCGGTGGAGTATGTGGTTTAATTCGATGCAACGCGAAGAACCTTACCTGGCCTTGACATGTCGAGAACTTTCCAGAGATG>662
    901>attgacgggggcccgcacaagcggtggagtatgtggtttaattcgatgcaacgcgaagaaccttacctggccttgacatgtcgagaactttccagagatg>1000
    901>attgacgggggcccgcacaagcggtggagtatgtggtttaattcgatgcaacgcgaagaaccttacctggccttgacatgtcgagaactttccagagatg>1000
```

continued

16*S* rDNA sequence of *Pseudomonas* sp. D2p compared with the sequence of *Pseudomonas genticula* (ATCC19374) and *Pseudomonas hibiscicola* (ATCC19867; third line).

```
              *         *         *         *         *         *         *         *         *         *
 663>GATTGGTGCCTTCGGGAACTCGAACACAGGTGCTGCATGGCGGTCGTCAGCTCGTGTCGTGAGATGTTGGGTTAAGTCCCGCAACGAGCGCAACCCTTGT>762
1001>gattggtgccttcgggaactcgaacacaggtgctgcatggctgtcgtcagctcgtgtcgtgagatgttgggttaagtcccgcaacgagcgcaacccttgt>1100
1001>gatgggtgccttcgggaactcgaacacaggtgctgcatggctgtcgtcagctcgtgtcgtgagatgttgggttaagtcccgcaacgagcgcaacccttgt>1100

              *         *         *         *         *         *         *         *         *         *
 763>CCTTAGTTGCCAGCACGTAATGGTGGGAACTTTAAGGAGACCGCCGGTGACAAACCGGAGGAAGGTGGGGATGACTTCAAGTCATCATGGCCCTTACGGC>862
1101>ccttagttgccagcacgtaatggtgggaactctaaggagaccgccggtgacaaaccggaggaaggtggggatgacgtcaagtcatcatggcccttacggc>1200
1101>ccttagttgccagcacgtaatggtgggaactctaaggagaccgccggtgacaaaccggaggaaggtggggatgacgtcaagtcatcatggcccttacggc>1200

              *         *         *         *         *         *         *         *         *         *
 863>CAGGG~~~~~~~~~~~~~~~~~~~~~~~~~~~~~~~~~~~~~~~~~~~~~~~~~~~~~~~~~~~~~~~~~~~~~~~~~~~~~~~~~~~~~~~~~~~~~~~~~>867
1201>cagggctacacacgtactacaatggtagggacagagggctgcaagccggcgacggtaagccaatcccagaaaccctatctcagtccggattggagtctgc>1300
1201>cagggctacacacgtactacaatggtagggacagagggctgcaagccggcgacggtaagccaatcccagaaaccctatctcagtccggattggagtctgc>1300

              *         *         *         *         *         *         *         *         *         *
 867>~~~~~~~~~~~~~~~~~~~~~~~~~~~~~~~~~~~~~~~~~~~~~~~~~~~~~~~~~~~~~~~~~~~~~~~~~~~~~~~~~~~~~~~~~~~~~~~~~~~~~~~~>867
1301>aactcgactccatgaagtcggaatcgctagtaatcgcagatcagcattgctgcggtgaatacgttcccgggccttgtacacaccgcccgtcacaccatgg>1400
1301>aactcgactccatgaagtcggaatcgctagtaatcgcagatcagcattgctgcggtgaatacgttcccgggccttgtacacaccgcccgtcacaccatgg>1400

              *         *         *         *         *         *         *         *         *         *
 867>~~~~~~~~~~~~~~~~~~~~~~~~~~~~~~~~~~~~~~~~~~~~~~~~~~~~~~~~~~~~~~~~~~~~~~~~~~~~~~~~~~~~~~~~~~~~~~~~~~~~~~~~>867
1401>gagtttgttgcaccagaagcaggtagcttaaccttcgggagggcgcttgccacggtgtnnnngatgactggggtnaagtcgtaacaaggtagccgta~~~>1497
1401>gagtttgttgcaccagaagcaggtagcttaaccttcgggagggcgcttgccacggtgtnnnngatgactggggtgaagtcgtaacaaggtagccgtatcg>1500

              *
 867>~~~~~~~~~~~~~~~~~~~>867
1497>~~~~~~~~~~~~~~~~~~~>1497
1501>gaaggtgcggctggatcac>1519
```

8.2 Structure elucidation of degradation products after anaerobic desulfonation of 3-(4'-sulfophenyl) butyrate and *p*-toluene sulfonate by *Clostridium* sp. EV4

3-(4'-(5''-deoxy-D-ribofuranos-5''-yl)phenyl) butanoic acid (SPP; natural product)

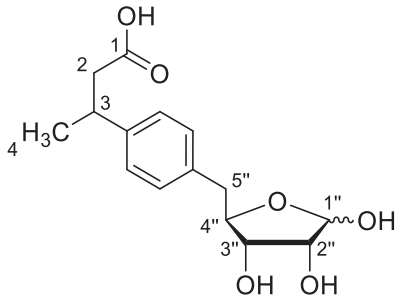

^{1}H NMR (600 MHz, Methanol-d_4)

α-form: δ = 7.17 (d, 1H, $^{3}J_{HH}$ = 4.2 Hz, arom. *ortho*-C**H**), 7.15 (d, 1H, $^{3}J_{HH}$ = 7.7 Hz, arom. *meta*-C**H**), 5.18 (d, 1H, $^{3}J_{HH}$ = 4.2 Hz, 1''-H), 4.20 (dt, 1H, $^{3}J_{HH}$ = 7.0, 5.0 Hz, 4''-H), 3.81 (t, 1H, $^{3}J_{HH}$ = 5.2 Hz, 2''-H), 3.76 (t, $^{3}J_{HH}$ = 5.3 Hz, 3''-H), 3.20 (h, 1H, $^{3}J_{HH}$ = 7.1 Hz, -C**H**-), 2.88 (dd, 1H, $^{2}J_{HH}$ = 14.2 Hz, $^{3}J_{HH}$ = 5.0 Hz, 5''-C**H**$_2$a), 2.73 (dd, 1H, $^{2}J_{HH}$ = 14.2 Hz, $^{3}J_{HH}$ = 7.0 Hz, 5''-C**H**$_2$b), 2.55 (dd, 1H, $^{2}J_{HH}$ = 15.1 Hz, $^{3}J_{HH}$ = 7.0 Hz, -C**H**$_2$a), 2.49 (dd, 1H, $^{2}J_{HH}$ = 15.1 Hz, $^{3}J_{HH}$ = 8.1 Hz, -C**H**$_2$b), 1.26 (d, 3H, $^{3}J_{HH}$ = 7.0 Hz, -C**H**$_3$).

β-form: δ = 7.21 (d, 2H, $^{3}J_{HH}$ = 7.9 Hz, arom. *ortho*-C**H**), 7.17 (d, 1H, $^{3}J_{HH}$ = 4.2 Hz, arom. H), 7.15 (d, 1H, $^{3}J_{HH}$ = 7.7 Hz, arom. *meta*-C**H**), 5.09 (d, 1H, $^{3}J_{HH}$ = 1.5 Hz, 1''-H), 4.03-3.99 (dt+s, 2H, $^{3}J_{HH}$ = 6.7, 3.6 Hz, 2''-H, 4''-H), 3.83 (dd, 1H, $^{3}J_{HH}$ = 4.3, 1.6 Hz, 3''-H), 3.20 (h, 1H, $^{3}J_{HH}$ = 7.1 Hz, -C**H**-), 2.97 (dd, 1H, $^{2}J_{HH}$ = 14.1 Hz, $^{3}J_{HH}$ = 3.3 Hz, 5''-C**H**$_2$a), 2.80 (dd, 1H, $^{2}J_{HH}$ = 14.0 Hz, $^{3}J_{HH}$ = 7.7 Hz, 5''-C**H**$_2$b), 2.55 (dd, 1H, $^{2}J_{HH}$ = 15.1 Hz, $^{3}J_{HH}$ = 7.0 Hz, -C**H**$_2$a), 2.49 (dd, 1H, $^{2}J_{HH}$ = 15.1 Hz, $^{3}J_{HH}$ = 8.1 Hz, -C**H**$_2$b), 1.26 (d, 3H, $^{3}J_{HH}$ = 7.0 Hz, -C**H**$_3$).

^{13}C NMR (100 MHz, Methanol-d_4)

α-form: δ = 176.9 (-**C**OOH), 145.5 (arom. *ipso*-C$_q$), 137.2 (arom. *para*-C$_q$), 130.6 (arom. *meta*-**C**H), 127.7 (arom. *ortho*-**C**H), 97.5 (1''-C), 84.4 (4''-C), 74.4 (3''-C), 72.1 (2''-C), 44.2 (-**C**H$_2$), 40.0 (5''-**C**H$_2$), 37.5 (-C**H**), 22.4 (-**C**H$_3$).

β-form: δ = 176.9 (-**C**OOH), 145.2 (arom. *ipso*-C$_q$), 138.0 (arom. *para*-C$_q$), 130.5 (arom. *meta*-**C**H), 127.6 (arom. *ortho*-**C**H), 103.0 (1''-C), 84.2 (4''-C), 77.2 (3''-H), 75.4 (2''-C), 44.2 (-**C**H$_2$), 41.8 (5''-**C**H$_2$), 37.5 (-C**H**), 22.4 (-**C**H$_3$).

3-(4’-(5’’-deoxy-D-ribofuranos-5’’-yl)phenyl) butanoic acid (SPP; natural product)

HR-MS

$[M+NH_4]^+$ = 314,16019

Δppm = 1,197

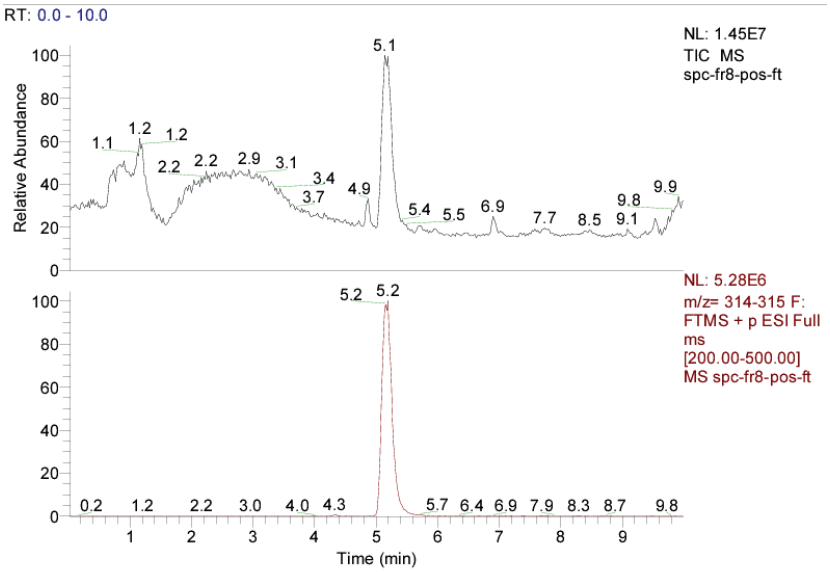

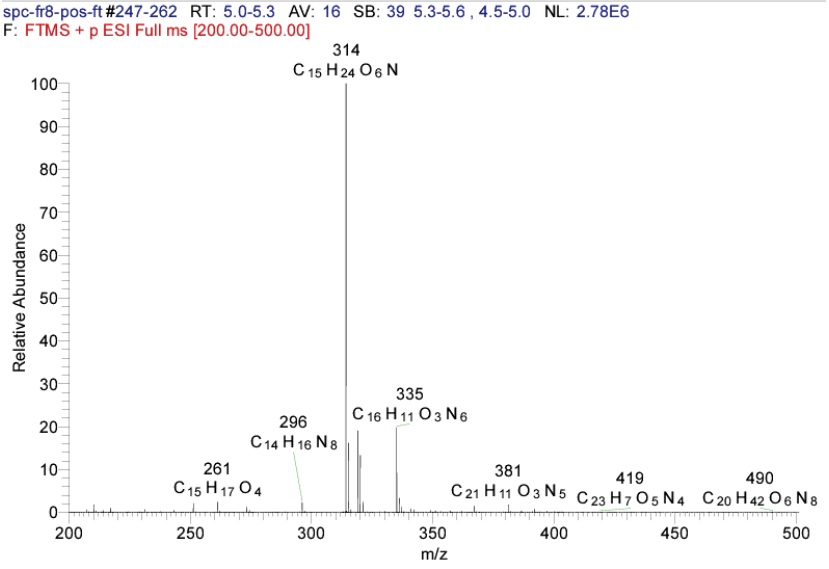

Elemental composition

Single mass

Mass: 314.16019

Max. results 7

Calculate

Idx	Formula	RDB	Delta ppm
1	$C_{15}H_{24}O_6N$	4.5	1.197
2	$C_{14}H_{18}ON_8$	10.0	1.214
3	$C_{16}H_{20}O_2N_5$	9.5	-3.060
4	$C_{13}H_{22}O_5N_4$	5.0	5.471
5	$C_{18}H_{22}O_3N_2$	9.0	-7.334
6	$C_{12}H_{26}O_9$	0.0	9.728
7	$C_{11}H_{20}O_4N_7$	5.5	9.745

File... List Simulate

Limits

Charge: 1

Nitrogen-Rule: Do not use

Mass tolerance 50.00 ppm

RDB equiv: -1.0-100.0

Elements in use

Isotope	Min	Max	DB eq.	Mass
16 O	0	15	0.0	15.995
12 C	0	30	1.0	12.000
1 H	0	60	-0.5	1.008
14 N	0	10	0.5	14.003

5-deoxy-5-tol-4'-yl-D-ribofuranose (TSP; natural product)

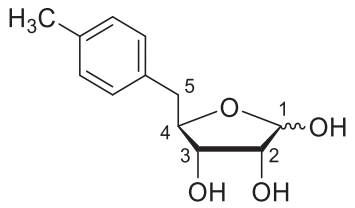

^{1}H NMR (600 MHz, Methanol-d_4)

α-form: δ = 7.12 (d, 1H, $^{3}J_{HH}$ = 7.9 Hz, arom. *ortho*-C**H**), 7.07 (d, 1H, $^{3}J_{HH}$ = 8.2 Hz, arom. *meta*-C**H**), 5.16 (d, 1H, $^{3}J_{HH}$ = 4.2 Hz, 1-H), 4.18 (dt, 1H, $^{3}J_{HH}$ = 6.8, 5.0 Hz, 4-H), 3.79 (dd, 1H, $^{3}J_{HH}$ = 5.8 Hz, 4.3 Hz, 2-H), 3.74 (t, $^{3}J_{HH}$ = 5.4 Hz, 3-H), 2.87 (dd, 1H, $^{2}J_{HH}$ = 14.2 Hz, $^{3}J_{HH}$ = 5.0 Hz, 5-C**H**$_2$a), 2.72 (dd, 1H, $^{2}J_{HH}$ = 14.2 Hz, $^{3}J_{HH}$ = 6.9 Hz, 5-C**H**$_2$b), 2.29 (s, 3H, -C**H**$_3$).

β-form: δ = 7.15 (d, 2H, $^{3}J_{HH}$ = 7.8 Hz, arom. *ortho*-C**H**), 7.07 (d, 1H, $^{3}J_{HH}$ = 8.2 Hz, arom. H), 7.15 (d, 1H, $^{3}J_{HH}$ = 7.7 Hz, arom. *meta*-C**H**), 5.08 (d, 1H, $^{3}J_{HH}$ = 1.5 Hz, 1-H), 4.00 (dt, 1H, $^{3}J_{HH}$ = 6.7, 4.0 Hz, 4-H), 3.99 (d, 1H, $^{3}J_{HH}$ = 4.0 Hz, 2-H), 3.81 (dd, 1H, $^{3}J_{HH}$ = 4.3, 1.6 Hz, 3-H), 2.95 (dd, 1H, $^{2}J_{HH}$ = 13.9 Hz, $^{3}J_{HH}$ = 3.5 Hz, 5-C**H**$_2$a), 2.79 (dd, 1H, $^{2}J_{HH}$ = 14.0 Hz, $^{3}J_{HH}$ = 7.7 Hz, 5-C**H**$_2$b), 2.29 (s, 3H, -C**H**$_3$).

^{13}C NMR (150 MHz, Methanol-d_4)

α-form: δ = 136.8 (arom. *ipso*-C$_q$), 136.2 (arom. *para*-C$_q$), 130.5 (arom. *meta*-**C**H), 129.8 (arom. *ortho*-**C**H), 97.6 (1-C), 84.3 (4-C), 74.4 (3-C), 72.1 (2-C), 39.9 (5-**C**H$_2$), 21.1 (-**C**H$_3$).

β-form: δ = 137.0 (arom. *ipso*-C$_q$), 136.6 (arom. *para*-C$_q$), 130.3 (arom. *meta*-**C**H), 129.8 (arom. *ortho*-**C**H), 103.0 (1-C), 84.3 (4-C), 77.2 (3-C), 75.4 (2-C), 41.7 (5-**C**H$_2$), 21.1 (-**C**H$_3$).

5-deoxy-5-tol-4'-yl-D-ribofuranose (TSP; natural product)

HR-MS

$[M+Na]^+$ = 247,09419

Δppm = 0,46

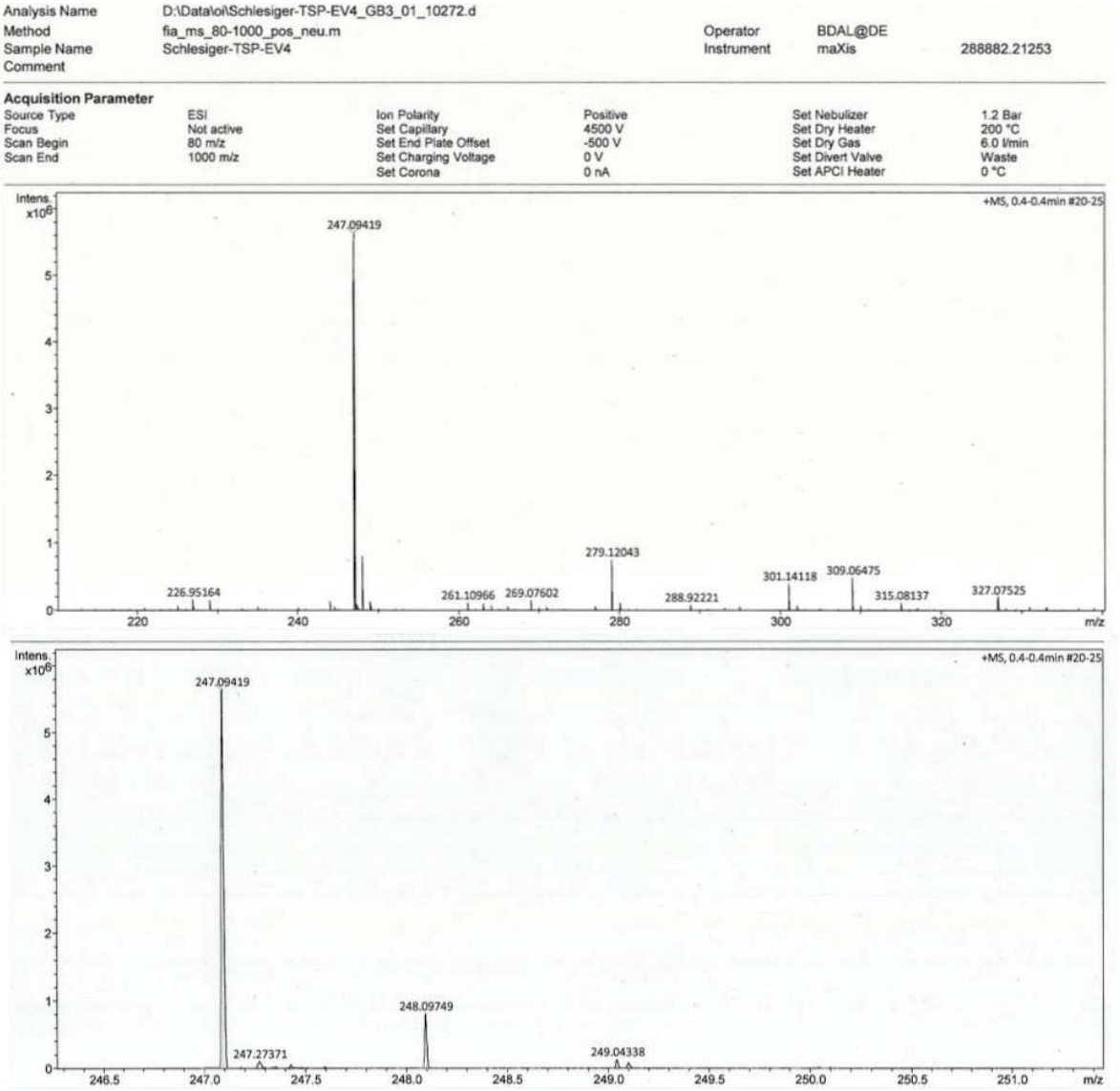

5-deoxy-5-(4'-tolyl)-D-ribose

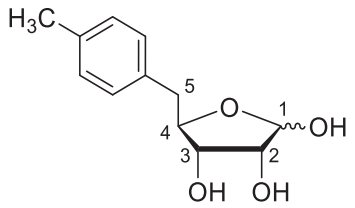

^{1}H NMR (600 MHz, Methanol-d_4)

α-form: δ = 7.12 (d, 1H, $^{3}J_{HH}$ = 7.8 Hz, arom. *ortho*-C**H**), 7.07 (d, 1H, $^{3}J_{HH}$ = 8.2 Hz, arom. *meta*-C**H**), 5.16 (d, 1H, $^{3}J_{HH}$ = 4.2 Hz, 1-H), 4.18 (dt, 1H, $^{3}J_{HH}$ = 6.9, 5.1 Hz, 4-H), 3.79 (dd, 1H, $^{3}J_{HH}$ = 5.8 Hz, 4.3 Hz, 2-H), 3.74 (t, $^{3}J_{HH}$ = 5.3 Hz, 3-H), 2.87 (dd, 1H, $^{2}J_{HH}$ = 14.2 Hz, $^{3}J_{HH}$ = 5.0 Hz, 5-C**H**$_2$a), 2.72 (dd, 1H, $^{2}J_{HH}$ = 14.2 Hz, $^{3}J_{HH}$ = 6.9 Hz, 5-C**H**$_2$b), 2.29 (s, 3H, -C**H**$_3$).

β-form: δ = 7.15 (d, 2H, $^{3}J_{HH}$ = 7.8 Hz, arom. *ortho*-C**H**), 7.07 (d, 1H, $^{3}J_{HH}$ = 8.2 Hz, arom. H), 7.15 (d, 1H, $^{3}J_{HH}$ = 7.7 Hz, arom. *meta*-C**H**), 5.08 (d, 1H, $^{3}J_{HH}$ = 1.4 Hz, 1-H), 4.00 (dt, 1H, $^{3}J_{HH}$ = 6.8, 4.0 Hz, 4-H), 3.99 (d, 1H, $^{3}J_{HH}$ = 4.0 Hz, 2-H), 3.81 (d, 1H, $^{3}J_{HH}$ = 3.2 Hz, 3-H), 2.95 (dd, 1H, $^{2}J_{HH}$ = 13.9 Hz, $^{3}J_{HH}$ = 3.5 Hz, 5-C**H**$_2$a), 2.79 (dd, 1H, $^{2}J_{HH}$ = 14.0 Hz, $^{3}J_{HH}$ = 7.6 Hz, 5-C**H**$_2$b), 2.29 (s, 3H, -C**H**$_3$).

^{13}C NMR (150 MHz, Methanol-d_4)

α-form: δ = 135.4 (arom. *ipso*-C$_q$), 134.8 (arom. *para*-C$_q$), 129.1 (arom. *meta*-**C**H), 128.4 (arom. *ortho*-**C**H), 96.2 (1-C), 82.8 (4-C), 73.0 (3-C), 70.7 (2-C), 40.3 (5-**C**H$_2$), 21.1 (-**C**H$_3$).

β-form: δ = 135.6 (arom. *ipso*-C$_q$), 135.2 (arom. *para*-C$_q$), 128.9 (arom. *meta*-**C**H), 128.4 (arom. *ortho*-**C**H), 101.6 (1-C), 82.8 (4-C), 75.7 (3-C), 74.0 (2-C), 38.5 (5-**C**H$_2$), 19.7 (-**C**H$_3$).

5-deoxy-5-(4'-tolyl)-D-ribose

HR-MS

$[M+Na]^+ = 247{,}09429$

$\Delta ppm = 0{,}83$

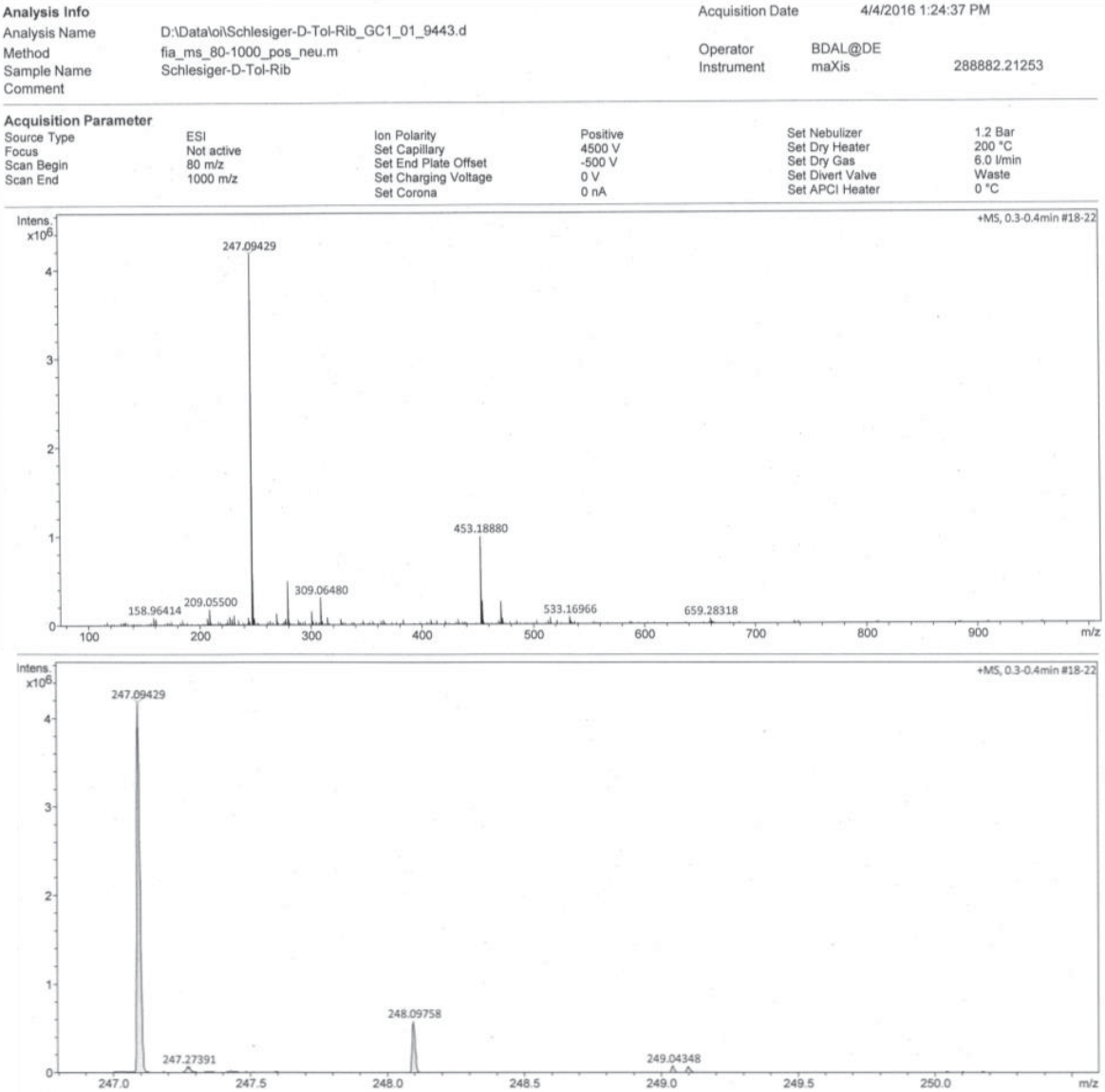

5-deoxy-5-(4'-tolyl)-L-ribose

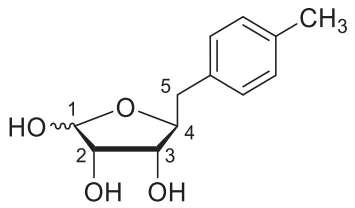

^{1}H NMR (600 MHz, Methanol-d_4)

α-form: δ = 7.12 (d, 1H, $^{3}J_{HH}$ = 7.9 Hz, arom. *ortho*-C**H**), 7.07 (d, 1H, $^{3}J_{HH}$ = 8.1 Hz, arom. *meta*-C**H**), 5.16 (d, 1H, $^{3}J_{HH}$ = 4.2 Hz, 1-H), 4.18 (dt, 1H, $^{3}J_{HH}$ = 6.3, 5.2 Hz, 4-H), 3.79 (t, 1H, $^{3}J_{HH}$ = 5.0 Hz, 2-H), 3.74 (t, $^{3}J_{HH}$ = 5.4 Hz, 3-H), 2.87 (dd, 1H, $^{2}J_{HH}$ = 14.2 Hz, $^{3}J_{HH}$ = 5.0 Hz, 5-C**H**$_2$a), 2.72 (dd, 1H, $^{2}J_{HH}$ = 14.2 Hz, $^{3}J_{HH}$ = 6.9 Hz, 5-C**H**$_2$b), 2.28 (s, 3H, -C**H**$_3$).

β-form: δ = 7.15 (d, 2H, $^{3}J_{HH}$ = 7.7 Hz, arom. *ortho*-C**H**), 7.07 (d, 1H, $^{3}J_{HH}$ = 8.2 Hz, arom. H), 7.15 (d, 1H, $^{3}J_{HH}$ = 7.7 Hz, arom. *meta*-C**H**), 5.08 (d, 1H, $^{3}J_{HH}$ = 1.4 Hz, 1-H), 4.00 (dt, 1H, $^{3}J_{HH}$ = 6.6, 4.2 Hz, 4-H), 3.99 (d, 1H, $^{3}J_{HH}$ = 3.9 Hz, 2-H), 3.81 (d, 1H, $^{3}J_{HH}$ = 3.3 Hz, 3-H), 2.95 (dd, 1H, $^{2}J_{HH}$ = 14.0 Hz, $^{3}J_{HH}$ = 3.4 Hz, 5-C**H**$_2$a), 2.79 (dd, 1H, $^{2}J_{HH}$ = 14.1 Hz, $^{3}J_{HH}$ = 7.6 Hz, 5-C**H**$_2$b), 2.28 (s, 3H, -C**H**$_3$).

^{13}C NMR (150 MHz, Methanol-d_4)

α-form: δ = 136.8 (arom. *ipso*-C$_q$), 136.2 (arom. *para*-C$_q$), 130.5 (arom. *meta*-**C**H), 129.8 (arom. *ortho*-**C**H), 97.6 (1-C), 82.8 (4-C), 74.4 (3-C), 72.1 (2-C), 41.7 (5-**C**H$_2$), 21.1 (-**C**H$_3$).

β-form: δ = 137.0 (arom. *ipso*-C$_q$), 136.6 (arom. *para*-C$_q$), 130.3 (arom. *meta*-**C**H), 129.8 (arom. *ortho*-**C**H), 103.0 (1-C), 84.2 (4-C), 77.2 (3-C), 75.4 (2-C), 39.9 (5-**C**H$_2$), 21.1 (-**C**H$_3$).

5-deoxy-5-(4'-tolyl)-L-ribose

HR-MS

$[M+Na]^+$ = 247,09418

Δppm = 0,42

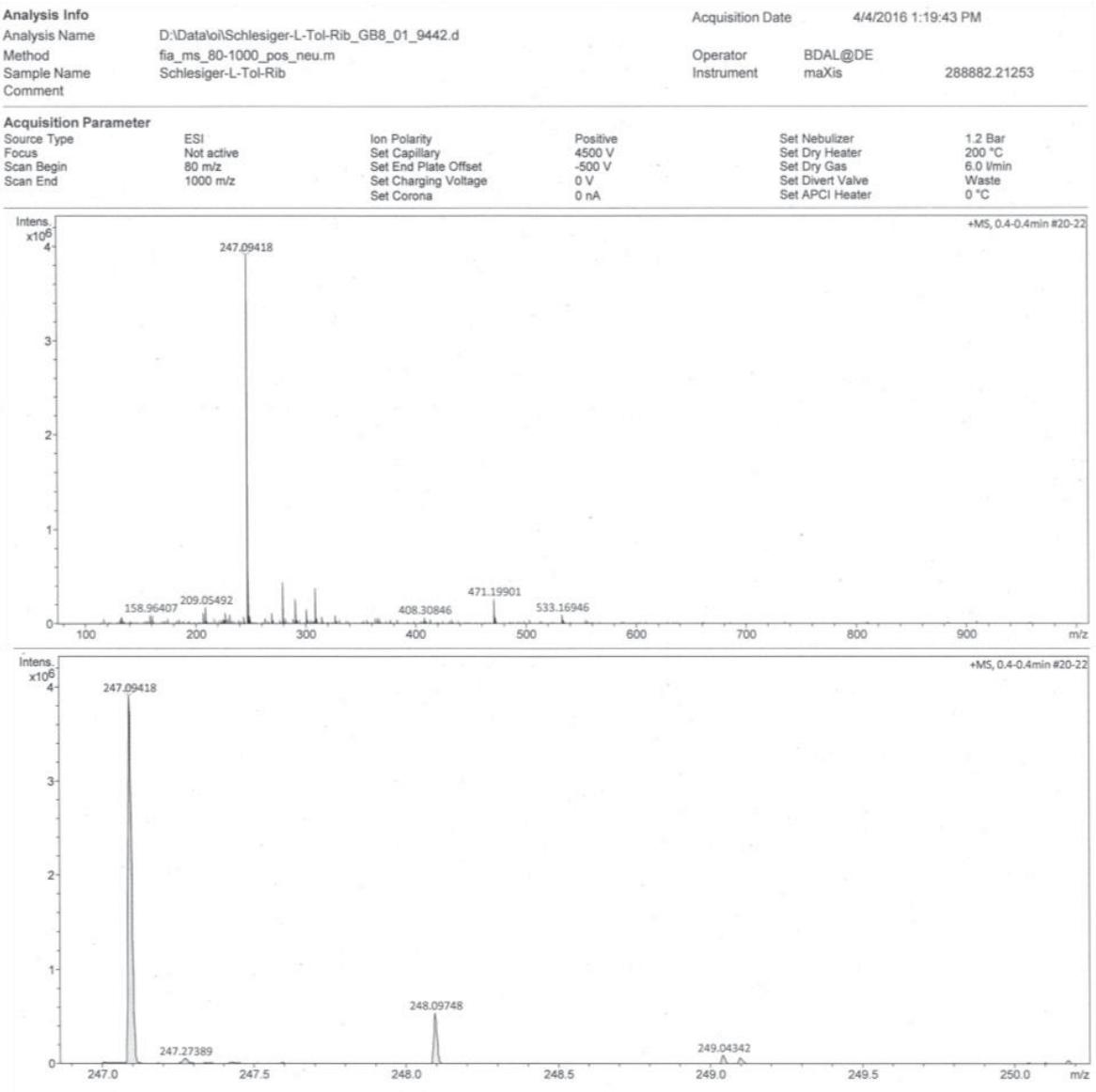

5-deoxy-5-(4'-tolyl)- D-lyxose

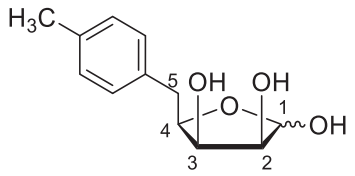

^{1}H NMR (600 MHz, Methanol-d_4)

α-form: δ = 7.13 (d, 1H, $^{3}J_{HH}$ = 7.5 Hz, arom. *ortho*-C**H**), 7.06 (d, 1H, $^{3}J_{HH}$ = 7.7 Hz, arom. *meta*-C**H**), 5.07 (d, 1H, $^{3}J_{HH}$ = 4.8 Hz, 1-H), 4.03 (dt, 1H, $^{3}J_{HH}$ = 6.7, 4.0 Hz, 4-H), 4.00 (t, 1H, $^{3}J_{HH}$ = 4.9 Hz, 2-H), 3.91 (t, $^{3}J_{HH}$ = 5.1 Hz, 3-H), 3.04 (dd, 1H, $^{2}J_{HH}$ = 13.8 Hz, $^{3}J_{HH}$ = 7.0 Hz, 5-C**H**$_2$a), 2.88 (dd, 1H, $^{2}J_{HH}$ = 13.7 Hz, $^{3}J_{HH}$ = 7.2 Hz, 5-C**H**$_2$b), 2.28 (s, 3H, -C**H**$_3$).

β-form: δ = 7.16 (d, 2H, $^{3}J_{HH}$ = 8.0 Hz, arom. *ortho*-C**H**), 7.06 (d, 1H, $^{3}J_{HH}$ = 7.7 Hz, arom. *meta*-C**H**), 5.19 (d, 1H, $^{3}J_{HH}$ = 2.5 Hz, 1-H), 4.27 (td, 1H, $^{3}J_{HH}$ = 7.0, 2.2 Hz, 4-H), 3.94 (d, 1H, $^{3}J_{HH}$ = 2.4 Hz, 2-H), 3.96-3.93 (m, 1H, 3-H), 2.96 (dd, 1H, $^{2}J_{HH}$ = 13.7 Hz, $^{3}J_{HH}$ = 6.7 Hz, 5-C**H**$_2$a), 2.81 (dd, 1H, $^{2}J_{HH}$ = 13.7 Hz, $^{3}J_{HH}$ = 7.3 Hz, 5-C**H**$_2$b), 2.28 (s, 3H, -C**H**$_3$).

^{13}C NMR (150 MHz, Methanol-d_4)

δ = 136.8 (arom. *ipso*-C$_q$), 136.6 (arom. *para*-C$_q$), 130.3 (arom. *meta*-**C**H), 129.9 (arom. *ortho*-**C**H), 103.0 (1-C), 82.6 (4-C), 80.0 (3-C), 73.2 (2-C), 36.2 (5-**C**H$_2$), 21.1 (-**C**H$_3$).

5-deoxy-5-(4'-tolyl)- D-lyxose

HR-MS

$[M+Na]^+ = 247{,}09418$

$\Delta ppm = 0{,}39$

Analysis Info

Analysis Name	D:\Data\oi\Schlesiger-D-Tollyx_GB7_01_9441.d	Acquisition Date	4/4/2016 1:14:47 PM
Method	fia_ms_80-1000_pos_neu.m	Operator	BDAL@DE
Sample Name	Schlesiger-D-Tollyx	Instrument	maXis 288882.21253
Comment			

Acquisition Parameter

Source Type	ESI	Ion Polarity	Positive	Set Nebulizer	1.2 Bar
Focus	Not active	Set Capillary	4500 V	Set Dry Heater	200 °C
Scan Begin	80 m/z	Set End Plate Offset	-500 V	Set Dry Gas	6.0 l/min
Scan End	1000 m/z	Set Charging Voltage	0 V	Set Divert Valve	Waste
		Set Corona	0 nA	Set APCI Heater	0 °C